Die approbierte Originalversion dieser Dissertation ist in der Hauptbibliothek der Technischen Universität Wien aufgestellt und zugänglich.
http://www.ub.tuwien.ac.at

The approved original version of this thesis is available at the main library of the Vienna University of Technology.
http://www.ub.tuwien.ac.at/eng

TECHNISCHE UNIVERSITÄT WIEN

DISSERTATION

Interaction of Building Envelope and Cooling Ceilings - System Analysis and System Modeling

ausgeführt zum Zwecke der Erlangung des akademischen Grades

Doktor/in der technischen Wissenschaften

eingereicht an der TU Wien, Fakultät für Maschinenwesen und Betriebswissenschaften

von

Katharina Eder

Matrikelnummer 0927763

unter der Leitung von

Univ.-Prof. Dipl.-Ing. Dr.techn. Thomas Bednar

Fakultät für Bauingenieruwesen, Institut für Hochbau und Technologie
Forschungsbereich für Bauphysik und Schallschutz, E206

begutachtet von

Ao.Univ.-Prof. Dipl.-Ing. Dr.techn. Karl Ponweiser
TU Wien
Fakultät für Maschinenwesen und Beriebswissenschaften
Institut für Energietechnik und Thermodynamik

Univ.-Prof. Dipl.-Ing. Dr.techn. Tobias Pröll
Universität für Bodenkultur Wien
Department für Materialwissenschaften und Prozesstechnik
Institut für Verfahrens- und Energietechnik

This work was supported by Vienna, University of Technology within the framework of the doctoral program “Energy Systems 2030 (ENSYS 2030)”.

I acknowledge, that the printing of the thesis “Interaction of Building Envelope and Cooling Ceilings - System Analysis and System Modeling” needs the confirmation of the examination committee.

Affidavit

I declare in lieu of oath, that I wrote this thesis and performed the associated research myself, using only literature cited in this volume. If text passages from sources are used literally, they are marked as such.

I confirm that this work is original and has not been submitted elsewhere for any examination, nor is it currently under consideration for a thesis elsewhere.

Wien, 22.06.2017

(Katharina Eder)

Publications

Publications included in this work

K. Eder, T. Bednar: “Effect of façade systems on the performance of cooling ceilings: In situ measurements”, Frontiers of Architectural Research, Volume 4, Issue 1, March 2015, Pages 68–78

K. Eder, H. Konder, T. Bednar: “Effect of different façade systems on the cooling capacity of a cooled ceiling – Tracer gas measurement of the air flow”, Proceedings of the 10th Nordic Symposium on Building Physics, NSB, 2014, Lund, 8 Seiten

K. Eder, M. Neusser, T. Bednar: “Effect of different façade systems on the cooling capacity of a cooled ceiling – CFD modeling”, Proceedings of the 10th Nordic Symposium on Building Physics, NSB, 2014, Lund, 8 Seiten

K. Eder, C. Steininger, T. Bednar: “Enhancing the performance of a cooling ceiling by an innovative façade system”; Proceedings of the 5th International Building Physics Conference, IBPC, 2012, Kyoto 8 Seiten

Publications not included in this work

K. Eder, E. Widl, B. Beigelböck, F. Judex, C. Gähler: “CO-Simulation for Control Design - a case study for cross domain collaboration”; ASHRAE and IBPSA-USA SimBuild 2016, Salt Lake City, UT

B. Beigelböck, M. Cichy, K. Eder, F. Judex: “Demand Response of Large Residential Buildings - A Case Study from “Seestadt Aspern””; IECON 2016 - 42nd Annual Conference of IEEE ndustrial Electronics Society, 2016, Florence, Italy

B. Beigelböck, K. Eder, F. Judex, I. Lindmeier: “Validierung dynamischer Gebäude- und Anlagensimulation am Beispiel eines Mehrfamilienhauses in der “Seestadt Aspern””; 20th International Congress e-nova 2016, Pinkafeld

B. Beigelböck, J. Emhofer, K. Eder, I. Lindmeier: “DCTune - Methodenentwicklung zur Effizienzsteigerung von Dessicant Evaporative Cooling Systemen”; 20th International Congress e-nova 2016, Pinkafeld

K. Eder, I. Lindmeier, S. Hauer, F. Judex, M. Blöchle, G. Zucker: “Methodenentwicklung zur signifikanten Verkürzung der Inbetriebnahmephase am Demonstrationsgebäude Post am Rochus”; 20th International Congress e-nova 2016, Pinkafeld

K. Eder, P. Horn: “Auswirkung verschiedener Systemkonfigurationen für Raumheizung und Warmwasserbereitung in Kombination mit thermo-chemischennSpeichern auf die Gesamtenergieeffizienz der Energiebereitstellung”; 20th International Congress e-nova 2016, Pinkafeld

E. Widl, F. Judex, K. Eder, P. Palensky: “FMI-based Co-Simulation of Hybrid Closed-loop Control System Models”, International Conference on Computer Science & Education, Juli ICCSE 2015

E. Widl, W. Müller, D. Basciotti, S. Henein, S. Hauer, K. Eder: “Simulation of Multi-domain Energy Systems Based on the Functional Mock-up Interface Specification”, International Symposium on Smart Electric Distribution Systems and Technologies, September 2015

F. Petrushevski , S. Hauer, F. Judex, S. Leal, und K. Eder: “Quality assessment of automatically generated simplified thermal building models”, in BS 2015, to be published Dec 2015, Hyderabad-India.

A. Bres, K. Eder, S. Hauer und F. Judex.: “Case study of energy performance analyses on different scales”, in 6th International Building Physics Conference, IBCP 2015

S.Leal, S. Hauer, F. Judex, K. Eder, and S. Gahr. “BAUSIM 2014: a prototypical automated building modeling tool.” Aachen, Germany: Fifth German-Austrian IBPSA Conference, 2014.

Acknowledgements

The doctoral program “Energy Systems 2030 (ENSYS 2030)” is an internal research project funded by Vienna University of Technology, which has the main goal to provide doctoral students within the research area Ënergy and Environment,ä remarkably structured and interdisciplinary education. Without the framework of the doctoral program for me writing a PHD theses would not have been possible. Undertaking this PhD has been an experience for me and it would not have been possible to do without the support and guidance that I received from many people.

First and foremost I wish to thank my advisor, Univ. Prof. Dipl-Ing. Dr.techn. Thomas Bednar. He has been supportive ever since the day we discussed the research topic. He guided me successfully with suggestions of improvement and development through all the years writing on my theses.

Second I want to thank Ao.Univ.Prof. Dipl.-Ing. Dr.techn. Karl Ponweiser for taking the part of the co-supervisor and the helpful discussions regarding thermal and air flow modeling, these discussions contributed decisively to the success of the work. Furthermore I want to thank Univ.-Prof. Dipl.-Ing. Dr.techn. Tobias Pröll for taking the time to review the theses.

For more than 10 years Christian Steininger supports me in the field of HVAC technology with his immense knowledge. He is full of curiosity and every discussion and critical question was expanding my spectrum of skills and knowledge. I’m thankful for every minute of time he took to support me in finding the research topic as well as discussing the results and outcomes and helping me finalizing this work.

Dozens of people have helped and taught me immensely at the Institute for Building Construction and Technology, Department for Building Physics and Building Acoustic. Im very grateful for the help I received from Manfred Grüner and Hannes Konder regarding the measurement equipment, measurement installation and the data recording. Special thanks goes also to Maximilian Neusser who impressed me deeply and it was a pleasure discussing the topic of air flow modelling with him. As part of the team I also want to send a special thanks to Marianne Rebel for all her administrative and even more for her personal support.

A special thanks to my family. Words cannot express how grateful I am to my mother and father for all their support and how proud I am to be one of their children. I would also like to thank all of my friends who supported me in writing, and incented me to strive towards my goal.

Abstract

The aim of the work is, to provide an easy to handle planning support tool that takes into account the different influencing parameters regarding the resulting room conditions and therefore the comfort in the room. The prediction of thermal comfort in buildings plays a key role in constructing energy efficient buildings and at the moment it cannot be fully implemented. In the completeness complex flow processes in different façade systems, the dynamic of building elements' performance in combination with the control system is a great, so far, unresolved challenge.

For the development of a simplified calculation model a series of measurements have been done in an existing office building with different façade systems. The measurement results show that there is an impact on the cooling capacity of a cooling ceiling and the operative temperature and therefore also on the comfort by different façade systems. Furthermore the measurements are used for the validation of the mathematical model.

For the thermal calculation a room model based on the program Matlab/Simulink was built. A CFD Model (with the program Comsol) realizes the mapping of the air flow. The boundary conditions for the CFD Model are the results of the thermal calculation. The goal is to define a sufficiently accurate picture of the flow characteristics in rooms. The results of the CFD calculations allow a simplified integration into the thermal model using distribution factors and mass balances.

The validation of the calculation results with the measurement results shows that a fully coupled simulation (coupling of thermal and air flow calculation) is not required for the prediction of room conditions and the thermal comfort in rooms. Neglecting the flow characteristics in rooms can lead to incorrect results, especially for complex façade systems in combination with component activation (e.g. cooling ceiling).

Based on the validated model, recommendations for future office and class room designs in net energy producing buildings can be formulated. To accomplish this, simulations over typical day to day cycles as well as yearly cycles can be conducted.

Contents

Publications **i**

Publications included in this work i

Publications not included in this work i

List of Figures **xi**

List of Tables **xxiii**

1 Basic Information and Motivation **1**

1.1 Motivation 1

1.2 State of the art 2

1.2.1 Studies on façade system 2

1.2.2 Studies on activated building element 2

1.2.3 ”Dominant” Building Energy Programs 3

1.2.4 Studies on co-Simulation 7

1.2.5 Conclusio State of the Art 7

1.3 Hypotheses 8

2 Description of Measurement Set-up **11**

2.1 Introduction 11

2.2 Building / Room Set up 11

2.2.1 Basic Building Information 12

2.2.2 Façade System 12

2.2.3 Cooling 15

2.2.4 Ventilation 20

2.3 Measurement Set up 21

2.3.1 Measurement equipment 21

2.3.2 Air Temperature / Moisture 23

2.3.3 Operative Temperature - Black Ball Measurement 26

2.3.4 Cooling Medium Temperature Measurement 28

2.3.5 Mass flow - cooling ceiling 29
2.3.6 Volume flow 30
2.3.7 Supply Air Temperature 31
2.3.8 Comfort Level Probe 32
2.3.9 Heat Flow Measurement 37
2.3.10 Intensity of Illumination 38
2.3.11 Solar Radiation 40
2.3.12 Tracer Gas Measurement 42

3 Measurement Operative Temperature 45
3.1 Introduction 45
3.2 Building / Room set up 45
3.2.1 Basic Building Information 45
3.2.2 Measurement positions operative temperature 47
3.3 Measurement Results on Operative Temperature 50
3.3.1 Adjustment of the Rooms 52
3.3.2 Results: Single Skin façade, Shading System completely closed . 53
3.3.3 Results: Single Skin Façade, Shading System half opened 54
3.3.4 Results: Single Storey Double Skin Façade, Shading System completely closed 56
3.3.5 Results: Single Storey Double Skin Façade, Shading System Half Opened 58
3.3.6 Summary of Measurement Results - First Summer Period 60
3.3.7 Measurement Results - Next to the Façade - Second Summer Period 62
3.3.8 Measurement Results - Centre of the Room - Second Summer Period 64
3.4 Summary in-situ Measurements - Operative Temperature 66

4 Cooling Capacity of the Cooling Ceiling 69
4.1 Introduction 69
4.2 Building / Room Set up 70
4.3 Cooling capacity for a day with solar radiation - single skin façade 72
4.3.1 Cooling capacity for a day with solar radiation - room type 1 72
4.3.2 Cooling capacity for a day with solar radiation - room type 3 73

4.3.3 Cooling capacity for a day with solar radiation - room type 5 74
4.4 Cooling capacity for a day with solar radiation - single storey double skin façade 75
4.4.1 Cooling capacity for a day with solar radiation - room type 2 75
4.4.2 Cooling capacity for a day with solar radiation - room type 4 76
4.4.3 Cooling capacity for a day with solar radiation - room type 6 77
4.5 Cooling capacity for a day without direct solar radiation 78
4.5.1 Cooling capacity for a day without direct solar radiation - room type 2 78
4.5.2 Cooling capacity for a day without direct solar radiation - room type 3 79
4.5.3 Cooling capacity for a day without direct solar radiation - room type 6 80
4.6 Single skin façade versus single storey double skin façade 81
4.7 Summary cooling capacity for all room types 83

5 Tracer Gas Measurement 85
5.1 Introduction 85
5.2 In-situ measurement - Building Information 85
5.2.1 Cooling 86
5.2.2 Ventilation 87
5.3 Measurement Set up 87
5.3.1 Sensor Location 88
5.3.2 Measurement Variations 89
5.4 Measurement results tracer gas measurement 91
5.4.1 Decay curves - CO_2 concentration 91
5.4.2 Location of Injection - Impact on the results 93
5.4.3 Summary of results for a day with solar radiation 94
5.4.4 Summary of results for a day without solar radiation 95
5.5 Conclusions tracer gas measurement 96

6 Thermal Modeling 97
6.1 Basic Information 97
6.1.1 Room Geometry / Zones 98
6.2 Mathematical Model 99

6.2.1 Energy Balance of Zones . . . 99
6.2.2 Calculation of Components - Heat Balance . . . 100
6.2.3 Partition walls . . . 101
6.2.4 Model description for the Heat Flow through a Layer . . . 102
6.2.5 Model Description for the Outward Heat Flow . . . 104
6.2.6 Model Description for the Inward Heat Flow . . . 108
6.2.7 Model Description for the Cooling Ceiling . . . 109

7 Air Flow Modeling 113
7.1 Introduction . . . 113
7.2 Method . . . 113
7.3 2D-Model . . . 114
7.3.1 Geometry and mesh properties . . . 114
7.3.2 Façade system . . . 115
7.3.3 Boundary Conditions . . . 116
7.3.4 Material Properties and initial Conditions . . . 117
7.3.5 Mesh and Solver Settings . . . 118
7.4 Results CFD Simulation . . . 120
7.4.1 Operative Temperature . . . 120
7.4.2 Cooling Capacity . . . 120
7.4.3 Air velocity . . . 124
7.5 Conclusions of the CFD calculation . . . 130

8 Air Flow Integrated Room Model 131
8.1 Introduction . . . 131
8.2 Model description . . . 131
8.2.1 Zone . . . 133
8.2.2 Geometry . . . 134
8.2.3 Façade . . . 136
8.2.4 Enclosing Surfaces . . . 140
8.2.5 Internal Gains . . . 143
8.2.6 Ventilation . . . 144
8.2.7 Weather . . . 145
8.3 Summary Air Flow Integrated Room Modeling . . . 146

9 Validation of the Integrated Room Model 147

9.1 Introduction: Validation Enhanced Room Model . . . 147
9.2 Air Flow Integration - Comparison of the Speed Factors . . . 147
9.3 Comparison Measurement Results and Calculated Results on the Cooling Capacity . . . 148
9.4 Comparison Measurement Results and Calculated Results on Operative Temperatures . . . 148
9.5 Calculation Results for the different Room Types - Design Day . . . 150
9.6 Summary Validation Air Flow Integrated Room Model . . . 151

10 Summary and Outlook **153**
10.1 Introduction . . . 153
10.2 Summary of the work . . . 154
10.2.1 Measurement Results . . . 154
10.2.2 Mathematical Modeling . . . 160
10.2.3 Air Flow Integrated Room Model . . . 163
10.3 Outlook . . . 167

Bibliography **169**

Curriculum Vitae **173**

List of Figures

1.1 Resistance network according to DIN 4715-1 [7] . . . 4
1.2 Resistance network according to EN 15377-1 [5] . . . 6
1.3 CO-simulation - state of the art . . . 8
1.4 Schematic overview of the 2 main parts of the work including the subtasks . 9
1.5 Schematic overview of the development of an enhanced room model . . . 10

2.1 floor plan - test room . . . 11
2.2 Room dimensions; left side: floor plan of the measurement room; right sight: section view of the measurement room . . . 12
2.3 schematic section of the two façade types; left side: single skin façade; right side: single storey double skin façade . . . 13

2.4 Schematic overview of the refrigeration supply; there a 2 chillers in the situated in the cellar each of 2900 kW 15
2.5 Pictures of the cooling ceiling 16
2.6 Schematic overview of the cooling system of the room, the location of the cooling ceiling is highlighted; the dark blue area represents the active cooling area in the room zone; the light blue area represents the active cooling area in the façade zone 16
2.7 active cooling area - room area; the active cooling area is 5.56 m^2 17
2.8 active cooling area - façade area; the active cooling area is 3.19 m^2 17
2.9 schematic overview - additional cooling element 18
2.10 schematic overview - additional cooling element 18
2.11 schematic overview of the ventilation system 20
2.12 schematic overview of the ventilation system of the measurement rooms . . . 20
2.13 Measurement equipment of the test rooms 22
2.14 Photo of the measurement of the air temperature and the humidity; LinPicco; no direct radiation on the sensor 23
2.15 Measurement points for the measurement of the air temperature and the humidity within the rooms 24
2.16 Measurement results for the air temperature in room 03 24
2.17 Measurement results for the air temperature in the area of the feet; room 02: LP18 and room 03: LP13 25
2.18 Measurement results for the air temperature in room 03 25
2.19 Pictures of the measurement of operative temperature; in the picture it is seen that the measurement was done with black balls (PT1000 sensors inside; diameter of 100 mm) in 3 depths of the room 26
2.20 Measurement operative temperature, where PT are the temperature sensors (PT1000) of the air temperatures 27
2.21 Measurement operative temperature, where PT are the temperature sensors (PT1000) of the air temperatures 27
2.22 Pictures of the flow / return temperature measurement 28
2.23 Measurement positioning flow / return temperature; the blue points mark the measurement positions; in total 10 sensors were available and the positions for the temperature measurements for the flow and return temperature were changed 28
2.24 Overview of cooling ceiling sections regarding mass flow of the cooling medium 29

2.25 Result of the measurement of the mass flow 29
2.26 Picture of the supply air outlet next to the façade 30
2.27 Measurement supply air temperature - positioning 31
2.28 Measurement results on the supply air temperature 31
2.29 Pictures of the comfort measurement; the measurements were carried out in the room on the basis of a grid; for each room set up 12 measurements were carried to evaluated the comfort 33
2.30 Schematic overview of the four room zones due to comfort measurements . . 33
2.31 Schematic overview of the tree different height of the measurement points for the measurements due to comfort; the heights represent the comfort near the feet (0.30 m), the comfort in the area of the head for sitting person (1.20 m) and the area of the head for a standing person (1.80 m 34
2.32 Measurement results - draught rate in % for the single storey double skin façade; the point in the diagram refer to the schematic overview of the measurement points in the floor plan (2.30) and the section of the measurement points (2.31); 1/3 means left side of the room, next to the façade in a height of 1.8 m 35
2.33 Measurement results - draught rate in % for the single skin façade; the point in the diagram refer to the schematic overview of the measurement points in the floor plan (2.30) and the section of the measurement points (2.31); 1/3 means left side of the room, next to the façade in a height of 1.8 m 35
2.34 Measurement results - draught rate in percentage for one week; comparison of the draught rate due to the additional cooling element, the red points how the measurement results without cooling elements, the orange ones the results with cooling elements; both measurements were done at point 1/2 which means 1.5 m from the façade and in a height of 1.2 m above the floor 36
2.35 measurement points for the measurement of the heat flow; th orang points are measurement points on the ceiling, the red ones those on the floor; with each measurement point two temperatures were taken - the air temperature (light green pints) and the surface temperature (dark green points) 37
2.36 Picture of the measurement of the intensity of illumination 38
2.37 Sensor location of the light meters; 2 meters are situated in room 01 - one in the middle of the room and the other one 1m from the entrance; 1 meter is situated in room 02 - 1m from the entrance 39

2.38 Measurement results of the light intensity for room 01 (LX1) and room 02 (LX2); both 1 m from the entrance of the room 39
2.39 Position of the radiation meters, one after the first glazing (PY1) and the second meter 1m from the façade (PY2) in room 03 - to measure incident radiation through the whole façade system 40
2.40 Measurement results - incident solar radiation; the yellow line represents the results for the measurement after the first glazing; the brown curve represents the measurement results of the incident radiation 1 m from the façade in room 03; the façade system referring to the measurement results is single storey double skin façade and fully closed shading elements 41
2.41 Pictures of the CO_2 meters; from left to right side: room, floor, ceiling, façade 42
2.42 Measurement set up – floor plan (left side) and section (right side) including the sensor numbers, where the first 4 numbers are the maximum concentration rate and the last 2 are the numbers are the unique sensor identification numbers 43

3.1 measurement points for operative temperature; left side: floor plan of the measurement rooms; right sight: section view; the red points mark the sensor positions 47
3.2 floor plan - test room 48
3.3 Visualization of the room types by section views; room type 0: single skin façade shading system 1 (screen type 1); room type 2 single skin façade, shading system 2 (screen type 2); room type 2: single storey double skin façade, shading system 2; room type 3: single skin façade, shading system 3 (blinds); room type 4: single storey double skin façade, shading system 3; room type 5: single skin façade, shading system 2, additional cooling elements; room type 6: single storey double skin façade, shading system 2, additional cooling elements 49
3.4 Comparison operative temperature test room and reference room - centre of the room 52
3.5 Comparison operative temperature test room and reference room - 1 m distance to the façade 52
3.6 Operative temperature next to the façade; façade: single skin façade; shading system fully closed; the colours in the diagram are referring to 3.2 53

3.7 Operative temperature in the centre of the room ; façade: single skin façade; shading system fully closed; the colours in the diagram are referring to 3.2 . . 53
3.8 Operative temperature next to the façade; façade: single skin façade; shading system half opened; the colours in the diagram are referring to 3.2 54
3.9 Operative temperature in the centre of the room ; façade: single skin façade; shading system is half opened; the colours in the diagram are referring to 3.2 55
3.10 Operative temperature next to the façade; façade: single storey double skin façade; shading system fully closed; the colours in the diagram are referring to 3.2 56
3.11 Operative temperature in the centre of the room ; façade: single storey double skin façade; shading system fully closed; the colours in the diagram are referring to 3.2 56
3.12 Operative temperature next to the façade; façade: single storey double skin façade; shading system half opened; the colours in the diagram are referring to 3.2 58
3.13 Operative temperature in the centre of the room ; façade: single storey double skin façade; shading system is half opened; the colours in the diagram are referring to 3.2 58
3.14 Operative temperature next to the façade; room types: table 3.2); red: fully closed shading elements; orange: half closed shading elements 60
3.15 Operative temperature in the centre of the room room types: table 3.2); red: fully closed shading elements; orange: half closed shading elements 61
3.16 Operative temperature next to the façade for a warm sunny day for 4 room types - room type 0: reference room; room type 2: screen type 2, single storey double skin façade; room type 3: shading type 3, single skin façade; room type 6: shading type 2, single storey double skin façade, additional cooling elements 62
3.17 Summary of measurement results regarding maximum operative temperature (5pm values) for the position next to the façade for the different room types for the second summer period 63
3.18 Operative temperature - centre of the room 64
3.19 Summary of measurement results regarding maximum operative temperature (5pm values) for the centre of the room for the different room types for the second summer period 65
3.20 Measurement results on operative temperature - centre of the room 66

3.21 Measurement results on operative temperature - 1 m distance to the façade . 67

4.1 Schema of the cooling ceiling in the test rooms; left side - floor plan; right side - section view; the cooling ceiling is divided into two parts - the room area (dark blue) and the façade area (light blue); these two parts are arranged overlapping to increase the cooling capacity next to the façade 70
4.2 Schema of the cooling ceiling in the test rooms; left side - floor plan; right side section view; the blue points mark the measurement points of the flow and return temperature of the cooling medium; the red points mark the measurement position of the operative temperature 71
4.3 Measurement results for the cooling capacity of the cooling ceiling for room type 1 (single skin façade, shading type 2 (screen)); the dots represent the measurement results, the line is the resulting approximation; the values are referring to the active cooling area and not the floor area. 72
4.4 Measurement results for the cooling capacity of the cooling ceiling for room type 3 (single skin façade, shading type 3 (blinds)); the dots represent the measurement results, the line is the resulting approximation; the values are referring to the active cooling area and not the floor area. 73
4.5 Measurement results for the cooling capacity of the cooling ceiling for room type 5 (single skin façade, shading type 2 (screen) plus additional cooling elements next to the façade); the dots represent the measurement results, the line is the resulting approximation; the values are referring to the active cooling area and not the floor area. 74
4.6 Measurement results for the cooling capacity of the cooling ceiling for room type 2 (single storey double skin façade, shading type 2 (screen)); the dots represent the measurement results, the line is the resulting approximation; the values are referring to the active cooling area and not the floor area. . . . 75
4.7 Measurement results for the cooling capacity of the cooling ceiling for room type 4 (single storey double skin façade, shading type 3 (blinds)); the dots represent the measurement results, the line is the resulting approximation; the values are referring to the active cooling area and not the floor area. . . . 76

4.8 Measurement results for the cooling capacity of the cooling ceiling for room type 6 (single storey double skin façade, shading type 2 (screen) plus additional cooling elements next to the façade); the dots represent the measurement results, the line is the resulting approximation; the values are referring to the active cooling area and not the floor area. 77
4.9 Measurement results for the cooling capacity of the cooling ceiling for room type 2 (single storey double skin façade, shading type 2 (screen)); the dots represent the measurement results, the line is the resulting approximation; the values are referring to the active cooling area and not the floor area. . . . 78
4.10 Measurement results for the cooling capacity of the cooling ceiling for room type 3 (single skin façade, shading type 3 (blinds)); the dots represent the measurement results, the line is the resulting approximation; the values are referring to the active cooling area and not the floor area. 79
4.11 Measurement results for the cooling capacity of the cooling ceiling for room type 6 (single storey double skin façade, shading type 2 (screen) plus additional cooling elements next to the façade); the dots represent the measurement results, the line is the resulting approximation; the values are referring to the active cooling area and not the floor area. 80
4.12 Measurement results regarding the change from single skin façade to single storey double skin façade; the measurement results are taken from room 01 . 81
4.13 Measurement results regarding the change from single skin façade to single storey double skin façade for all room types; room 01: room type 1 and 2; room 02: room type 3 and 4; room 03: room type 5 and 6 82
4.14 Difference on cooling capacity due to the change from single skin façade (left side) to single storey double skin façade (right side); dotted lines: results cloudy days; continuous lines: results clear days 82
4.15 Comparison of the cooling capacity of different room types 83

5.1 Floor plan (left side) / section (right side); location of tracer gas injection is highlighted; floor plan: direct injection to the room (1); concrete ceiling (2) cooling ceiling (3); supply air area (4); façade area (5) 86
5.2 Measurement set up – floor plan (left side) and section (right side) including the sensor numbers, where the first 4 numbers are the maximum concentration rate and the last 2 are the numbers referring to the evaluation diagrams . 88

5.3 Schematic overview of the four different room types; from left to right: single skin façade+closed suspended cooling ceiling; single skin façade+open suspended cooling ceiling, single storey double skin façade+closed suspended cooling ceiling; single storey double skin façade+open suspended cooling ceiling 89
5.4 Schematic overview of measurement points and colours referring to the results in figure 5.5 91
5.5 Measurement result of CO_2 concentration a different location in the room with the impact in the room for room type 4, the numbers shown in the legend are referring to the numbers of the sensor (last two numbers in fig 2). The diagrams show that there is no big difference in concentration within the defined zones. 92
5.6 Measurement result of CO_2 concentration by different impact location for room type 4 (dskin+openc); with solar radiation; measurement period 1 hour for each variant; different concentrations in the specified areas within the first 10 minutes, after the first 10 minutes the concentration is equal in each area independent of the impact location 93
5.7 Measurement results of CO_2 concentration for the different room types with solar radiation, the tracer gas injection directly into the room (floor area). The diagram shows an increase of concentration in the ceiling area due to the single stores double skin façade and a decrease due to the lack of natural ventilation for the cases with the closed suspended ceiling. 94
5.8 Measurement results of CO_2 concentration for the different room types without solar radiation, the tracer gas injection directly into the room (floor area). The diagram shows that there is almost no difference of concentration between the room types. 95

6.1 Schematic overview - room model 98
6.2 Influences on the energy balance of a zone 99
6.3 Schematic illustration of the layer based model for dividing components (e.g. walls between zones) 101
6.4 Schematic illustration of the heat flow though a layer 102
6.5 schematic illustration of the heat flow of the outside construction layer 104
6.6 Schematic illustration of the heat flow from the outside construction layer . . 107
6.7 schematic illustration of the heat flow for the inside construction layer 108

6.8 Schematic overview the cooling ceiling construction and its thermal design values according to the description done in Glück (2003) [23] 109
6.9 Summary of input values and calculation scheme for the cooling ceiling . . . 110

7.1 Simplification of the model geometry from three dimensions to two dimensions 114
7.2 Façade type 1 (left side): single skin façade with internal shading element / façade type 2 (right side): single storey double skin façade with a shading element between the glazing elements 115
7.3 Heat capacity (cp), dynamic viscosity (η) and thermal conductivity (k) in dependence of the temperature in °C 117
7.4 Density (ρ) in dependence of the temperature in K and the pressure in Pa . . 118
7.5 Visualisation of mesh geometry for the simplified modeling (wall functions) for the single storey double skin façade 119
7.6 Comparison of operative temperature and the cooling capacity for façade type 1 (left side) and façade type 2 (right side); the temperature is below 27°C with façade type 2, the cooling capacity is increasing with the increasing solar radiation; with façade type 1 the operative temperature is getting above 27°C and the cooling capacity is lower. 120
7.7 Cooling capacity in dependence of the room depth for façade system 2; temperature difference between mean medium temperature and operative temperature in the room is 9 K 121
7.8 Cooling capacity in dependence of the depth of the room with an incident solar radiation of 800 W/m^2 and a temperature difference of 9 K between the mean medium temperature and the operative temperature in the middle of the room. 121
7.9 Resulting cooling capacity in dependence of the incident solar radiation; the temperature difference between the mean medium temperature and the operative temperature in the middle of the room is 9 K. 122
7.10 Measurement results on operative temperature (left side) and cooling capacity (right side; (M)..measurement; (C)..CFD calculation) – there is a good accordance between the measurement results and the CFD calculation; the difference of operative temperature is about 0.2 K 123
7.11 Visualization of the regarded areas for the velocity study; the colours of the cutting lines are referring to the diagrams 124

7.12 velocity field within the façade area (left diagram) and the ceiling gap (right diagram) for façade system 1 (single skin façade), simulation result for an incident solar radiation of 800 W/m^2 and an external temperature of 32 °C . . 125
7.13 Visualization of the regarded areas for the velocity study; the colours of the cutting lines are referring to the diagrams 125
7.14 velocity field within the façade area (left diagram) and the ceiling gap (right diagram) for façade system 2 - single storey double skin façade, simulation result for an incident solar radiation of 800 W/m^2 and an external temperature of 32 °C 126
7.15 Air distribution for the two façade systems for an incident radiation of 800 W/m^2; left side: single skin façade; right side: single storey double skin façade126
7.16 Design Day - external temperature and solar radiation 127
7.17 Simulation results regarding the mean velocity in the considered areas for the design day for façade system 1 - single skin façade; results regarding the façade: v_mean_fas(fs1); results regarding the ceiling: v_mean_ceil(fs1) 128
7.18 Simulation results regarding the mean velocity in the considered areas for the design day for façade system 2 - single storey double skin façade; results regarding the façade: v_mean_fas(fs2); results regarding the ceiling: v_mean_ceil(fs2) 129
7.19 Comparison of the velocity - thermal calculation (velocity is calculated from the convective heat flow due the temperature difference air temperature and surface temperature; left side - façade area; right side - ceiling area) 129

8.1 schematic overview of the **room model**; the main parts of the model are highlighted - room, enclosing surfaces, façade/façade types/shading control; cooling ceiling; ventilation; internal heat gains; geometry; input and output . . 132
8.2 schematic overview of the model part - **zone**; summary of the various input parameters like geometry (grey frame), the calculation of the components (turquoise frame), the internal loads (red frame), the ventilation (violet frame), the calculation of the cooling ceiling (light blue frame) and the radiation (yellow frame); Output: resulting temperatures (blue frame) 133
8.3 schematic overview of the model part - **geometry**; overview of the geometric input and calculated output parameters 134

8.4 schematic overview of the façade types, the colours refer to the model components in figure 8.5; the air flow for the different façade types is highlighted with the violet arrows 137
8.5 schematic overview of the model part - **façade type**; the picture show the façade type: single storey double skin façade plus shading; the red lines mark the calculation of the layers - the layers were adjusted to the façade type; the green field mark the integration of the air flow 138
8.6 schematic overview of the model part - **control façade and shading system**; the red field mark the selection of the façade type; the upper switch is for façade type 01 (single skin façade) and the lower switch is for façade type 2 (single storey double skin façade); the marked field on the right side summarize the output 139
8.7 schematic overview of the model part - **partition walls**; 1st red frame (top): inputs coming from zone modeling; 2nd red frame (middle): modules for the layer calculation; 3rd red frame (bottom): link to the input data for the calculation; blue frame: outputs and results of the partition wall calculation . . 140
8.8 schematic overview of the model part - **raised floor**; red frame: thermal calculation of the floor; blue frame: integration / coupling to the ventilation of the room 141
8.9 schematic overview of the model part - **cooling ceiling**; red frame: thermal calculation of the construction layers; blue frames: calculation of the layer ”air”; green frames: integration of the simplified air flow modeling 142
8.10 schematic overview of the model part - **internal gains**; red frame: input values - heat gains due to lights, technical equipment and people; blue frame: control of the internal gains 143
8.11 schematic overview of the model part - **ventilation**; red frame: input of volume flow rate; blue frame: control strategy of ventilation system and supply air temperature 144
8.12 Schematic overview of the model part - **weather**; red frame: input data file; blue frame: output for further calculation; yellow frame: calculation of the radiation on the surface 145

9.1 Comparison of the speed factors - result of the air flow calculation (lines) and output of the air flow integrated room model simulation (dots) for the façade area (red) and the cooling ceiling area (blue) 147

9.2 Comparison of the capacity of the cooling ceiling in dependence of the temperature difference between the mean medium temperature and the operative temperature in the centre of the room; red: calculation results, blue measurement results 148
9.3 Comparison of the measurement results (blue line) and the results of the developed room model (red line) for room type 2; the difference between the measurement results and the simulation results around 5pm is due to the gap between the façade and the screen - direct sun is shining on the black ball meter (see figure 9.4) 149
9.4 Comparison of the measurement results (blue line) and the results of the developed room model (red line) for room type 2 - **explanation of the differences** 149
9.5 simulation results - room type 0 / 1 / 2 / 3 / 5; the simulation results are in a good accordance to the measurement results (see figure 3.20) 150

10.1 Schematic overview of the development of an enhanced room model 153
10.2 Visualization of the room types by section views - summary (detailed description see chapter 2.3.3) 154
10.3 Measurement equipment of the test rooms 155
10.4 Measurement results on operative temperature - centre of the room 156
10.5 Measurement results on operative temperature - 1 m distance to the façade . 157
10.6 Comparison of the cooling capacity of different room types 158
10.7 location of tracer gas injection - summary (detailed description see 2.2) . . . 159
10.8 Measurement results of CO_2 concentration for the different room types with solar radiation, the tracer gas injection directly into the room (floor area). The diagram shows an increase of concentration in the ceiling area due to the single stores double skin façade and a decrease due to the lack of natural ventilation for the cases with the closed suspended ceiling. 160
10.9 Schematic overview - room model 161
10.10 Measurement results on operative temperature (left side) and cooling capacity (right side; (M)..measurement; (C)..CFD calculation) – summary 162
10.11 Air distribution for the two façade systems for an incident radiation of 800 W/m^2; left side: single skin façade; right side: single storey double skin façade 163
10.12 Comparison of the air velocity –> resulting speed factors - summary (detailed description see chapter 7.4.3) 164

10.13schematic overview of the **room model**; the main parts of the model are highlighted - room, enclosing surfaces, façade/façade types/shading control; cooling ceiling; ventilation; internal heat gains; geometry; input and output . . 165
10.14Comparison of the measurement results (blue line) and the results of the developed room model (red line) for room type 2 - summary 166
10.15simulation results - room type 0 / 1 / 2 / 3 / 5; 166

List of Tables

2.1 Summary of active cooling area for each room 19
2.2 Measurement results for the supply air flow for each air outlet 30
2.3 Supply air flow for each air outlet 30

3.1 Summary of the differences regarding optical properties of the tested shading systems 46
3.2 summary measurement variation, room types, where room type 0: single skin façade shading system 1 (screen type 1); room type 2 single skin façade, shading system 2 (screen type 2); room type 2: single storey double skin façade, shading system 2; room type 3: single skin façade, shading system 3 (blinds); room type 4: single storey double skin façade, shading system 3; room type 5: single skin façade, shading system 2, additional cooling elements; room type 6: single storey double skin façade, shading system 2, additional cooling elements 49
3.3 Summary of measurement set up - first measurement period 50
3.4 Summary of measurement set up for the “long term” measurement during the second summer period 51
3.5 Summary of measurement results of the maximum operative temperature in the centre of the room and next to the façade for the first measurement period. The results are for the façade system: single skin façade and the shading system is fully closed 54

3.6 Summary of measurement results of the maximum operative temperature in the centre of the room and next to the façade for the first measurement period. The results are for the façade system: single skin façade and the shading system is half closed 55
3.7 Summary of measurement results of the maximum operative temperature in the centre of the room and next to the façade for the first measurement period. The results are for the façade system: single storey double skin façade and the shading system is fully closed 57
3.8 Summary of measurement results of the maximum operative temperature in the centre of the room and next to the façade for the first measurement period. The results are for the façade system: single storey double skin façade and the shading system is half closed 59
3.9 Maximum operative temperature (5pm) next to the façade for three different days during the second summer period measurement for 4 room types - room type 0: reference room; room type 2: screen type 2, single storey double skin façade; room type 3: shading type 3, single skin façade; room type 6: shading type 2, single storey double skin façade, additional cooling elements 62
3.10 Maximum operative temperature (5pm) in the centre of the room for three different days during the second summer period measurement for 4 room types - room type 0: reference room; room type 2: screen type 2, single storey double skin façade; room type 3: shading type 3, single skin façade; room type 6: shading type 2, single storey double skin façade, additional cooling elements 64
3.11 Summary of measurement results of the maximum operative temperature in the centre of the room 66
3.12 Summary of measurement results of the maximum operative temperature next to the façade 67

4.1 summary measurement variation, room types (detailed description see chapter 3 in section 3.2.2) 71
4.2 Summary measurement variation, room types (detailed description see chapter 3 in section 3.2.2) 83

5.1 Overview of the measurement variants 90

7.1 Summary of the room / model dimensions taken for the 2D air flow model of the room . . . 115
7.2 Summary of the technical data for the façade systems, single skin façade: column 2 and 3; single storey double skin façade: coloum 2, 3 and 4 . . . 116
7.3 Summary of the temperatures of the surrounding surfaces for the basic simulation with an solar radiation of 800 W/m^2 . . . 116
7.4 Summary of the material data - input values for the air flow calculation . . . 117
7.5 Summary of the surface emissivity for the different material within the room . 118
7.6 Solver settings . . . 119
7.7 Summary of the temperature range for the surrounding surfaces for the design day simulation . . . 127

8.1 Summary of the geometric input parameters . . . 134
8.2 Summary of the geometric output data . . . 135
8.3 Summary of the differences regarding optical properties of the tested shading systems . . . 136

9.1 Summary of boundary conditions referring to figure 9.5 . . . 150

10.1 measurement variation, room types - summary (detailed description see chapter 2.3.3) . . . 155
10.2 Summary of measurement results of the maximum operative temperature in the centre of the room . . . 156
10.3 Summary of measurement results of the maximum operative temperature next to the façade . . . 157

1 Basic Information and Motivation

1.1 Motivation

In the field of energy efficient buildings massive changes due to building standards took place over the last 10 years. At the moment the goal is to develop plus energy buildings (residential and non-residential) and the vision is to build plus energy districts and cities.

Necessary aspects such as energy efficient devices, avoidance of stand-by losses, reduction of losses due to building service systems, highly efficient delivery systems, innovative façade systems and components with integrated energy supply by photovoltaic or solar thermal are the focus of current research topics in this field.The research and development in the field of sustainable design led to improvement in methods, the design process and products.

The calculation or prediction of the thermal comfort in the common areas of buildings plays a key role and at the moment it cannot be fully implemented. In the completeness complex flow processes in closed and open façades, the dynamic of building elements' performance in combination with the control system which should guarantee a flexible usage of rooms are a great, so far unresolved challenge.

One of the key influence factor on comfort is the air velocity in the occupational area. The aim of this research is to develop a mathematical model that rebuilds the necessary detail of the calculation focusing on the effect of air flow on the capacity of cooling ceilings and the comfort in the room. The calculation should include the interaction of complex façade systems and the rooms' ventilation and cooling system.

The vision is, to provide an easy to handle planing support tool that takes into account the different influencing parameters regarding the resulting room conditions and therefore the comfort in the room. One of the requirements for the use of design tools also in an early planing phase is, that they need to be fast and flexible.

1.2 State of the art

At the moment there are detailed studies for the different disciplines like on the building physics part (especially façades) and on the building service systems part (e.g. cooling ceilings). The interaction of the different disciplines is known by now but not well investigated by now. One of the results of the work of Fonseca (2011) [21] which describes the modeling of a hydronic ceiling system is, that the influence of the façade needs to be considered.

The following sections give an overview on studies regarding the modeling of façade systems and on activated building elements. Furthermore the implementation in dominant building simulation programs like TRNSYS, Energy Plus, ESP-r and IDA Ice is discussed.

1.2.1 Studies on façade system

Regarding façade systems there are detailed studies investigating the topic of the efficiency of façade systems and the influence on the building like the review on solar façades (Quesada et al. 2012) [38] or the effect of multi skin façades on the energy demand of Radhi et al. (2013) [39]. The effect of façade systems on the energy demand are also part of the work of Hamza (2008) [27] where double skin façades are compared to single skin façades. The focus within this study is set on hot and arid regions. The details of double skin façades are discussed in Hien (2005) [29] and Shameri et al. (2011) [42].

Details on energy efficiency of glazing and shading systems regarding design, physical properties and economy can be found in Wagner (2007) [52].

Mathematical models for the detailed calculation of façades system are developed amongst others the work of Ghadamian et al. [22] which describes the analytical solution for energy modeling of double skin façades.

Most of the existing models are for external double skin façades, this work deals with the effect of single storey double skin façade (internal) on the HVAC system and the comfort within the room. The diving force of the natural ventilated single storey double skin façade is natural buoyancy, therefore the air flow is not easy to control and the dependence on weather conditions (mainly solar radiation) makes it discontinuous.

1.2.2 Studies on activated building element

Detailed studies of the behaviour and efficiency of cooling ceilings and the impact on the room, like the work of Causone et al. (2009) [16] which describes the experimental

evaluation of heat transfer coefficients between radiant ceiling and room or the experimental evaluation of the cooling capacity like it is done in Chictote et al. (2012) [15] are existing.

The description of the thermal behaviour of cooling ceilings is done by Beck (2002). Detailed descriptions of the heat transfer coefficients of cooling ceilings are made by the work of Bernd Glück in (Glück, 1999 [25] and 2003 [23]). The book TABS Control (Tödtli et al., 2009 [49]) gives a good summary and overview about possible control strategies for energy efficient operation of thermal activated building elements.

The study of Fonseca (2011) [21] worked out, that mathematical models of cooling ceilings were developed as stand-alone tools to evaluate their performance under test bed conditions. These models does not take into account influencing factors like buoyancy regarding to different façade systems and cannot be used to make reliable predictions regarding room conditions and comfort within the room.

1.2.3 ”Dominant” Building Energy Programs

TRNSYS

TRNSYS is a transient simulation software tool developed in 1975, it is a modular structured program, where components are described by different so called ”types” and there is a graphical interface (TRNSYS simulation studio) to link the different types together.

According to the program documentation [44] and the mathematical reference [45] the modeling of a cooling ceiling panel is done by integrating an active layer to the construction within the building description. The German standard DIN 4715-1 [7] for chilled ceiling panels is the basis for the model. Parameters like pipe spacing, inside diameter and specific heat coefficient of fluid have to be defined, additional values (specific norm power, specific norm mass flow rate, norm area and norm number of loops) for the definition of the performance at test conditions after the German norm DIN 4715-1 [7] for the chilled ceiling panel are needed. The German standard DIN 4715-1 [7] has been replaced by the DIN EN 14240 [4].

The division of the radiative norm power into a radiative and a convective part is normally done by the knowledge of the mean surface temperature $t_{o,kd}$. According to DIN 4715-1 [7] the mean fluid temperature t_W is the standard output for a cooling ceiling panel. To get a heat transfer coefficient $U_{w}rx$ the resistance network at test conditions is calculated by the given input. In figure 1.1 the resistance model for chilled ceiling test conditions after DIN 4715-1 [7] is shown.

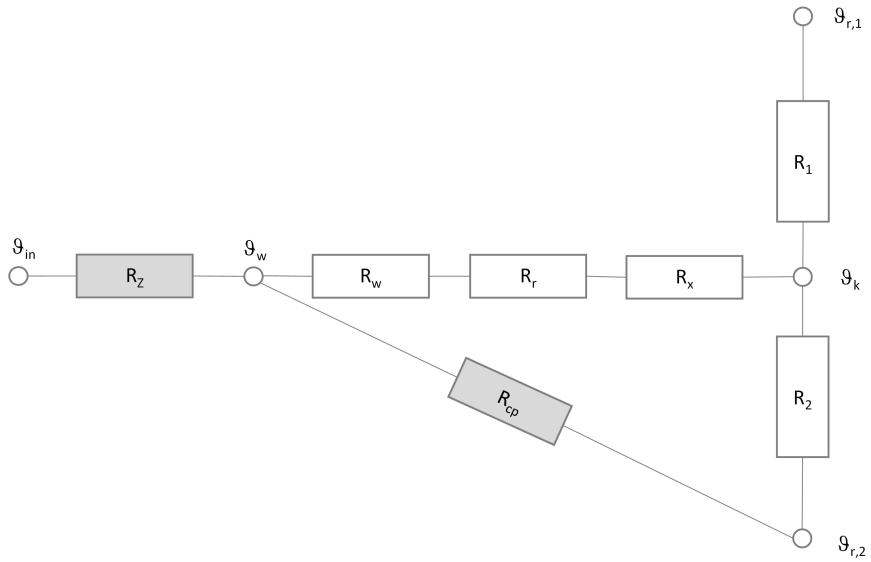

Figure 1.1: Resistance network according to DIN 4715-1 [7]

where

R_w ... thermal resistance fluid to pipe in $(m^2\ K)/W$

R_r ... thermal resistance pipe in $(m^2\ K)/W$

R_x ... thermal resistance in x-direction in $(m^2\ K)/W$

R_{cp} ... thermal resistance of chilled ceiling panel at test conditions in $(m^2\ K)/W$

R_1 ... thermal resistance upper wall at test conditions well insulated in $(m^2\ K)/W$

R_2 ... thermal resistance combined heat transfer to the room in $(m^2\ K)/W$

ϑ_w ... mean fluid temperature in °C

ϑ_k ... mean temperature of chilled ceiling in °C

$\vartheta_{r,2}$ ... operative temperature room in °C

$\vartheta_{r,1}$ ... operative outside temperature in °C

The resulting heat transfer coefficient is calculated according to equation 1.1

$$U_{wrx} = 0.6 \quad \exp\left(\frac{0.0469 \quad P_{sp_norm}}{3.6}\right) \tag{1.1}$$

where

U_{wrx} ... heat transfer coefficient in $kJ/(h\ m^2\ K)$

P_{sp_norm} ... specific norm power after DIN 4715-1 [7] in $kJ/(h\ m^2)$

The details regarding the calculation can be found in the TRNSYS documentation Volume 5 - Multizone Building modeling with Type56 and TRNBuild [43].

The test according to DIN 4715-1 [7] is useful to compare different types of chilled ceiling elements, but it is not taking influences of HVAC systems (like ventilation) or

different effects due to façade systems into account. Furthermore it is considered that the load distribution is homogeneous.

Energy Plus

The development of the Energy Plus program started in 1996, actually there were developed two software tools - first DOE-2 and second BLAST - both were supported by the department of Energy (DOE) from the United States of America. The Energy Plus program [36] combines these two tools

The modeling of active elements is done by electric resistance wires embedded in a component. The calculation of cooling ceilings is done according to the description done by Karadag (2009) [31] , for active ceiling components this model is selected as default by Energy Plus. In the work of Karadag (2009) [31] the development of radiative and convective heat transfer coefficients for cooling ceilings are described. The convective part is simulated numerically first (by ignoring the radiative part), the radiative part is calculated theoretically for different surface emissivities, room dimensions and thermal conditions in a second step. Out of this studies new equations regarding the convective and the total heat transfer coefficients for cooling ceilings were developed. The resulting equation for the heat transfer coefficient for cooling ceilings is shown in equation 1.2

$$h_c = 3.1\ \Delta T^{0.22} \tag{1.2}$$

where

h_c ... surface exterior convective heat transfer coefficient in $W/(m^2\ K)$

ΔT ... temperature difference between surface temperature and air temperature in K

For the calculation it is considered as a stationary building element and that the temperature (medium + surface) is constant.

IDA ICE

The program IDA Indoor Climate and Energy (IDA ICE) is a thermal simulation tool based on a modular system which was developed since the early 90's. The main focus of the program is whole year detailed and dynamic multi-zone simulation of indoor climate and energy demand. For the calculation of active building elements the program provides the "Slab Cooling and Heating" extension.

According to the program documentation if IDA ICE [13] the cooling ceiling object is inserted on the ceiling of a zone by dividing the construction into two parts. The calculation is done by a heat exchanger model which is corresponding to the piping layer.

The active layer can be treated as an infinitely conductive plane within the ceiling, which means all 2D effects are not considered. The heat transfer is calculated by a logarithmic temperature difference between the fluid and the active layer (which has a constant temperature). The total heat transfer coefficients are an user defined input and includes:

- Convection between medium and tube wall
- Heat conduction through the tube walls
- "Fin efficiency" corresponding to the distance between immersed tubes or actual fins

For the steady state case the modeling is done according to the resistance method of the standard EN 15377-1 [5]. The schematic overview of the method is shown in figure 1.2 the calculation details can be found in the standard EN 15377-1 [5]

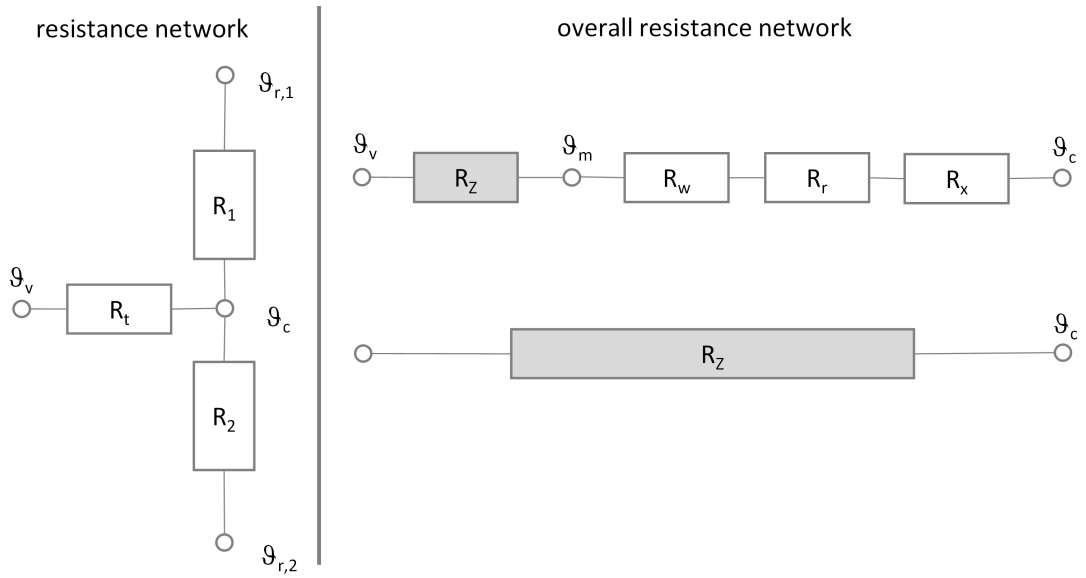

Figure 1.2: Resistance network according to EN 15377-1 [5]

where

R_t	...	thermal resistance between supply temperature and the average temperature of the conductive layer in $(m^2\ K)/W$
R_w	...	thermal resistance fluid to pipe in $(m^2\ K)/W$
R_r	...	thermal resistance pipe in $(m^2\ K)/W$
R_x	...	thermal resistance in x-direction in $(m^2\ K)/W$
R_1	...	thermal resistance upper wall at test conditions well insulated in $(m^2\ K)/W$
R_2	...	thermal resistance combined heat transfer to the room in $(m^2\ K)/W$
ϑ_v	...	supply temperature of cooling medium °C
ϑ_c	...	mean temperature of the conductive medium in °C
ϑ_m	...	mean cooling medium temperature in °C
$\vartheta_{r,2}$	...	operative temperature room in °C
$\vartheta_{r,1}$	...	operative outside temperature in °C

ESP-r

The ESP-r system is a building simulation program as a result of sustained developments since 1974 and it's still ongoing. The main goals are

- describe real-life performance,
- support early design phase of buildings, and
- performance assessments

The way of modeling cooling ceilings in ESP-r is to model the panel as a thin zone bounded by the metal of the panel and with high internal heat transfer coefficients. With the two zone model there is the possibility to extract heat from the room zone. The way of modeling gives a good representation of the radiant and convective heat transfer with the room (depending on the used boundary conditions) but there is no information regarding the fluid temperature.

The review of the program documentations shows that at the moment the interaction between complex facade systems and the capacity of the cooling ceiling is not covered by any of the common building simulation tools. There is the possibility of coupling air flow simulations and thermal simulations tools to close the gap and get reliable results on room conditions and thermal comfort.

1.2.4 Studies on co-Simulation

Due to multiple coupled physical phenomena (air flow, convection, conduction and radiation) the behaviour of double skin façades is very complex. Both, experimental and numerical models for the optimization of the performance of double skin façades have been developed e.g. network models (Tanimoto et al., 1997) [48], zonal models (Jiru et al., 2008 [30, vgl.]), energy simulation with coupled air flow models (Stec et al. 2005) [47] and detailed computational fluid dynamics studies (Manz, 2005) [35].

Currently, all linked methods of flow-, radiation- and building element simulation are very time intensive the calculation scheme follows the illustration in figure 1.3. The aim of this work is to develop an approximation that provides a sufficiently accurate picture of the influence of three-dimensional flow phenomena in rooms on the heat and mass flow at surfaces for low flow-rates.

1.2.5 Conclusio State of the Art

The literature review shows, that non of the discussed (mostly used) building energy programs (TRNSYS, Energy Plus, IdaIce and ESP-r) can simulate the interaction of complex façade systems and cooling ceilings with the required level of detail. Although there are "work-arounds" if specific parameters are known. For example in ESP-r it

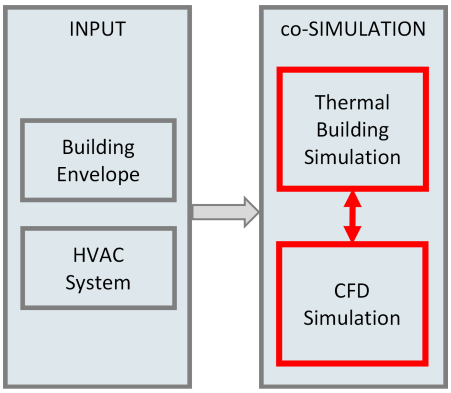

Figure 1.3: CO-simulation - state of the art

is possible to integrate a simplified air flow modeling by mass balances, which allows to describe the effect of buoyancy in dependence of façade systems and the cooling ceiling within the model if they are defined by a second party tool.

There is the possibility of doing coupled air flow and thermal simulations to get reliable results on room conditions and thermal comfort. These simulations are very time consuming at the moment and therefore not appropriate for the use of early planing phase support.

1.3 Hypotheses

The focus of the dissertation is set on the cooling of buildings the behaviour of cooling ceilings in interaction with complex façade systems should be described by a mathematical model. To achieve the goal of energy efficient buildings, zero emission buildings or energy active buildings there is the need of new and in some parts complex building concepts. For the acceptance and success of new concepts the comfort for users compared to conventional systems should have a significant improvement, at least it should not get lower. This makes it no longer possible to separate the civil engineering and building physics design from the service systems design of a building.

The cooling ceiling is a system which guarantees high comfort because of the high proportion of radiation, but with the current office building standard the limit of the capacity is reached. Due to the combination of high glass content and high internal heat gains and the rising share of engineering (architecture and user comfort due to electrical equipment) the cooling capacity is not sufficient. Within the work studies on increasing the cooling capacity of a cooling ceiling with different façade systems should be discussed.

The goal of the work is to develop a mathematical model as a first step for an easy to handle design tool that can predict comfort in room for different building concepts. The

key issue is the integration of a simplified model of complex flow phenomena within the room.

According to Feist (1994) [20] mathematical modeling and measurement have different functions in a process of understanding and complement each other. Neither can the mathematical modeling make measurements completely unnecessary (measurement are the only way for the validation of modeling) - nor is it feasible and reasonable to want to answer any questions by measurements (generalizable statements are limited by finitely amount of measurement variants and cannot be done).

Therefore the work is divided in two main parts (see figure 1.4), on the one hand there are in-situ measurements in an existing office building for

- temperatures (air, surface and operative),
- humidity,
- capacity of the cooling ceiling and
- air flow measurements done by tracer gas measurements.

Measurements on comfort with comfort level probes are carried out too. On the other hand there is the part of the mathematical modeling, which is divided into 3 subtasks itself

- the thermal modeling,
- the air flow modeling and the combination of these two model parts
- the development of the air flow integrated room model

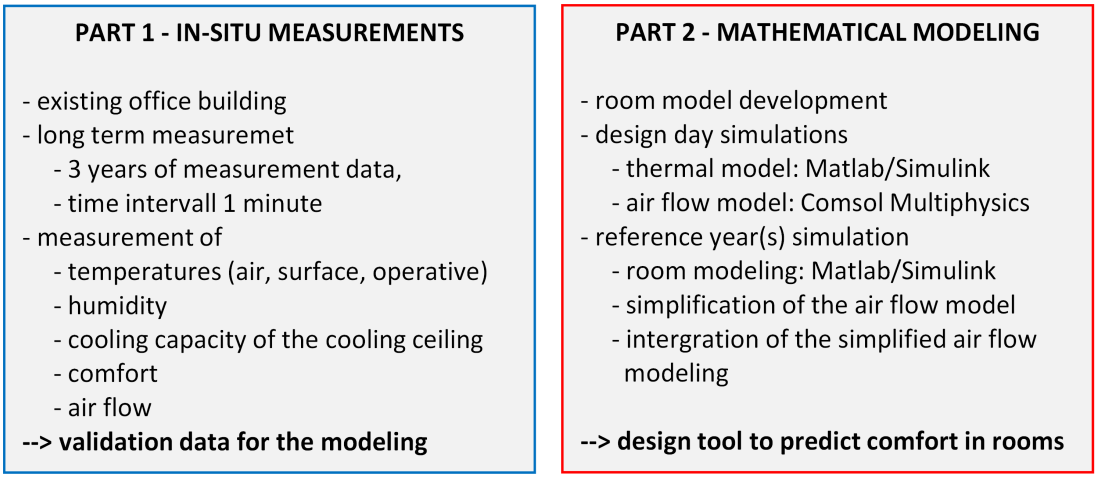

Figure 1.4: Schematic overview of the 2 main parts of the work including the subtasks

In figure 1.5 the schematic overview of the development of the room model is shown. The grey marked area includes the input data which are the building informations like the envelope, but also the geometric data and the information regarding the HVAC system, in this case it is the information regarding the cooling ceiling (mass flow, flow and return temperature and active cooling area).

The blue marked area refers to the measurement results taken from the in-situ measurements, they were used for the validation of the mathematical model in different steps of the model development. The main measurement results which were compared are the operative temperature in the room, the capacity of the cooling ceiling and the measurement results on the air distribution in within the room.

The red area in the figure represents the modeling part. To keep the model simple and as fast as possible and needed for the planning phase of a building the idea is to make a design day simulation part to define inputs for the reference year(s) simulation part. The design day simulation can be a coupled thermal and air flow simulation that provides information of the interaction between building elements and building service systems. For example an output could be the capacity of the cooling ceiling in dependence of the solar radiance and the room conditions or the air velocity within different room areas regarding different façade systems.

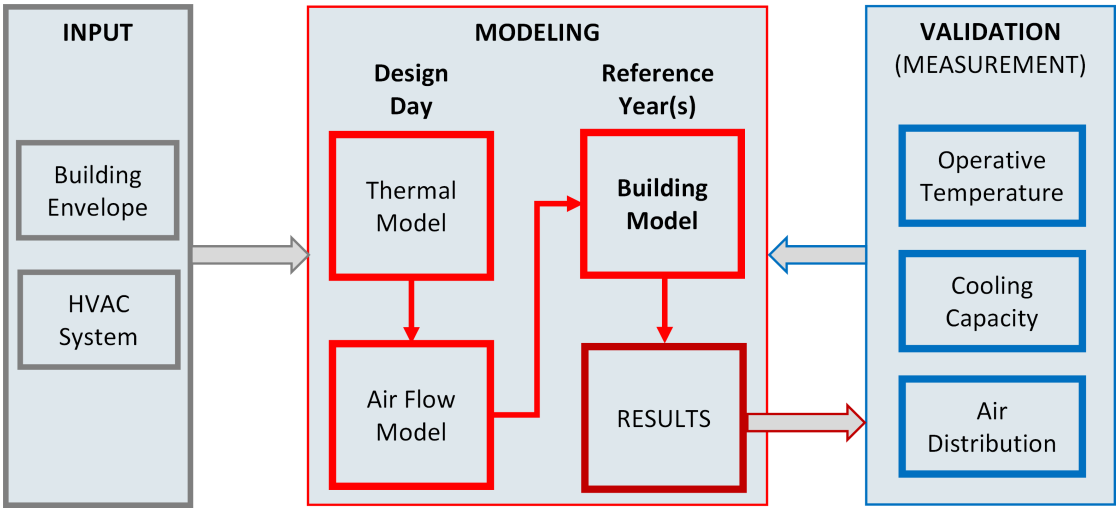

Figure 1.5: Schematic overview of the development of an enhanced room model

The development of the air flow integrated room model is an interactive work between different mathematical model parts (thermal modeling, air flow modeling) and measurement results to validate the model parts and the final room model.

2 Description of Measurement Set-up

2.1 Introduction

According to Feist (1994) [20] the reliable measurement of building physical parameters is a challenge in itself: the basic for correct measurement results of the room air temperatures is a good knowledge of the theory (sensor screening against radiation, time constant of the sensor, self-heating, long-term stability, ...). Consumption measurements are often based on the volume or flow rate measurement. Volume flow measuring devices often have start-up volume flows, below which they do not run or at least they have an extremely inaccuracy. Such aspects have to be considered carefully when doing measurements. A reliance on measured values is therefore justified only if you know exactly what was measured.

2.2 Building / Room Set up

A series of measurements have been done in an existing office building with different room set ups (different façade systems due to the combination of glazing and shading and differences on the active cooling area of the room). On the 34th floor there were built 4 identical rooms, each of about 11 m^2. The façade is a west-orientated totally glazed surface, as the rooms are situated on the 34th floor, there is no shading due to other buildings or geographical surroundings. The floor plan of the tested rooms is shown in figure 2.1. The configuration of the test rooms is typical for single person offices in Austria.

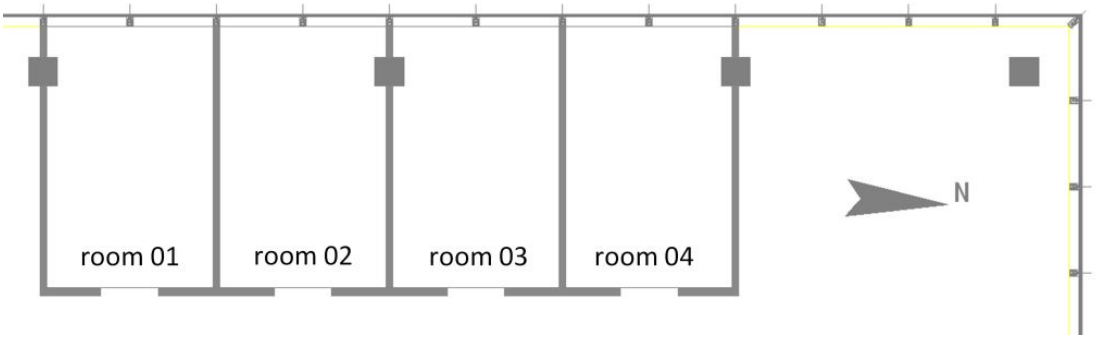

Figure 2.1: floor plan - test room

In figure 2.2 the dimensions of the room are visualized. On the left side there is the floor plan for one room with a room depth of 4.10 m and a width of 2.6 m. On the right side the section view is shown, the main heights are marked. The room height is 2.8 m the occupied area of the room, the height in the façade area is 3.0 m, the floor height is

3.5 m. The test rooms are adjacent and are separated by a gypsum plasterboard wall. The floor is a raised floor which is caused to it's air leading properties (the supply air is realized over the raised floor) open throughout the whole storey. It's not possible to close the floor, because than the test rooms would be without fresh air. The suspended ceiling of the measurement rooms is separated by a foreclosure (mineral wool) around the rooms and also between these rooms.

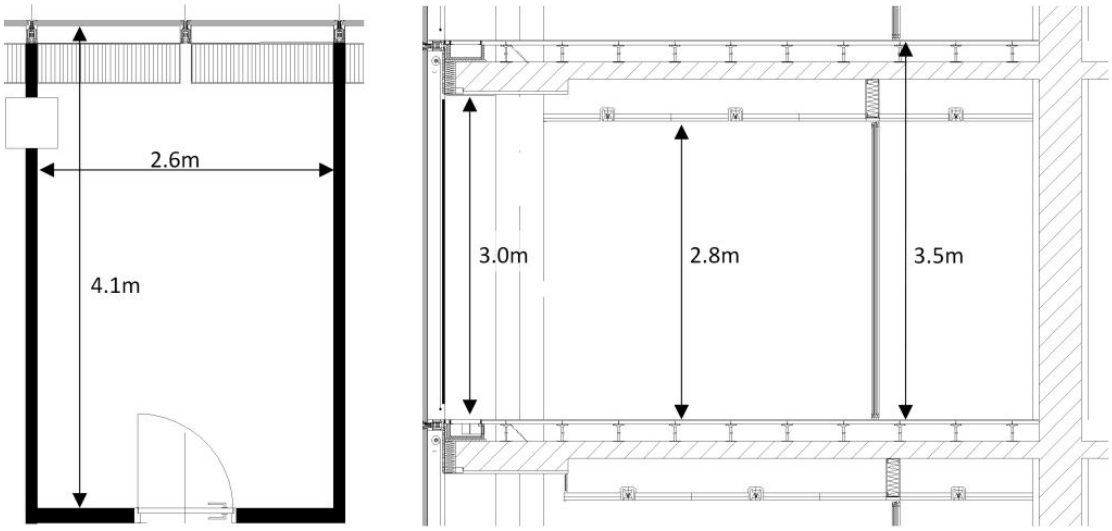

Figure 2.2: Room dimensions; left side: floor plan of the measurement room; right sight: section view of the measurement room

2.2.1 Basic Building Information

The office building is located in Vienna, Austria and it's a tower with a fully glazed façade. The U-Value of the room envelope:

- glazing: U = 1.10 $W/(m^2\ K)$
- frame (percentage 8 %): U = 2.95 $W/(m^2\ K)$
- ceiling / floor: U = 1.45 $W/(m^2\ K)$
- Interior wall (gypsum cardboard): U = 0.65 $W/(m^2\ K)$
- interior door: U = 1.80 $W/(m^2\ K)$

Within the building there is the possibility to test different façade systems by changing the shading element and due to the possible change from single skin façade to single storey double skin façade.

2.2.2 Façade System

Four rooms were realized for the measurements, one of them was used as a reference room, which means that the conditions in this room were not changed during the whole measurement time. The basic set up is a single skin façade and a fully closed screen

(shading system 1). The technical data of the shading system (reference room – type 1) is:

- solar transmittance: τ = 0.19
- reflectance: ρ = 0.37
- absorptance: α = 0.44
- light transmittance: τ_L = 0.19

Different façade systems were tested, the schematic overview of the single skin façade and the single storey double skin façade is shown in figure 2.3. The following bullet list summarize the 5 different façades systems (combination of glazing and shading)

- Façade system 1: single skin façade with internal shading element type 1
- Façade system 2: single skin façade with internal shading element type 2
- Façade system 3: single storey double skin façade with internal shading element type 2
- Façade system 4: single skin façade with internal shading element type 3 (blinds)
- Façade system 5: single storey double skin façade with internal shading element type 3 (blinds)

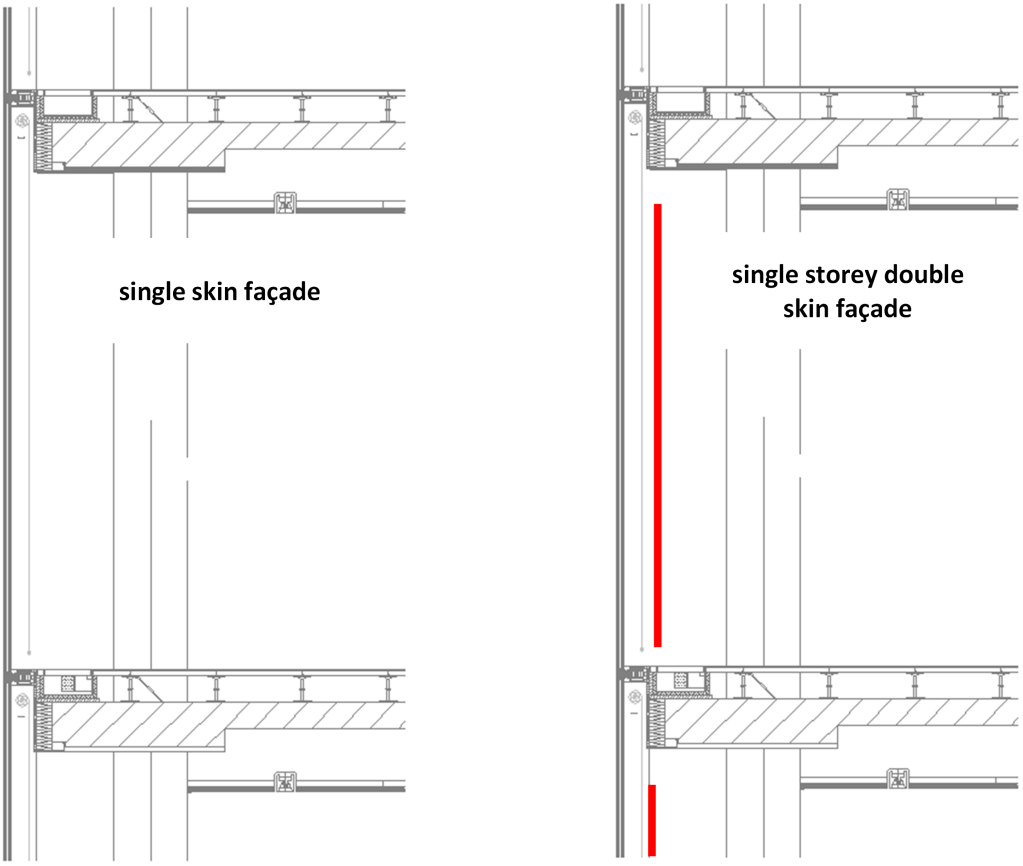

Figure 2.3: schematic section of the two façade types; left side: single skin façade; right side: single storey double skin façade

The technical data for the façade system is described in the following part

Technical data of the outside pane:

- Outside pane: 6 mm coated
- 16mm gap between the panes (argon filled)
- Inside pane 10 mm laminated safety glass
- Total solar energy transmittance: g = 0.35
- Solar transmittance: τ = 0.33
- Reflectance: ρ = 0.41
- Absorptance outside pane: α_c = 0.25
- Absorptance inside pane: α_i = 0.01
- Heat transfer coefficient U = 1.29 $W/(m^2\ K)$

The technical data of the shading system - type 2 (screen) is:

- Solar transmittance: τ = 0.11
- Reflectance: ρ = 0.39
- Absorptance: α = 0.50
- Light transmittance: τ_L = 0.10

The technical data of the shading system - type 3 (blinds) is:

- Solar transmittance: τ = 0.08
- Reflectance: ρ = 0.39
- Absorptance: α = 0.54
- Light transmittance: τ_L = 0.08

The technical data for the 2nd glazing is summarized in the following itemisation

- insulation glass pane
- heat transfer coefficient U = 1.1 $W/(m^2\ K)$

2.2.3 Cooling

Refrigeration Supply

The energy supply is a conventional system. For the cooling of the building there are two chillers, each of 2900 kW and the re-cooling units are situated on the top of the building. The schematic overview of the cooling system for the building for the part of the cooling ceiling is shown in figure 2.4

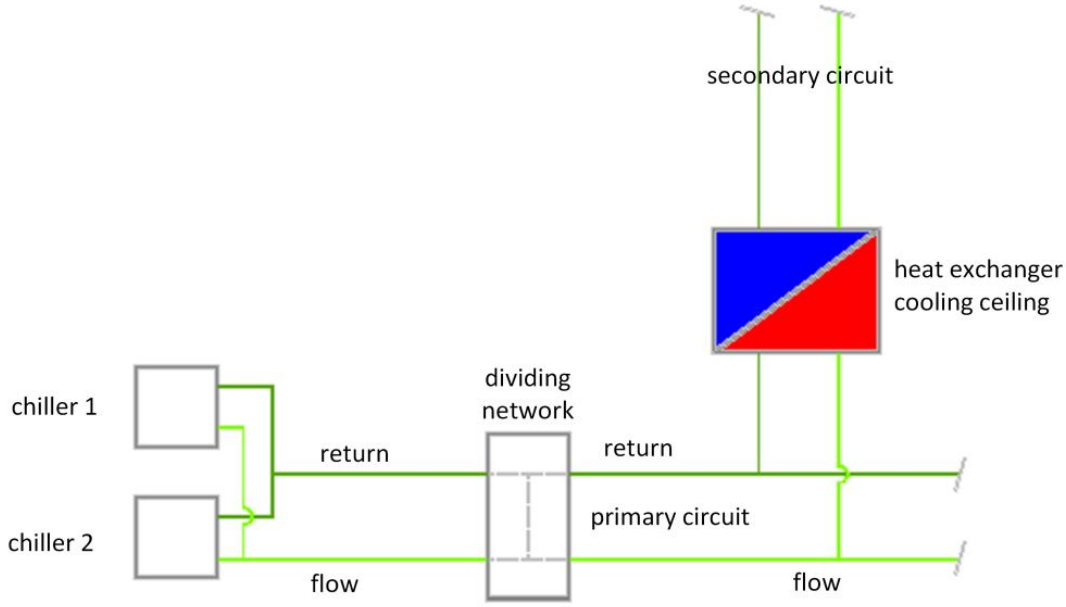

Figure 2.4: Schematic overview of the refrigeration supply; there a 2 chillers in the situated in the cellar each of 2900 kW

Cooling of the Room

The cooling of the rooms is mainly done with a suspended cooling ceiling. The cooling ceiling consist of capillary pipes which were integrated within the suspended ceiling (aluminium panels). The cooling ceiling is shown in figure 2.5. The description of the cooling is done in this section.

Figure 2.5: Pictures of the cooling ceiling

The cooling area is splitted into a façade area and a room area. The cooling medium temperature can variate between 14 °C to 19 °C in dependence of the ambient temperature. The schematic overview of the cooling area is shown in figure 2.6.

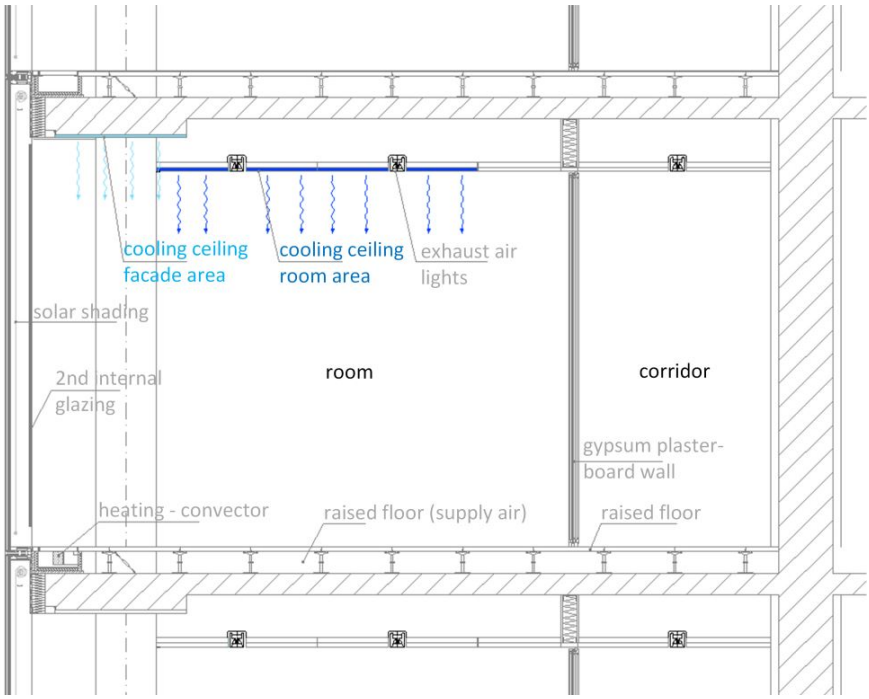

Figure 2.6: Schematic overview of the cooling system of the room, the location of the cooling ceiling is highlighted; the dark blue area represents the active cooling area in the room zone; the light blue area represents the active cooling area in the façade zone

Active Cooling Area

According to EN 14240 [4] the cooling capacity is referenced to the active cooling area and not to the room area. In figure 2.7 on the left side, the active cooling area of the cooling ceiling regarding the room area is shown and you can see that 4 rows of ceiling panels are activated, the first row next to the corridor is not activated. A reduction of the cooling area due to columns is not given in the room area. The active area of the cooling ceiling in the room area for the 2-axis measurement rooms is 5.56 m^2.

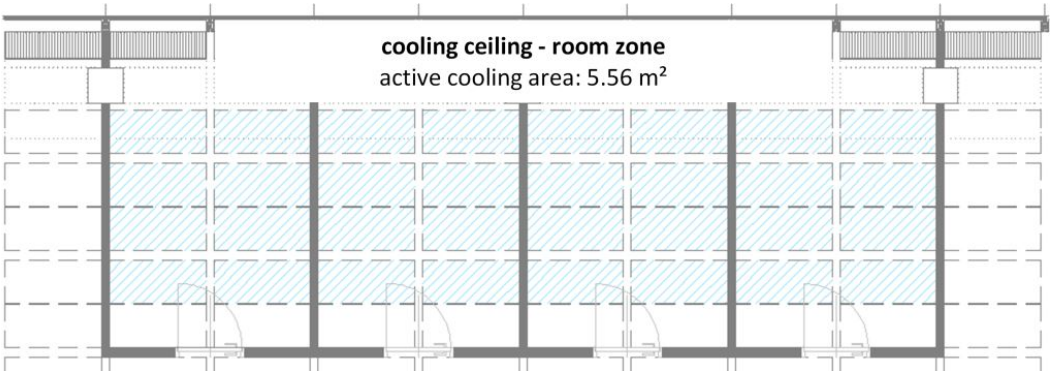

Figure 2.7: active cooling area - room area; the active cooling area is 5.56 m^2

In figure 2.8 on the right side you can see that 3 ceiling panels are occupied by the façade towards the corridor with capillary pipe mats. This area describes the cooling ceiling of the façade area. Furthermore it is important to note that in every fourth window axis the cooling area is reduced by a column. The active area of the cooling ceiling in the façade area for the 2-axis measurement rooms is 3.19 m^2.

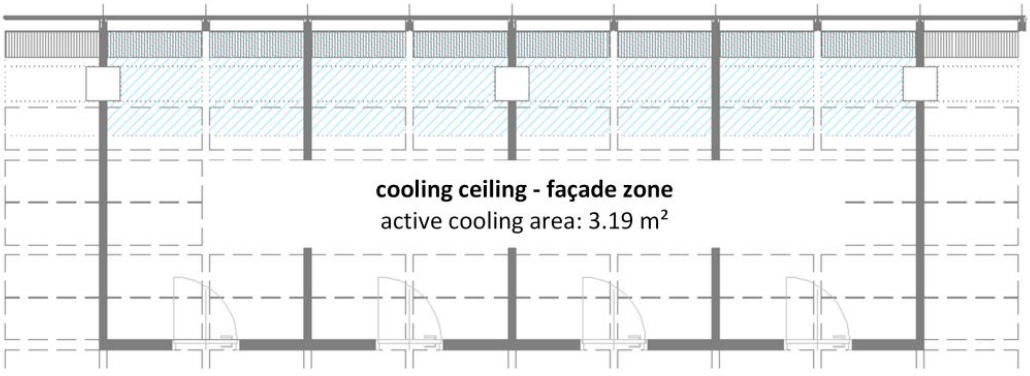

Figure 2.8: active cooling area - façade area; the active cooling area is 3.19 m^2

In total there is an active cooling area of 8.75 m^2 for each of the 2-axis measurement rooms, the cooling areas (façade and room) are overlapping in order to increase the cooling capacity next to the façade. Based on the room area there is a rate of cooling area of about 80 %.

One room was tested with additional cooling elements (the picture of the mounted cooling elements are shown in figure 2.9) which were placed in the area next to the façade. Due to the additional cooling elements there is an increase of the cooling area of 0.84 m^2. In figure 2.10 the additional area is highlighted

Figure 2.9: schematic overview - additional cooling element

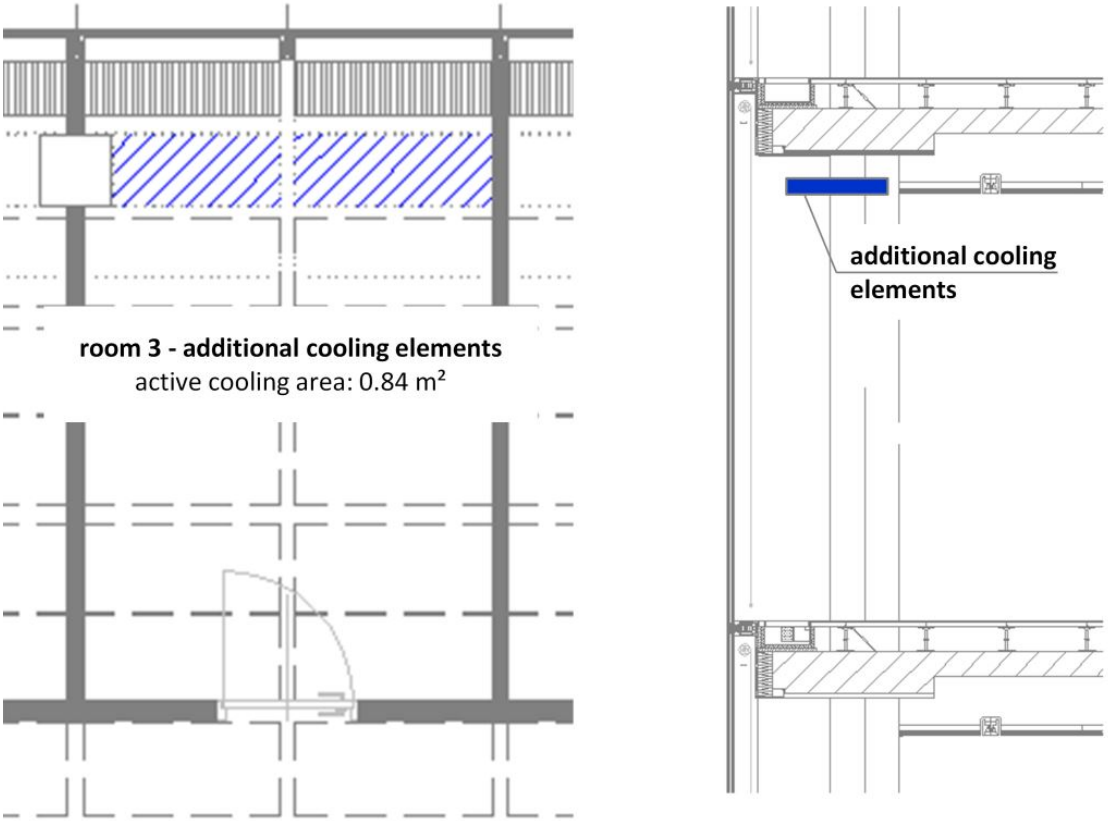

Figure 2.10: schematic overview - additional cooling element

Summary of the Active Cooling Area for the Measurement Rooms

The summary of the active cooling area is visualized in table 2.1 for each room.

Table 2.1: Summary of active cooling area for each room

		amount	m	m	m^2
room 01	left	4	0.57	1.22	2.78
		2	0.45	1.22	1.10
		1	0.45	1.00	0.45
					4.33
	right	4	0.57	1.22	2.78
		3	0.45	1.22	1.65
		0	0.45	1.00	0.00
					4.42
	total				**8.75**
room 02	left	4	0.57	1.22	2.78
		3	0.45	1.22	1.65
		0	0.45	1.00	0.00
					4.42
	right	4	0.57	1.22	2.78
		2	0.45	1.22	1.10
		1	0.45	1.00	0.45
					4.33
	total				**8.75**
room 03	left	4	0.57	1.22	2.78
		2	0.45	1.22	1.10
		1	0.45	1.00	0.45
					4.33
	right	4	0.57	1.22	2.78
		3	0.45	1.22	1.65
		0	0.45	1.00	0.00
					4.42
	total				**8.75**
	add. cooling el. - left	1	0.42	1.10	0.46
	add. cooling el. - right	1	0.42	0.90	0.38
	add. cooling el. - total				**0.84**
room 04	left	4	0.57	1.22	2.78
		3	0.45	1.22	1.65
			0.45	1.00	0.00
					4.42
	right	4	0.57	1.22	2.78
		2	0.45	1.22	1.10
		1	0.45	1.00	0.45
					4.33
	total				**8.75**

2.2.4 Ventilation

The fresh air supply is done by a mechanical ventilation system. The design of the ventilation system is as full air conditioning – heating, cooling / dehumidification and humidification. Due to the hight of the building and the single skin façade there is no possibility of natural ventilation by windows. The ventilation system has a heat and moisture recovery. The schematic overview of the ventilation plant is shown in 2.11.

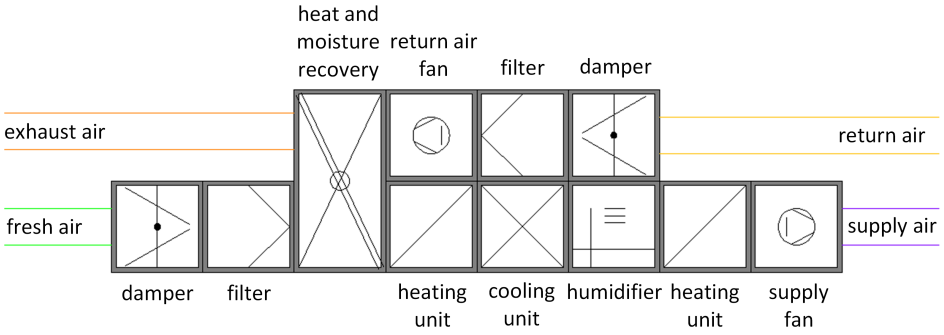

Figure 2.11: schematic overview of the ventilation system

The schematic overview of the ventilation system for the test rooms is shown in figure 2.12. The supply air for the rooms is realized via the raised floor, the whole floor is air leading (marked by the violet area). The air outlet is over “slot diffusers” next to the façade. There is a volume flow rate of about 50 m^3/h for each room with a supply air temperature of about 21 °C. The exhaust air is realized by exhaust air lights. There are flexible ducts between the lights and the suspended ceiling in the corridor. The suspended ceiling in the corridor is air leading as well (yellow range).

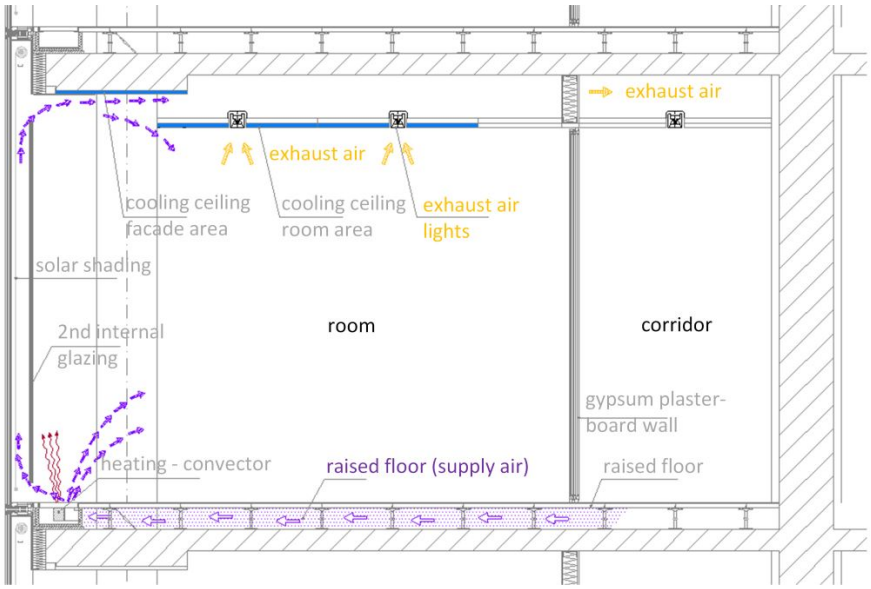

Figure 2.12: schematic overview of the ventilation system of the measurement rooms

2.3 Measurement Set up

The measurement set-up for the test rooms is described in this section, all measurement categories are mentioned and the description and positioning of the individual sensing elements is done. Due to the volume of measurement results some are presented in own chapters, like the results on the operative temperature (see chapter 3), the cooling capacity of the cooling ceiling (see chapter 4) and the tracer gas measurements (see chapter 5). The other results are briefly presented within this section.

2.3.1 Measurement equipment

The measuring system is situated next to the measurement rooms and contain the following elements

- Agilent 34980A: 2 module cards 34922A, 1 module card 34921A
- Keithley 2010: 1 module card

- 25 temperature / moisture sensors type: LinPicco moisture and temperature modules
- 40 PT 1000 temperature sensors - type: Heraeus PT1000
- 10 medium temperature meters type: thermocouples type K, 1.5 mm
- 2 comfort level probe type: ThermoAir 6
- heat flow measurement: 2 x Phymeas 250 mm x 250 mm / 4 x Ahlborn 250 mm x 250 mm
- 5 illumination meters type: Voltkraft
- 1 illumination meter type: Testo 545
- 3 pyranometers type: CM3

To record the outdoor conditions, a weather station with a temperature and humidity sensor and the measurement of the radiation was installed on the roof of the building. The radiation measurement was situated on the west side façade using a pyranometer. The values for these parameters were taken every minute.

The impact of internal loads is realized by a heat mat with a load of about 45 W/m^2 and it is activated by a timer. The operating time is from 8am to noon and from 1pm to 5pm.

The schematic overview of the measurement equipment for the rooms s shown in figure 2.13, where the green marked positions are regarding temperature measurements, the blue ones are regarding humidity measurements and the red ones are referencing to the heat flow measurements. The measurement interval is on minute and the main measurement parameters are:

- operative temperature
- air temperature
- surface temperature
- humidity
- heat flow
- flow and return temperature of the cooling medium

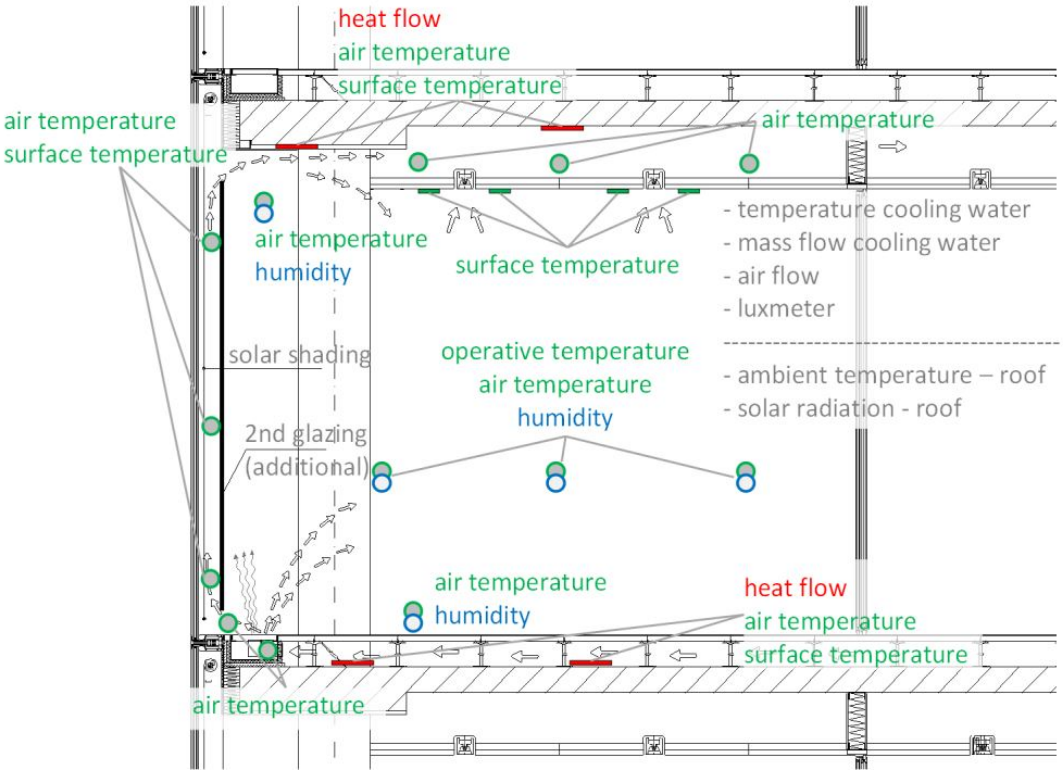

Figure 2.13: Measurement equipment of the test rooms

Additionally the mass flow of the cooling medium and the air flow were measured periodically. The main measurement points for the cooling capacity are also described separately in the section 2.3.5.

2.3.2 Air Temperature / Moisture

The moisture and temperature measurement was done with LinPicco temperature and humidity modules like the pictures in figure 2.14 show. The air temperature and the humidity was measured in different positions as is it marked in figure 2.15 to get an overview of the temperature and humidity range within the test area of the building. The measurement was done with humidity plus temperature transducers based on polymer capacitive sensor. The available field for moisture measurement is from 5 % to 95 % while for temperature measuring is from –10 °C to +70 °C. The sensors are like mm-icrophonettype container in size. The measuring accuracy for humidity is ± 3 % between 20 % and 80 % and otherwise ± 5 %, for temperature there is a measuring accuracy of $\pm$ 1.5 K.

Figure 2.14: Photo of the measurement of the air temperature and the humidity; LinPicco; no direct radiation on the sensor

The schematic overview of the measurement point is shown in figure 2.15, the position of the air temperature and moisture meters is marked by the green points. In total there were measured 25 positions in different room heights. The height of the sensors is written next to the sensor number, when no height is described th logger is mounted in the height of the operative temperature meters (1.20 m above the floor).

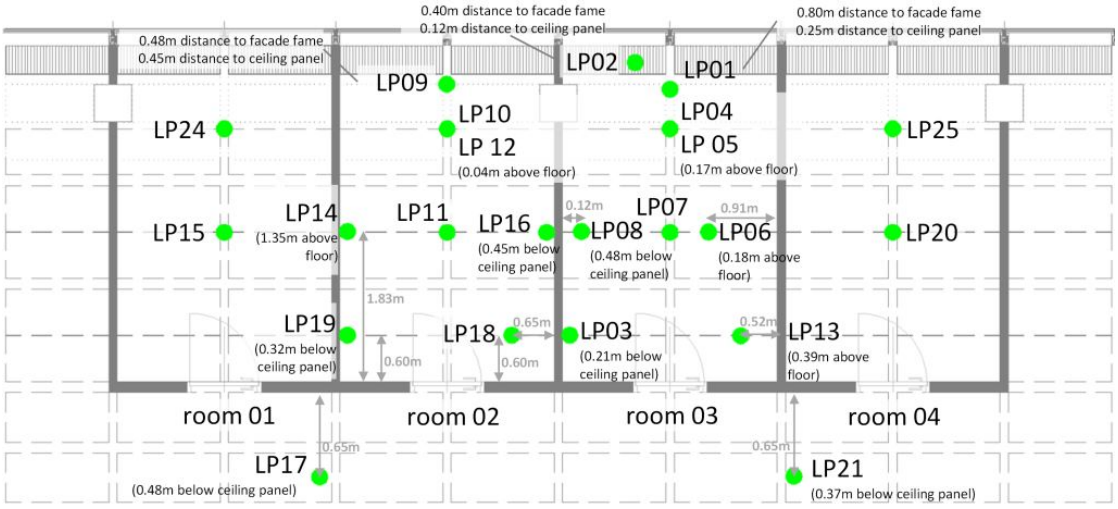

Figure 2.15: Measurement points for the measurement of the air temperature and the humidity within the rooms

The air temperature within the room area from 0.20 m above the floor to 0.20 m below the cooling ceiling panel is very similar for the different measurement locations (see figure2.16). The air temperature close to the cooling ceiling varies between 16 °C and 21 °C, there is a difference of about 2 K compared to the room air temperature. In figure 2.16 the line for LP02 represents the measurement results for the air temperature 0.20 m below the cooling ceiling next to the façade and LP03 is regarding teh area next to the door. The air temperature next to the floor show a very constant value of about 21 °C (see figure 2.16).

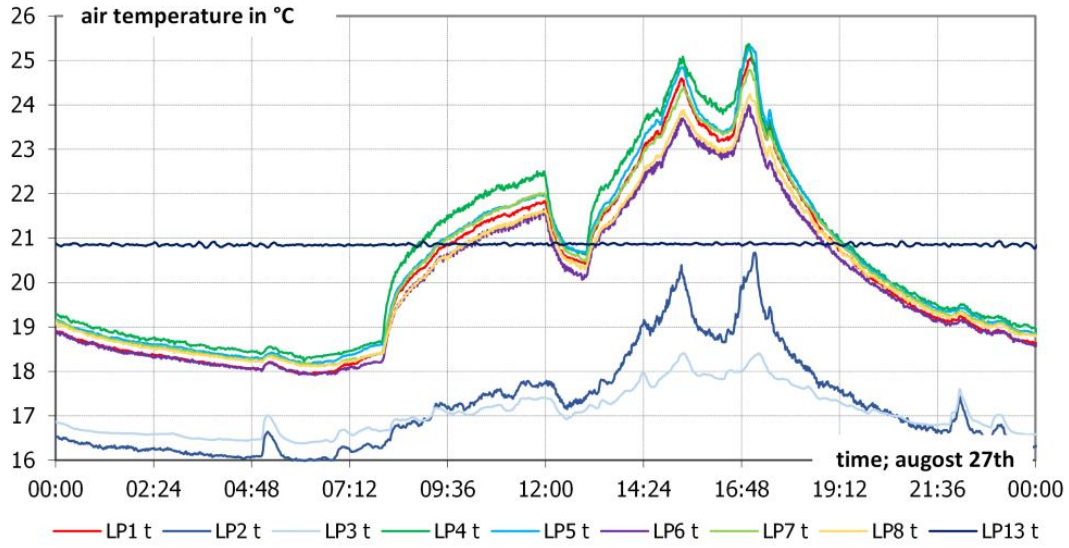

Figure 2.16: Measurement results for the air temperature in room 03

In figure 2.17 the measurement results for the air temperature in the area of the feet for room 02 (LP18) and for room 03 (LP13) are compared. The results show that the temperature is more or less constant during the whole day, the mean value of the air temperature in regarding the floor area is 20.85 °C.

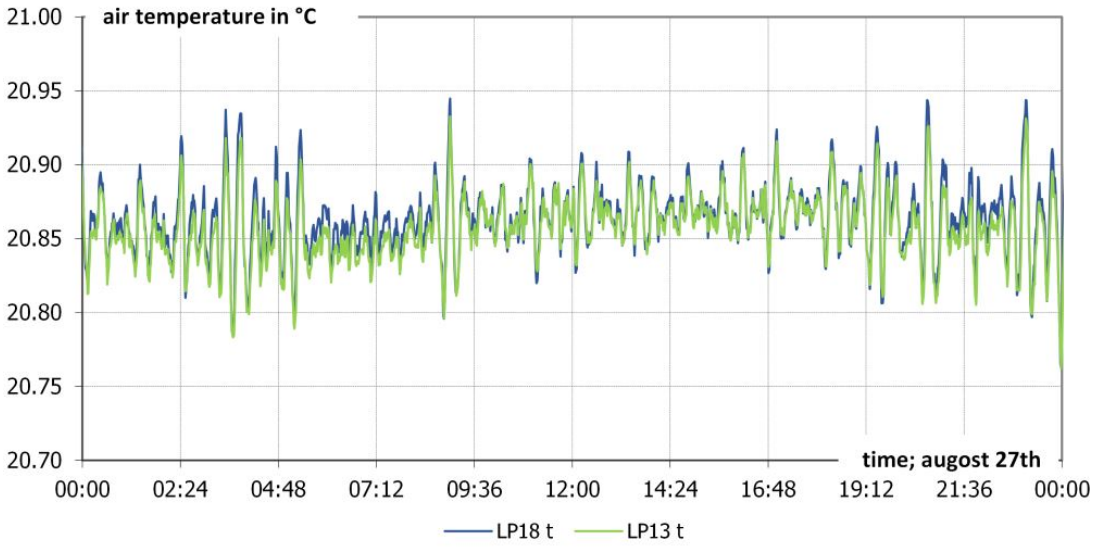

Figure 2.17: Measurement results for the air temperature in the area of the feet; room 02: LP18 and room 03: LP13

The measurement results on relative humidity are shown in figure 2.18 for room 03. The results show that the relative humidity is between 50 % and 60 % within the room area. Next to the cooling ceiling it's higher (around 70 %) which is due to lower temperatures.

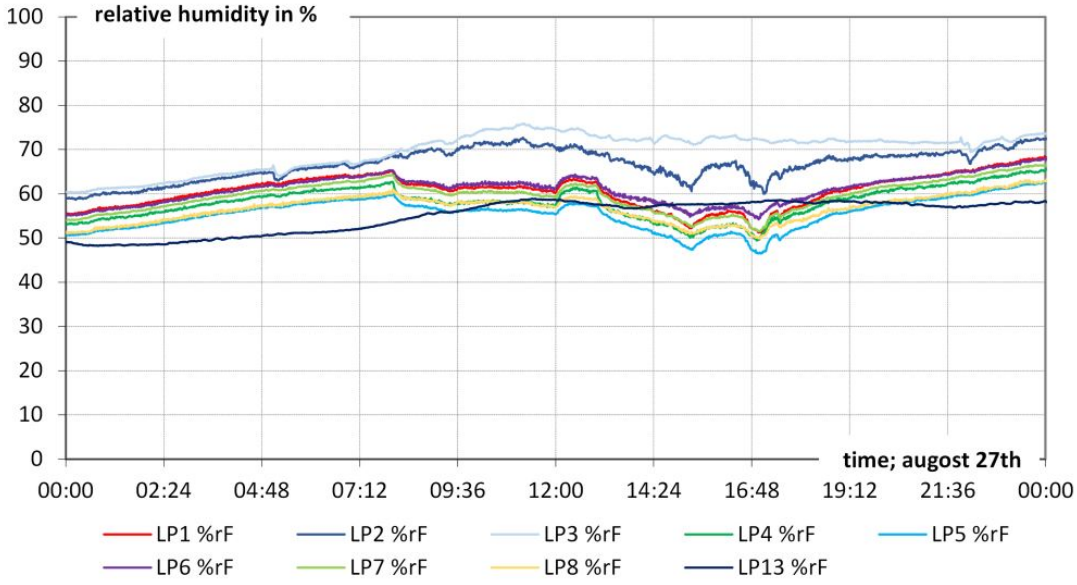

Figure 2.18: Measurement results for the air temperature in room 03

2.3.3 Operative Temperature - Black Ball Measurement

The temperature measurement was done with PT1000 temperature sensors Heraeus M22. Platinum temperature sensors of the M-series are characterized by long-term stability and accuracy over a wide temperature range and compatibility. They are used in particular for applications with high consumption volumes, typically uses are for the automotive industry, white goods, HVAC systems, power generation, and equipment and machinery for medicine and industry.

The specification is done in accordance with DIN EN 60751 [9], the sensors are suitable for a temperature range from -70 °C to +500 °C, with the following classes apply for the following temperature ranges:

- -70 °C bis +500 °C: class B
- -50 °C bis +300 °C: class A
- $\pm$0 °C bis +150 °C: class 1/3 DIN

The self-heating of the sensor is 0.4 K/mW at 0 °C, and the response for air streams (velocity v = 2 m/s) are:

- $t_{0.5}$ = 3.0 seconds
- $t_{0.9}$ = 10.0 seconds

The operative temperature was measured in different depths of the room in a black ball with a diameter of 100 mm, each at a height of 1.20 meters. Figure 2.19 shows pictures of the measurement set up.

Figure 2.19: Pictures of the measurement of operative temperature; in the picture it is seen that the measurement was done with black balls (PT1000 sensors inside; diameter of 100 mm) in 3 depths of the room

The schematic overview of the measurement points for the floor plan is shown in figure 2.20. The section view is shown in figure 2.21. In total 10 points within the 4 rooms were measured. In room 01 and room 4 the operative temperature in the middle of the

room and next to the façade (1 m distance) were measured. In room 2 and room 3 the operative temperatures next to the door were measured additionally to get an idea of the temperature range within the room.

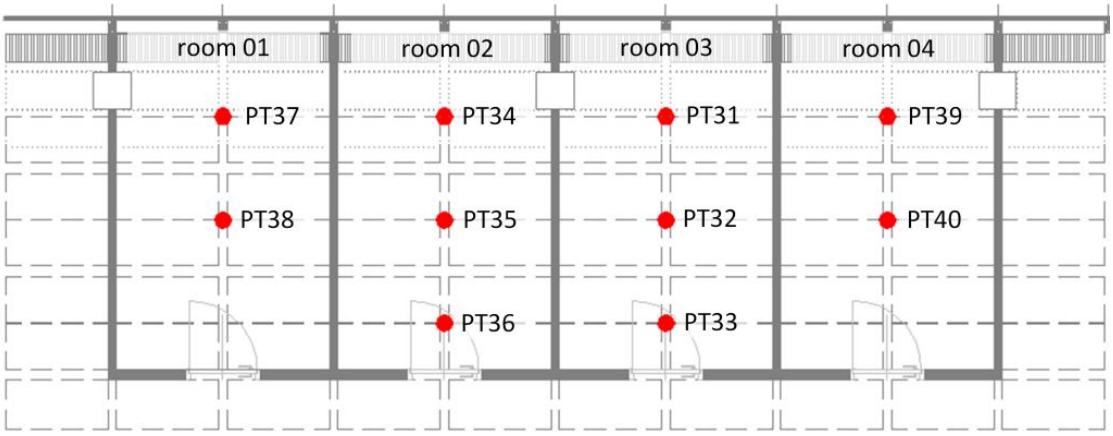

Figure 2.20: Measurement operative temperature, where PT are the temperature sensors (PT1000) of the air temperatures

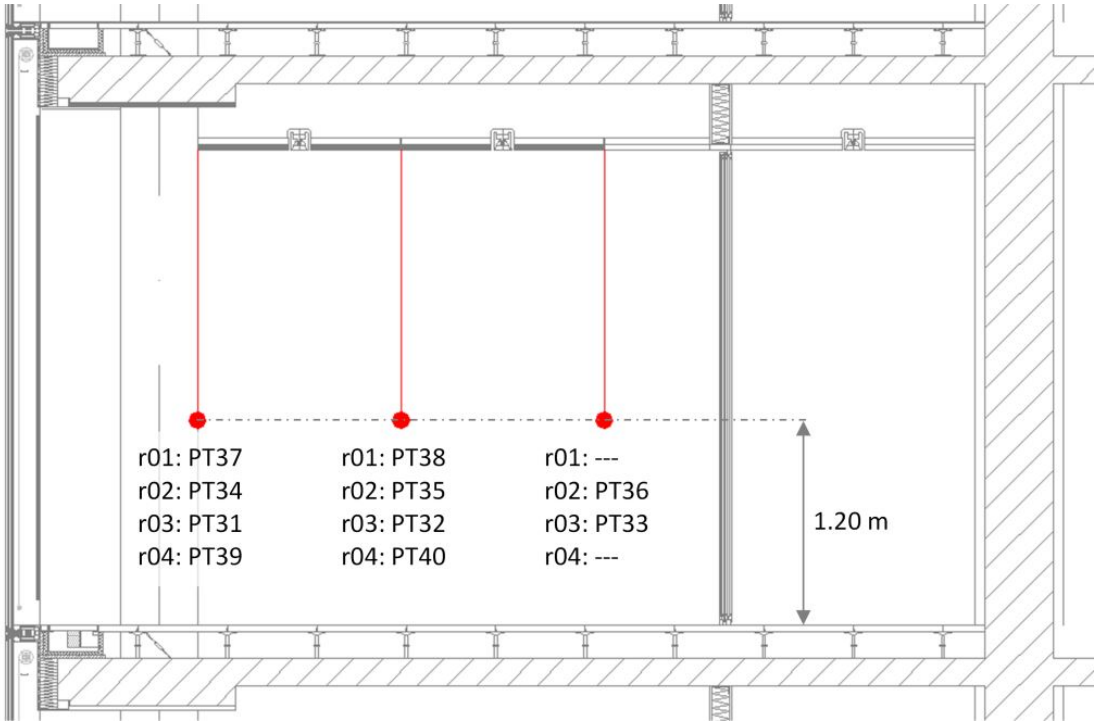

Figure 2.21: Measurement operative temperature, where PT are the temperature sensors (PT1000) of the air temperatures

The results on operative temperatures and the conclusions are shown in chapter 3, section 3.3, the summary of the measurement results is done in section 3.4.

2.3.4 Cooling Medium Temperature Measurement

The flow and return temperatures of the cooling medium are measured by insertion probes like they are shown in figure 2.22. As temperature sensors thermocouples type K were used, the are characterized as class 1 according to the standard EN 60584-1 [8]. They are valid in a temperature range from -40 °C to + 375 °C, with a allowed tolerance of ±1.5 °C. The response time of the sensor is specified by $t_{0.9}$ = 3 seconds

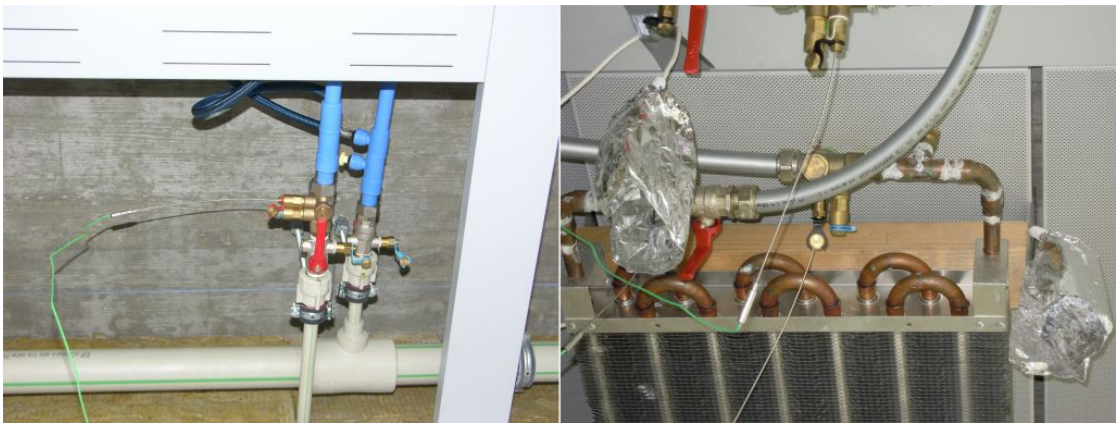

Figure 2.22: Pictures of the flow / return temperature measurement

The measurement points for the flow and return temperatures of the cooling medium are shown in figure 2.23, where the blue points mark the measurement locations. In total 10 sensors were available and the positions for the temperature measurements for the flow and return temperature were changed.

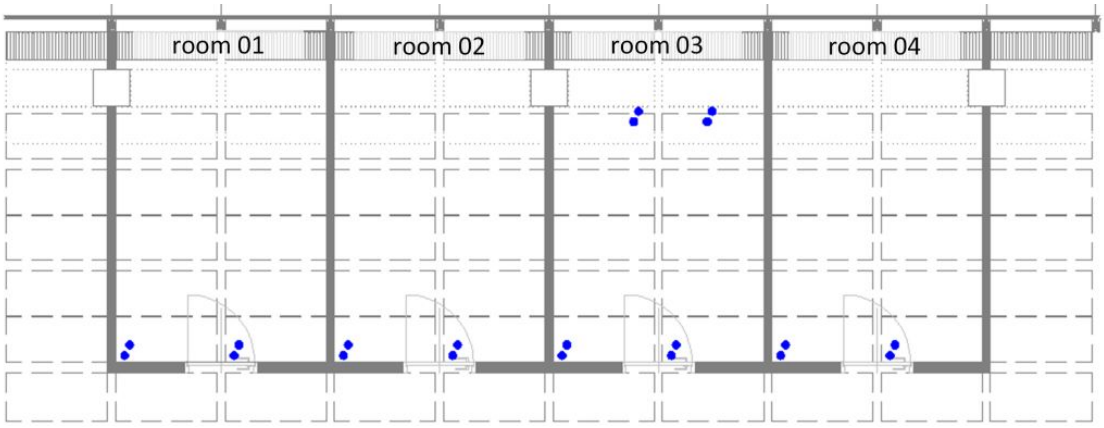

Figure 2.23: Measurement positioning flow / return temperature; the blue points mark the measurement positions; in total 10 sensors were available and the positions for the temperature measurements for the flow and return temperature were changed

2.3.5 Mass flow - cooling ceiling

The measurement of the mass flow through the capillary pipes was measured by differential pressure meter compatible to the mounted valves, which were fabricated of the company Oventrop. The measurement uncertainty is 2 % of the measured value due to the manufacturer's information. In figure 2.24 the areas which are supplied by one mass flow are highlighted. In the plan there are 6 different zones, 2 zones for each room for the cooling ceiling and 2 additional zones for the cooling elements next to the façade in room 3. The colours of the floor plan are referring to the measurement results (see figure 2.25)

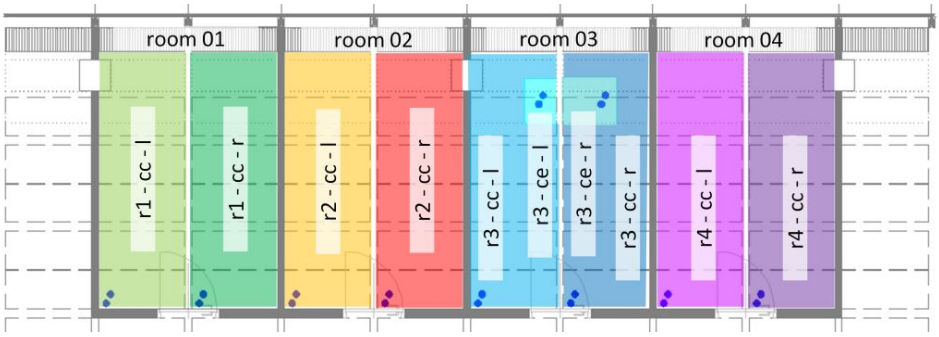

Figure 2.24: Overview of cooling ceiling sections regarding mass flow of the cooling medium

The measurement was done by point measurements, and the result is shown in figure 2.25 for 3 point measurements. The measurement results are very similar, only in room 4 the results of the first measurement show a higher mass flow rate than the other two measurements shown in this diagram.

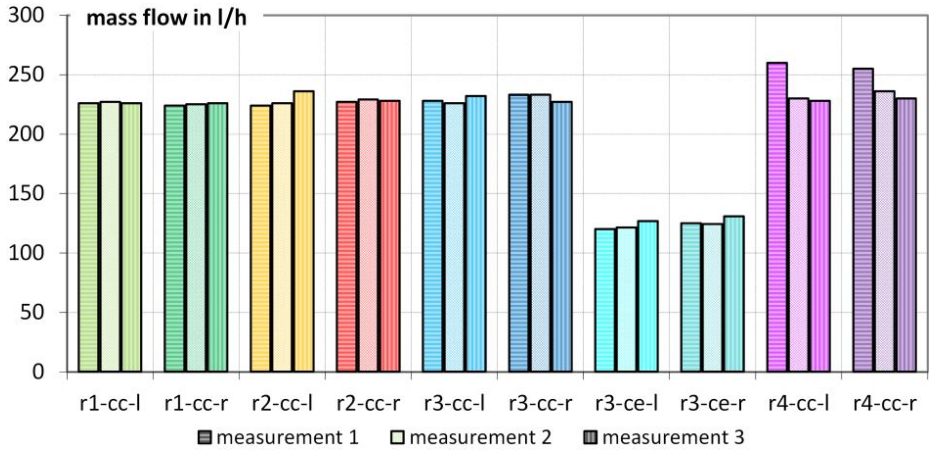

Figure 2.25: Result of the measurement of the mass flow

The mass flow was measured periodically, the measurements did not show relevant differences. For further investigations the mass flow was assumed to be 225 l/h for the cooling ceiling and 120 l/h for the additional cooling elements. Control measurements took place in with respect to the measurements, in relevant time periods every 2 days and were done by an ultrasonic flow measuring meter.

2.3.6 Volume flow

The supply air is realised by slot diffusers next to the façade, each room has two supply air outlets, pictures of the air outlet is shown in figure 2.26.

Figure 2.26: Picture of the supply air outlet next to the façade

The supply air volume flow was measured by point measurements with a special meter which was built to measure the air flow in this building. The measurement results are shown in table 2.2.

Table 2.2: Measurement results for the supply air flow for each air outlet

room 1		room 2		room 3		room 4	
convector right side	convector left side	convector right side	convector left side	convector right side	convector left side	convector right side	convector left side
23 m³/h	23 m³/h	20 m³/h	20 m³/h	20 m³/h	22 m³/h	23 m³/h	23 m³/h

To get the real supply air flow the measurement results have to be multiplied by 1.2 (according to manufacturer information). The actual supply air flow for each axes is shown in table 2.3

Table 2.3: Supply air flow for each air outlet

room 1		room 2		room 3		room 4	
convector right side	convector left side	convector right side	convector left side	convector right side	convector left side	convector right side	convector left side
27.6 m³/h	27.6 m³/h	24.0 m³/h	24.0 m³/h	24.0 m³/h	26.4 m³/h	27.6 m³/h	27.6 m³/h

According to the measurement there is an air change rate between 1.6 1/h to 1.8 1/h. The supply air flow was not changed during the whole measurement period. For all further investigations it was assumed to be 25 m^3/h for each axes. The supply air flow was controlled manually every two month.

2.3.7 Supply Air Temperature

The supply air temperature measurement was done by LinPicco temperature and humidity modules, the description and the specification of the inaccuracy of the sensors is done in subsection 2.3.2. The measurement of the supply air temperature was done in 2 rooms (room 02 and room 03) with a time step of one minute during the whole measurement period. The temperature was taken directly at the air outlet (slot diffusers next to the façade, see figure 2.26). In figure 2.27 the position of the temperature meters is highlighted.

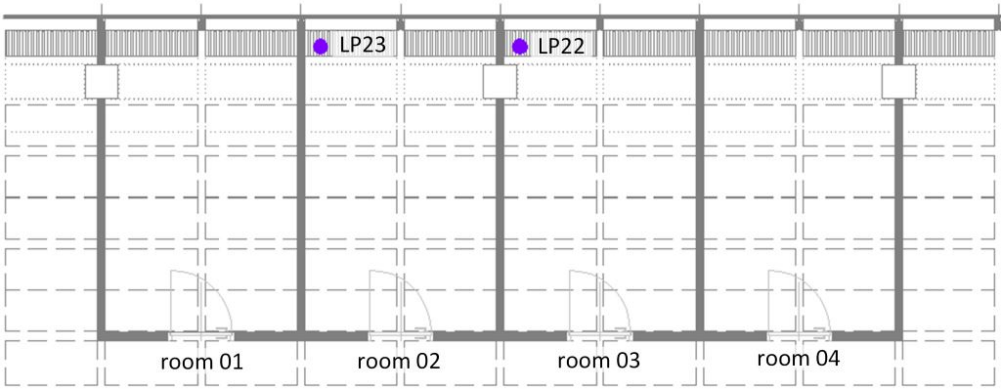

Figure 2.27: Measurement supply air temperature - positioning

The measurement results shown in figure 2.28 show that the supply air temperature variate between 20.5 °C and 22.5 °C and the results for both measurement locations do not have significant differences. The supply air temperature was measured during the whole measurement period wit a time step of 1 minute for 2 locations. The results do not show significant differences due to the supply air outlet. The supply air variate between 20.5 °C and 22.5 °C during the measurement period.

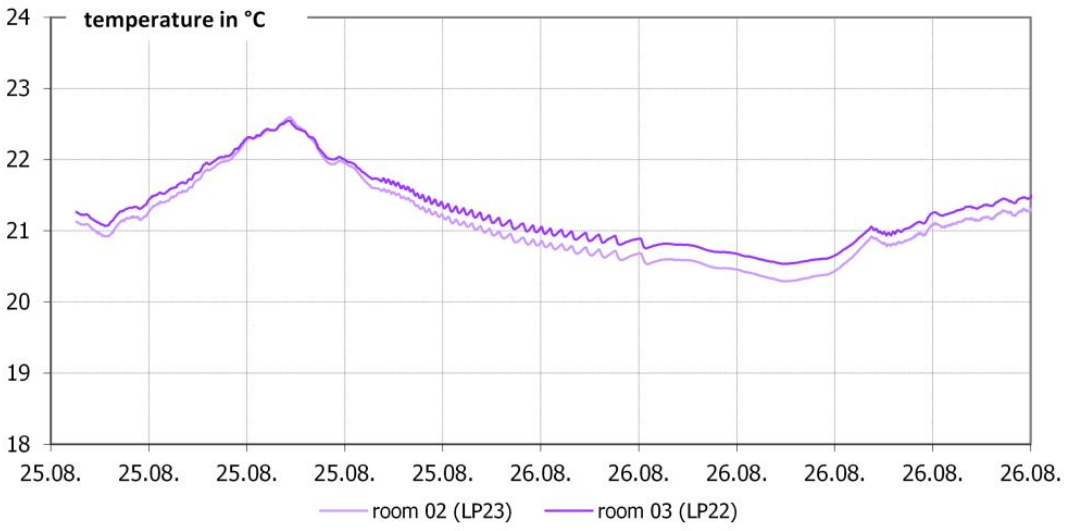

Figure 2.28: Measurement results on the supply air temperature

2.3.8 Comfort Level Probe

The determination of the resulting thermal comfort is an important issue during the design of façade systems. Especially for highly glazed office spaces the correct calculation of the local heat balance is not often well known. Using EN ISO 7730 [11] could lead to underestimation of the energy balance if the direct solar radiation is not accounted for.

The comfort in rooms is one of the most influencing factors due to new building concepts. For the acceptance and success of new concepts the comfort for the users compared to conventional systems should have a significant improvement, at least it should not get lower.

Therefore measurement on thermal comfort for the room types were done. The measurements were done according to EN ISO 7726 [10]. In the standard a measurement period of 180 seconds with 5 measurements per second is required. The air temperature is measured too. For the calculation of the draught rate (according to EN ISO 7730 [11]) the values of the air temperature should be between 20 °C and 26 °C.

The output data is summarized in the following bulleted list:

- highest air velocity: highest value of the test series
- mean air velocity: arithmetic mean value of the test series
- minimum air velocity: lowest value of the test series
- standard deviation: standard deviation of the test series
- intensity of turbulence: intensity of turbulence of the test series
- draught rating DR: according to EN ISO 7730 [11]

The measurement was done with comfort level probe type ”Thermo Air6”, in combination with PT1000 temperature sensors the degree of turbulence was measured. The probe ThermoAir6 is suited for measuring small flow ranges of gaseous media. It has an integrated temperature compensation and an individual calibration in the company’s accredited SCS wind tunnel are a guarantee of high precision. The flow sensor ThermoAir6 has a measuring range of 0.01 m/s to 1.0 m/s and 0.15 m/s to 5 m/s. The measuring accuracy of the air flow at a temperature of 22 °C is $\pm 1\,\%\text{fs.}$ and $\pm 1.5\,\%\text{rdg.}$ between 0.01 m/s and 0.1 m/s between 0.15 m/s and 5.0 m/s it is $\pm 0.5\,\%\text{fs.}$ and $\pm 1.5\,\%\text{rdg.}$. In figure 2.29 the comfort sondes are shown.

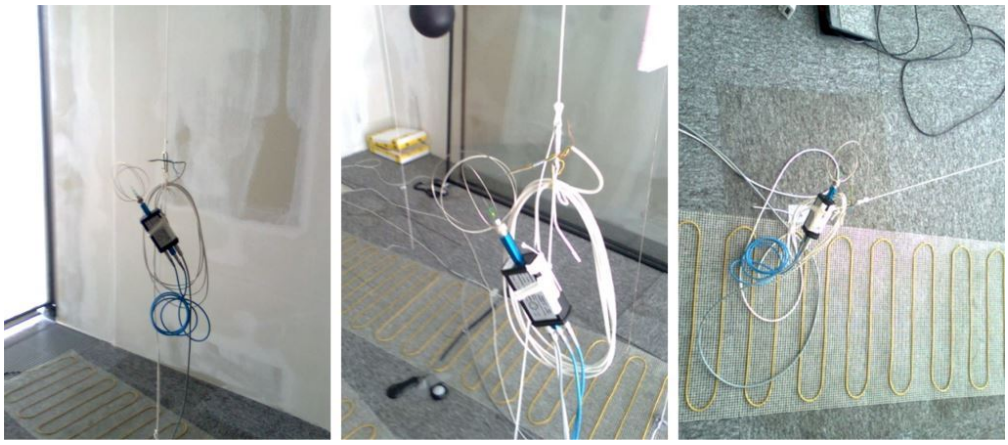

Figure 2.29: Pictures of the comfort measurement; the measurements were carried out in the room on the basis of a grid; for each room set up 12 measurements were carried to evaluated the comfort

To evaluate the comfort of the room, for each room 12 measurements points were taken. The rooms were divided into four zones (see figure 2.30) and the for each position the comfort was measured in three different heights - 0.30 m above the floor, 1.20 m above the floor and 1.80 m above the floor as it is shown in figure 2.31. The tree heights represent the comfort near the feet (0.30 m), the comfort in the area of the head for sitting person (1.20 m) and the area of the head for a standing person (1.80 m).

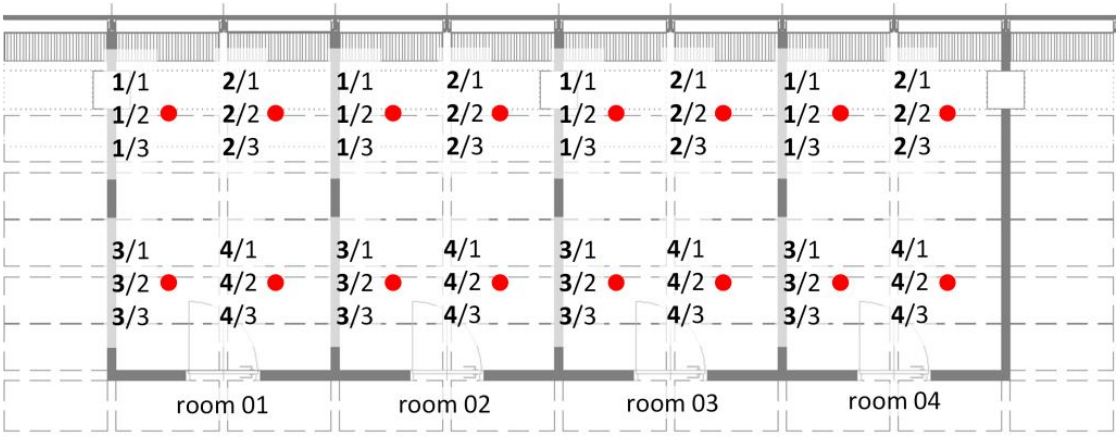

Figure 2.30: Schematic overview of the four room zones due to comfort measurements

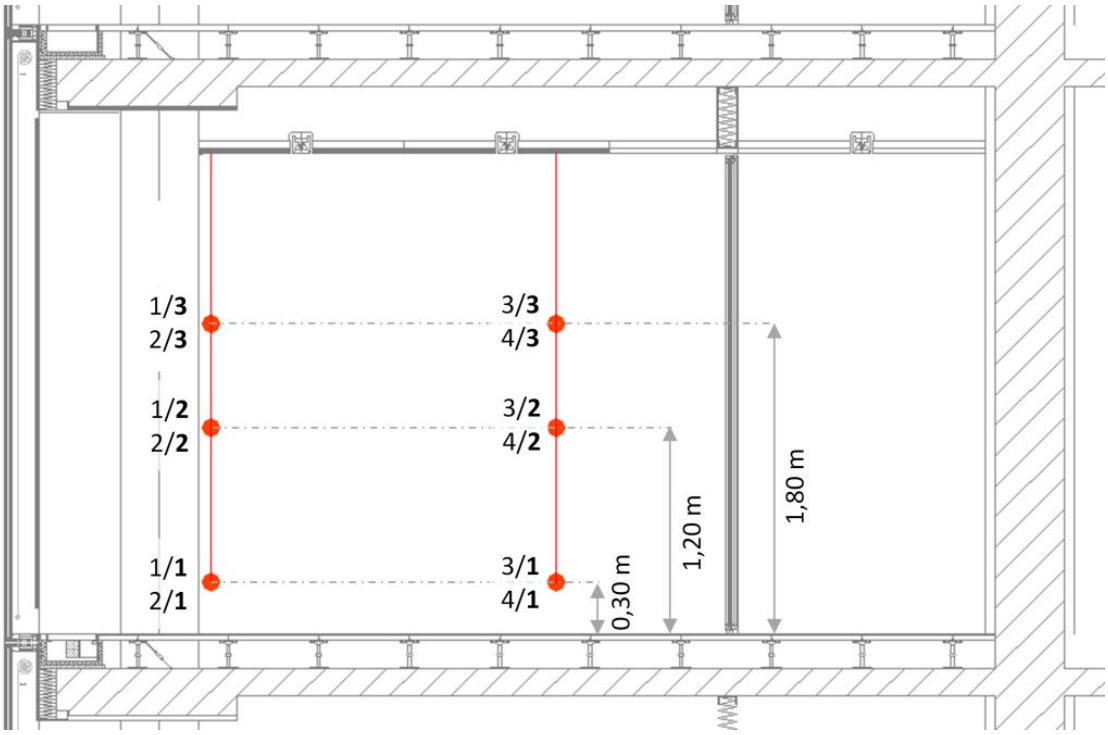

Figure 2.31: Schematic overview of the tree different height of the measurement points for the measurements due to comfort; the heights represent the comfort near the feet (0.30 m), the comfort in the area of the head for sitting person (1.20 m) and the area of the head for a standing person (1.80 m

The measurement results show a good acceptance for the single storey double skin façade. The results are shown in figure 2.32. According to figure 2.32 the highest percentage of dissatisfied is expected in the area of the feet. The results show a draught rate of about 16 %. Compared with the results on the single skin façade (see figure 2.33) there is a reduction of the percentage of dissatisfied, especially in the area of the head (sitting person).

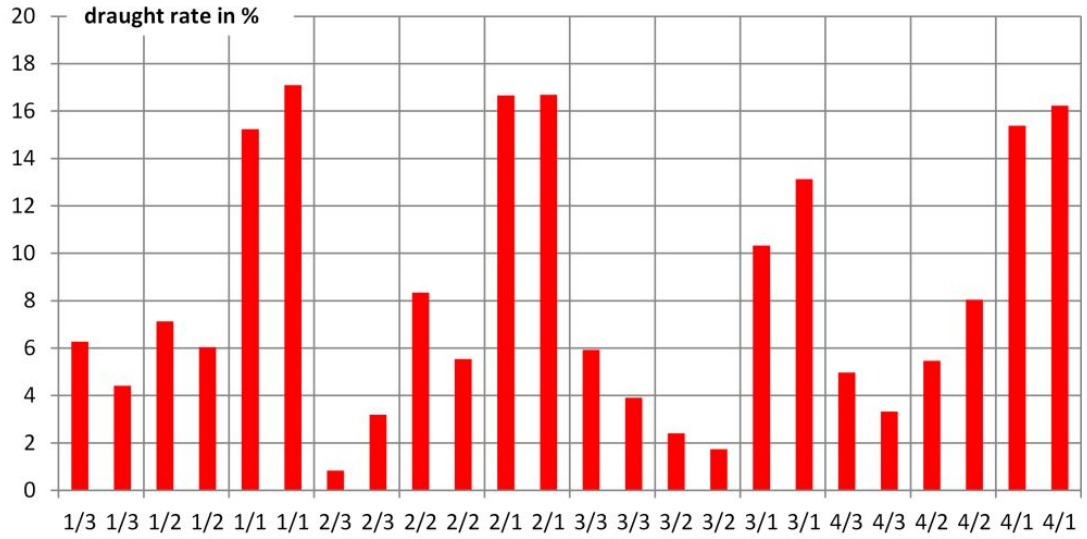

Figure 2.32: Measurement results - draught rate in % for the single storey double skin façade; the point in the diagram refer to the schematic overview of the measurement points in the floor plan (2.30) and the section of the measurement points (2.31); 1/3 means left side of the room, next to the façade in a height of 1.8 m

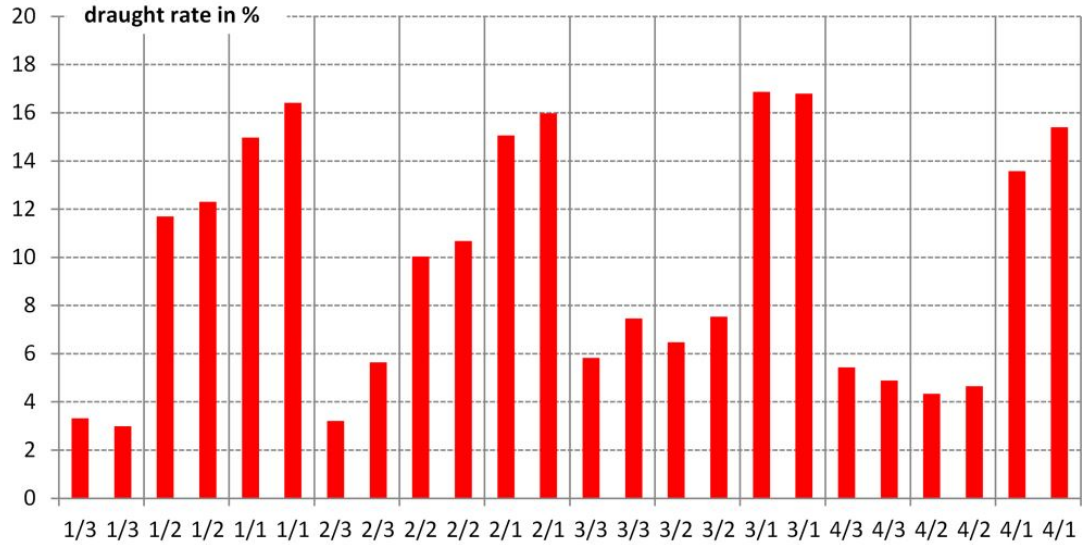

Figure 2.33: Measurement results - draught rate in % for the single skin façade; the point in the diagram refer to the schematic overview of the measurement points in the floor plan (2.30) and the section of the measurement points (2.31); 1/3 means left side of the room, next to the façade in a height of 1.8 m

The additional cooling elements next to the façade increase the active cooling area and therefore the cooling capacity for the room. This room concept is reviewed in terms of comfort. The measurement results show that there is a decrease of comfort due to the cooling elements In figure 2.34 the measurement results for one week for the point 1/2 (1.5 m from the façade, height 1.2 m above the floor) are shown. The comfort draught rate increase from about 15 % to 22 % due to the additional cooling elements. The low surface temperature of the elements leads to an cold air flow and therefore to discomfort.

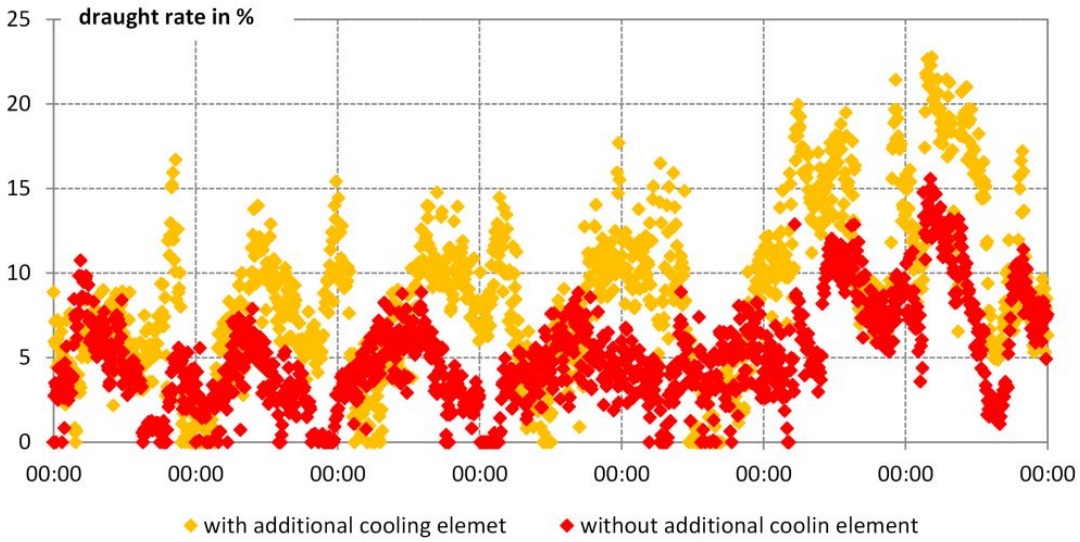

Figure 2.34: Measurement results - draught rate in percentage for one week; comparison of the draught rate due to the additional cooling element, the red points how the measurement results without cooling elements, the orange ones the results with cooling elements; both measurements were done at point 1/2 which means 1.5 m from the façade and in a height of 1.2 m above the floor

The measurement results on comfort measurement show that there is an increase of comfort due to the change from single skin façade to the single storey double skin façade. The additional cooling elements lead to an increasing draught rate.

2.3.9 Heat Flow Measurement

In figure 2.35 the positioning of the heat flow measurement is shown, the orange marked squares represent the measuring point on the ceiling of the room, the red one these on the floor. For each measurement point the air temperature and the surface temperature next to the heat flow measurement was taken. In figure 2.35 these two measurements are marked with the green points, the light green ones for the air temperature and the dark green ones for the surface temperature. The heat flow measurement was done to validate the thermal model regarding the heat flow.

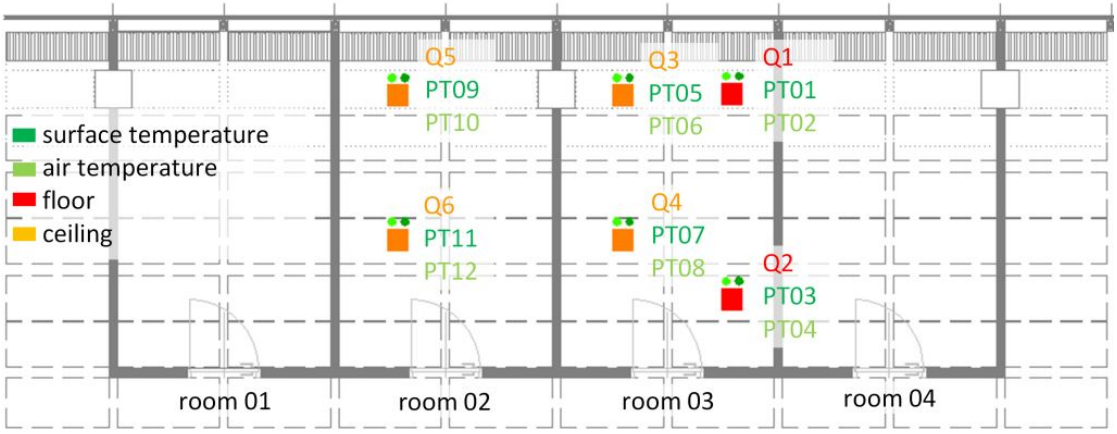

Figure 2.35: measurement points for the measurement of the heat flow; th orang points are measurement points on the ceiling, the red ones those on the floor; with each measurement point two temperatures were taken - the air temperature (light green pints) and the surface temperature (dark green points)

In technical data for the heat flow measurement according to the data sheets is summarized in the following paragraph. The heat-flow plates have a dimension of 250 mm x 250 mm, wherein the active surface has a dimension of 180 mm x 180 mm. The relationship between heat flux and thermal voltage is set according to test reports, the results are shown in the following list:

- Phymeas 137004: 1 mV –> 5.21 W/m^2
- Phymeas 137005: 1 mV –> 4.52 W/m^2
- Ahlborn 1030007: 1 mV –> 4.80 W/m^2
- Ahlborn 1030008: 1 mV –> 4.59 W/m^2
- Ahlborn 3100009: 1 mV –> 4.72 W/m^2
- Ahlborn 3100010: 1 mV –> 4.74 W/m^2

The calibration was carried out with a single plate equipment at an average temperature of 23 °C and a heat flux of about 100 W/m^2. For the measurement the sensor was embedded between two moss rubber sheets. The relative uncertainty is 5 %

2.3.10 Intensity of Illumination

The measurement of the intensity of illumination was done in 2 rooms (room 01 and room 02) with a time step of one minute during the whole measurement period with luxmeter (pictures of the measurement are shown in figure 2.36). To compare the results on operative temperature there should not be a difference on the light intensity due to shading systems (comparison of screen and blinds). If the blinds are fully closed, the illuminance is not high enough for a working place and additional lighting would be used. To compare the effectiveness of the different shading systems the position of the elements of the blinds were adapted manually so that the light impact is the same compared to the screen. To get comparable measurement results of the light meters the were adjusted in a first step. The sensors were positioned in one room next to each other, to make sure that they measure the same illuminance.

Figure 2.36: Picture of the measurement of the intensity of illumination

The measurement points of the light intensity are highlighted in figure 2.37. There are 3 measurement points, 2 in room 01 and 1 in room 2. In room 01 the light intensity was measured in the middle of the room and with a distance of 1 m from the entrance to the room (deepest point of the occupied zone). In room 02 the measurement point is 1 m from the entrance to the room.

Figure 2.37: Sensor location of the light meters; 2 meters are situated in room 01 - one in the middle of the room and the other one 1m from the entrance; 1 meter is situated in room 02 - 1m from the entrance

The intensity of illuminance was compared by the deepest point within the occupied zone. In figure 2.38 the measurement results of the light intensity are shown. As the controlöf the blinds was done manually there are some differences in light intensity. The biggest difference is after the attendance time, there is an higher illuminance due to the screen. From the morning till around 5.30 pm there is a good accordance of the light intensity of the two rooms.

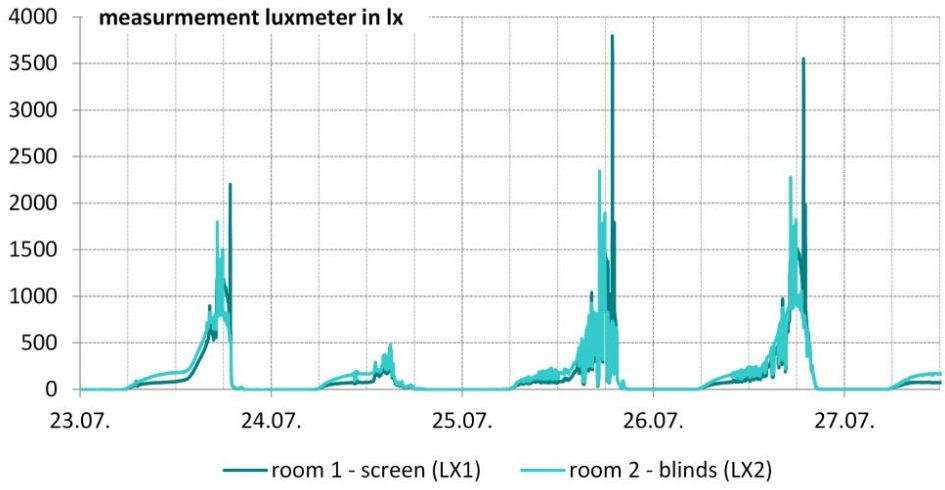

Figure 2.38: Measurement results of the light intensity for room 01 (LX1) and room 02 (LX2); both 1 m from the entrance of the room

For the results on operative temperature the light impact into the room should be taken into account to compare different shading systems (in this case screens with blinds). To get comparable results on operative temperature the blinds were controlledmmanually so that there is the same intensity of illumination compared to the screen. The measurement results show a good accordance of the light intensity for the two rooms.

2.3.11 Solar Radiation

The measurement of the incident solar radiation was done with pyranometer type Kipp & Zonen CM3. The sensor CM3 is an instrument to measure the solar irradiance, it's a second class pyranometer according to the definition of the standard ISO 9060 [12]. It measures the solar energy that is received from the whole hemisphere (180 degrees field of view).

According to the inspection reports the sensors were calibrated by comparison with an outdoors calibrated reference pyranometer (CM3 FT014), they were mounted horizontally side by side. The source for the calibration is a 1000 W tungsten-halogen lamp wit a colour temperature of 3300 K. The calibration measurement was done with an normal angle of incident. The sensitivity of the CM3 sensors was specified at a temperature of 20 °C and an irradiation of 500 W/m^2 with $\pm$0.5 % for all three sensors that were used for the measurement.

One of the radiation meters was used on the outside of the building, the incident radiation on the façade was measured and the other two radiation meters were placed in the measurement area (see figure 2.39), one meter measure the radiation after the first glazing without shading. The second meter was placed 1m from the façade in room 03, the incident radiation through the whole façade system (single skin façade plus shading or single storey double skin façade plus shading) was measured.

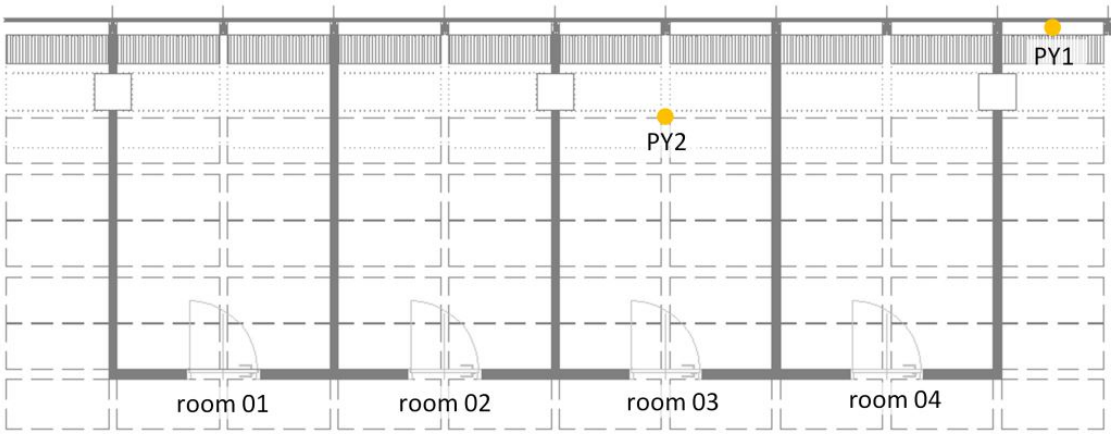

Figure 2.39: Position of the radiation meters, one after the first glazing (PY1) and the second meter 1m from the façade (PY2) in room 03 - to measure incident radiation through the whole façade system

In figure 2.40 the results of solar radiation are shown for the measurement point 1 m from the façade and after the first glazing. The façade system for the measurement is single storey double skin façade and a fully closed shading system. The results show a strong reduction of solar radiation due to the façade system.

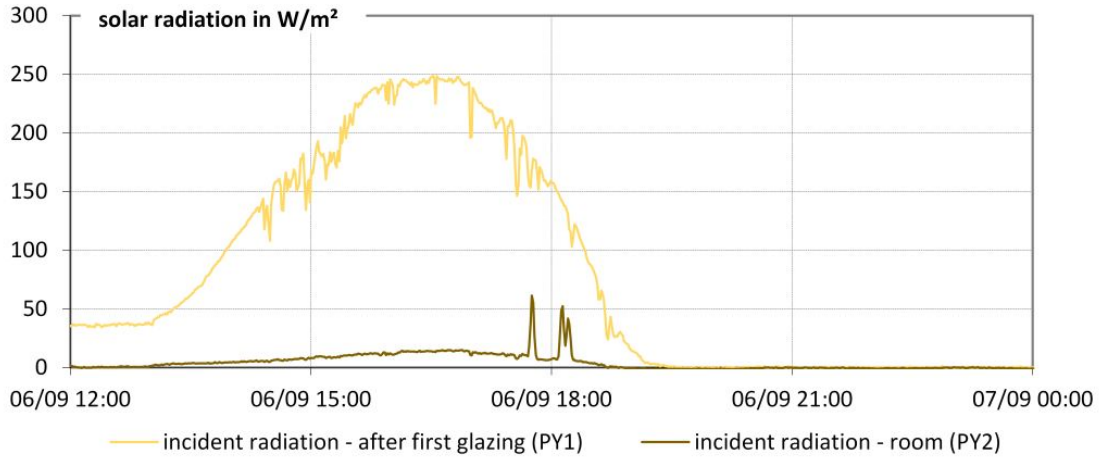

Figure 2.40: Measurement results - incident solar radiation; the yellow line represents the results for the measurement after the first glazing; the brown curve represents the measurement results of the incident radiation 1 m from the façade in room 03; the façade system referring to the measurement results is single storey double skin façade and fully closed shading elements

2.3.12 Tracer Gas Measurement

This section gives an short overview of the measurement set up, the details on measurement variations and results can be found in chapter 5, section 5.3 and section 5.4..

As tracer gas CO_2 was used, as sensors Johnson Controls CD-W00-00-0 CO_2 transmitter were applied. They are suitable for measuring and transmitting CO_2 levels, ranging from 0 to 2000 parts per million (ppm). The accuracy at 25 °C is specified with to be smaller than $\pm$40 ppm CO_2 + 3.0 % of reading, these specification includes manufacturing deviation and drift. The operating temperature is specified between -5 °C to +45 °C, the humidity range should be between 0 % and 85 %. The sensors have a warm-up time of 1 minute and the response time (0 % to 63 %) is 1 minute.

In figure 2.41 photographs of the measurement set-up are shown, where the first figure from the left side to the right side shows a view into the room from the door side, the second one gives a picture of the sensor in the raised floor, the third one visualize the meters in the ceiling area and the last one shows the position of the sensor above the second layer glazing.

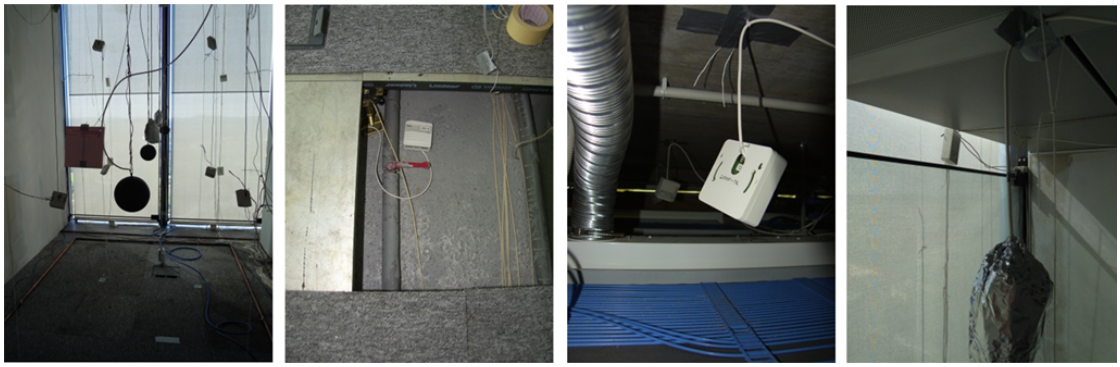

Figure 2.41: Pictures of the CO_2 meters; from left to right side: room, floor, ceiling, façade

To measure the air flow in the room, a grid of 27 CO_2 sensors was set up. In figure 2.42 the position of the CO_2 sensors is shown, where the left side is the floor plan and the right side shows the section of the room.

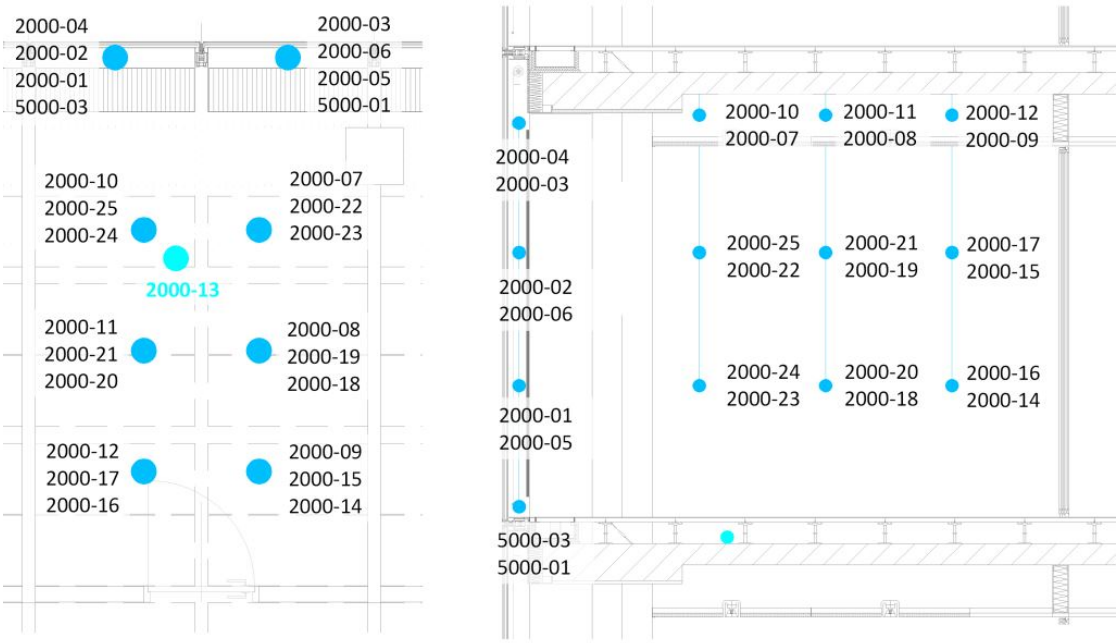

Figure 2.42: Measurement set up – floor plan (left side) and section (right side) including the sensor numbers, where the first 4 numbers are the maximum concentration rate and the last 2 are the numbers are the unique sensor identification numbers

The measurement itself was done by CO_2 injections and the concentration at the measurement points was logged. A defined amount of CO_2 was injected on five different positions of the room:

- Inj 1: directly into the room, floor area (by a frame with small openings)
- Inj 2: ceiling – height of the concrete ceiling
- Inj 3: ceiling – height of the suspended cooling ceiling
- Inj 4: Supply air area
- Inj 5: Façade area

3 Measurement Operative Temperature

3.1 Introduction

According to EN ISO 7730 [11], the operative temperature shall be determined as the average size of air temperature and the radiation temperature. This temperature is measured with a globe thermometer according to EN ISO 7726 [10]. The standard ball has a diameter of d_k = 150 mm and an emissivity of ε = 0.95. Regarding the shape and the diameter of the ball there is much discussion and various statements what shape, size and colour represents best of the human being. For the measurements of the operative temperatures in this case black balls with a diameter of d_k = 100 mm are used.

3.2 Building / Room set up

A series of measurements have been done with different room types. The detailed description of the in-situ measurements is found in chapter 2, section 2.2. The relevant data for the measurement of the operative temperature is summarized in this section.

3.2.1 Basic Building Information

Four rooms were realized for the measurements in an existing office building which is located in Vienna, Austria. It is a tower with a fully glazed façade. The test-rooms are adjacent and are separated by a gypsum plasterboard wall. The suspended ceiling of the measurement rooms is separated by a foreclosure (mineral wool) around the rooms and between these rooms. The floor is a raised floor which is caused to its air leading properties (the supply air is realized over the raised floor) open throughout the whole storey. It is not possible to close the floor, because than the test rooms would be without fresh air.

For detailed description regarding the ventilation system see chapter 2, section 2.2.4. The ventilation of the rooms is done by an mechanical ventilation system, where the supply air is done by the raised floor. The return air from the room is realized by exhaust air lights. In total there is an air change rate of 1.6 1/h to 1.8 1/h with an supply air temperature between 20.5 °C and 22.5 °C. The measurement results on the air change rate and the supply air temperature are described in chapter 2, section 2.3.7 and section 2.3.6.

Within the building there is the possibility to test different façade systems by changing the shading element furthermore there is also the possibility to change the single skin façade to a single storey double skin façade. Another change on boundary conditions is due to the active cooling area in the room.

The effect on operative temperature by the change by changing the boundary conditions of the room were tested. In total there were tested 5 different façade systems, the overview is shown in the following list, the differences regarding the optical properties of the shading systems are summarized in table 3.1.

- Façade system 1: single skin façade with internal shading element type 1
- Façade system 2: single skin façade with internal shading element type 2
- Façade system 3: single storey double skin façade with internal shading element type 2
- Façade system 4: single skin façade with internal shading element type 3 (blinds)
- Façade system 5: single storey double skin façade with internal shading element type 3 (blinds)

Table 3.1: Summary of the differences regarding optical properties of the tested shading systems

optical properties	shading system 1	shading system 2	shading system 3
Solar transmittance τ	0.19	0.11	0.08
Reflectance ρ	0.37	0.39	0.39
Absorptance α	0.44	0.50	0.54
Light transmittance τ_L	0.19	0.10	0.07

The cooling of the room is done by suspended cooling ceilings. The detailed description is found in chapter 2, section 2.2.3. The cooling ceiling is equal in each room. In one room there were mounted additional cooling elements in the façade area to measure the effect of an additional active cooling area on the operative temperature and the comfort in the room. The detailed description of the cooling elements and the results on the comfort can be found in chapter 2, section 2.2.3 and section 2.3.8.

3.2.2 Measurement positions operative temperature

The schematic overview of the measurement points of the operative temperature is shown in figure 3.1. On the left side there is the floor plan, on the right side the section view is shown.

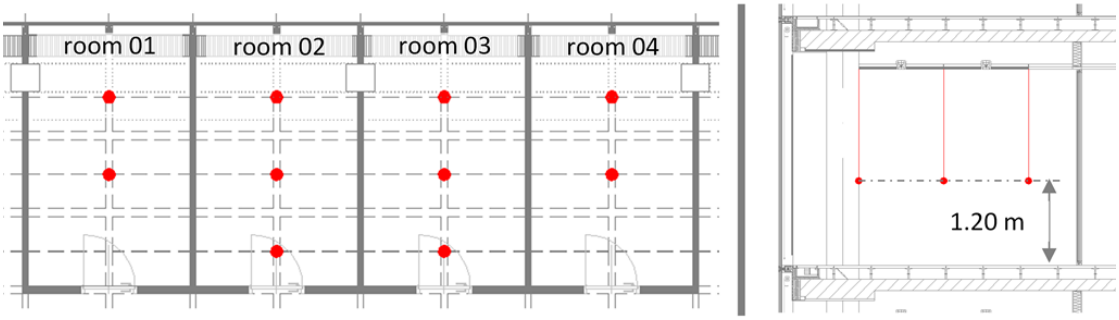

Figure 3.1: measurement points for operative temperature; left side: floor plan of the measurement rooms; right sight: section view; the red points mark the sensor positions

The aim of the measurements is to figure out the influence on the operative temperature and the cooling capacity of a cooled ceiling by changing the room set up in the following three categories:

- change of façade system
- change of shading system
- change of active cooling area

figure 3.2 shows an overview of the room types and measurement variations.

One of the rooms was used as a reference room (room 04). In this room the boundary conditions (façade system, shading type, active cooling area) were not changed. The other rooms serve as test room where different set-ups due to façade system, shading types and active cooling area were realized. Room 01 is the room with shading element type 2, which is a screen and the measurement was done for the single skin façade (façade type 1) and the single storey double skin façade (façade type 2). Room 02 has the same measurement variation as room 01, this room has shading elements type 3 (blinds). Room 03 has the same boundary conditions as room 01 (façade system and shading type), the difference to room 01 are the additional cooling elements which were situated nest to the façade to increase the active cooling area and therefore the cooling capacity for the room.

On the pictures at the right corner of each room the view to the outside through the shading elements is shown. There is a difference between room 04 and room 01/room 03, shading type 1 (screen in room 04) is more transparent than shading type 2 (screen in room 01 and room 03), but with both shading systems there is a view to the outside. The picture for room 02, shading type 3 (blinds) shows that with closed blinds there is no view to the outside.

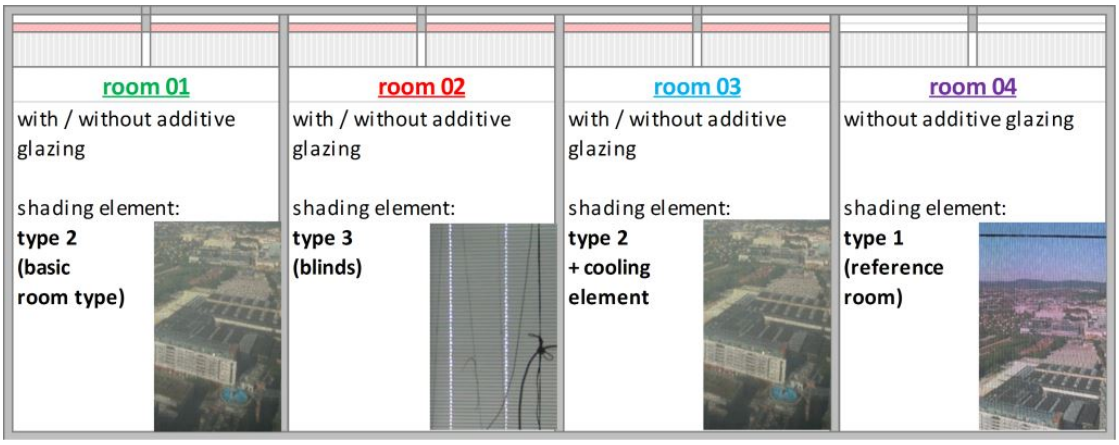

Figure 3.2: floor plan - test room

In total 7 room types were tested. A short overview of the measurement variations due to façade system, shading system and cooling system is shown in figure 3.3 and is summarized in table 3.2.

In figure 3.3 the 7 room types are visualized in the section view, the used colours refer to the colours in figure 3.2 and table 3.2. The first picture shows room type 0 - which is the reference room with a single skin façade and shading type 1 (screen type 1), which is highlighted by the violet line in the façade area. The next picture describes room type 1 - the difference to room type 0 is the shading system, it is changed from shading system 1 to shading system 2 (another screen type), the change is highlighted by the green line in the façade area. On the third picture room type 2 is visualized, the change from room type 1 to room type 2 is regarding the façade, the façade is changed from single skin façade to single storey double skin façade. The next picture shows room type 3, the difference to room type 0 is again the shading system, is is changed to shading system 3 (blinds). The 5th picture visualize room type 4, the difference between room type 3 and room type 4 is the façade system, it is changed from single skin façade to single storey double skin façade. The last two pictures are describing room type 5 and 6, these to room types have additional cooling elements in the façade area where room type 5 is representing the single skin façade room set up and room type 6 has façade system 2 (single storey double skin façade). The shading of room type 5 and 6 is shading system 2 (screen type 2).

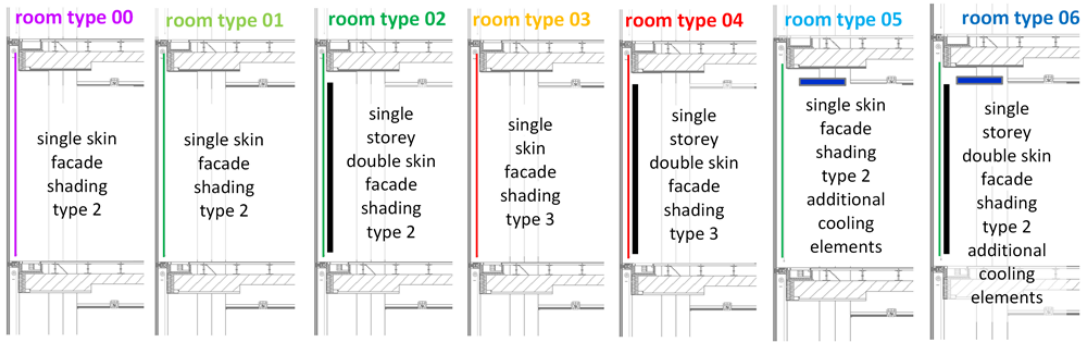

Figure 3.3: Visualization of the room types by section views; room type 0: single skin façade shading system 1 (screen type 1); room type 2 single skin façade, shading system 2 (screen type 2); room type 2: single storey double skin façade, shading system 2; room type 3: single skin façade, shading system 3 (blinds); room type 4: single storey double skin façade, shading system 3; room type 5: single skin façade, shading system 2, additional cooling elements; room type 6: single storey double skin façade, shading system 2, additional cooling elements

Table 3.2: summary measurement variation, room types, where room type 0: single skin façade shading system 1 (screen type 1); room type 2 single skin façade, shading system 2 (screen type 2); room type 2: single storey double skin façade, shading system 2; room type 3: single skin façade, shading system 3 (blinds); room type 4: single storey double skin façade, shading system 3; room type 5: single skin façade, shading system 2, additional cooling elements; room type 6: single storey double skin façade, shading system 2, additional cooling elements

name	room	façade	shading	additional cooling element
Room type 0	4	single skin	screen $\tau_L = 0.19$	---
Room type 1	1	single skin	screen $\tau_L = 0{,}10$	---
Room type 2	1	single storey double skin	screen $\tau_L = 0{,}10$	---
Room type 3	2	single skin	blinds	---
Room type 4	2	single storey double skin	blinds	---
Room type 5	3	single skin	screen $\tau_L = 0{,}10$	yes
Room type 6	3	single storey double skin	screen $\tau_L = 0{,}10$	yes

To make is easier to read the colour of the font can be found in the following diagrams, so the purple line show the results of the reference room (type 0), the green ones the results of room number 1 (type 1 + 2), the red ones room number 2 (type 3 + 4) and the blue ones room number 3 (type 5 + 6).

3.3 Measurement Results on Operative Temperature

The operative temperature is one of the influencing factors on comfort. According to EN ISO 7730 [11] there are 3 categories (A, B and C) with different acceptance of predicted percentage of dissatisfied people (PPD). To reach category B the maximum operative temperature in summer should be lower than 26 °C. Category B means that the PPD is less than 10 %.

In the reference room (room type 0) the boundary conditions were not changed during the whole measurement period, in order to compare the operative temperatures of the different room types. During the measurement period it was noticed that most of the screens are used half opened, regarding this fact the measurement of the operative temperature was done with full closed and half closed (1.25 m distance from the floor) shading systems.

In the first measuring period (first summer period) there were 19 days, which could be used for the evaluation of the operative temperature regarding different room set-ups. In table 3.3 the days and the room boundary conditions are summarized.

Table 3.3: Summary of measurement set up - first measurement period

	1	2	3	4	5	6	7	8	9	10	11	12	13	14	15	16	17	18	19
single skin facade																			
single sorey double skin facade																			
shading system fully closed																			
shading system half opened																			

The measurement results of the first measurement period were validated with a second measurement period in the second summer. Especially the results on screen type 3 were proven, because the values seems not to be correct. After the validation of the measurement results of the first summer period, the boundary conditions of the room set up were not changed in the second summer period. During the llong time measurementöf the second summer period the room conditions were as listed in table 3.4. The Evaluation is shown for 3 days (27.07 / 19.08 and 20.08) because these days have almost similar boundary conditions in terms of incident solar radiation and eternal temperature and were the only days with solar radiation during the whole day.

Table 3.4: Summary of measurement set up for the “long term” measurement during the second summer period

name	room	façade	shading	additional cooling element
Room type 0	4	single skin	screen $\tau_L = 0.19$	---
Room type 2	1	single storey double skin	screen $\tau_L = 0{,}10$	---
Room type 3	2	single skin	blinds	---
Room type 6	3	single storey double skin	screen $\tau_L = 0{,}10$	yes

For the conclusion regarding the operative temperature the maximum values for the operative temperatures (5 pm values) were compared.

3.3.1 Adjustment of the Rooms

The first step before starting testing different façade systems was to do the adjustment of the rooms. The comparison of the operative temperatures is shown in figure 3.4 (centre of the room) and figure 3.5 (1 m distance to the façade). The room temperatures were measured with the single skin façade and without shading. That is also the reason for the high temperatures. In figure 3.4 and figure 3.5 you can see that in all four rooms the same temperature is measured in the middle of the room and next to the façade.

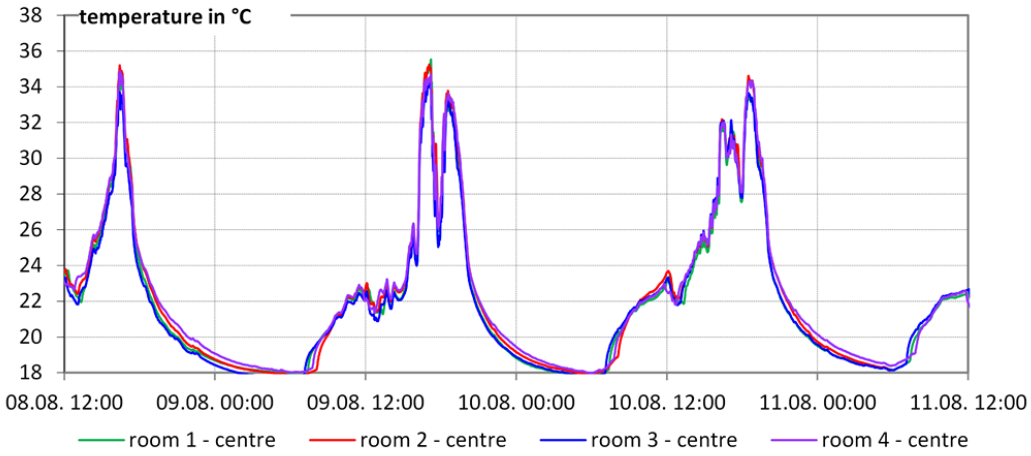

Figure 3.4: Comparison operative temperature test room and reference room - centre of the room

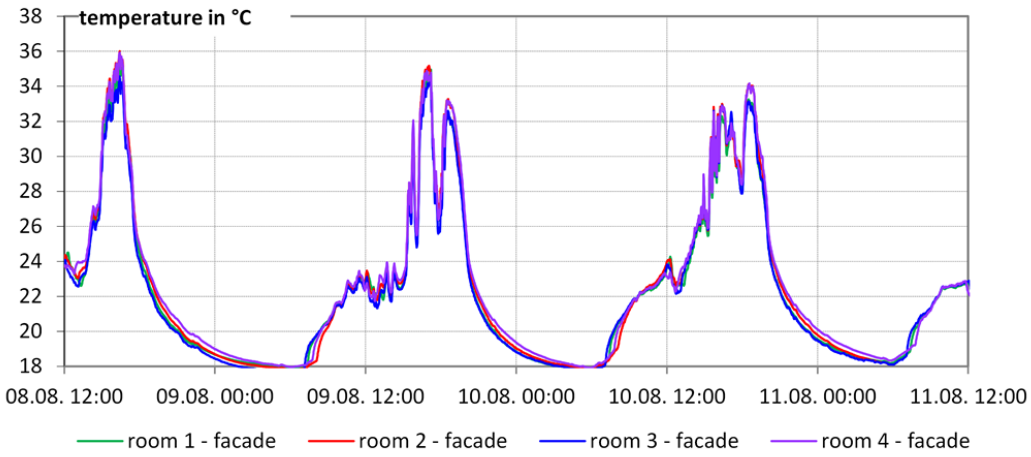

Figure 3.5: Comparison operative temperature test room and reference room - 1 m distance to the façade

3.3.2 Results: Single Skin façade, Shading System completely closed

The measurement results for the maximum operative temperature are shown in figure 3.6 for the measurement points next to the façade (1 m distance to the façade) and in figure 3.7 for the measurement points in the centre of the room.

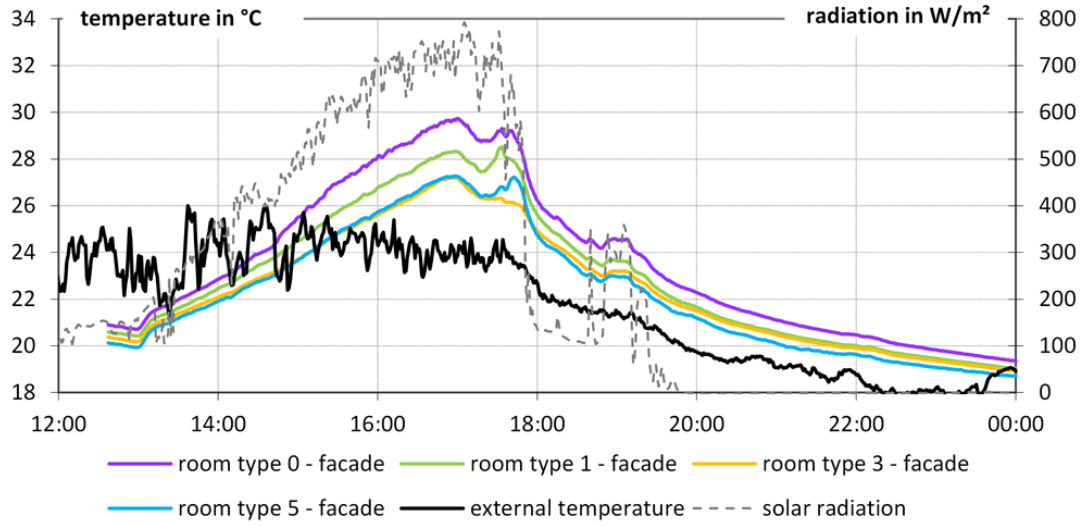

Figure 3.6: Operative temperature next to the façade; façade: single skin façade; shading system fully closed; the colours in the diagram are referring to 3.2

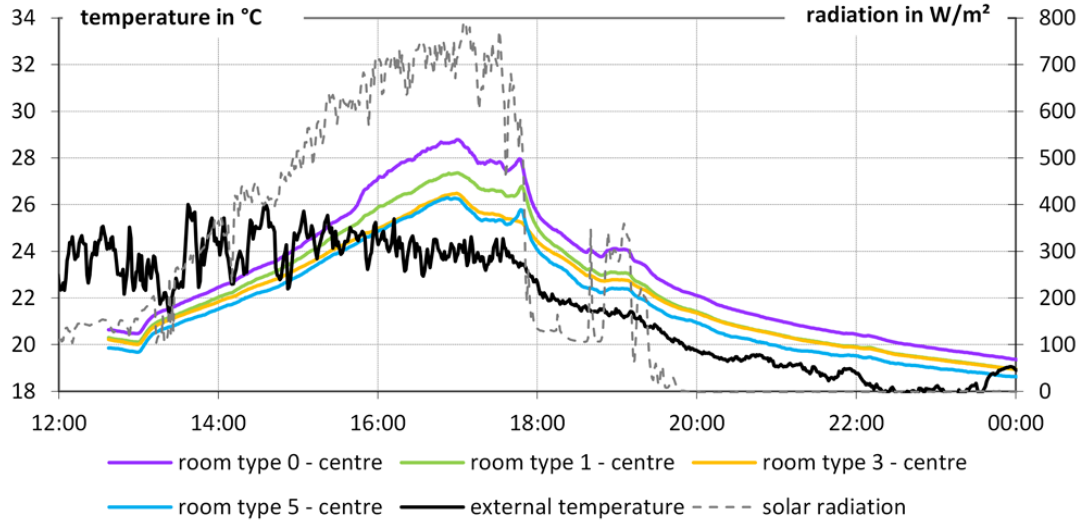

Figure 3.7: Operative temperature in the centre of the room ; façade: single skin façade; shading system fully closed; the colours in the diagram are referring to 3.2

The summary of the measurement results regarding the maximum operative temperature for the single skin façade and with fully closed shading system is done in table 3.5.

Due to the change from room type 0 to room type 01 (change of the screen type) the operative temperature next to the façade is reduced of 1.0 K, in the middle of the room the reduction is 1.4 K. The additional cooling element within the façade area leads to a temperature reduction of 1.1 K for both measurement points (next to the façade / middle of the room) compared to room type 1.

Table 3.5: Summary of measurement results of the maximum operative temperature in the centre of the room and next to the façade for the first measurement period. The results are for the façade system: single skin façade and the shading system is fully closed

room type	sensor location	
	1 m distance to the **façade**	**centre** of the room
room type 0	29.7 °C	28.8 °C
room type 1	28.3 °C	27.4 °C
room type 3	27.4 °C	27.3 °C
room type 5	26.8 °C	26.2 °C

3.3.3 Results: Single Skin Façade, Shading System half opened

The results for the façade area are shown in figure 3.8 and for the centre of the room in figure 3.9.

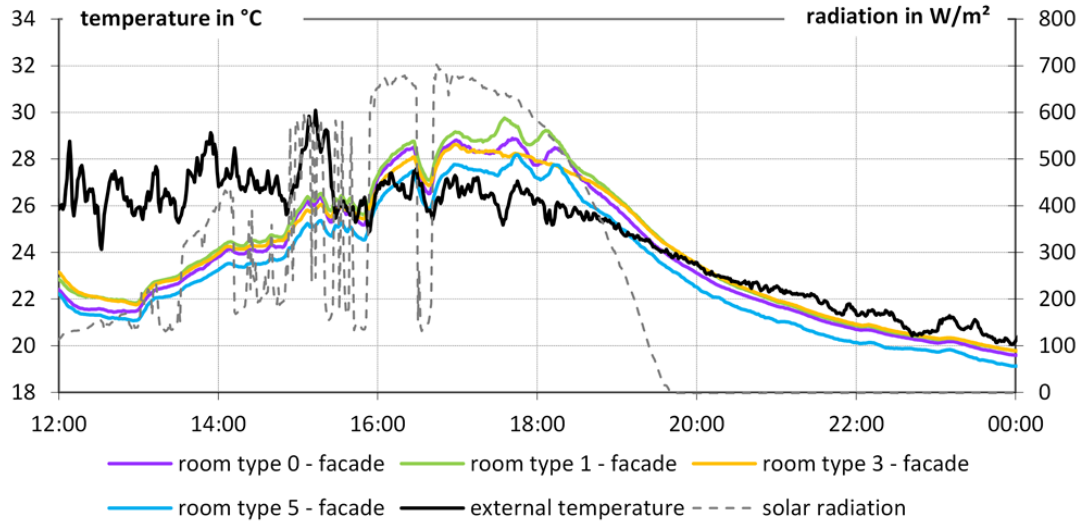

Figure 3.8: Operative temperature next to the façade; façade: single skin façade; shading system half opened; the colours in the diagram are referring to 3.2

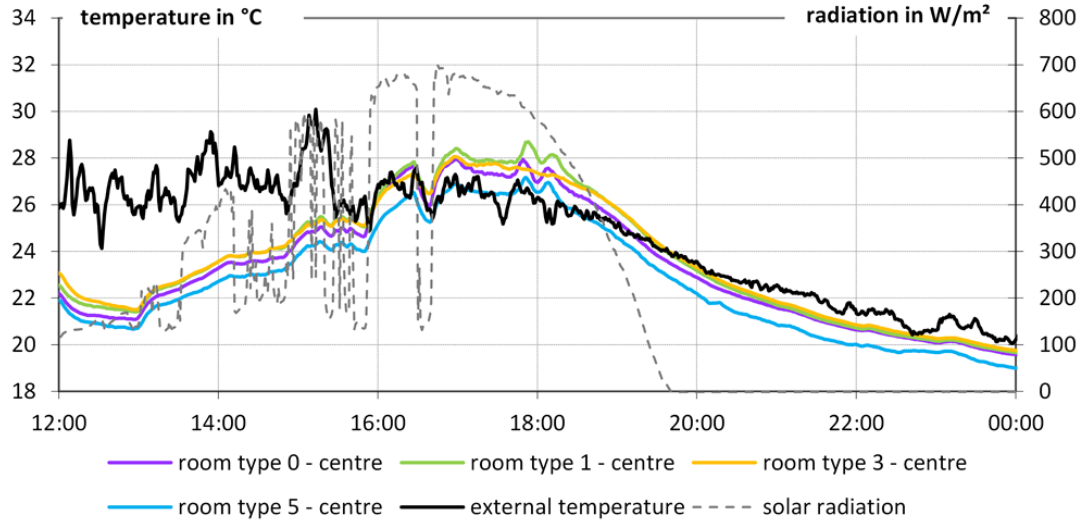

Figure 3.9: Operative temperature in the centre of the room ; façade: single skin façade; shading system is half opened; the colours in the diagram are referring to 3.2

The summary of the measurement results regarding maximum operative temperature for the single skin façade and with half closed shading system is done in table 3.6.

Due to the change of the shading system (change from screen to blinds) there is a temperature reduction of 0.3 K in the centre of the room and of 0.4 K next to the façade. Compared to the room type 1 the additional cooling elements lead to a reduction of the operative temperature of 1.4 K next to the façade and 1.8 K in the middle of the room.

Table 3.6: Summary of measurement results of the maximum operative temperature in the centre of the room and next to the façade for the first measurement period. The results are for the façade system: single skin façade and the shading system is half closed

room type	sensor location	
	1 m distance to the **façade**	**centre** of the room
room type 0	-	-
room type 1	30.1 °C	29.3 °C
room type 3	29.6 °C	29.0 °C
room type 5	28.3 °C	27.9 °C

3.3.4 Results: Single Storey Double Skin Façade, Shading System completely closed

The change from the single skin façade to the single storey double skin façade leads to a reduction of the operative temperature. Figure 3.10 show the influence regarding different boundary conditions like shading type and cooling area next to the façade for a reference day, in figure 3.11 the results in the centre of the room are shown.

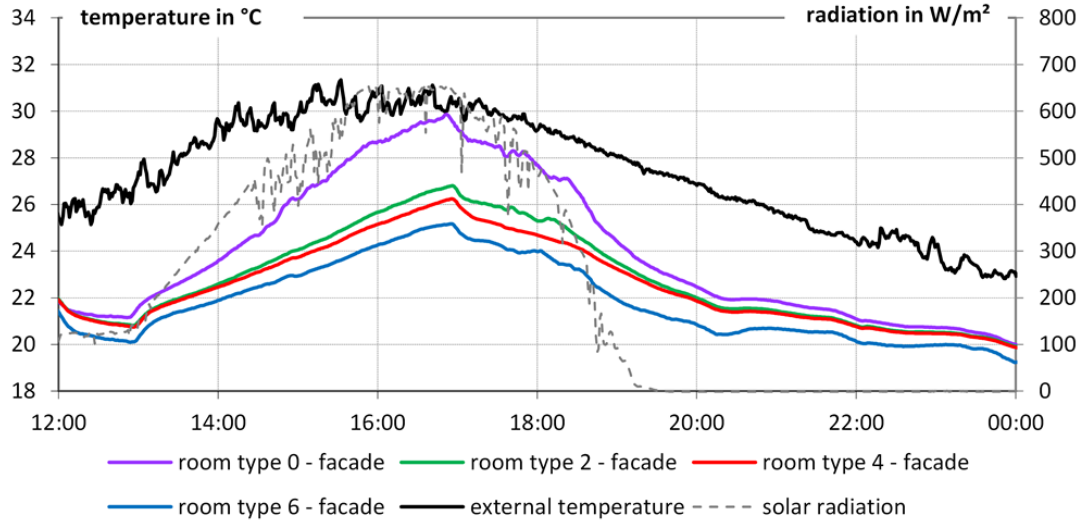

Figure 3.10: Operative temperature next to the façade; façade: single storey double skin façade; shading system fully closed; the colours in the diagram are referring to 3.2

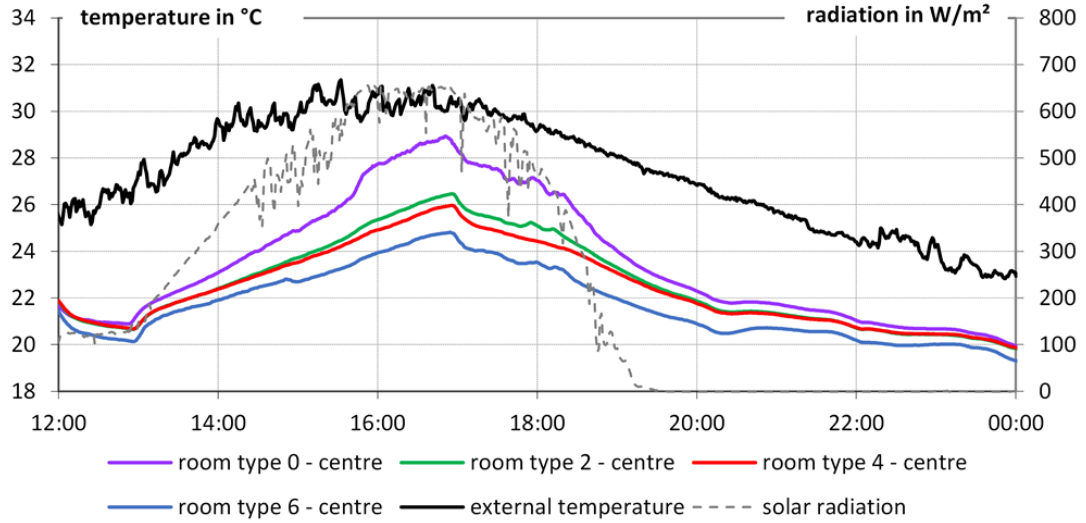

Figure 3.11: Operative temperature in the centre of the room ; façade: single storey double skin façade; shading system fully closed; the colours in the diagram are referring to 3.2

The summary of the measurement results for the single storey double skin façade and with fully closed shading system is done in table 3.7.

The change from single skin façade to single storey double skin façade leads to a reduction of the operative temperature of 1.2 K next to the façade and 0.7 K in the centre of the room (both values are for room 02, comparison of room type 1 and 2). The change of the shading system from screen to blinds (comparison of room type 2 and 4) show a reduction of 0.3 K next to the façade and an increase of 0.3 K in the centre of the room. The results of room type 6 (additional cooling elements) show a reduction of operative temperature of 1.7 K next to the façade and in the centre of the room (comparison with room type 2).

Table 3.7: Summary of measurement results of the maximum operative temperature in the centre of the room and next to the façade for the first measurement period. The results are for the façade system: single storey double skin façade and the shading system is fully closed

description	sensor location	
	1 m distance to the **façade**	**centre** of the room
room type 0	28.7 °C	28.0 °C
room type 2	27.1 °C	26.7 °C
room type 5	26.8 °C	27.0 °C
room type 6	25.4 °C	25.0 °C

3.3.5 Results: Single Storey Double Skin Façade, Shading System Half Opened

Figure 3.12 show the influence of different boundary conditions like shading type and cooling area for half closed shading systems. In figure 3.13 the results for the centre of the room are shown.

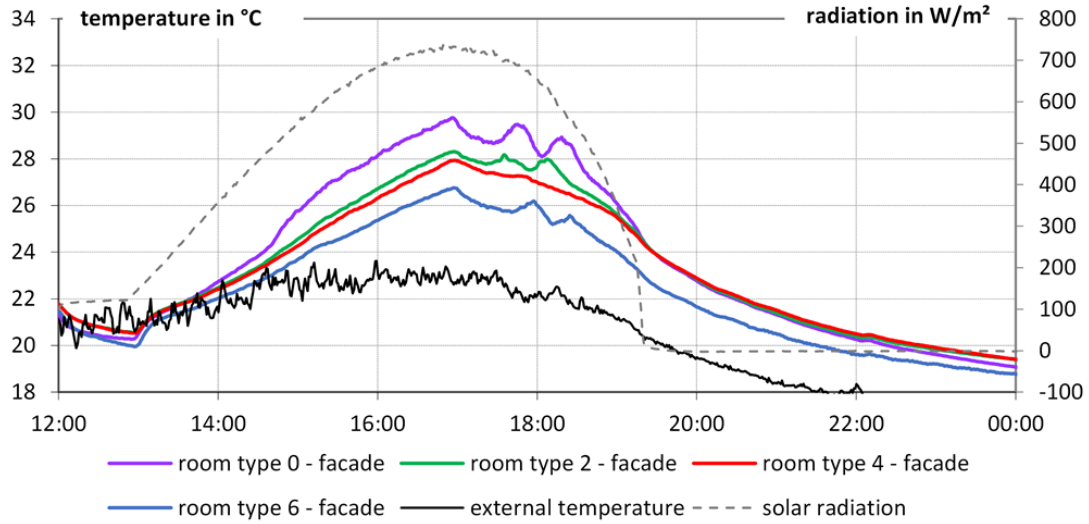

Figure 3.12: Operative temperature next to the façade; façade: single storey double skin façade; shading system half opened; the colours in the diagram are referring to 3.2

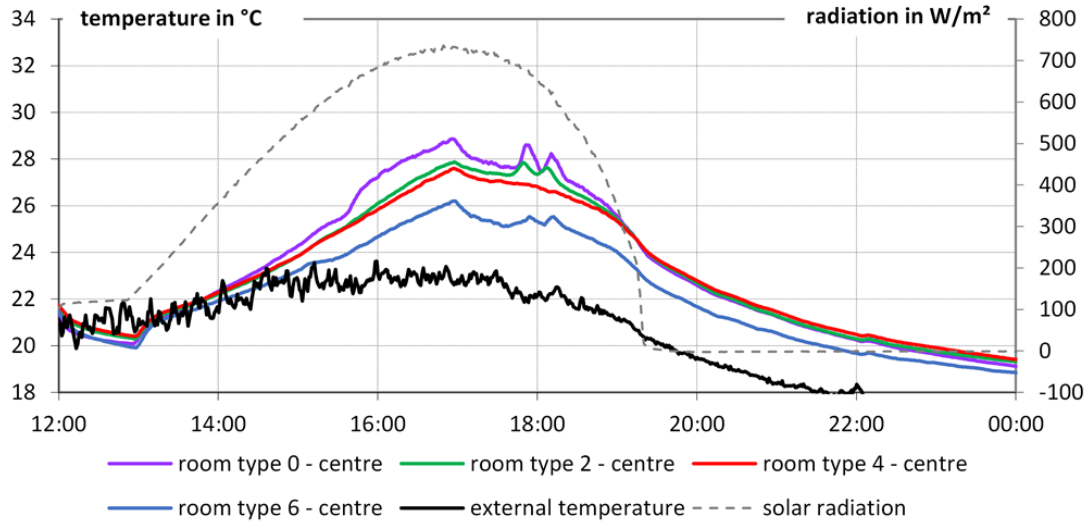

Figure 3.13: Operative temperature in the centre of the room ; façade: single storey double skin façade; shading system is half opened; the colours in the diagram are referring to 3.2

The summary of the measurement results regarding maximum operative temperature for the single storey double skin façade and with half closed shading system is done in table 3.8.

The change from single skin façade to single storey double skin façade leads to a reduction of the operative temperature of 1.6 K next to the façade and 1.2 K in the centre of the room (both values are for room 02, comparison of room type 1 and 2). The change of the shading system from screen to blinds (comparison of room type 2 and 4) show a reduction of 0.3 K for both measurement positions. The results of room type 6 (additional cooling elements) show a reduction of operative temperature of 1.6 K next to the façade and 1.8 K in the centre of the room (comparison with room type 2).

Table 3.8: Summary of measurement results of the maximum operative temperature in the centre of the room and next to the façade for the first measurement period. The results are for the façade system: single storey double skin façade and the shading system is half closed

description	sensor location	
	1 m distance to the **façade**	**centre** of the room
room type 0	-	-
room type 2	28.5 °C	28.1 °C
room type 5	28.2 °C	27.8 °C
room type 6	26.9 °C	26.3 °C

3.3.6 Summary of Measurement Results - First Summer Period

The measurement results show the impact of different boundary condition (see definition of the room types (3.2) on the operative temperature in the room on two positions - the first one next is to the façade and the second one is in the centre of the room. The results are summarized separately for the two measurement points.

Operative Temperature next to the Façade

In figure 3.14 the measurement results on operative temperature next to the façade are shown. The values represent the maximum operative temperature during the operative time (5pm values). The measurement results show a temperature difference of 1.4 K due to the change from screen type (different optical properties, see table 10.1). The enhanced façade system with the single storey double skin façade (room type 2) leads to a reduction of 1.2 K compared to room type 1 (single skin façade). The additional cooling elements in the façade area cause a reduction of the operative temperature of 1.1 K (also compared to room type 1.

The reduced use of the shading elements (half opened; the shading systems were opened 1.25 m from the bottom) to increase the sight to the outside (most used in this building) leads to the following differences on operative temperature: The change of the shading element from type 2 to type 3 (screen to blinds) reduces the operative temperature of 0.5 K (both situation with the single skin façade). The additional cooling elements lead to a reduction of the operative temperature of 1.4 K (compared with room type 1). The comparison of the single skin façade to the single storey double skin façade (values for room 2, comparison of room type 1 and 2) show a temperature difference of 1.5 K.

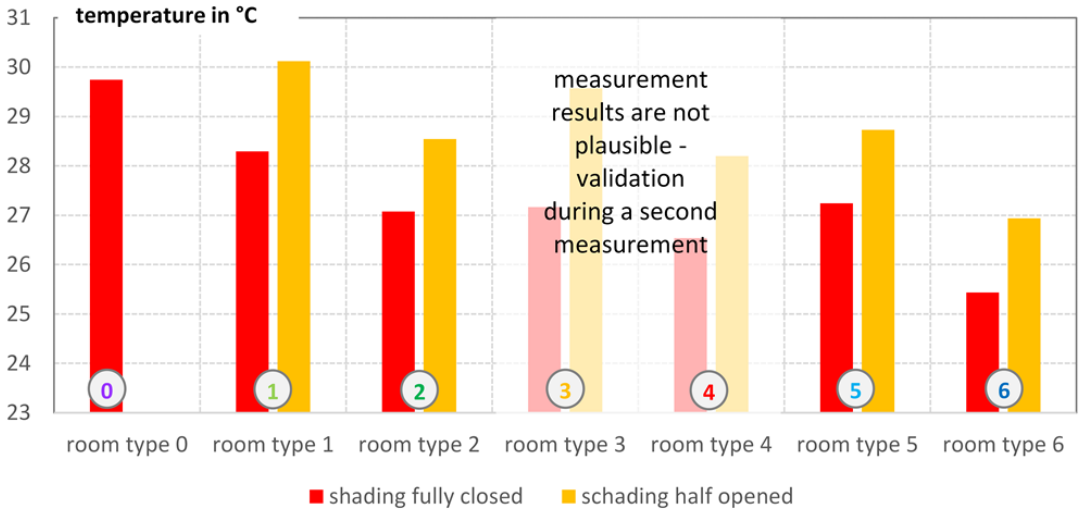

Figure 3.14: Operative temperature next to the façade; room types: table 3.2); red: fully closed shading elements; orange: half closed shading elements

Operative Temperature in the Centre of the Room

The measurement results with fully closed shading elements show, that the change of the screen type from type 1 to type 2 lead to a reduction of the operative temperature of 1.4 K. The change of the façade system from a single skin façade to the single storey double skin façade reduces the operative temperature in the middle of the room of about 0.6 K. The additional cooling elements in the façade area causes a reduction of the operative temperature of 1.1 K.

The change of the shading element from type 2 to type 3 (screen to blinds) reduces the operative temperature of 0.3 K (both situation with the single skin façade). The additional cooling elements lead to a reduction of the operative temperature of 1.5 K (compared with room type 1). The comparison of the single skin façade to the single storey double skin façade (values for room 2, comparison of room type 1 and 2) show a temperature difference of 1.3 K.

In figure 3.15 the results on maximum operative temperature during the operative time (5.00 pm values) for the different room types (description see table 3.2) are show. The red bars are regarding the results on fully closed shading elements, the orange ones represent the measurement results for half closed shading systems.

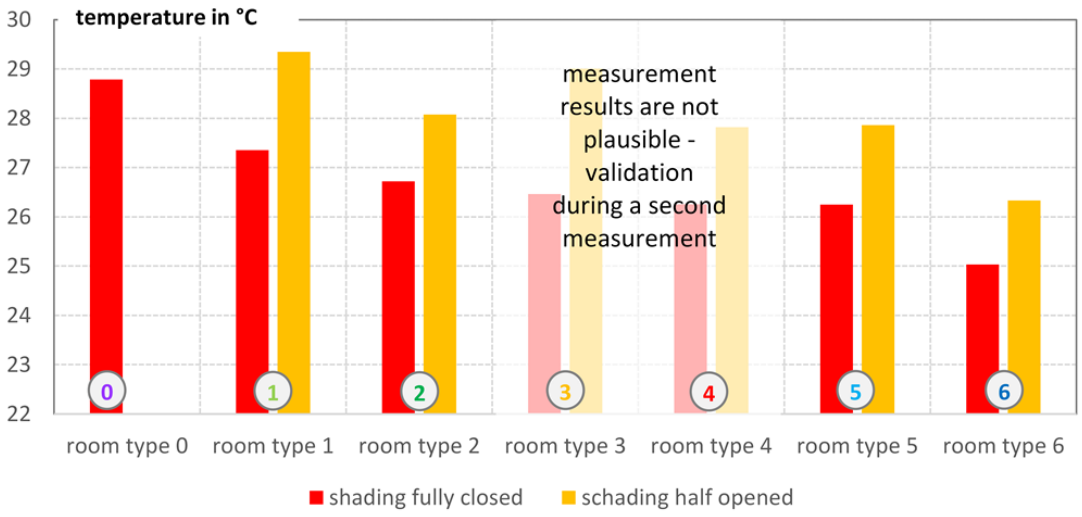

Figure 3.15: Operative temperature in the centre of the room room types: table 3.2); red: fully closed shading elements; orange: half closed shading elements

3.3.7 Measurement Results - Next to the Façade - Second Summer Period

Figure 3.16 shows the different operative temperatures during a warm sunny day for four different façade systems for one of the reference days during the second summer period. The black line is the ambient temperature, the dotted grey one the solar radiation (global; beam + diffuse) on the west façade. The maximum values for operative temperature are summarized in table 3.9 for three reference days with solar radiation during the second summer period. The results show that there is a temperature difference of about 5 K due to the different room set-up (different façade + shading system, additional cooling element).

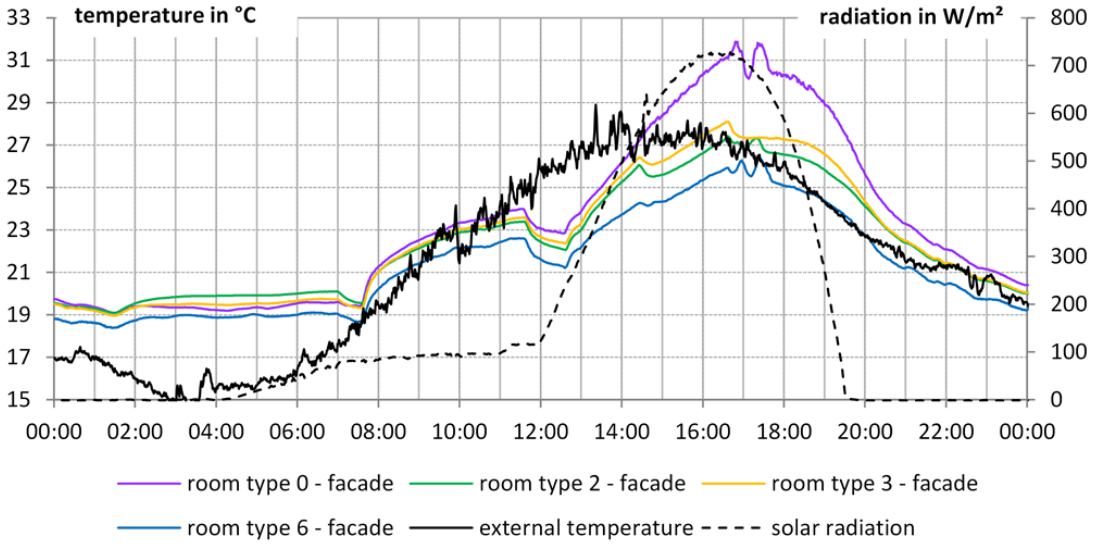

Figure 3.16: Operative temperature next to the façade for a warm sunny day for 4 room types - room type 0: reference room; room type 2: screen type 2, single storey double skin façade; room type 3: shading type 3, single skin façade; room type 6: shading type 2, single storey double skin façade, additional cooling elements

Table 3.9: Maximum operative temperature (5pm) next to the façade for three different days during the second summer period measurement for 4 room types - room type 0: reference room; room type 2: screen type 2, single storey double skin façade; room type 3: shading type 3, single skin façade; room type 6: shading type 2, single storey double skin façade, additional cooling elements

room type / measurement days		27.07.	19.08.	20.08.
room type 00	°C	31.0	29.8	30.0
room type 02	°C	26.8	26.3	26.5
room type 03	°C	27.4	26.5	26.7
room type 06	°C	26.1	24.8	25.0
external air temperature	°C	26.8	25.7	27.8
solar radiation	W/m²	710.6	583.3	615.8

In figure 3.17 results regarding maximum operative temperature (5pm values) for the measurement position next to the façade for the different room types are visualized. The measurements show that there is a decrease of 1.4 K due to the change of the shading type (from type 1 to type 2). The change from shading type 2 to shading type 3 cause a decrease of 0.9 K. The comparison of the operative temperature with the single skin façade and the single storey double skin façade show a temperature difference of 1.2 K (both measurements with shading type 2). With the additional cooling elements there is a reduce of the operative temperature of 1.5 K (comparison of room type 1 and room type 5)

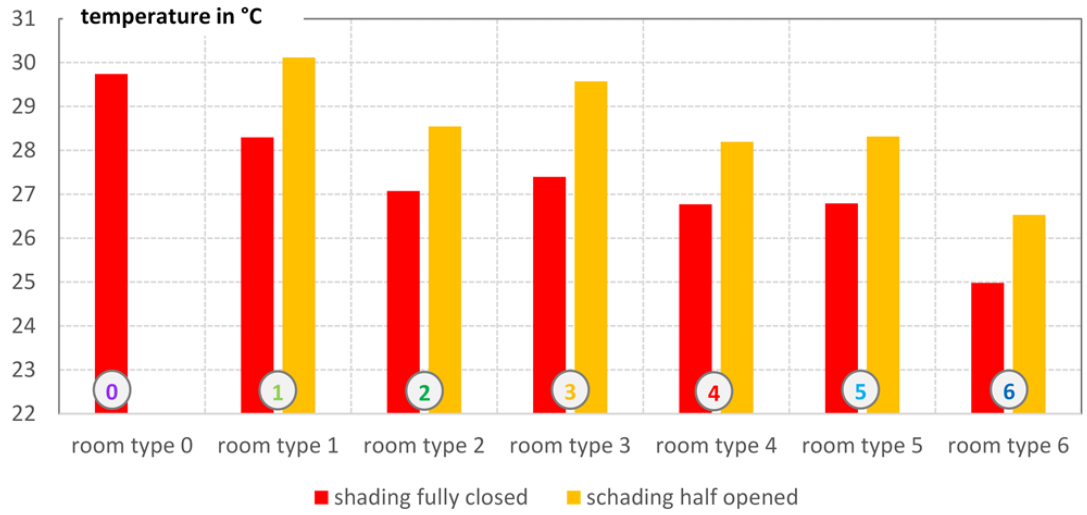

Figure 3.17: Summary of measurement results regarding maximum operative temperature (5pm values) for the position next to the façade for the different room types for the second summer period

3.3.8 Measurement Results - Centre of the Room - Second Summer Period

Figure 3.18 shows the different operative temperatures during a warm sunny day for four different room types. The black line is the ambient temperature, the dotted grey one the global solar radiation on the west façade. The maximum values for operative temperature are summarized in table 3.10 for three days with solar radiation during the second summer period. The results show that there is a temperature difference of about 4.5 K due to the different room set-up (different façade + shading system, additional cooling element).

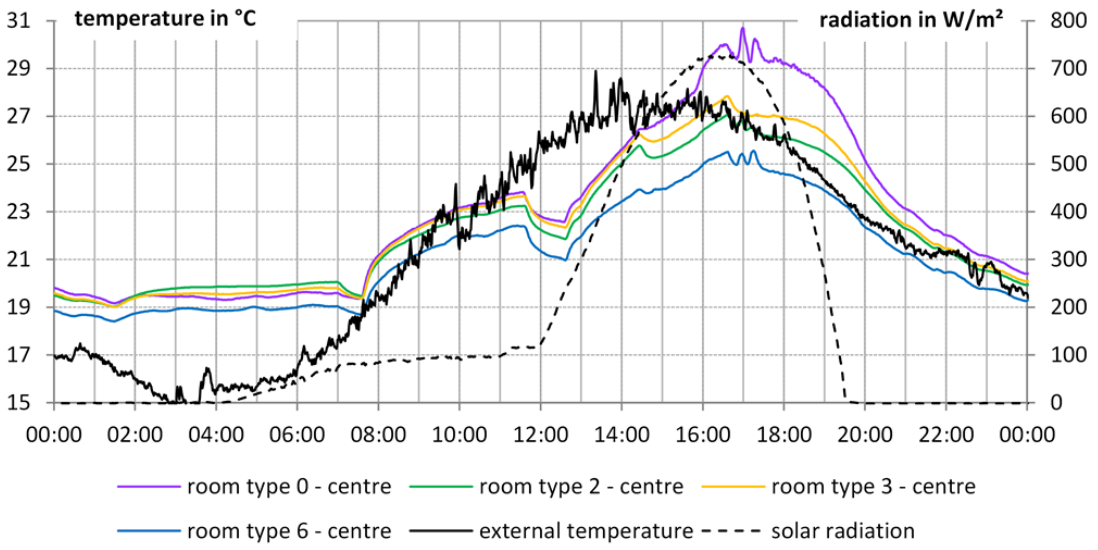

Figure 3.18: Operative temperature - centre of the room

Table 3.10: Maximum operative temperature (5pm) in the centre of the room for three different days during the second summer period measurement for 4 room types - room type 0: reference room; room type 2: screen type 2, single storey double skin façade; room type 3: shading type 3, single skin façade; room type 6: shading type 2, single storey double skin façade, additional cooling elements

room type / measurement days		27.07.	19.08.	20.08.
room type 00	°C	30.7	28.3	28.7
room type 02	°C	26.6	25.6	25.8
room type 03	°C	27.2	26.2	26.4
room type 06	°C	25.3	24.3	24.5
external air temperature	°C	26.8	25.7	27.8
solar radiation	W/m²	710.6	583.3	615.8

In figure 3.19 results regarding maximum operative temperature (5pm values) for the centre of the room for the different room types are visualized. The measurements show that there is a decrease of 1.4 K due to the change of the screen type (from type 1 to type 2). The change from screen type 2 to screen type 3 cause a decrease of 0.1 K, so these two shading systems are moretheless equal to the operative temperature in the centre of the room. The comparison of the operative temperature with the single skin façade and the single storey double skin façade show a temperature difference of 0.6 K (both measurements with screen type 2). With the additional cooling elements there is a reduce of the operative temperature of 1.1 K (comparison of room type 1 and room type 5)

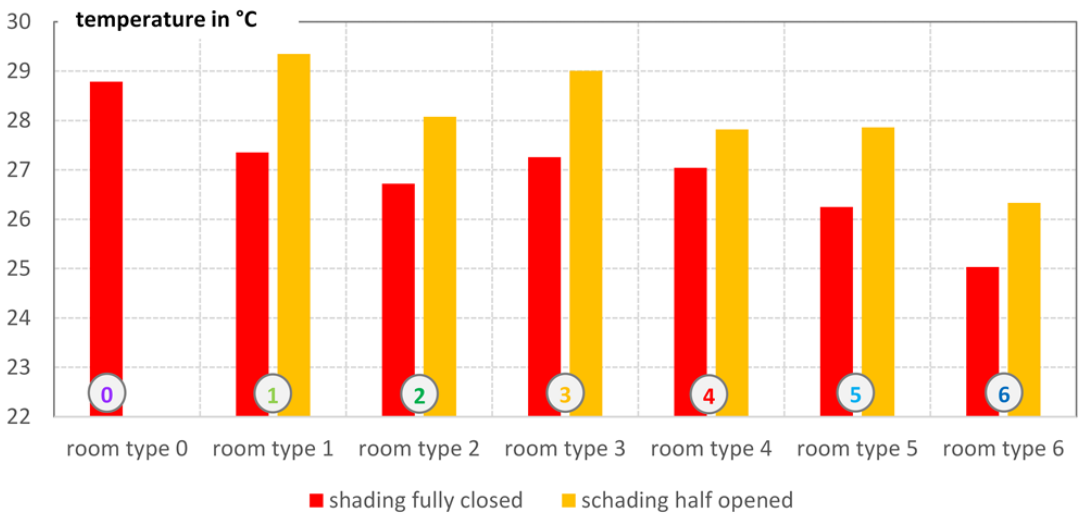

Figure 3.19: Summary of measurement results regarding maximum operative temperature (5pm values) for the centre of the room for the different room types for the second summer period

3.4 Summary in-situ Measurements - Operative Temperature

Through an intensive set of measurements different façade systems were tested due to the operative temperature in the centre of the room and close to the façade and the resulting cooling capacity. The room conditions were changed in the following three fields:

- change of shading system
- additional cooling element
- additional internal glazing

In figure 3.20 the result on the maximum operative temperature in the centre of the room for the different room types is shown. The change of the shading type from shading type 1 to shading type 2 reduces the maximum operative temperature of 1.4 K. The maximum operative temperature with room type 1 (shading type 2) is 27.4 °C. Due to the second glazing the operative temperature can be reduced of 0.7 K. With the additional cooling element the maximum operative temperature can be reduced of 2.5 K. The measured maximum operative temperatures and temperature difference to the reference room is shown in table 3.11.

Table 3.11: Summary of measurement results of the maximum operative temperature in the centre of the room

	Room type 0	Room type 1	Room type 2	Room type 3	Room type 4	Room type 5	Room type 6
temperature – totally closed	28.8 °C	27.4 °C	26.7 °C	27.3 °C	27.0 °C	26.2 °C	25.0 °C
temperature difference	-	- 1.4 K	- 2.1 K	- 1.5 K	- 1.7 K	- 2.5 K	- 3.8 K
temperature – half closed	-	29.3 °C	28.1 °C	29.0 °C	27.8 °C	27.9 °C	26.3 °C
temperature difference	-	+ 2.0 K	+ 1.4 K	+ 1.7 K	+ 0.8 K	+ 1.6 K	+ 1.3 K

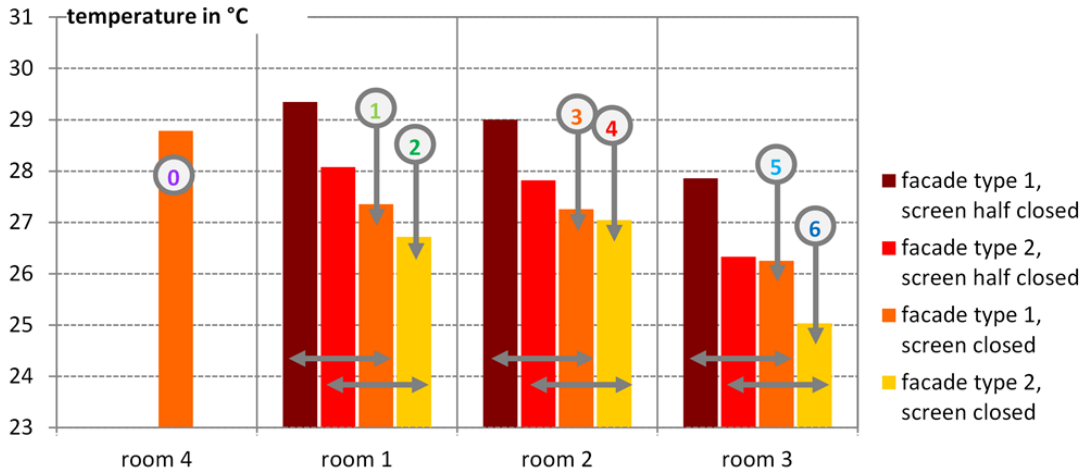

Figure 3.20: Measurement results on operative temperature - centre of the room

The measurement results next to the façade (distance of 1 m to the façade at the beginning of the working area) show a higher reduction of the maximum operative temperature. The results of the measurement are shown in figure3.21, the summary of the measured temperatures and the temperature difference to the reference room is shown in table 3.12. The change of the shading type from shading type 1 to shading type 2 reduces the maximum operative temperature of 1.4 K. The maximum operative temperature can be reduced of 1.2 K due to the second glazing from 28.3 °C (façade type 1) to 27.1 °C (façade type 2). With the additional cooling element there is a reduction of the maximum operative temperature of 2.9 K.

Table 3.12: Summary of measurement results of the maximum operative temperature next to the façade

	Room type 0	Room type 1	Room type 2	Room type 3	Room type 4	Room type 5	Room type 6
temperature – totally closed	29.7 °C	28.3 °C	27.1 °C	27.4 °C	26.8 °C	26.8 °C	25.4 °C
temperature difference	-	- 1.4 K	- 2.6 K	- 2.3 K	- 3.0 K	- 2.9 K	- 4.3 K
temperature – half closed	-	30.1 °C	28.5 °C	29.6 °C	28.2 °C	28.3 °C	26.9 °C
temperature difference	-	+ 1.8 K	+ 1.4 K	+ 2.4 K	+ 1.7 K	+ 1.5 K	+ 1.5 K

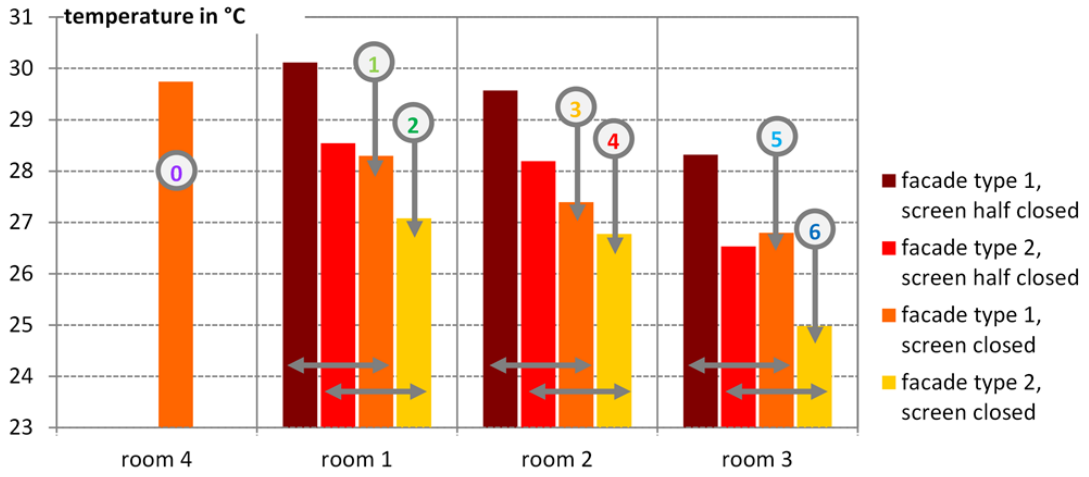

Figure 3.21: Measurement results on operative temperature - 1 m distance to the façade

4 Cooling Capacity of the Cooling Ceiling

4.1 Introduction

Using the existing regulations to calculate the capacity of cooling ceilings could lead to wrong results. The cooling load calculation according to VDI 2078 [6] considers the cooling load as a purely convective load and is unsuitable. Basic differences and potential error in calculating the cooling load according to standard - VDI 2078 [6] (simplified procedure) are:

- The calculation of the cooling load is carried out for a room air temperature, because of the high proportion of the radiation of the cooling ceiling the calculation regarding a room temperature, is more appropriate
- The storage capacity of the ceiling is significantly reduced by the installation of a cooling ceiling in the relevant ceiling surface. The premise of the weight factors according to the standard is a storable ceiling, therefore, the thermal storage capacity which is used in the calculation according to standard is too high.
- The convective heat transfer is significantly higher for cooling ceilings compared to horizontal ceiling surfaces
- The absorbed radiation of the cooled surface need to be dissipated by the cooling medium immediately, the calculation according to the standard is assuming a proportional distribution of the radiation within the room area. This assumption is very inconvenient for cooling ceilings

An extension of the standard (sheet 1) [1] has been worked out, these differences are intended to compensate. A new cooling load standard is in preparation which will take into account the potential errors in the load calculation for radiant cooling ceilings.

Furthermore the different effect of gains due to the façade system can result in a relevant difference of the capacity of cooling ceilings and on the comfort in rooms. Using EN ISO 7730 [11] could lead to underestimation of the energy balance if the direct solar radiation is not accounted for. The detailed calculation of the total solar energy transmittance for solar protection devices combined with glazing is given in the EN 13363-2 [3].

The literature study has shown that the cooling capacity of the cooling ceiling is affected by many boundary conditions and for a consideration and overall assessment, the cooling power must be considered as a function of the physical building constraints. To determine the cooling capacity of the test rooms (detailed description see chapter 2) measurements were performed and the results are summarized in this chapter.

4.2 Building / Room Set up

To develop methods to integrate the cooling capacity of cooling ceiling and the comfort in the room to an enhanced room model a series of measurements has been done in an existing office building with different room types (combination of façade system, shading system and active cooling area). The detailed description of the measurement set-up is done in chapter 2, a short summary regarding the main points of the measurement is done within this section.

There were built 4 identical rooms with 11 m^2, with west orientated glazed surfaces. The cooling of the test rooms is provided by cooling ceilings, the schema of the cooling is shown in figure 4.1.

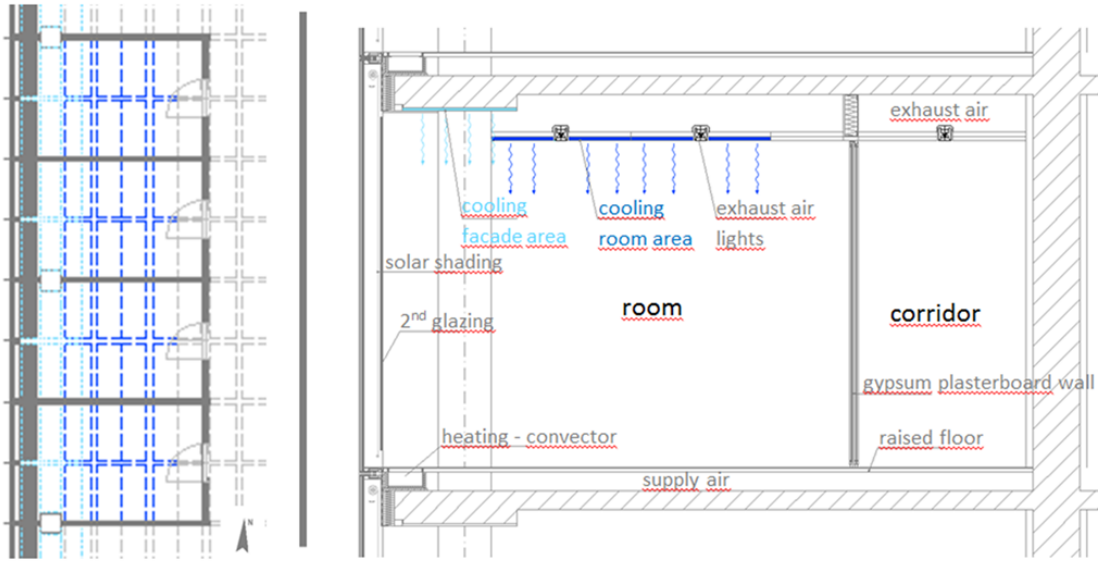

Figure 4.1: Schema of the cooling ceiling in the test rooms; left side - floor plan; right side - section view; the cooling ceiling is divided into two parts - the room area (dark blue) and the façade area (light blue); these two parts are arranged overlapping to increase the cooling capacity next to the façade

The flow and return temperature was measured by temperature meters. The mass flow was measured by differential pressure meter. Furthermore, the operative temperature was measured in different depths of the room by PT1000 temperature sensors in a black balls with a diameter of 10 cm, each at a height of 1.20 meter. Figure 4.2 shows the schematic diagram of the measuring points.

In total there the cooling capacity of 6 room types was measured. the summary of the measurement variations is shown in table 4.1, for the detailed description of the different room types see chapter 3 in section 3.2.2.

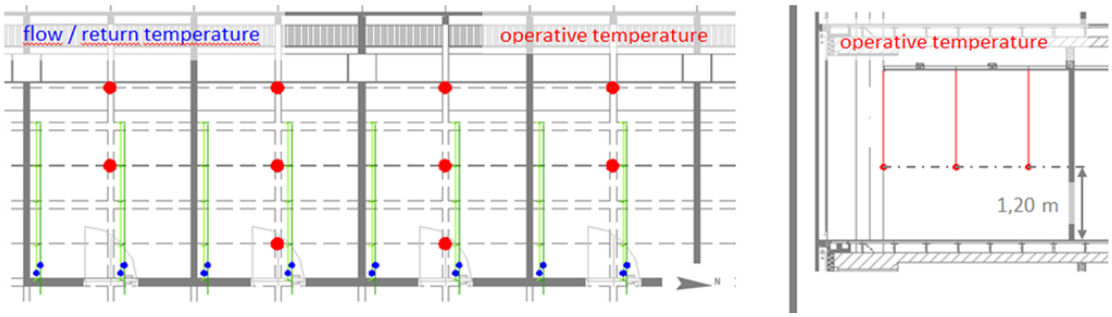

Figure 4.2: Schema of the cooling ceiling in the test rooms; left side - floor plan; right side section view; the blue points mark the measurement points of the flow and return temperature of the cooling medium; the red points mark the measurement position of the operative temperature

Table 4.1: summary measurement variation, room types (detailed description see chapter 3 in section 3.2.2)

name	room	façade	shading	additional cooling element
Room type 1	1	single skin	screen $\tau_L = 0{,}10$	---
Room type 2	1	single storey double skin	screen $\tau_L = 0{,}10$	---
Room type 3	2	single skin	blinds	---
Room type 4	2	single storey double skin	blinds	---
Room type 5	3	single skin	screen $\tau_L = 0{,}10$	yes
Room type 6	3	single storey double skin	screen $\tau_L = 0{,}10$	yes

The basis for the measurement of the cooling capacity of cooling ceilings is the EN 14240. The measurements were done in a real office building and not by test plant conditions. The system boundary of the measured rooms is the surrounding surfaces.

The cooling capacity is based on the average temperature difference between the operative temperature in the middle of the room and the mean medium temperature (see equation 4.1)

$$\Delta t = t_i - \frac{t_v + t_r}{2} \tag{4.1}$$

where

- t_i ... reference temperature (operative temperature in the centre of the room) in °C
- t_V ... flow temperature of the cooling water in °C
- t_R ... return temperature of the cooling water in °C

4.3 Cooling capacity for a day with solar radiation - single skin façade

The calculation of the specific cooling capacity is based on the active cooling area. The following sections describe the measurement results for the single skin façade (room type 1, room type 3 and room type 5).

The measurement results on cooling capacity are shown in dependence of the temperature difference between the operative temperature in the middle of the room and the mean medium temperature for each room. The dots represent the measurement results and the lines are the resulting approximation.

All measurement results are referring to a clear sunny day (with direct solar radiation).

4.3.1 Cooling capacity for a day with solar radiation - room type 1

In figure 4.3 the measurement results regarding the cooling capacity for room type 1 (single skin façade, shading type 2 (screen)) are shown. The points represent the measurement results and the line is the resulting approximation. Room type 1 represents the basic room conditions, the other room types are compared to room type 1.

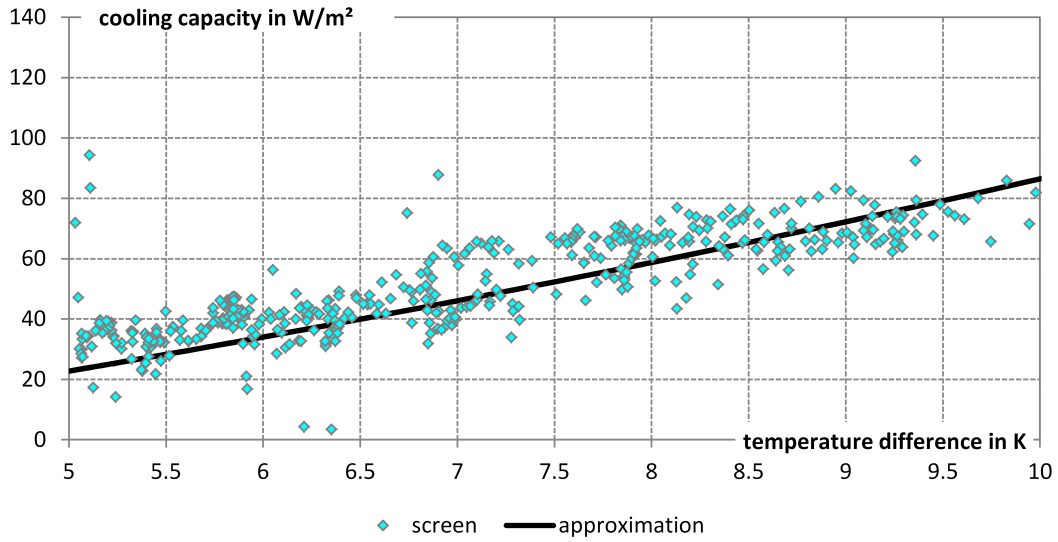

Figure 4.3: Measurement results for the cooling capacity of the cooling ceiling for room type 1 (single skin façade, shading type 2 (screen)); the dots represent the measurement results, the line is the resulting approximation; the values are referring to the active cooling area and not the floor area.

The measurement results for room type 1 show a cooling capacity of 82 $W/m^2_{coolingarea}$ in dependence of 9 K temperature difference between the operative temperature in the middle of the room and the mean medium temperature for room 01.

4.3.2 Cooling capacity for a day with solar radiation - room type 3

In figure 4.4 the measurement results regarding the cooling capacity for room type 3 (single skin façade, shading type 3 (blinds)) are shown. The points represent the measurement results and the line is the resulting approximation.The difference to room type 1 is the shading system - room type 1 uses screens and room type 3 blinds. The optical properties of these two shading systems can be found in chapter 2, section 2.2.2.

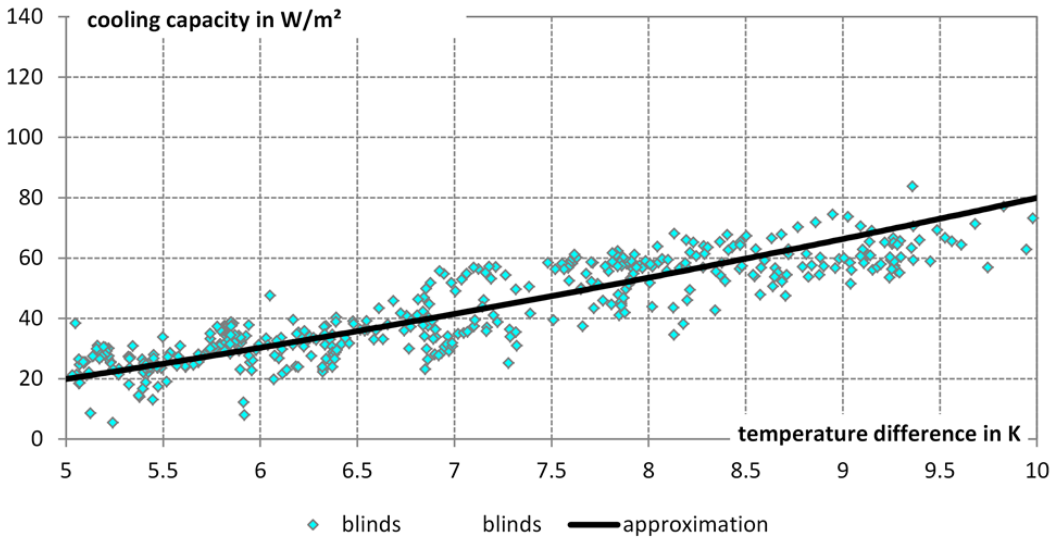

Figure 4.4: Measurement results for the cooling capacity of the cooling ceiling for room type 3 (single skin façade, shading type 3 (blinds)); the dots represent the measurement results, the line is the resulting approximation; the values are referring to the active cooling area and not the floor area.

The measurement results for room type 03 show a cooling capacity of 77 $W/m^2_{coolingarea}$ in dependence of 9 K temperature difference between the operative temperature in the middle of the room and the mean medium temperature for room 03. Compared to room type 01 the change of the shading system leads to a reduction of the cooling capacity of about 5 $W/m^2_{coolingarea}$.

4.3.3 Cooling capacity for a day with solar radiation - room type 5

In figure 4.5 the measurement results regarding the cooling capacity for room type 5 (single skin façade, shading type 2 (screen) plus additional cooling elements next to the façade) are shown. The points represent the measurement results and the line is the resulting approximation. The difference to room type 1 is the additional active cooling area due to the cooling elements next to the façade.

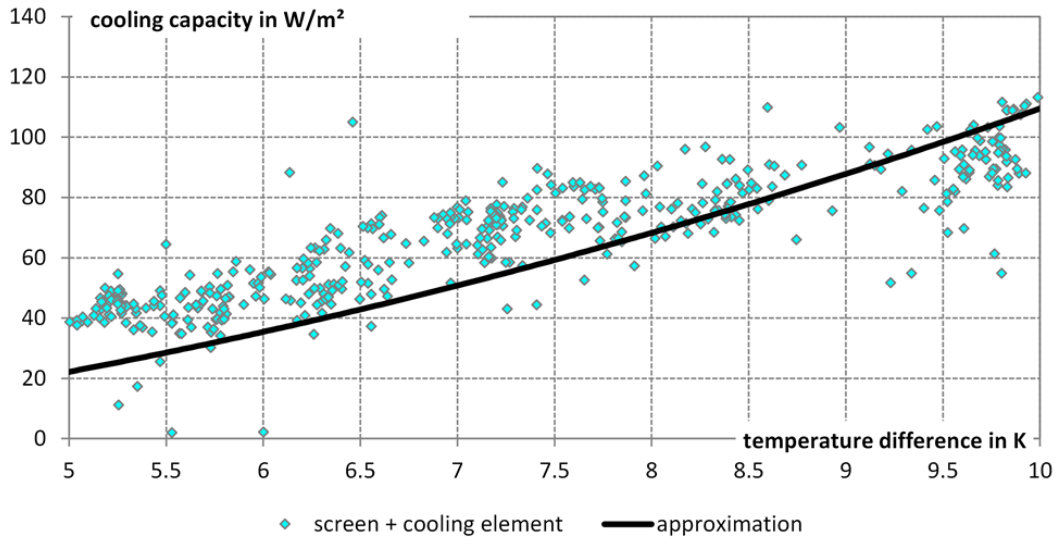

Figure 4.5: Measurement results for the cooling capacity of the cooling ceiling for room type 5 (single skin façade, shading type 2 (screen) plus additional cooling elements next to the façade); the dots represent the measurement results, the line is the resulting approximation; the values are referring to the active cooling area and not the floor area.

The measurement results for room type 05 show a cooling capacity of 88 $W/m^2_{coolingarea}$ in dependence of 9 K temperature difference between the operative temperature in the middle of the room and the mean medium temperature for room 03. Compared to room type 01 the additional cooling elements lead to an increase of the cooling capacity of about 6 $W/m^2_{coolingarea}$.

4.4 Cooling capacity for a day with solar radiation - single storey double skin façade

The calculation of the specific cooling capacity is based on the active cooling area. The following sections describe the measurement results for the single storey double skin façade (room type 2, room type 4 and room type 6).

The measurement results on cooling capacity are shown in dependence of the temperature difference between the operative temperature in the centre of the room and the mean medium temperature for each room. The dots represent the measurement results and the lines are the resulting approximation.

All measurement results are referring to a clear sunny day (with direct solar radiation).

4.4.1 Cooling capacity for a day with solar radiation - room type 2

In figure 4.6 the measurement results regarding the cooling capacity for room type 02 (single storey double skin façade, shading type 2 (screen)) are shown. The points represent the measurement results and the line is the resulting approximation. The difference to room type 11 is the change of the façade system from single skin façade to single storey double skin façade.

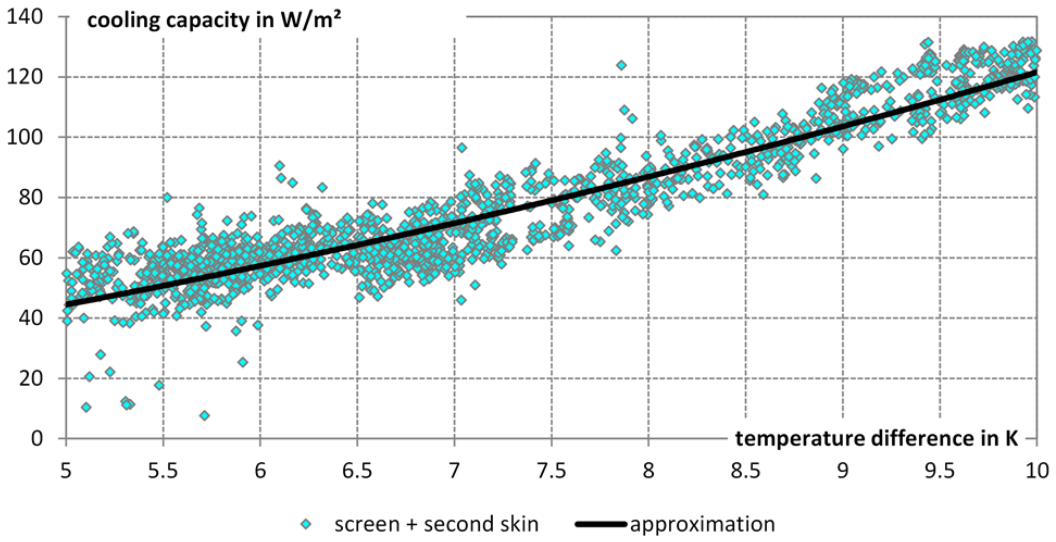

Figure 4.6: Measurement results for the cooling capacity of the cooling ceiling for room type 2 (single storey double skin façade, shading type 2 (screen)); the dots represent the measurement results, the line is the resulting approximation; the values are referring to the active cooling area and not the floor area.

The measurement results for room type 02 show a cooling capacity of 102 $W/m^2_{coolingarea}$ in dependence of 9 K temperature difference between the operative temperature in the

middle of the room and the mean medium temperature for room 03. Compared to room type 01 the change from single skin façade to single storey double skin façade leads to an in increase of the cooling capacity of about 20 $W/m^2_{coolingarea}$.

4.4.2 Cooling capacity for a day with solar radiation - room type 4

In figure 4.7 the measurement results regarding the cooling capacity for room type 04 (single storey double skin façade, shading type 3 (blinds)) are shown. The points represent the measurement results and the line is the resulting approximation. There are two differences to room type 1, first the change of the shading system from screens to blinds and second the change of the façade system from single skin façade to single storey double skin façade.

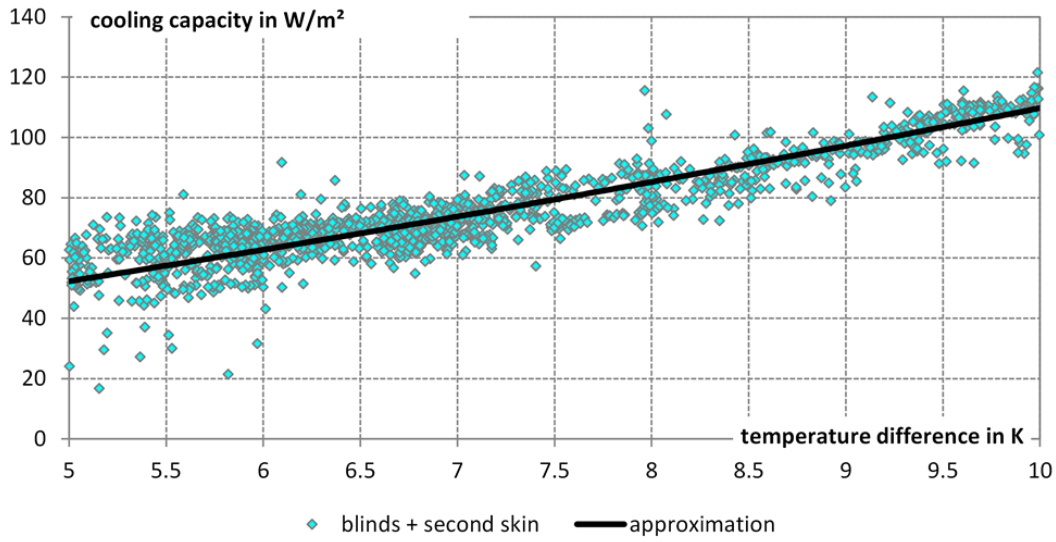

Figure 4.7: Measurement results for the cooling capacity of the cooling ceiling for room type 4 (single storey double skin façade, shading type 3 (blinds)); the dots represent the measurement results, the line is the resulting approximation; the values are referring to the active cooling area and not the floor area.

The measurement results for room type 02 show a cooling capacity of 98 $W/m^2_{coolingarea}$ in dependence of 9 K temperature difference between the operative temperature in the middle of the room and the mean medium temperature for room 03. The comparison to the basic room set-up (room type 1) show that the change from single skin façade to single storey double skin façade and the change of the shading system leads to an in increase of the cooling capacity of about 16 $W/m^2_{coolingarea}$. The change of the shading system tends to result in a small decrease of the cooling capacity. Compared to room type 03 the change from single skin façade to single storey double skin façade leads to an in increase of the cooling capacity of about 21 $W/m^2_{coolingarea}$.

4.4.3 Cooling capacity for a day with solar radiation - room type 6

In figure 4.8 the measurement results regarding the cooling capacity for room type 06 (single storey double skin façade, shading type 2 (screen) plus additional cooling elements next to the façade) are shown. The points represent the measurement results and the line is the resulting approximation. The differences to room type 1 are the façade system - single storey double skin façade instead of single skin façade and the additional active cooling area in the façade zone.

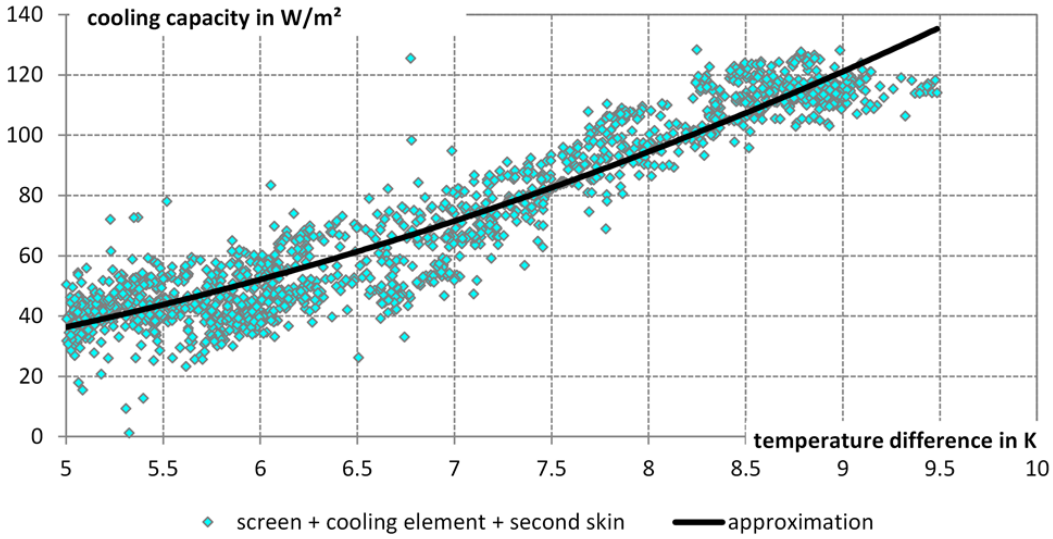

Figure 4.8: Measurement results for the cooling capacity of the cooling ceiling for room type 6 (single storey double skin façade, shading type 2 (screen) plus additional cooling elements next to the façade); the dots represent the measurement results, the line is the resulting approximation; the values are referring to the active cooling area and not the floor area.

The measurement results for room type 2 show a cooling capacity of 120 $W/m^2_{coolingarea}$ in dependence of 9 K temperature difference between the operative temperature in the middle of the room and the mean medium temperature for room 03. The comparison to the basic room set-up (room type 1) show that the change from single skin façade to single storey double skin façade and the additional cooling elements lead to an in increase of the cooling capacity of about 38 $W/m^2_{coolingarea}$. Compared to room type 5 the change from single skin façade to single storey double skin façade leads to an in increase of the cooling capacity of about 18 $W/m^2_{coolingarea}$.

4.5 Cooling capacity for a day without direct solar radiation

The measurement was evaluated for a cloudy day too, the results are presented in this section. The mean impact for the cooling capacity for the cloudy days is due to internal loads and there is an impact because of diffuse radiation. The measurement results show rather flat lines and there is only a small difference between the room types. In detail there were presented the results for 3 room types - room type 2 (single storey double skin façade, shading system 2 (screen)), room type 3 (single skin façade, shading system 3 (blinds)) and room type 6 (single storey double skin façade, shading system 2 (screen), additional cooling elements). There are no significant differences between the room types, therefore not all results were presented. These three room types represent the full range of applied values.

4.5.1 Cooling capacity for a day without direct solar radiation - room type 2

In figure 4.9 the measurement results regarding the cooling capacity for room type 2 (single storey double skin façade, shading type 2 (screen)) are shown. The points represent the measurement results and the line is the resulting approximation.

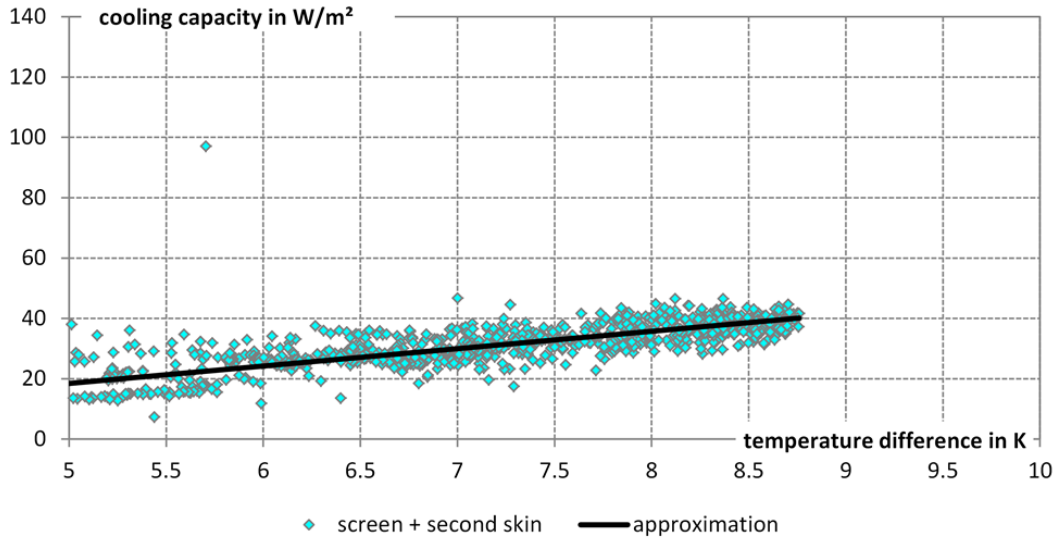

Figure 4.9: Measurement results for the cooling capacity of the cooling ceiling for room type 2 (single storey double skin façade, shading type 2 (screen)); the dots represent the measurement results, the line is the resulting approximation; the values are referring to the active cooling area and not the floor area.

The measurement results for room type 2 show a cooling capacity between 20 $W/m^2_{coolingarea}$ and 40 $W/m^2_{coolingarea}$ in dependence of the temperature difference between the operative temperature in the middle of the room and the mean medium temperature.

4.5.2 Cooling capacity for a day without direct solar radiation - room type 3

In figure 4.10 the measurement results regarding the cooling capacity for room type 3 (single skin façade, shading type 3 (blinds)) are shown. The points represent the measurement results and the line is the resulting approximation.

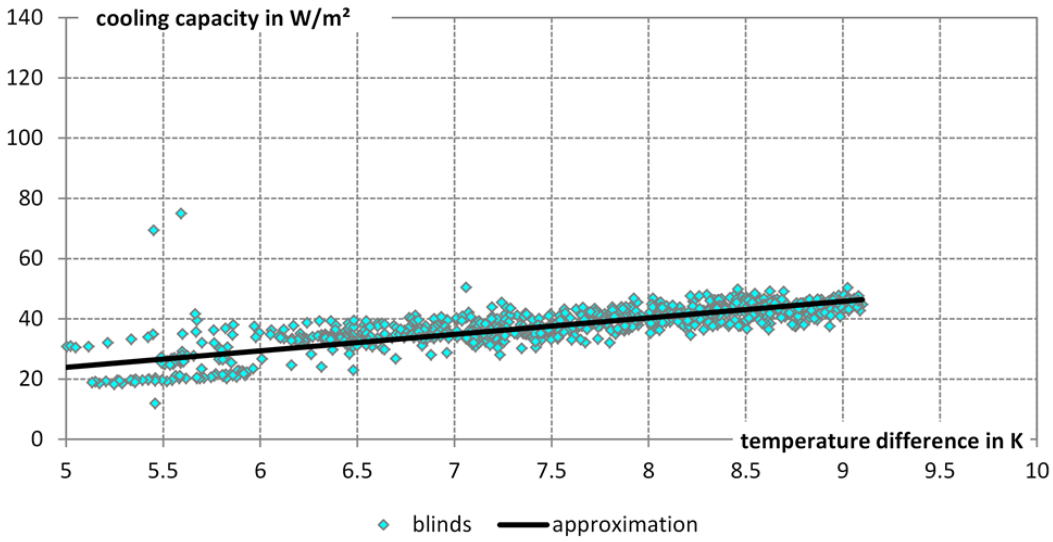

Figure 4.10: Measurement results for the cooling capacity of the cooling ceiling for room type 3 (single skin façade, shading type 3 (blinds)); the dots represent the measurement results, the line is the resulting approximation; the values are referring to the active cooling area and not the floor area.

The measurement results for room type 3 show a cooling capacity between 22 $W/m^2_{coolingarea}$ and 42 $W/m^2_{coolingarea}$ in dependence of the temperature difference between the operative temperature in the middle of the room and the mean medium temperature. Compared with the results of room type 2 there are no significant differences.

4.5.3 Cooling capacity for a day without direct solar radiation - room type 6

In figure 4.11 the measurement results regarding the cooling capacity for room type 6 (single storey double skin façade, shading type 2 (screen) plus additional cooling elements next to the façade) are shown. The points represent the measurement results and the line is the resulting approximation.

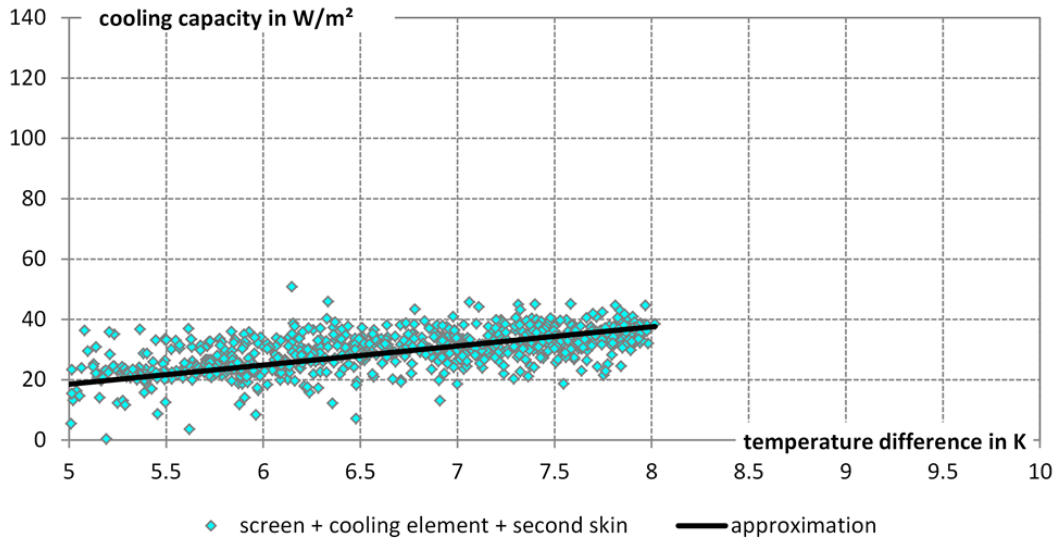

Figure 4.11: Measurement results for the cooling capacity of the cooling ceiling for room type 6 (single storey double skin façade, shading type 2 (screen) plus additional cooling elements next to the façade); the dots represent the measurement results, the line is the resulting approximation; the values are referring to the active cooling area and not the floor area.

The measurement results for room type 6 show a cooling capacity between 20 $W/m^2_{coolingarea}$ and 40 $W/m^2_{coolingarea}$ in dependence of the temperature difference between the operative temperature in the middle of the room and the mean medium temperature. Compared with the results of room type 2 and 3 there are no significant differences.

4.6 Single skin façade versus single storey double skin façade

For the summary the results between the single skin façade and the single storey double skin façade were figured out.

The calculation of the specific cooling capacity is based on the active cooling area. In figure 4.12 there are shown the measurement results on the cooling capacity in dependence of the temperature difference between the operative temperature in the centre of the room and the mean medium temperature for room type 01 on the left side and for room type 02 on the right side. The dots represent the measurement results and the line is the resulting approximation. The measurement results show an increase due to the change from single skin façade to double skin façade.

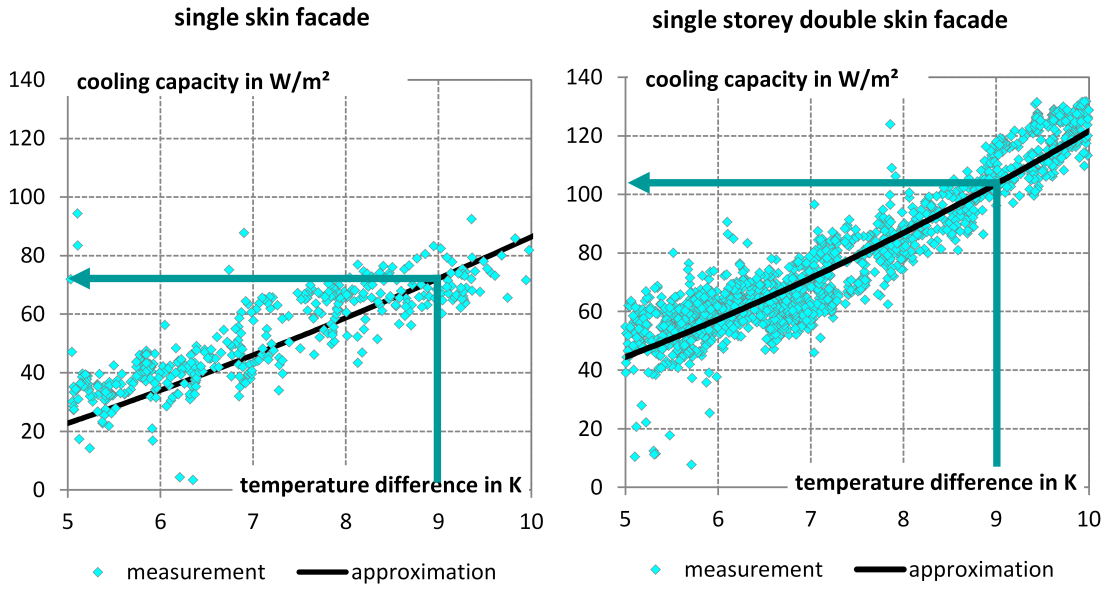

Figure 4.12: Measurement results regarding the change from single skin façade to single storey double skin façade; the measurement results are taken from room 01

In figure 4.13 the difference is shown for each room type, the results are summarized in the following itemization:

- comparison of room type 1 and 2 show an in crease of about 20 $W/m^2_{coolingarea}$
- comparison of room type 3 and 4 show an in crease of about 21 $W/m^2_{coolingarea}$
- comparison of room type 5 and 6 show an in crease of about 18 $W/m^2_{coolingarea}$

The measurements were done for each room system for a clear sunny day and for a cloudy day. The difference between the cooling capacities for these two days is shown in figure 4.14 for room type 1 on the left side and room type 2 on the right side. The dotted lines shows the cloudy day, where the mean impact is due to internal loads and there is an impact because of diffuse radiation. The line is rather flat and there is only

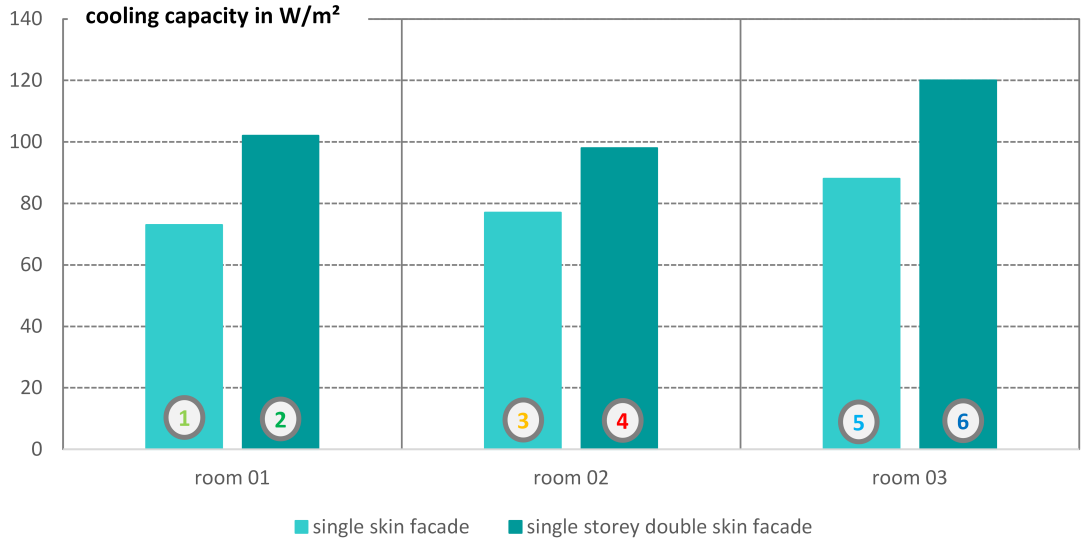

Figure 4.13: Measurement results regarding the change from single skin façade to single storey double skin façade for all room types; room 01: room type 1 and 2; room 02: room type 3 and 4; room 03: room type 5 and 6

a small difference between room type 01 and room type 02. The continuous line shows the approximation of the measurement result of the cooling capacity on a clear sunny day and there is a stronger increase due to the solar impact and a difference between the two façade systems.

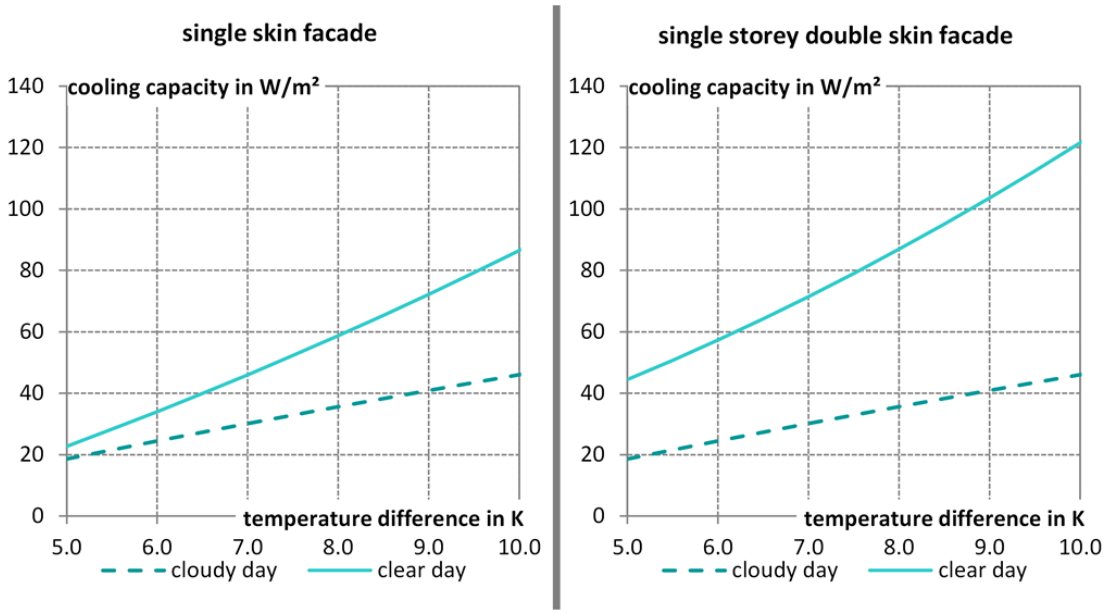

Figure 4.14: Difference on cooling capacity due to the change from single skin façade (left side) to single storey double skin façade (right side); dotted lines: results cloudy days; continuous lines: results clear days

4.7 Summary cooling capacity for all room types

The summary of the measurement results visualize, that there is an impact on the cooling capacity by different room set-ups. There is an increase of the cooling capacity of about 20 $W/m^2_{coolingarea}$ in dependency of the temperature difference between the operative temperature in the centre of the room and the mean medium temperature due to the change of the façade system from single skin façade to single storey double skin façade. The resulting cooling capacities of the different room types are shown in figure 4.15. The colour of the lines is referring to the description of the room types, which is summarized in table 4.2, the detailed description of the room types can be found in chapter 3 in section 3.2.2

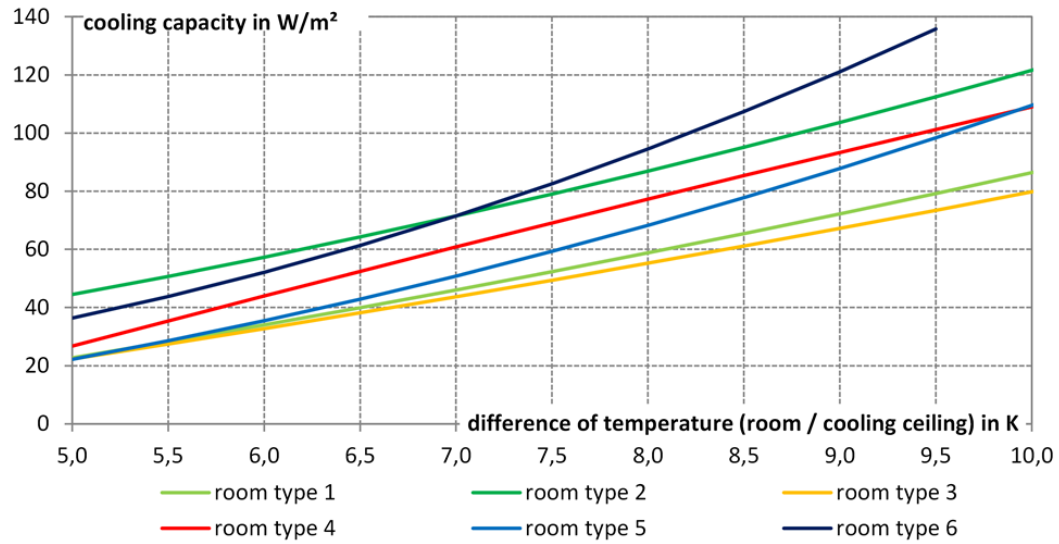

Figure 4.15: Comparison of the cooling capacity of different room types

Table 4.2: Summary measurement variation, room types (detailed description see chapter 3 in section 3.2.2)

name	room	façade	shading	additional cooling element
Room type 1	1	single skin	screen $\tau_L = 0{,}10$	---
Room type 2	1	single storey double skin	screen $\tau_L = 0{,}10$	---
Room type 3	2	single skin	blinds	---
Room type 4	2	single storey double skin	blinds	---
Room type 5	3	single skin	screen $\tau_L = 0{,}10$	yes
Room type 6	3	single storey double skin	screen $\tau_L = 0{,}10$	yes

The measurement results show that there is an increase of the cooling capacity due to different façade systems. The verification of the assumption, that the capacity increase is because of a higher air flow rate over the ceiling and therefore a higher convection load, can be done by the mathematical model and is one of the topic for further analysis.

5 Tracer Gas Measurement

5.1 Introduction

The aim of the tracer gas measurements is to clarify how the façade system and the cooling ceiling impacts the air movement within a room. Therefore the measurements with different inject locations and different room set ups were done.

One part of the results show the impact of different façade systems – single skin façade versus single storey double skin façade on the air movement. The measurements show an increase of concentration within the ceiling zone which is attributed to a higher air flow rate over the ceiling. Furthermore different set ups of the cooling ceilings were measured – one with natural ventilation over the suspended cooling ceiling and the other one without natural ventilation. The measurement results show that there is a decrease of concentration due to the missing natural ventilation.

The measurement results show a clear difference in the rate of concentration on different room points due to the solar radiation, the location of impact and the room set up.

5.2 In-situ measurement - Building Information

The detailed description of the test rooms and the general measurement set-up is done in chapter 2.2. A short summary regarding the main points of the tracer gas measurements is done in this section.

The measurement was done in an existing office building. On the 34th floor a test room of about 11 m^2 is situated, this is typical for a single person office in Austria. As the room is situated on the 34th floor, there is no shading due to other buildings or geographical surroundings. The façade is a west-orientated totally glazed façade.

Figure 5.1 shows the floor plan (left side) and the section view (right side) of the measurement room. The floor is raised which is caused to its air leading properties (the supply air is realized over the raised floor) open throughout the whole storey. It is not possible to close the floor, because then the test room would be without fresh air. The suspended ceiling of the measurement rooms is separated by a foreclosure (mineral wool) around the room. The suspended ceiling in the corridor area is used as exhaust air duct.

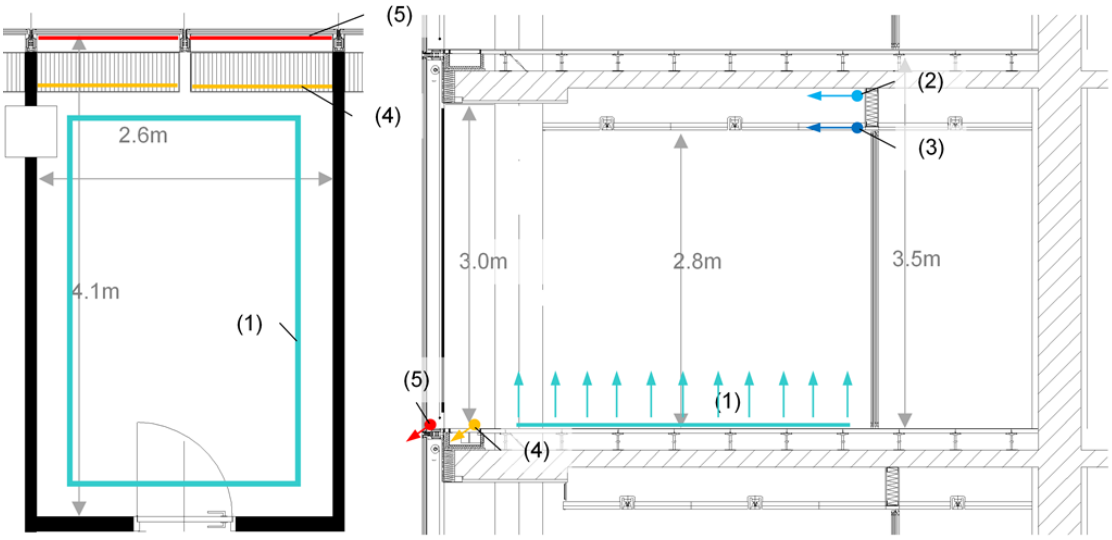

Figure 5.1: Floor plan (left side) / section (right side); location of tracer gas injection is highlighted; floor plan: direct injection to the room (1); concrete ceiling (2) cooling ceiling (3); supply air area (4); façade area (5)

The U-Values of the surrounding areas of the room are summarized in the following list:

- glazing: U = 1.10 $W/(m^2\ K)$
- frame (percentage 8%): U = 2.95 $W/(m^2\ K)$
- ceiling / floor: U = 1.47 $W/(m^2\ K)$
- interior wall (gypsum cardboard): U = 0.65 $W/(m^2\ K)$
- interior door: U = 1.80 $W/(m^2\ K)$

There is the possibility to change the façade system from a single skin façade to a single storey double skin façade by adding a second internal glazing element. These two façade systems were tested, both with an internal shading element. The difference between these two façade variations are shown in figure 3, there the difference is highlighted between picture 1 and 3, or between 2 and 4.

5.2.1 Cooling

The cooling of the rooms is done by a suspended cooling ceiling with capillary pipe mats, which are place in the ceiling panels. The cooling area is slitted into a façade area and a room area, these are overlapping so that there is a higher capacity in the façade area. For the room area of the measurement room the active area of the cooling ceiling is 5.56 m^2 and for the façade area it is 3.19 m^2. Overall there is an active cooling area of 8.75 m^2, based on the room area there is a rate of cooling area of about 80 %.

Through the measurement the boundary conditions of the suspended cooling ceiling was changed, one time with and one time without natural ventilation over the cooling ceiling. The difference on room conditions is shown in figure 5.3, for the cooling ceiling

picture 1 and 3 are without natural ventilation and the 2nd and the 4th one are with natural ventilation.

5.2.2 Ventilation

There is a mechanical ventilation system. The design of the ventilation system is as full air conditioning – heating, cooling / dehumidification and humidification.

The supply air for the room is realized via the raised floor, the whole floor is air leading. The air outlet is over “slot diffusers” next to the façade. There is a design volume flow rate of about 50 m^3/h (2.0 1/h) for the room with a supply air temperature of about 21 °C.

The exhaust air is realized by exhaust air lights (light fixture combined with extract air terminals). There are flexible ducts between the lights and the suspended ceiling in the corridor the idea of doing the return air in this way is to remove the heat were it is generated. The suspended ceiling in the corridor is air leading as well.

5.3 Measurement Set up

The goal of the measurement is to paint a picture of the air flow movement in the room and to see if it’s changing by different façade situations. Therefore a series of tracer gas measurements was done. The ASHREA Handbook of fundamentals (2009) [14] describes three different tracer gas methods to determine the air change rate:

- concentration decay or growth method
- constant concentration method
- constant injection method

The concentration decay method, measuring the decay of tracer gas is the simplest and most often used method. Using single point measurements the following three conditions should strictly be satisfied. For single point measurements the tracer gas should be uniformly mixed in the enclosure, there should be no unknown tracer gas sources and the ventilation flow should be the dominant means of the tracer gas removal from space to get reliable results (according ASHREA Handbook of fundamentals (2009) [14]).

According Charlesworth (1988) [37] it is very difficult to achieve a uniformly mixture of the tracer gas in the entire enclosure of in-situ measurements. To solve this problem tracer gas concentrations should be measured at several points of the considered areas and it’s assumed that the mean value is the average concentration for the entire enclosure. As tracer gas carbon dioxid (CO_2) was used, as described in Laussmann (2011) [34] it fulfils the specification of a good tracer gas.

5.3.1 Sensor Location

To measure the room a grid of 27 CO_2 sensors was set up. In figure 5.2 the position of the CO_2 sensors is shown, where the left side is the floor plan and the right side shows the section of the room.

The measurement itself was done by CO_2 injections and the concentration at the measurement points was logged. A defined amount of CO_2 was injected on five different positions of the room, the different impact locations are highlighted in figure 5.1:

- Inj 1: directly into the room, floor area (by a frame with small openings)
- Inj 2: ceiling – height of the concrete ceiling
- Inj 3: ceiling – height of the suspended cooling ceiling
- Inj 4: Supply air area
- Inj 5: Façade area

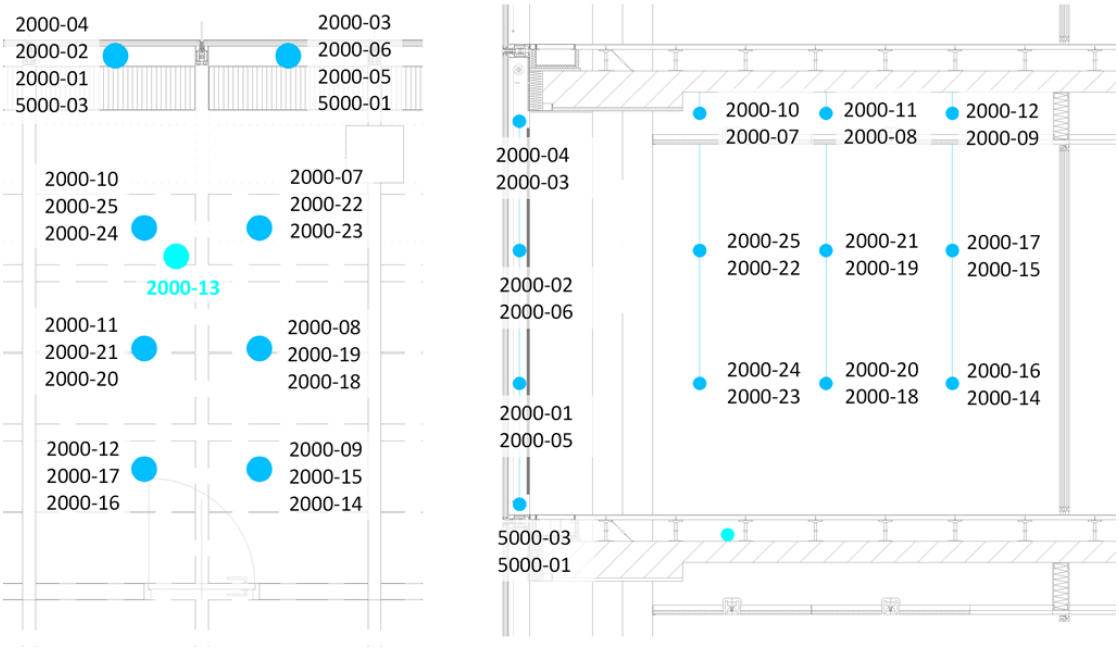

Figure 5.2: Measurement set up – floor plan (left side) and section (right side) including the sensor numbers, where the first 4 numbers are the maximum concentration rate and the last 2 are the numbers referring to the evaluation diagrams

5.3.2 Measurement Variations

The measurement was done with a single skin façade and a single storey double skin façade and with an open suspended ceiling and a closed suspended ceiling (figure 5.3). For the tracer gas measurement the following 4 room types were tested:

- Room type 1: single skin façade, closed suspended cooling ceiling (sskin+closedc)
- Room type 2 single skin façade, open suspended cooling ceiling (sskin+openc)
- Room type 3: single storey double skin façade, closed suspended cooling ceiling (dskin+closedc)
- Room type 4: single storey double skin façade, open suspended cooling ceiling (dskin+openc)

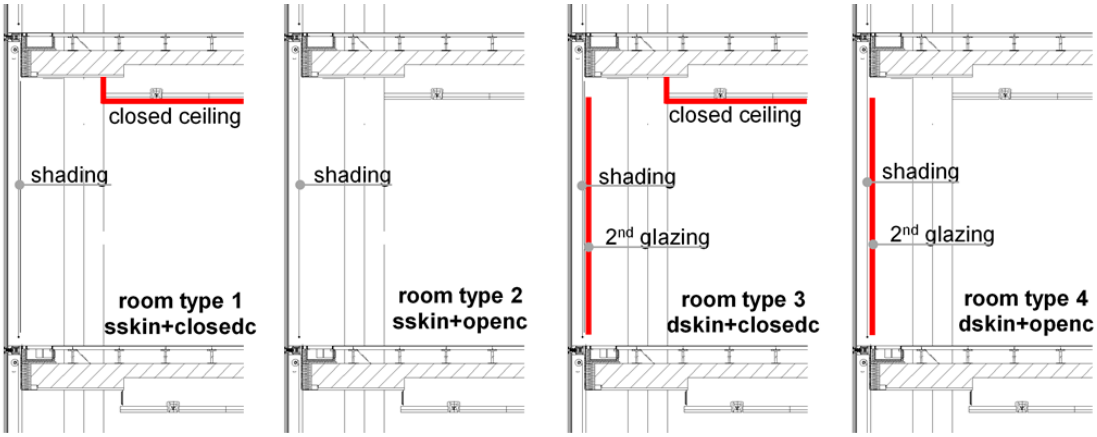

Figure 5.3: Schematic overview of the four different room types; from left to right: single skin façade+closed suspended cooling ceiling; single skin façade+open suspended cooling ceiling, single storey double skin façade+closed suspended cooling ceiling; single storey double skin façade+open suspended cooling ceiling

In total there were measured 40 different variants with different boundary conditions (overview see table 5.1). Each variant was measured twice, one time with a clear sunny sky and the other time with a cloudy sky. The measurement period for each variant is 1 hour due to the air change rate of the room. The measurement interval is 10 seconds.

Table 5.1: Overview of the measurement variants

Nr.	location of injection					solar radiation		room type			
	Inj 01	Inj 02	Inj 03	Inj 04	Inj 05	with	With-out	1	2	3	4
1	x					x		x			
2		x				x		x			
3			x			x		x			
4				x		x		x			
5					x	x		x			
6	x					x			x		
7		x				x			x		
8			x			x			x		
9				x		x			x		
10					x	x			x		
11	x					x				x	
12		x				x				x	
13			x			x				x	
14				x		x				x	
15					x	x				x	
16	x					x					x
17		x				x					x
18			x			x					x
19				x		x					x
20					x	x					x
21	x						x	x			
22		x					x	x			
23			x				x	x			
24				x			x	x			
25					x		x	x			
26	x						x		x		
27		x					x		x		
28			x				x		x		
29				x			x		x		
30					x		x		x		
31	x						x			x	
32		x					x			x	
33			x				x			x	
34				x			x			x	
35					x		x			x	
36	x						x				x
37		x					x				x
38			x				x				x
39				x			x				x
40					x		x				x

5.4 Measurement results tracer gas measurement

5.4.1 Decay curves - CO_2 concentration

As a result of the measurement there are curves of concentration for each variant and each sensor. The measurement period for one variant is 1 hour, but the main air movement is within the first 10 minutes, then the concentration is equal within the room (see figure 5.5 and 5.6)

Figure 5.5 visualize the measurement results for room type 4 (single storey double skin façade+open ceiling) for the different locations in the room. The results are for a clear sunny day and the CO_2 impulse was injected directly into the room. In the diagram there are results for different room heights, where the green line represents the measurement points in 1 m height, the orange dotted line the measurement results for 2 m room height and the red line the measurement results for the ceiling (schematic overview of measurement points and colours referring to the results in figure 5.5 are shown in figure 5.4).

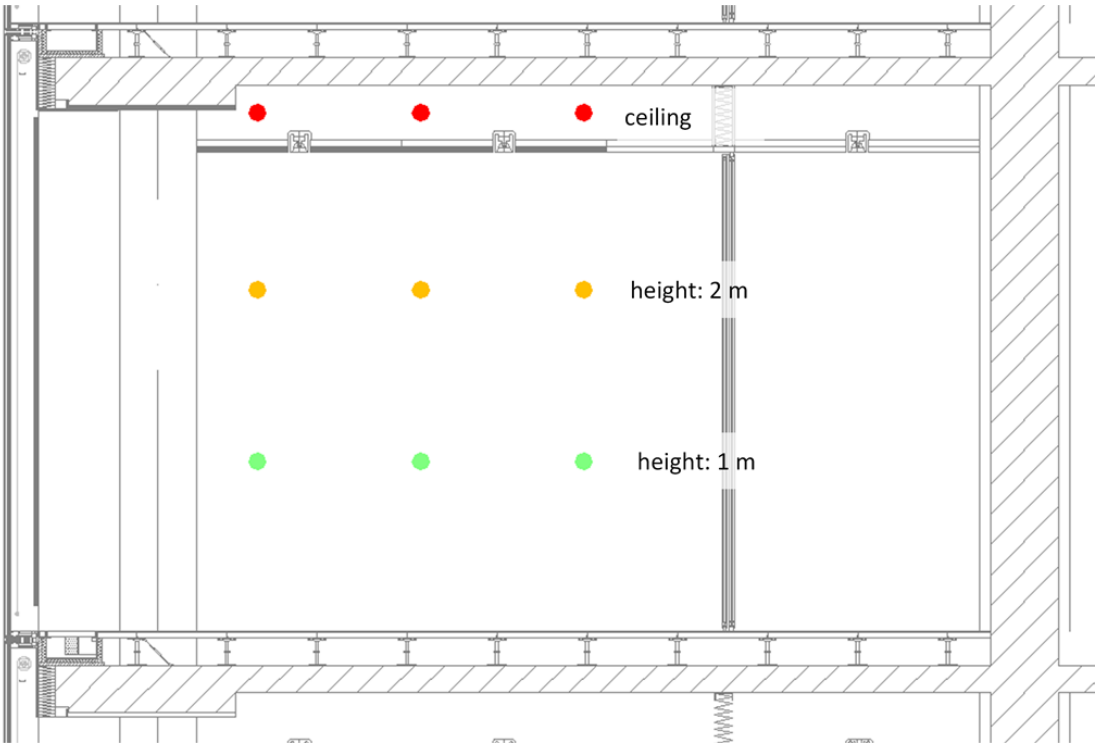

Figure 5.4: Schematic overview of measurement points and colours referring to the results in figure 5.5

The location of the measurement is marked in the diagram at the right corner. The figure shows the change of concentration for different locations within the room and the measurement results indicate that there is no big difference of concentration due to the room location.

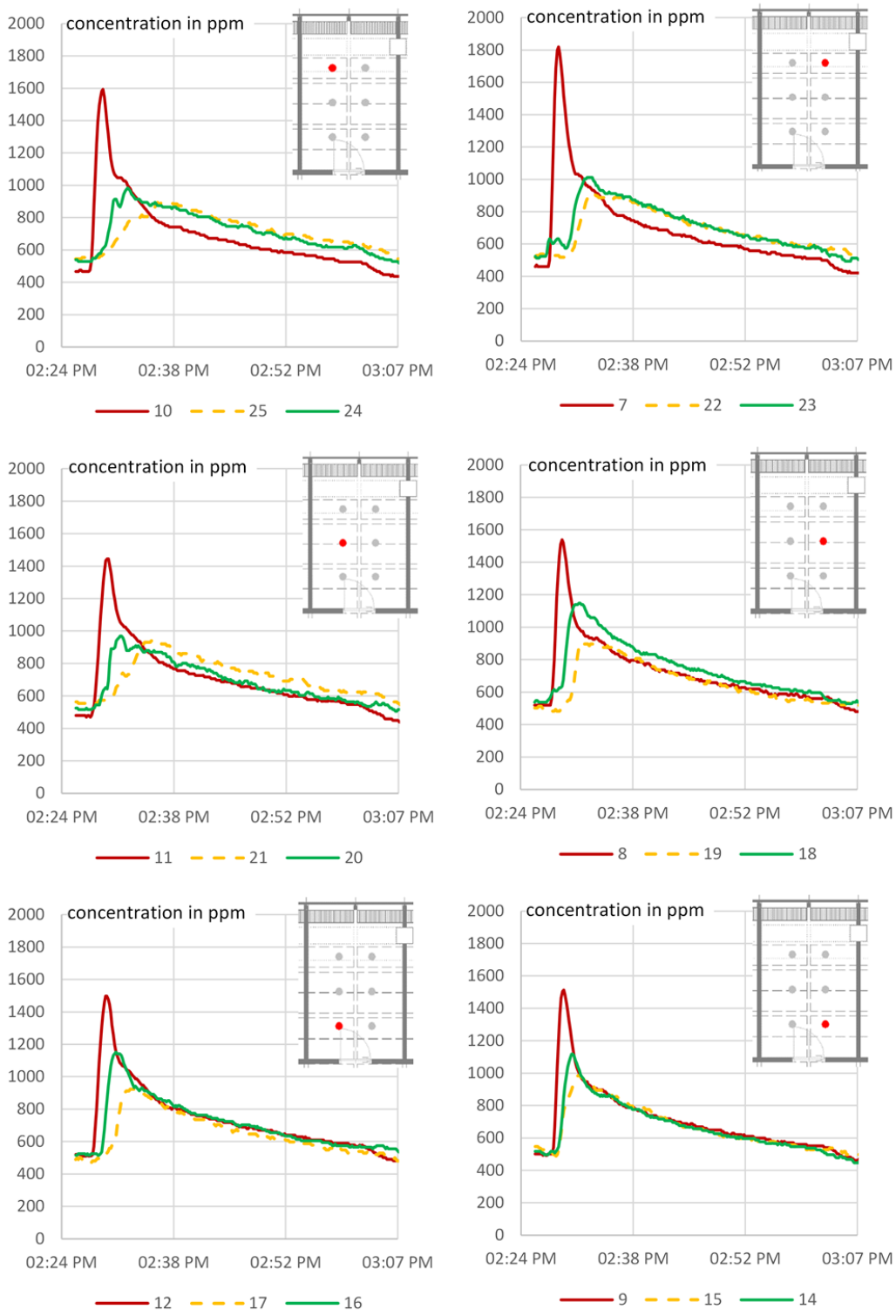

Figure 5.5: Measurement result of CO_2 concentration a different location in the room with the impact in the room for room type 4, the numbers shown in the legend are referring to the numbers of the sensor (last two numbers in fig 2). The diagrams show that there is no big difference in concentration within the defined zones.

5.4.2 Location of Injection - Impact on the results

The summary of the results for the difference of the CO_2 concentration in the different room areas by different location of injection are shown in figure 5.6 for room type 4 (single storey double skin façade+open suspended ceiling) with solar radiation.

The green line represents the concentration in the raised floor and is constant within the whole measurement period. The other lines show the different room areas (the room itself (blue dotted), the façade area (yellow) and the ceiling area(red)). The diagram shows that there is an “air roll”, the highest concentration rate with the injection direct to the room is in the façade area, the second highest concentration rate is in the ceiling area and the room itself has the smallest concentration rate. With the injection of tracer on the cooled layer (3rd part of the diagram) the results show a rapid declension of a cold air-stream, first the concentration raises within the room area and then in the façade area and the ceiling area.

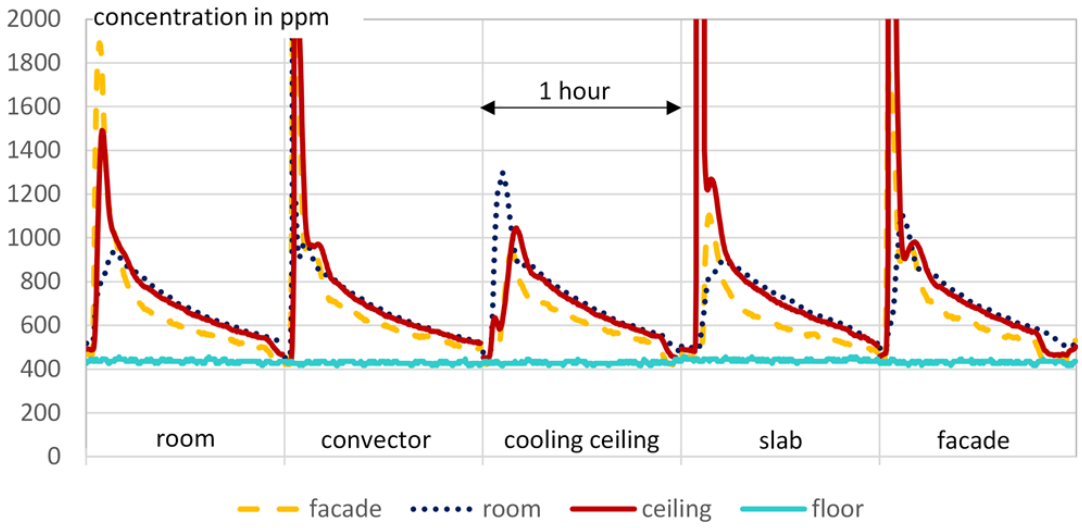

Figure 5.6: Measurement result of CO_2 concentration by different impact location for room type 4 (dskin+openc); with solar radiation; measurement period 1 hour for each variant; different concentrations in the specified areas within the first 10 minutes, after the first 10 minutes the concentration is equal in each area independent of the impact location

5.4.3 Summary of results for a day with solar radiation

In figure 5.7 there is the summary of the measurement results for the four different room types for a day with solar radiation visualized.

Figure 5.7 shows the first 10 minutes after the CO_2 injection directly into the room. The values in the diagram are the mean values of concentration for the room area, the façade area, the suspended ceiling and the raised floor. The concentration of the raised floor is not changing during the whole measurement, so there is no mass flow from the room to the floor.

The different rate of concentration in the suspended cooling ceiling show the difference in the air flow over the cooling ceiling. The measurement results show an increase of air flow due to the single storey double skin façade (comparing room type sskin+openc and dskin+openc) and a decrease of air flow due to the closed ceiling (comparing room type sskin+openc and sskin+closedc to room types dskin+openc and dskin+closedc).

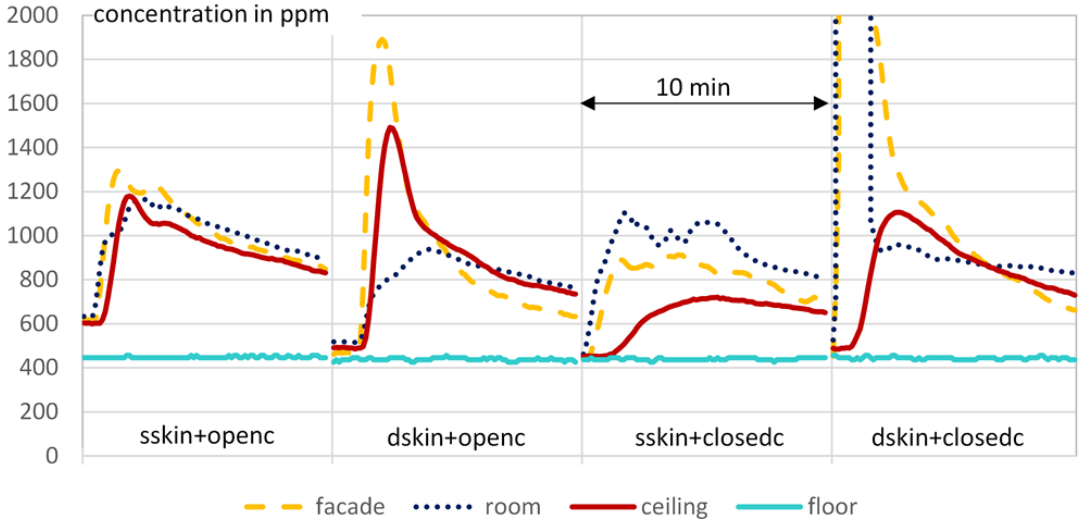

Figure 5.7: Measurement results of CO_2 concentration for the different room types with solar radiation, the tracer gas injection directly into the room (floor area). The diagram shows an increase of concentration in the ceiling area due to the single stores double skin façade and a decrease due to the lack of natural ventilation for the cases with the closed suspended ceiling.

5.4.4 Summary of results for a day without solar radiation

In figure 5.8 the results for the four different room types for a day without solar radiation are visualized. There is almost no difference of concentration between the room types. Due to the lack of buoyancy there is no air roll and the air movement is very small.

In figure 5.8 the first 10 minutes after the CO_2 injection direct into the room are shown. The values in the diagram are the mean values of concentration for the room area (blue), the façade area (yellow), the suspended ceiling (red) and the raised floor (green).

The different rate of concentration in the suspended cooling ceiling show the difference in the air flow over the cooling ceiling due to the tested boundary conditions of the room. The measurement results for the case without solar radiation show almost no difference of concentration.

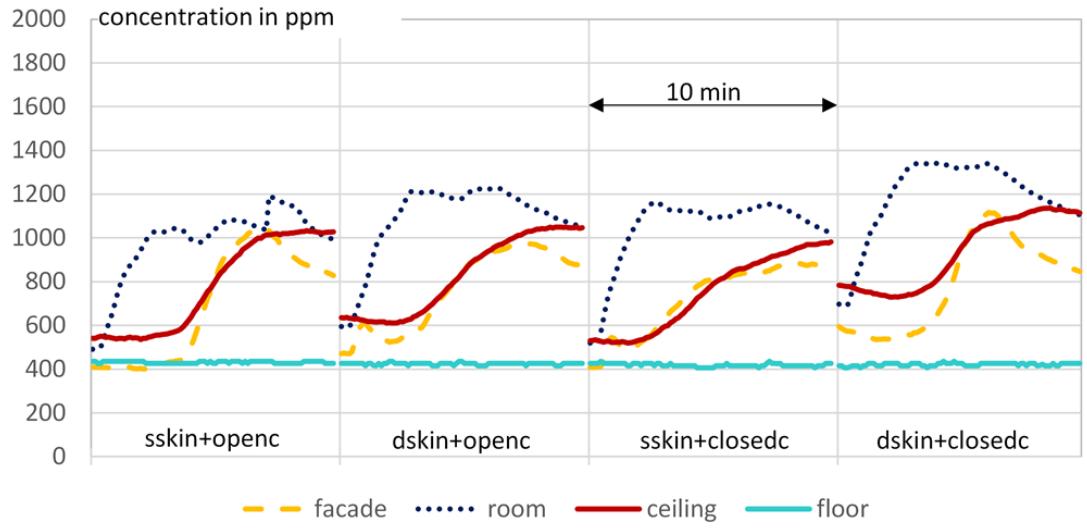

Figure 5.8: Measurement results of CO_2 concentration for the different room types without solar radiation, the tracer gas injection directly into the room (floor area). The diagram shows that there is almost no difference of concentration between the room types.

5.5 Conclusions tracer gas measurement

Through an set of tracer gas measurements the impact of air flow due to different room conditions (façade system, cooling system) were evaluated. The tracer gas measurement results show the impact by different concentration rates. The location of injections has no impact on the decay curves after the first 10 minutes.

The single storey double skin façade leads to a significant increase of tracer gas concentration within the ceiling zone. The maximum concentration within the suspended ceiling variate between 720 ppm (room type 1) and 1491 ppm (room type 4). Due to the second glazing there is an increase of 350 ppm. The difference between the open and the closed ceiling is about 420 ppm.

The measurement results show an impact on the air flow due to different boundary conditions. The next step for the model development is the detailed mathematical modeling of the air flow network within the room, which is done by CFD. To reach the aim of the research, which is the development of a simplified room model which includes the dynamic of three dimensional flow phenomena and can determine the impact on comfort with reasonable accuracy, the set of tracer gas measurement is one part of the model validation.

6 Thermal Modeling

6.1 Basic Information

The thermal modeling of buildings is done to fully understand the thermal behaviour of buildings. A huge range of thermal simulation tools like Energy Plus, Ida Ice, ESP-r, TRNSYS,... exist to investigate the thermal performance of buildings. Each of these programs have advantages and disadvantages within the models. The comparison of simulation tools is done in Crawley et al. (2005) [19] were twenty simulation programs were compared in terms of

- general model features like
- zone loads like
- Building Envelope, Daylighting and Solar like
- infiltration, ventilation, room air and multizone airflow
- renewable energy systems
- electrical systems and equipment
- HVAC systems
- HVAC equipment
- environmental emissions
- climate data availability
- economic evaluation
- resulting reports
- validation
- user interface, links to other programs and availability

Smaller research studies in the comparison of simulation programs is done e.g. by Veken et al. (2004) [50] and Sousa (2014) [46]. The study of Veken et al. (2004) [50] compares the simlation tools EPW, TRNSYS and ESP-r regarding their calculation of the net energy demand. The resarch work in Sousa (2014) [46] is regarding features in the programs Energy Plus, ESP-r, IDA ICE, IES VE and TRNSYS.

Feist [20] gives a good overview of different aspects in thermal building simulation. Different model approaches are described and compared like:

- instationary thermal conduction processes (Fourier)
- air flow networks (Navier-Stokes)
- radiation exchange between surfaces (Planckssches law)
- transmission, absorption and reflection of solar radiation
- control strategies for heating systems
- heat gains within the room

- infiltration and ventilation

For the development of a simplified room model a thermal model was set up in Matlab/Simulink. The mathematical model is based on separate modules, the model of the ”international Building Physics Toolbox” by Angela Sasic Kalagasidis (2007) [41] was used as template. The thermal model consists of four main groups - (1) construction, (2) zone, (3) systems and (4) sources and weather. The calculation of the room temperature and the capacity of the cooling ceiling was done with linked energy balances, wherein the calculation of components was done one-dimensional. In the following sections the boundary conditions, the geometry and the calculation of the heat flow through the individual layers is described.

6.1.1 Room Geometry / Zones

For the calculation, the rooms were divided into 5 zones like it's shown in figure 6.1. The calculation zones are listed in the following list:

- zone 01: room
- zone 02: façade
- zone 03: cooling ceiling - façade area
- zone 04: cooling ceiling - room area
- zone 05: raised floor

In figure 6.1 the main impaction parameters are visualized, like the external influences due to temperature and radiation, the infiltration, the mechanical ventilation system and the heating and cooling system.

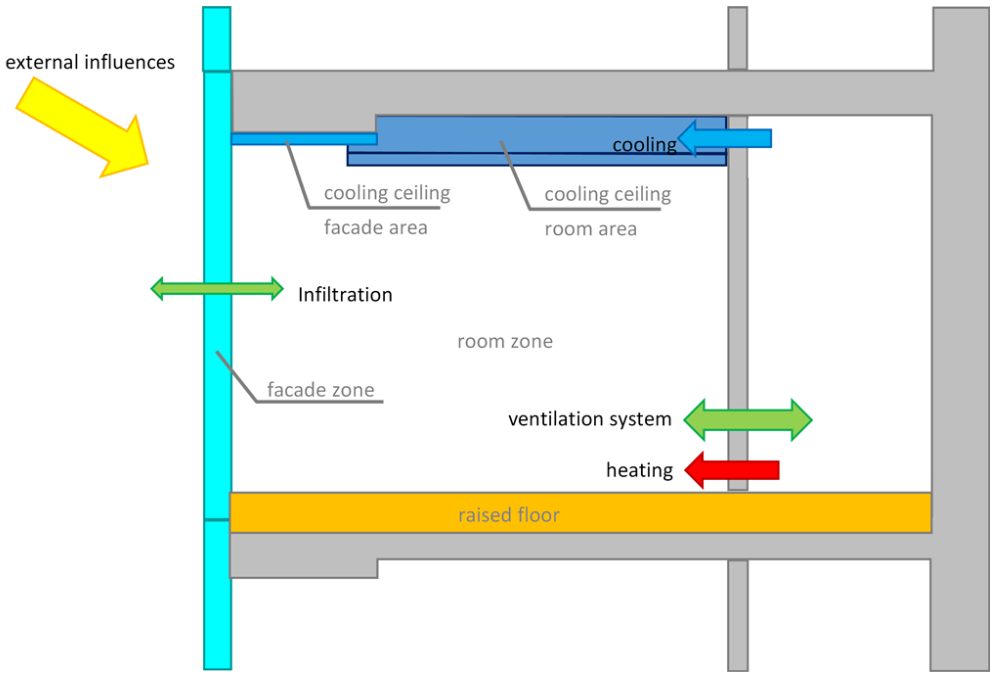

Figure 6.1: Schematic overview - room model

6.2 Mathematical Model

6.2.1 Energy Balance of Zones

The calculation follows the principle of conversation of energy, which means that sum of the energy flow must be equal to the periodic change of stored energy. In figure 6.2 the influences on the energy balance for a room are shown, where the red line marks the zone's border. The incoming gains are solar gains and gains from the building system services like heating, cooling and mechanical ventilation. Within the zone the internal gains like heat impact due to people, lighting and technical equipment have to be considered within the energy balance. The outgoing energy flow can be summarized to the part of the ventilation losses and the part of the transmission losses.

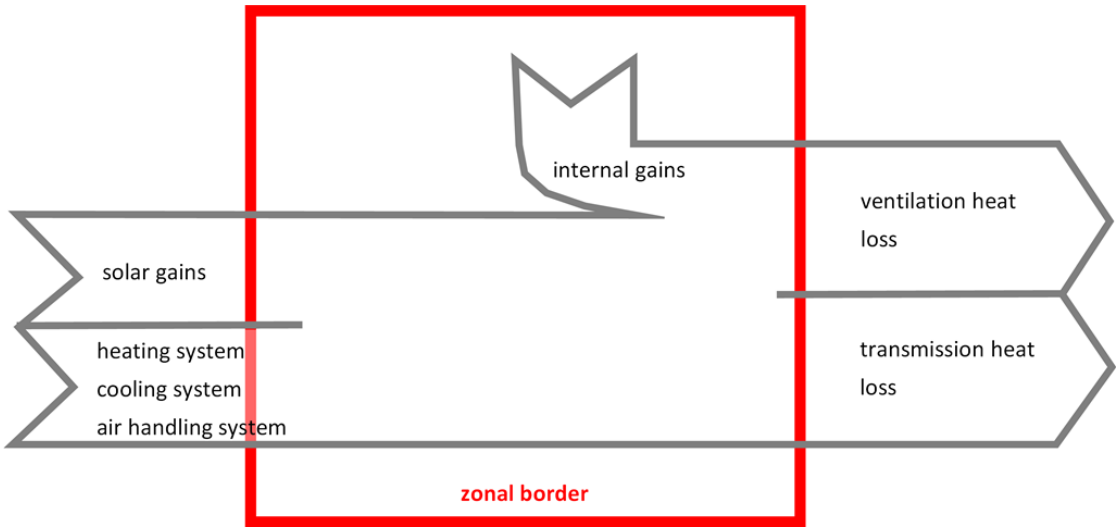

Figure 6.2: Influences on the energy balance of a zone

6.2.2 Calculation of Components - Heat Balance

The calculation of the components is done equal to the calculation of the zone - it follows the law of the conservation of energy. The components are divided into layers and the energy balance is formed for each individual layer.

The physical model for heat storage and heat transport is calculated using the following equations and is described in the following section for the individual component types in detail (dividing component, component with outward heat flow component with inward heat flow) .

The calculation follows the description done in Clarke (2001) [18] and is summarized in this chapter.

$$\left(c_{tr}\varrho_{tr} + c_{H_2O}\varrho_{H_2O}u_V\left(\tilde{x},t\right)\right)\frac{\delta T\left(\tilde{x},t\right)}{\delta t} = \nabla\lambda_T\left(w,T\right)\nabla T\left(\tilde{x},t\right) \tag{6.1}$$

where

c_{tr}	...	specific heat capacity in J/(kg K)
ρ_{tr}	...	density of the material in dry condition in kg/m^3
u_v	...	percentage water content in kg/m^3
T	...	temperature in K
$\lambda_T(w,T)$	...	thermal conductivity in W/(m K)

The calculation of the of convective heat transfer, the infra-red radiation exchange and absorption of solar radiation used as boundary conditions can be calculated by equation 6.2 and equation 6.3).

$$\alpha_{conv}\left(T_{air} - T_{surf}\right) + \varepsilon\sigma\left(T_s^4 - T_{surf}^4\right) + \alpha I_{sol} = -\lambda_T\left(w,T\right)\nabla T\left(\tilde{x},t\right)|_{\tilde{x}=\Omega} \tag{6.2}$$

where

α_{conv}	...	convective heat transfer coefficient in W/(m^2 K)
T_{air}	...	air temperature in K
T_{surf}	...	surface temperature in K
ε	...	effective emissivity dimensionless
T_s	...	temperature of the space confinement surfaces in K
α	...	absorption of solar radiation dimensionless
I_{sol}	...	solar radiation in W/m^2

$$T_s = \sqrt[4]{F_{sky}T_{sky}^4 + (1 \quad - F_{sky})\,T_{air}^4} \tag{6.3}$$

where

F_{sky}	...	view factor of the surface to the sky dimensionless
T_{sky}	...	sky temperature in K

6.2.3 Partition walls

The partition walls are computationally divided into 5 layers, whereby the heat flow through the layers or in the boundary layers is calculated. The calculation scheme of the partition walls is shown in figure 6.3.

In figure 6.3 the computational structure is illustrated. The balance equation for thermal energy has to be fulfilled in each node. Material depended respectively surface or weather conditions resistances are between the calculation nodes. Each node corresponds to a temperature node, the balance equations are explained for each node.

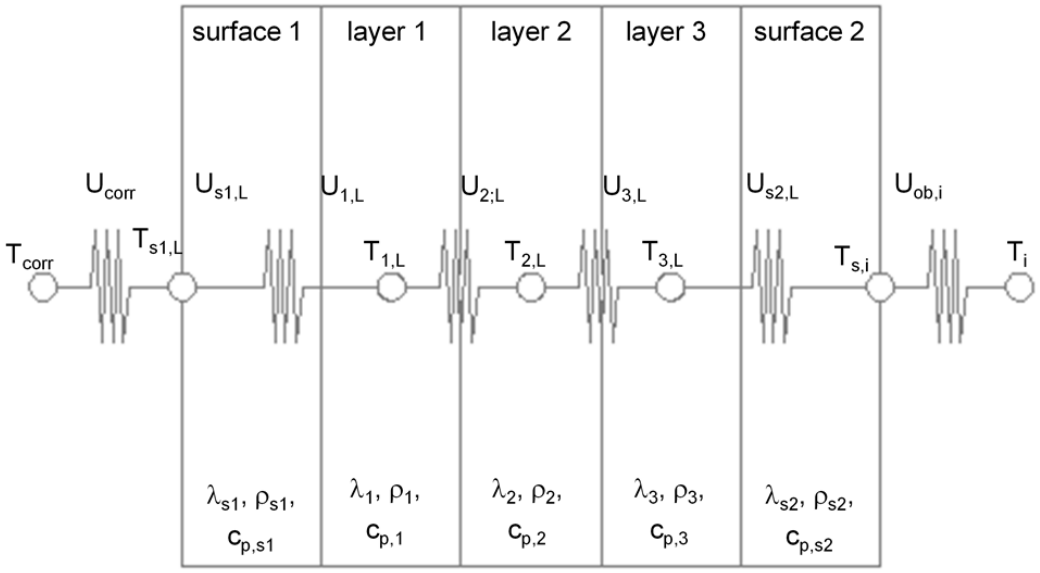

Figure 6.3: Schematic illustration of the layer based model for dividing components (e.g. walls between zones)

6.2.4 Model description for the Heat Flow through a Layer

The mathematical modeling of the heat flow through a layer is described in this chapter. In figure 6.4 the schematic overview of the heat flow and the influencing parameters is shown.

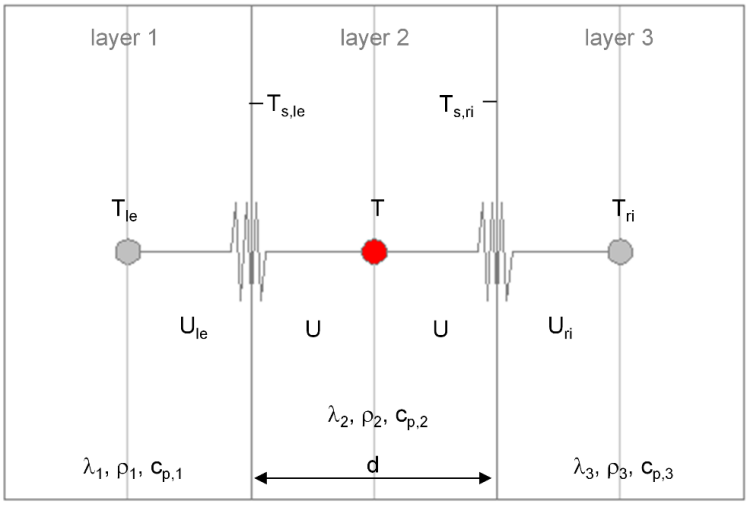

Figure 6.4: Schematic illustration of the heat flow though a layer

The heat flow through the layer is carried out according to the following calculation scheme and is regarded as the basis for the calculation of all layers. The principle of calculation is the energy conservation law, which states that the sum of the inflowing and outflowing energy in the considered control volume at constant pressure is equal to the change of the stored energy. For the temperature calculation, the total heat flow into and out of the control volume describe the change in the temperature is (see equation 6.4 to equation 6.9).

$$\frac{dT}{dt} = \frac{1}{C}\left(q_{le} + q_{ri}\right) \tag{6.4}$$

where

- dT ... temporal alternation of the layer temperature in K/s
- C ... heat capacity of the layer in relation to the surface area in J/(m^2 K)
- q_{le} ... heat flux density - left side in J/(m^2 s)
- q_{ri} ... heat flux density - right side in J/(m^2 s)

The heat capacity of each layer is calculated by equation 6.5.

$$C = \rho c_p d \tag{6.5}$$

where

- C ... heat capacity of the layer in relation to the surface area in J/(m^2 K)
- ρ ... density of the material in kg/m^3
- q_p ... specific heat capacity of the material in J/(kg K)
- d ... thickness of the layer in m

The heat flux density of the respective direction is calculated by equation 6.6.

$$q = q_{cond} + q_{conv} \tag{6.6}$$

where

- q_{cond} ... conductive heat flux density in J/(m^2 s)
- q_{conv} ... convective heat flux density in J/(m^2 s)

The heat flux from thermal conduction consists of the portion of the left side and the right side, the thermal coefficient of the half layer is calculated using equations 6.7 and 6.8.

$$q_{cond,le} = U\,(T_{s,le} - T) \tag{6.7}$$

$$q_{cond,ri} = U\,(T_{s,ri} - T) \tag{6.8}$$

where

- $q_{cond,le}$ ... conductive heat flux density - left side in J/(m^2 s)
- $q_{cond,re}$ ... conductive heat flux density - right side in J/(m^2 s)
- U ... thermal transition coefficient of the half of the layer in W/(m^2 K)
- $T_{s,le}$ ... temperature on the left boundary layer in K
- $T_{s,ri}$ ... temperature on the right boundary layer in K
- T ... layer temperature in K

$$U = \frac{\lambda}{\frac{d}{2}} \tag{6.9}$$

where

- U ... thermal transition coefficient of the half of the layer in W/(m^2 K)
- λ ... thermal conductivity in W/(m K)
- d ... thickness of the layer in m

Equation 6.10 shows principle of the calculation of the temperature at the layer boundary ($T_{s,le}$ and $T_{s,ri}$), the calculation is shown on the left side layer, the right sided layer temperature is calculated analogously

$$T_{s,le} = \frac{UT + U_{le}T_{le}}{U + U_{le}} \tag{6.10}$$

where

$T_{s,le}$ ... surface temperature, left-sided layer boundary in K
T ... layer temperature in K
T_{le} ... left layer temperature in K
U ... thermal transition coefficient of the half of the layer in W/(m^2 K)
$U_{s,le}$ ... thermal transition coefficient of the left layer in W/(m^2 K)

6.2.5 Model Description for the Outward Heat Flow

The difference of the outer surface layer node to the inside layer node is that the node is positioned on the outer layer boundary, therefore, the heat transmission coefficient (u-value) is based on the total layer thickness. Furthermore, the heat flux density is calculated from the outside by the adjacent air.

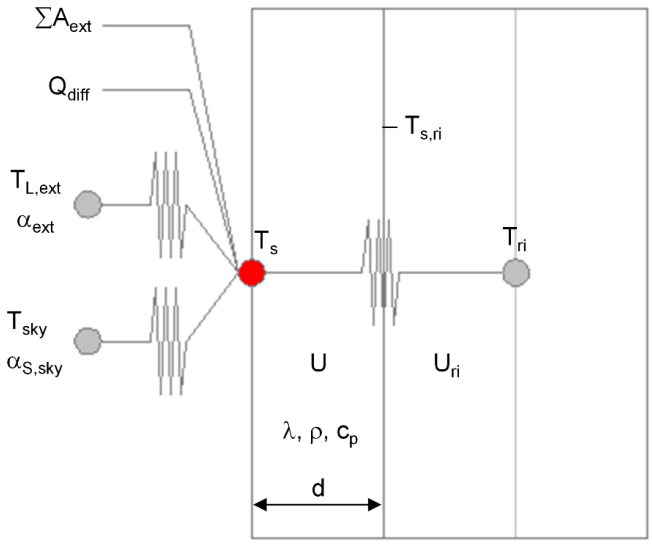

Figure 6.5: schematic illustration of the heat flow of the outside construction layer

The balance equation (equation 6.4) is valid also for the calculation of this node. The definition of the heat flux density from the outside is done according to equation 6.11.

$$q = (T_{ext} - T_{surf})\,\alpha_c + (I_{diff} + I_{dir})\,\alpha + (T_r - T_{surf})\,\varepsilon\alpha_r \tag{6.11}$$

where

T_{ext} ... outside air temperature in K
T_s ... surface temperature in K
α_c ... convective heat transfer coefficient in W/(m^2 K)
I_{diff} ... diffuse solar radiation on the surface in W/m^2
I_{dir} ... direct solar radiation on the surface in W/m^2
α ... absorption coefficient of the surface
T_r ... temperature of radiation of the surroundings in K
ε ... emissivity value of the surface
α_r ... radiant heat transfer coefficient in W/(m^2 K)

For the components with heat flow from the outside the solar heat gains, which have a significant impact on energy demand / energy consumption of the building as well as on the comfort of the room, are added as an additional and essential factor. Basically, the solar irradiation is influenced by building on Riccabona (2008) [40] by various factors like the following itemisation shows:

- the season
- location
- above sea level
- haze, cloudiness, fog
- horizon
- neighbouring buildings
- Overhanging components
- window recesses

The solar gains are depending of the intensity of the global radiation and the energy transmission of the outer shell. The calculation regarding a monthly balance sheet procedure is done by equation 6.12, analogues this equation can be applied with variable time steps.

$$Q_S = \sum_j \left(I_{S,j} \sum_m A_{G,m,j} \right) \tag{6.12}$$

where

Q_s ... monthly solar gains in kWh
$I_{S,j}$ ... total energy of the solar radiation on a area unit with an orientation j during the respective month in kWh/m^2
$A_{G,m,j}$ ... effective collector area of the glazing area in m^2

The solar heat gain through the façade construction are described by the following balance equations.
The input variables include the sun angle, the direct solar radiation, diffuse solar radiation and the reflected radiation.

Equation 6.13 describes the direct radiation on a surface. For $\cos(y_{SF})$ the relationship of equation 6.14 is valid.

$$I_{dir,S} = (1 - r_F)\, I_{dir} \cos(y_{SF}) \tag{6.13}$$

where

- $I_{dir,S}$ ... direct solar radiation on a surface in W/m^2
- rF ... reflectivity of the surface
- $I_{dir,n}$ ... direct solar radiation on a surface normal to the sun in W/m^2

$$\cos(y_{SF}) = \cos(y_F)\sin(y_S) + \sin(y_F)\cos(y_S)\cos(|a_s - a_F|) \tag{6.14}$$

where

- y_F ... degree of slope in radians (horizontal = 0)
- y_S ... solar altitude in radians (horizontal = 0)
- a_S ... orientation of the sun in radians (north = 0)
- a_F ... orientation of the surface in radians (north = 0)

The diffuse radiation on a surface is described by the relationship shown in equation 6.15.

$$I_{diff,S} = (1 - r_F)\, I_{diff,H} (\cos\frac{y_F}{2})^2 \tag{6.15}$$

where

- $I_{diff,S}$ ... diffuse solar radiation on a surface in W/m^2
- $I_{diff,H}$ ... diffuse solar radiation on a horizontal surface in W/m^2
- rF ... reflectivity of the surface
- y_F ... degree of slope in radians (horizontal = 0)

The environment reflected radiation on a surface is determined by equation 6.16.

$$I_{diff,refl} = r_U (\sin\frac{y_F}{2})^2 (I_{dir,n}\sin(y_S) + I_{diff,H}) \tag{6.16}$$

where

- 1 ... 1
- $I_{dir,S}$ ... diffuse reflecting solar radiation on a surface in W/m^2
- $I_{diff,H}$ ... diffuse solar radiation on a horizontal surface in W/m^2
- $I_{dir,n}$ ... direct solar radiation on a surface normal to the sun in W/m^2
- y_F ... degree of slope in radians (horizontal = 0)
- y_S ... solar altitude in radians (horizontal = 0)
- rF ... reflectivity of the surface

For the evaluation of the heat input from solar radiation the total solar energy transmittance factor (g-value) is the factor to determine. The g-value indicates what percentage

of the incident radiation energy becomes effective. For the evaluation of the heat impact the g-value of the whole façade system is relevant, the values for a component alone is not relevant for the calculation of the total heat impact. The combination of glazing and shading defines the effective g-value for the room, significant factors on the g-value are summarized in the following list according to Riccabona (2008) [40].

- characteristics of the glazing
- type, fittig position and position of the shading system
- direction of arrival of the radiation
- wind velocity and wind direction

The three characteristic parameters absorption, transmission and reflection the requirement of equation 6.17 is valid.

$$\alpha + \delta + \tau = 1 \tag{6.17}$$

where

α ... absorption coefficient
δ ... reflection coefficient
τ ... transmission coefficient

A part of the incident solar radiation on the outer pane is reflected, one absorbed and one part passes through. The transmittance percentage apply to the interior surfaces and is again divided into three parts. The reflective part again applies on the outer glass. The unit size is depending on the spectral range and the properties of the building materials.

In figure 6.6 the influences on the façade due to radiation are illustrated schematically.

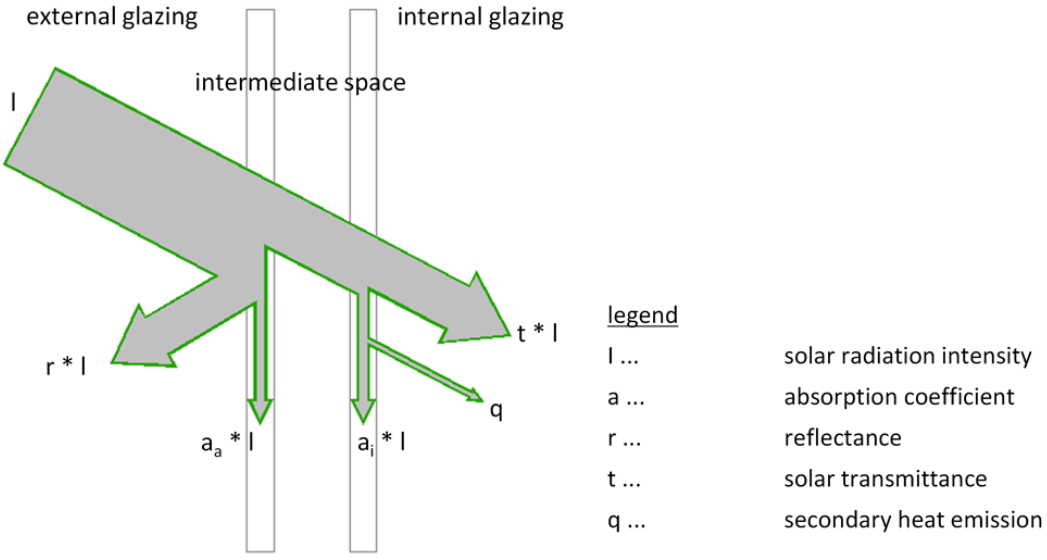

Figure 6.6: Schematic illustration of the heat flow from the outside construction layer

6.2.6 Model Description for the Inward Heat Flow

The inner surface layer nodes is, as the outer layer positioned on the boundary of the surface. Therefore the heat transfer coefficient (u-value) is based on the total layer thickness as a change to a internal node calculation. Furthermore, the heat flux density is calculated from the inside through the adjacent indoor room conditions.

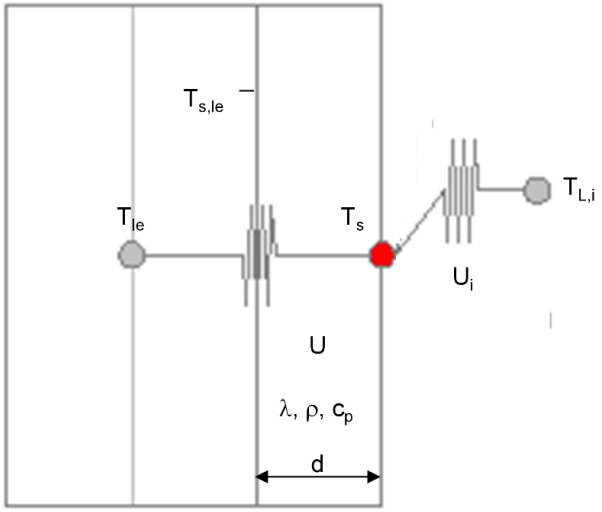

Figure 6.7: schematic illustration of the heat flow for the inside construction layer

The balance equation (equation 6.4) is valid also for the calculation of this node. The definition of the heat flux density from the inside is done according to equation 6.18.

$$q = (T_a - T_{surf})\,\alpha_c + q_{rad} \tag{6.18}$$

where

- T_a ... inside air temperature in K
- T_{surf} ... surface temperature in K
- α_c ... convective heat transfer coefficient in W/(m^2 K)
- q_{rad} ... radiation on the surface in W/m^2

6.2.7 Model Description for the Cooling Ceiling

The modeling of the cooling ceiling is divided in two parts, one part is the modeling of the concrete ceiling which is done according to the layer description of components. The second part is the modeling of the cooling layer and the air gap between the concrete ceiling and the cooling elements. The schematic overview of the thermal design values of the cooling ceiling and the ceiling construction is shown in figure 6.8.

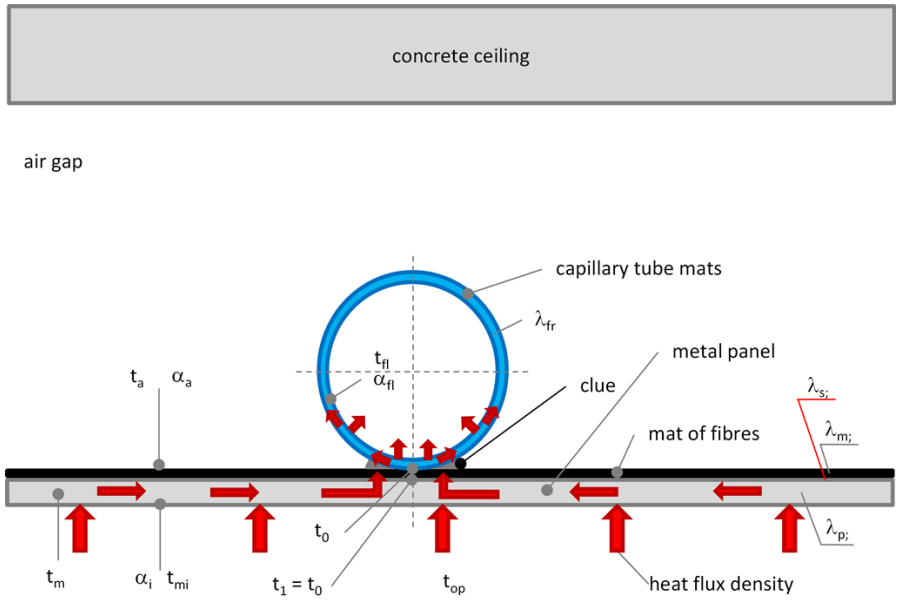

Figure 6.8: Schematic overview the cooling ceiling construction and its thermal design values according to the description done in Glück (2003) [23]

where

- t_a ... temperature air gap
- t_m ... temperature metal panel
- t_{mi} ... surface temperature metal panel
- t_{fl} ... cooling medium temperature
- t_0 ... surface temperature capillary pipes
- t_1 ... surface temperature fibre mats / capillary pipe facing surface of the metal panel
- t_{op} ... operative temperature of the room
- α_a ... heat transfer coefficient air gap
- α_i ... heat transfer coefficient room
- α_{fl} ... heat transfer coefficient cooling medium
- λ_{fl} ... thermal conductivity cooling medium
- λ_s ... thermal conductivity gap between fibre mats and metal panel
- λ_m ... thermal conductivity fibre mats
- λ_p ... thermal conductivity metal panel

The calculation was done according to the descriptions for capillary pipe cooling systems done in Glück (2003) [23] and are summarized in this section. The inputs and out-

puts characterizing the cooling ceiling layers ”air”, ”cooling medium” and ”metal panel” are shown in figure 6.9. The assumption for the calculation is, that there is a good heat conductivity between the the cooling medium and the surface of the metal panel facing the room. By Glück (2003) [23] a characteristic parameter describing the part heat transfer coefficient (see equation 6.19) was defined where the mean influencing factors on the heat transfer coefficient and therefore on the capacity are the tube distance and the intensity of the connection between the pipes and the metal panel.

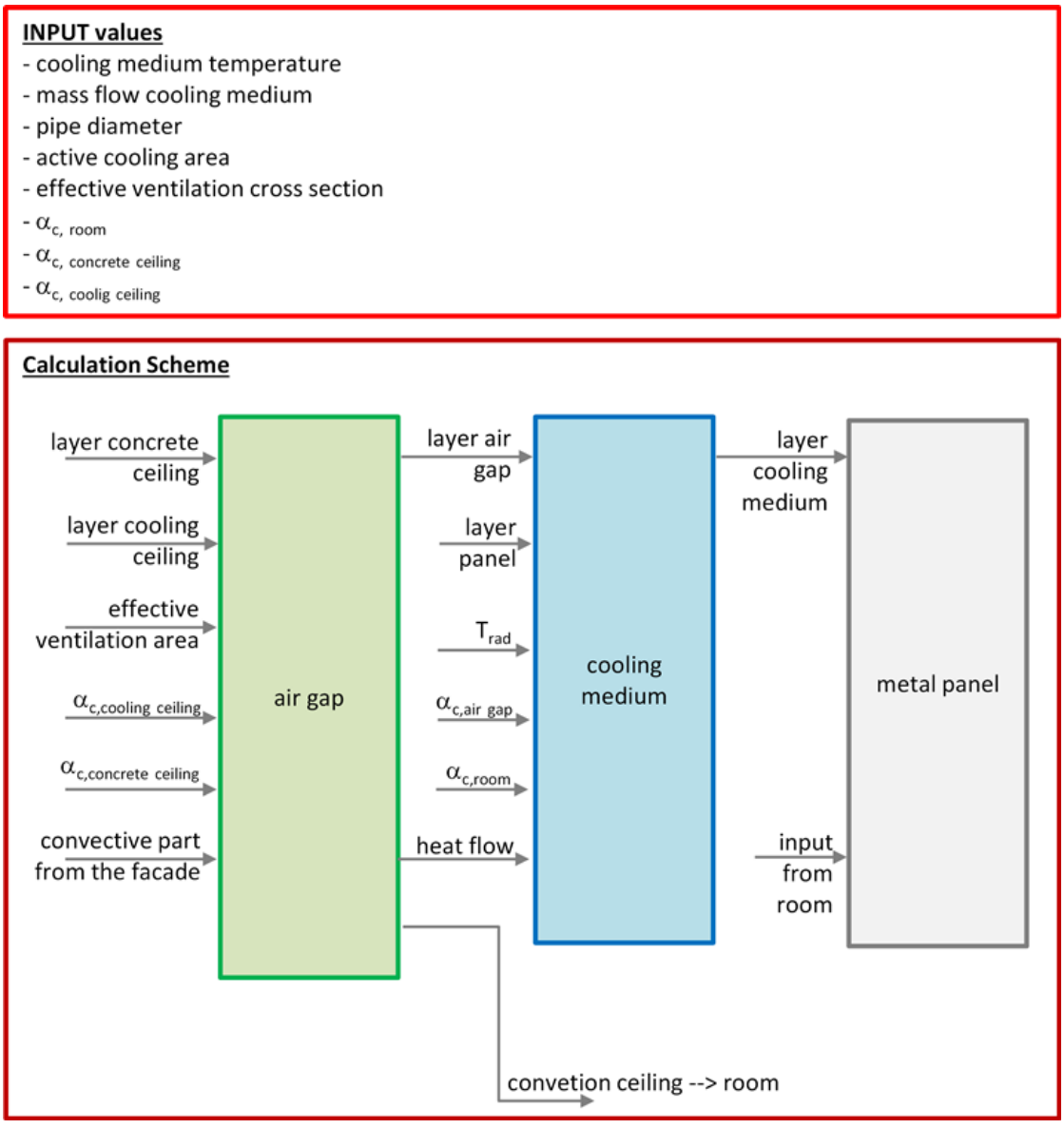

Figure 6.9: Summary of input values and calculation scheme for the cooling ceiling

$$\kappa = \frac{|\dot{q}|}{|t_m - t_{fl}|} \tag{6.19}$$

where

κ ... part heat transfer coefficient in W/(m^2 K)
$\dot{q}$ ... specific power (heat flow density) in W/m^2
t_m ... mean ceiling panel temperature (facing room) in K
T_{fl} ... mean cooling medium temperature in K

The heat flow is defined between the the room with an operating temperature t_{op} in direction of the suspended ceiling surface with the temperature t_{mi} as long as the requirement $t_{op} > t_{mi}$ is true. The heat transfer is described by the basic characteristic for underfloor heating systems according to DIN EN 1264 [2], which is shown in equation 6.20. This approach has been proven by scientific studies like the PhD of Külpmann (1991) [33] and test bed measurements like shown in Glück (1997) [24].

$$\alpha_i = 8.92 \quad |t_m - t_{op}|^{0.1} \tag{6.20}$$

where

α_i ... heat transfer coefficient in W/(m^2 K)
t_m ... mean ceiling panel temperature (facing room) in K
T_{op} ... operative temperature of the room in K

The heat flows is along the metal panel towards the contact point with the capillary pipe. The fibre mat is practically not involved in this heat transfer ($\lambda_{(\text{fibremat})} < \lambda_{\text{metalpanel}}$). The one-dimensional heat conduction is anzusetzten for the calculation of the heat conduction of the metal panel. For perforated metal panel elements the share of perforation has to be considered by a equivalent thickness of the panel. Furthermore the absorbed heat flow of the metal panel has to be transported through the fibre mat to the capillary pipes. To achieve a acceptable heat transfer process the contact area between the tubes, the fibre mats and the metal panel should be as big as possible. Finally the heat flow of the pipe wall to the cooling medium (water) needs to be calculated. Due to the small contact area (pipe dimensions) the calculation needs to be two-dimensional.

The definition of the heat transfer coefficients is depending on the connection of the capillary tube mats with the fibre mats and the metal panels. The studies done in Glück (2003) [23] show that there is a difference in the cooling capacity of 40 % to 50 % in dependence of the contact type (inlaid or glued capillary pipes).

7 Air Flow Modeling

7.1 Introduction

The air flow model is one part of the development of a air flow integrated room model which should calculate reliable results on comfort including the interaction of the envelope and the HVAC system.

One of the key issues for the calculation of a rooms condition and the resulting thermal comfort is the knowledge of the air flow distribution in the room. A simplified but still accurate enough air flow model should be built to determine the effect of different façade types on the cooling capacity of a cooling ceiling. A parametric study using the program COMSOL Multiphysics 4.3a was done. The output of the calculations was compared with the results of the in-situ measurements.

7.2 Method

The software program COMSOL Multiphysics version 4.3a was used, with the aim to calculate the impact of air movement with different façade systems on the cooling capacity of the cooling ceiling. The influence on the cooling capacity due to the façade systems was measured by an intensive set of measurement and the results presented in chapter 2, 3, 4 and 5 are used for the validation of the mathematical model.

The physical model ”non isothermal flow” was used for the air flow calculation. The main equations are summarized in the following list

- Navier Stokes (momentum balance and mass balance),
- heat balance and
- energy transport (convection and conduction)

One of the main topics is the modelling of the façade, because the simulation program COMSOL Multiphysics version 4.3a consider all radiation as the same, it’s not possible to make a distinction between large infra-red radiation and the solar spectrum (UV, light and short IR). This problem can be solved by calculating with temperatures around 0 K if only the façade is considered. With the calculation around 0 K the infra-red radiation is negligibly small compared to the incident solar radiation. This “simplification” is no longer possible if the room is also part of the analysis, because the surface to surface radiation should be taken into account and thus both types of radiation have to be considered. The incident solar radiation is taken into consideration by heat inputs in

the individual layers of the façade according to its absorption and solar transmission coefficient in this model.

7.3 2D-Model

7.3.1 Geometry and mesh properties

The geometry of the simulation model is according to the architectural plans a section through the room. A simplification of the model, from three dimensions to two was done. The symmetry is along the depth of the room (see figure 7.1). The main geometric data of the room is summarized in table 7.1.

In figure 7.1 on the left side picture the section through the 3D model is marked with a red area, the cut is in the middle of one façade axes and not in the centre of the façade length for a room. The room consists of two similar façade axes and between the two parts there the frame of the façade and the suspension of the ceiling elements is situated.

On the right side the simplified 2D model is sketched, the additional second skin is marked by the red line at the inside of the single skin façade. The cooling ceiling is highlighted by the light blue lines. The air in let position is visualized by the violet line on the floor of the room, and the return air position is between the cooling ceiling panels regarding the room area and is shown by the two yellow lines.

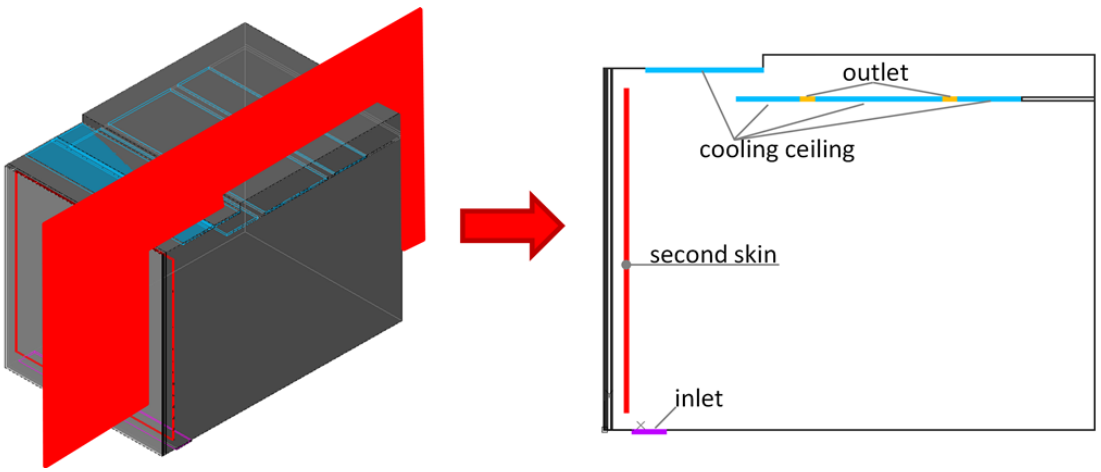

Figure 7.1: Simplification of the model geometry from three dimensions to two dimensions

Table 7.1: Summary of the room / model dimensions taken for the 2D air flow model of the room

Description	Height in m	Width in m
Room height	3.40	-
Room depth	4.10	-
Façade – exterior glass	3.07	0.01
Argon	3.07	0.01
Façade – interior glass	3.07	0.01
Gap between glass and screen	3.07	0.03
Screen	3.07	0.01
Gap between screen and 2nd glazing	3.07	0.11
2nd glazing extern	2.74	0.01
2nd glazing argon	2.74	0.01
2nd glazing intern	2.74	0.01

7.3.2 Façade system

With the CDF Model the impact of two façade systems

- Façade system 1: single skin façade with internal shading element and
- Façade system 2: single storey double skin façade with a shading element between the 2 glazing elements

on the capacity of the cooling ceiling should be tested. Figure 7.2 shows the schematic overview both façade systems, where the left picture visualize the single skin façade and the right one the single storey double skin façade. s of the glazing and shading according to the technical data shown in table 7.2.

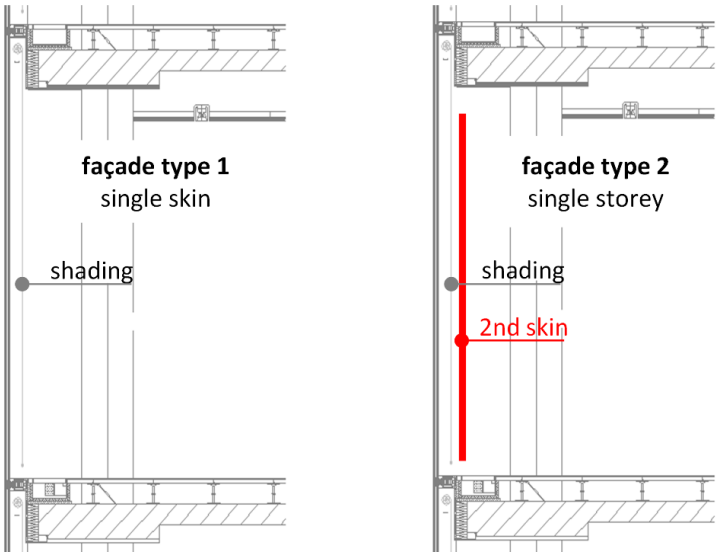

Figure 7.2: Façade type 1 (left side): single skin façade with internal shading element / façade type 2 (right side): single storey double skin façade with a shading element between the glazing elements

In table 7.2 the technical data for the façade systems is summarized. The detailed description of the façade systems and the technical data is done in chapter 2. The total solar energy transmittance g-value of the glazing of the single skin façade is g = 0.35 according the technical data sheet. The modeling of the solar radiation through the façade systems and the impact on the room is done by heat sources to the layer

Table 7.2: Summary of the technical data for the façade systems, single skin façade: column 2 and 3; single storey double skin façade: coloum 2, 3 and 4

Parameter description	Outside pane	Shading system	2nd skin
Total solar energy transmittance:	g = 0.35		
Solar transmittance:	τ = 0.33	τ = 0.11	τ = 0.55
Reflectance:	ρ = 0.41	ρ = 0.39	ρ = 0.24
Absorptance outside pane:	α_c = 0.25	α = 0.50	α_c = 0.25
Absorptance inside pane:	α_i = 0.01	---	α_i = 0.01
Light transmittance:	---	τ_L = 0.10	---
Heat transfer coefficient:	U = 1.29 W/m²K		U = 1.1 W/m²K

7.3.3 Boundary Conditions

The heat flux of the external wall is defined by an inward heat flux according to equation 1, the heat transfer coefficient for the external wall is 20 W/(m^2 K) and the external temperature is text is 32 °C for the basic simulation with an solar radiation of 800 W/m^2. The temperatures of the enclosing surfaces for the basic condition variant are summarized in table 7.3. The surface temperatures regarding the floor, the partition walls and the non-activated part of the ceiling is an input of a simplified thermal design day simulation of the room, the surface temperatures of the cooling ceiling are due to the results of the thermal imaging of the cooling ceiling which was done within the framework of this work.

Table 7.3: Summary of the temperatures of the surrounding surfaces for the basic simulation with an solar radiation of 800 W/m^2

Description	Temperature in °C
Floor	23.0
Partition wall	25.0
Ceiling – room	23.0
Ceiling façade	32.0
Cooled ceiling (bottom)	18.5
Cooled ceiling (top)	18.5

7.3.4 Material Properties and initial Conditions

The material properties of the surrounding surfaces and used materials are shown in table 7.4. The dynamic viscosity, the heat capacity and the thermal conductivity of the layer ”air” are temperature dependent and the values are shown in figure 7.3. The density of the layer ”air” is calculated in dependency of the air temperature and the air pressure and the values are shown in figure 7.3.

Table 7.4: Summary of the material data - input values for the air flow calculation

Description	Dynamic viscosity	Ration of specific heat	Heat capacity at a constant pressure	Density	Thermal conductivity
	Pa s	-	J/(kg K)	kg / m³	W/(m K)
Air (room)	ε(T[1/K])	1.4	cp(T[1/K])	ρ(pA[1/Pa],T[1/K])	k(T[1/K])
Façade external glazing	---	---	480	2200.000	1.100
Argon	---	---	520	1.784	0.018
Façade internal glazing	---	---	480	2200.000	1.100
Screen	---	---	1700	1150.000	0.260
2nd skin– external	---	---	480	2200.000	1.100
2nd skin – internal	---	---	480	2200.000	1.100
Aluminium	---	---	900	2700.000	160.000

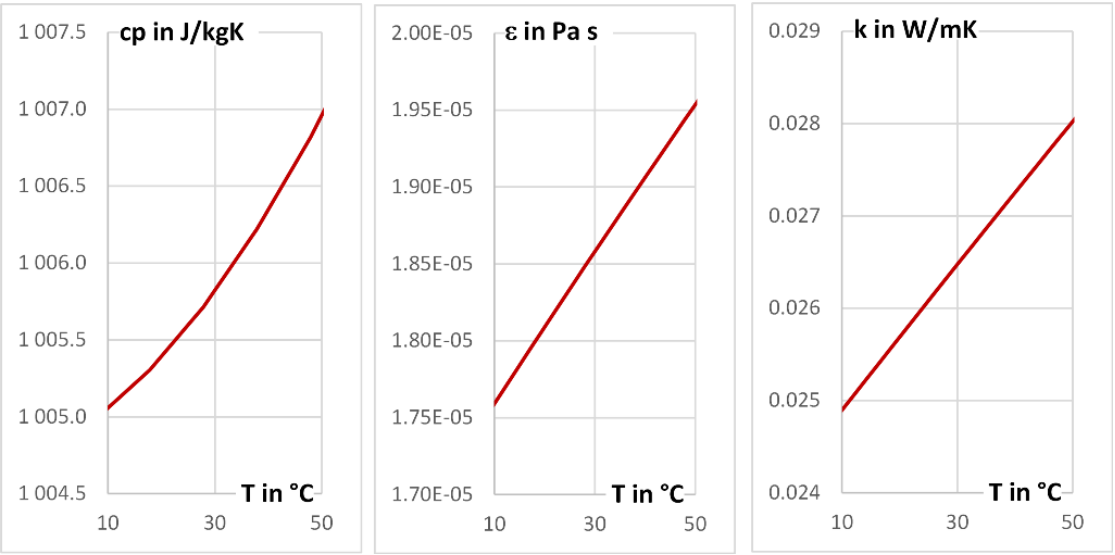

Figure 7.3: Heat capacity (cp), dynamic viscosity (η) and thermal conductivity (k) in dependence of the temperature in °C

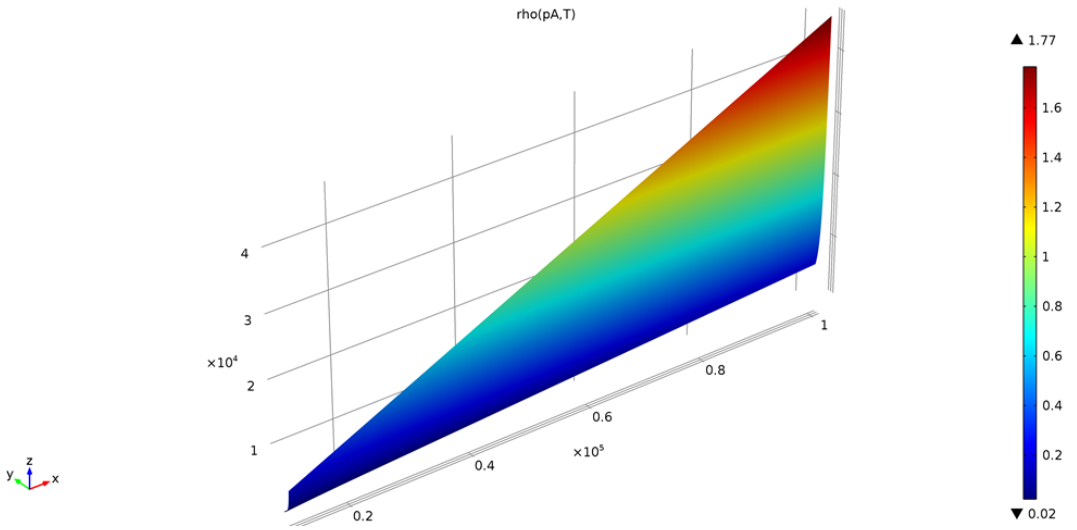

Figure 7.4: Density (ρ) in dependence of the temperature in K and the pressure in Pa

The surface emissivity for the surfaces is shown in table 7.5, the references for the emissivity values are the handbook of Chemistry and Physics (2009) [28], the DMIC Report (1962) [17], the Thermal Radiation Properties Survey (1960) [26], the "Leitfaden zur Infrarottechnik" (guidline for infrared technologies) [32] provides by testo and the data provided at the homepage of viZaar AG [51]. The initial temperature condition t_0 is 294.15 K, the initial pressure p_{ref} is 1 atm.

Table 7.5: Summary of the surface emissivity for the different material within the room

Description	Surface emissivity
Floor	0.70
Aluminium - grey paint	0.95
Glass	0.80
Screen	0.88
Concrete – ceiling	0.94
Plaster – partition wall	0.94

7.3.5 Mesh and Solver Settings

One output of the CFD calculation is the cooling capacity of the cooling ceiling, due to this issue, the calculation was done with the Low Reynolds number $k - \epsilon$ turbulence model. The mesh of the complete model consists of 100698 (façade type 1) and 120508 (façade type 2) elements. The summary of the solver settings is shown in table 7.6

The CFD modeling was also done with the simplification of wall factors, in figure 7.5 the picture of the mesh regarding the single storey double skin façade is shown. With boundary setting of the wall factor calculation the elements can be reduced from 100698

Table 7.6: Solver settings

Description	Type
Type of analysis: non isothermal flow	Non-isothermal flow
Linear system solver:	MUMPS
Relative tolerance	0.001
Pivot threshold	0.1
Memory allocation factor	1.2

to 37657 for façade type 1 and from 120508 to 51539 for façade type 2 and the calculation time is reduced. The evaluation of the results show, that the values for the temperatures in within the room area and the surface temperatures as well as the velocity fields are similar, statement regarding the cooling capacity cannot be done with the simplified model.

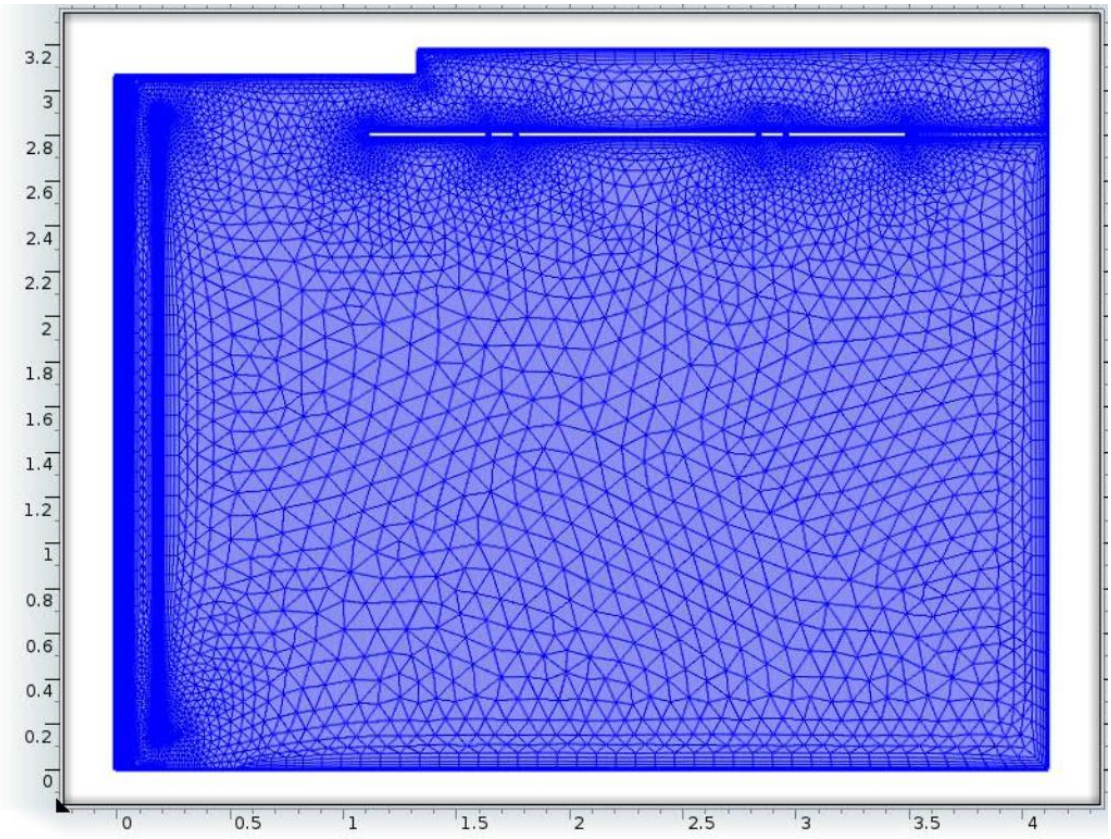

Figure 7.5: Visualisation of mesh geometry for the simplified modeling (wall functions) for the single storey double skin façade

7.4 Results CFD Simulation

7.4.1 Operative Temperature

In figure 7.6 the results of the operative temperature in the middle of the room are shown for the two façade systems. The results for the single skin façade show an increase of the operative temperature from 24.7 °C to 28.5 °C with an increasing solar impact. The mean capacity of the cooling ceiling variate between 40 W/m^2 and 80 W/m^2 cooling area. The effect of the single storey double skin façade is a smaller increase of the operative temperature in the middle of the room due to a higher efficiency of the cooling ceiling. The diagram shows, that the operative temperature stay around 26 °C and the cooling capacity increase due to the solar impact.

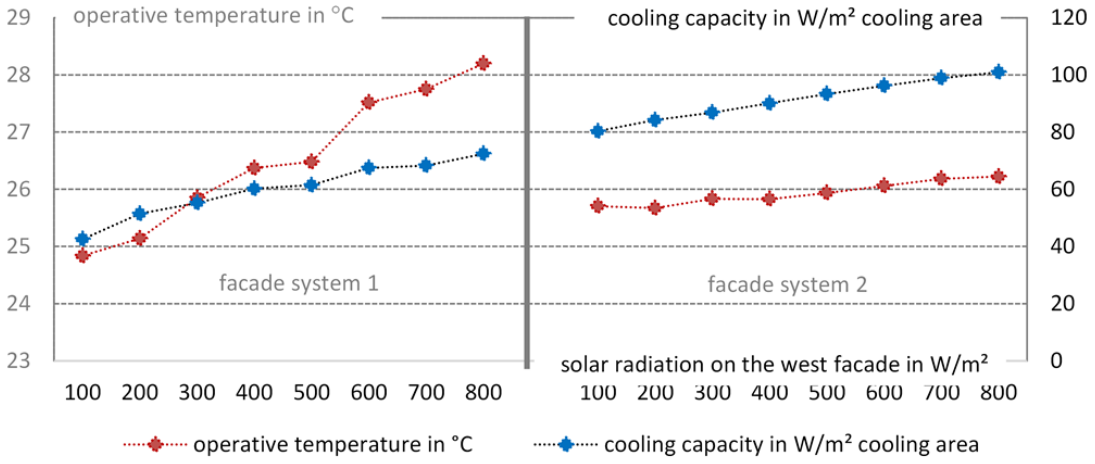

Figure 7.6: Comparison of operative temperature and the cooling capacity for façade type 1 (left side) and façade type 2 (right side); the temperature is below 27°C with façade type 2, the cooling capacity is increasing with the increasing solar radiation; with façade type 1 the operative temperature is getting above 27°C and the cooling capacity is lower.

7.4.2 Cooling Capacity

The cooling capacity was calculated for both façade types with different incident radiation (from 100 W/m^2 to 800 W/m^2): In figure 7.7 the results on cooling capacity in relation to the room depth for façade type 2 for a temperature difference between the mean medium temperature and the operative temperature in the middle of the room of 9 K are visualized.

The results for the cooling capacity of the cooling ceiling as a function of the depth of the room for the 2 façade systems is shown in figure 7.8. The calculation results show that there is an increase of the cooling capacity by comparing the single skin façade (grey line) and the double skin façade (black line). Especially next to the façade but also

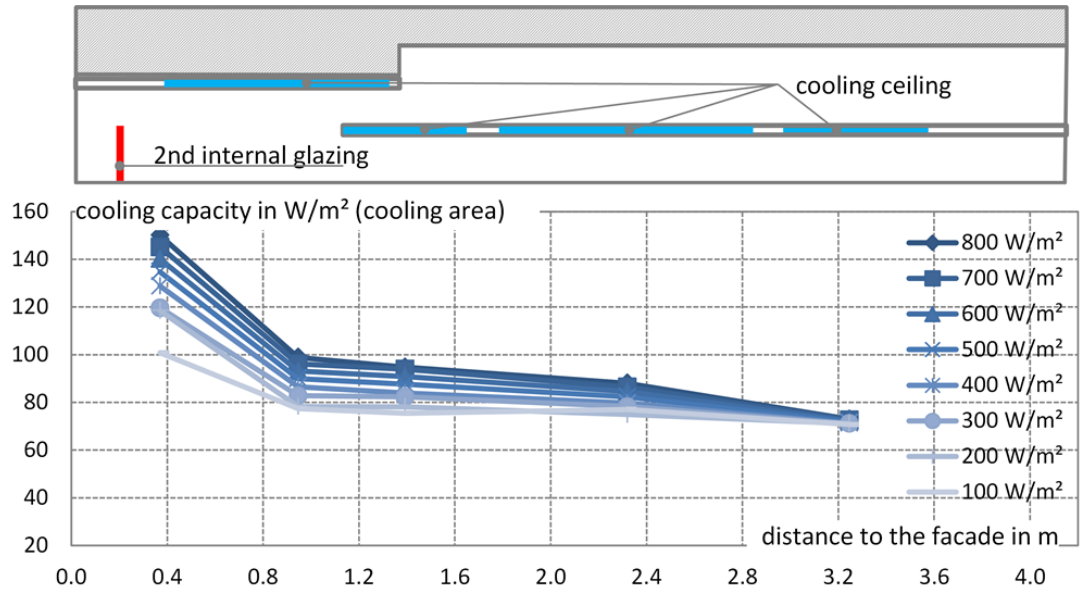

Figure 7.7: Cooling capacity in dependence of the room depth for façade system 2; temperature difference between mean medium temperature and operative temperature in the room is 9 K

throughout the room. The difference is minimal where the cooling ceiling is arranged overlapping.

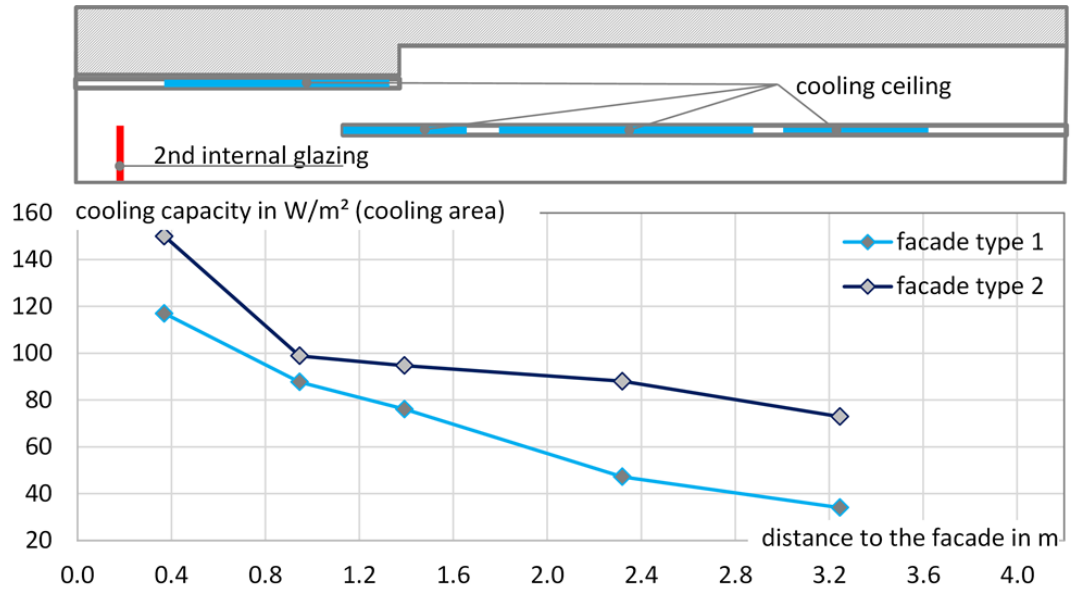

Figure 7.8: Cooling capacity in dependence of the depth of the room with an incident solar radiation of 800 W/m^2 and a temperature difference of 9 K between the mean medium temperature and the operative temperature in the middle of the room.

Figure 7.9 shows the resulting mean cooling capacity with different impacts due to the incident solar radiation for the two façade systems. The temperature difference between the mean medium temperature and the operative temperature in the middle of the room is 9 K.

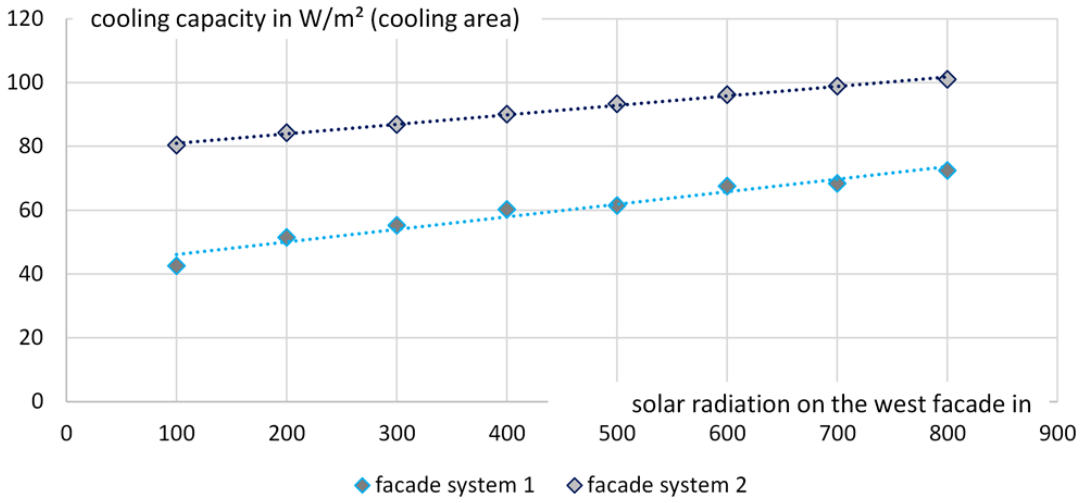

Figure 7.9: Resulting cooling capacity in dependence of the incident solar radiation; the temperature difference between the mean medium temperature and the operative temperature in the middle of the room is 9 K.

The comparison of the measurement results and the results of the CFD calculation is shown in figure 7.10. There is a good agreement between both for the operative temperature and the cooling capacity. The measurement results are taken by a series of measurement in an existing building. The description for the measurement set-up is done in chapter 2. The results on operative temperature are presented in chapter 3. Chapter 4 describes the measurement results regarding the cooling capacity of the cooling ceiling.

In figure 7.10 on the left side the operative temperatures for two façade systems single skin façade and singe storey double skin façade with screen type 2 as shading system are shown. The left part in this diagram represents the result of the CFD calculation and the right part the measurement results, where the light blue colour refers to façade system 1 and the dark blue is regarding façade system 2. The compared value are for the position in the centre of the room, and the difference of the operative temperature in the middle of the room is about 0.2 K.

The right side diagram in figure 7.10 show the results regarding the cooling capacity of the cooling ceiling. The lines represent the measurement approximation done by the measurement results (detailed description see chapter 4). The points view the results out of the CFD calculation for the different tested boundary conditions. The diagram show a good agreement between the measurement results and the results of the CFD calculation for the cooling capacity of the cooling ceiling for both façade systems.

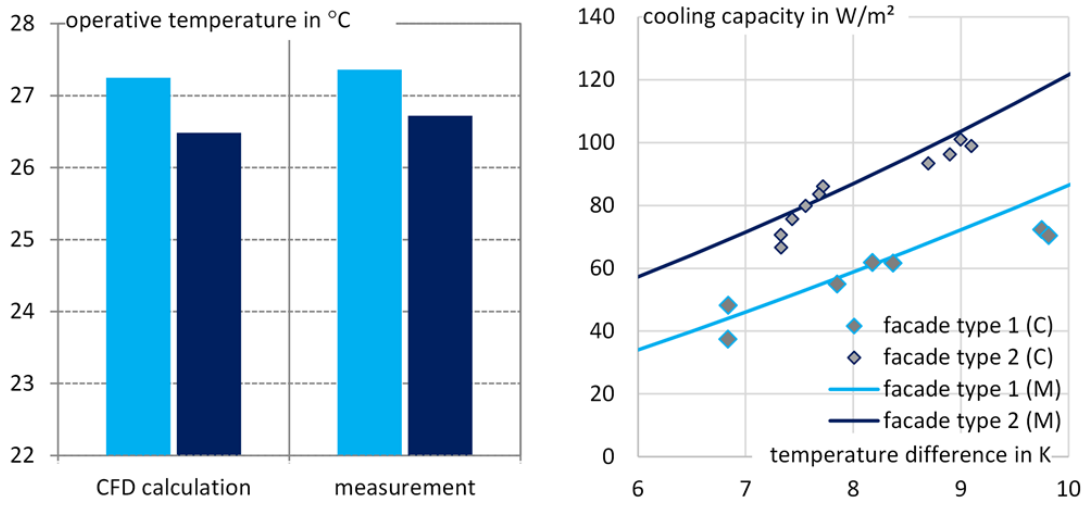

Figure 7.10: Measurement results on operative temperature (left side) and cooling capacity (right side; (M)..measurement; (C)..CFD calculation) – there is a good accordance between the measurement results and the CFD calculation; the difference of operative temperature is about 0.2 K

7.4.3 Air velocity

In this section the results on air velocity are discussed for the two façade systems (single skin façade and single storey double skin façade).

Velocity Single Skin Façade

The velocity was evaluated for two areas of the room, once in three different heights of the façade and second on the entrance to the open cooling ceiling ceiling. The areas are marked in figure 7.11 for the single skin façade (fs1)

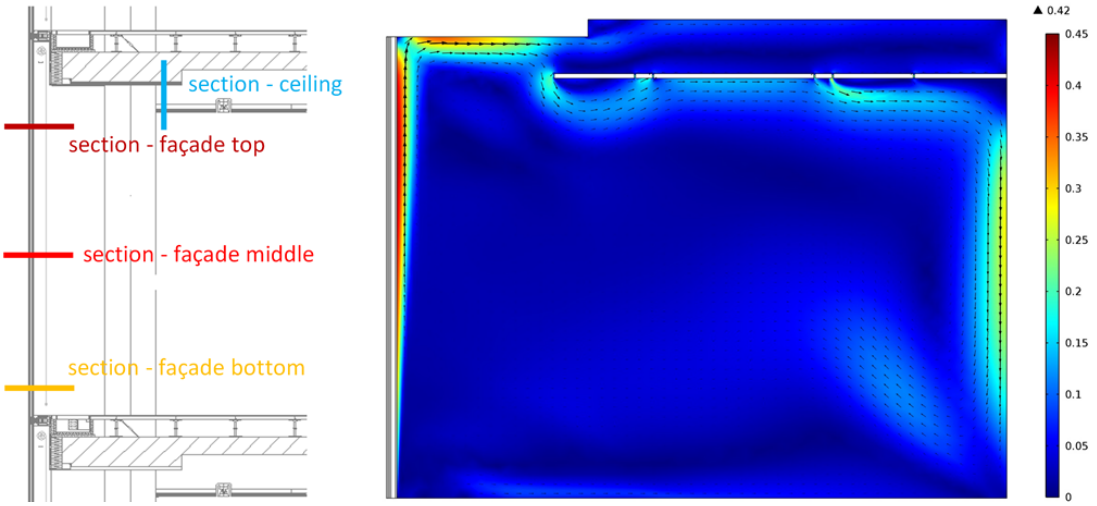

Figure 7.11: Visualization of the regarded areas for the velocity study; the colours of the cutting lines are referring to the diagrams

The results for an incident radiation of 800 W/m^2 and an external temperature of 32 °C for façade system 1 - single skin façade - are shown in figure 7.12, were the left side represents the results for the façade area and the right side represent the result for the ceiling gap. The mean velocity within the façade gap is 0.04 m/s, for the ceiling gap there is a mean velocity of 0.03 m/s.

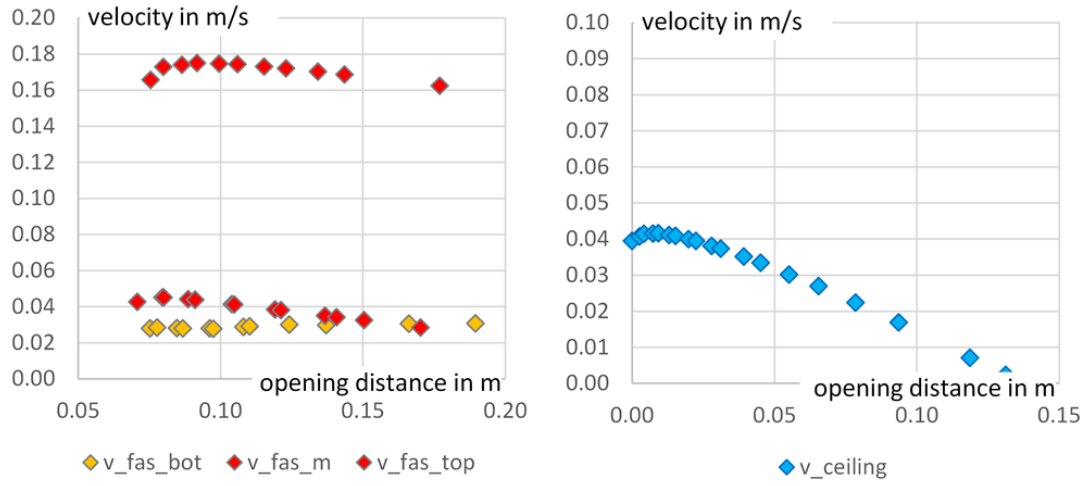

Figure 7.12: velocity field within the façade area (left diagram) and the ceiling gap (right diagram) for façade system 1 (single skin façade), simulation result for an incident solar radiation of 800 W/m^2 and an external temperature of 32 °C

Velocity Single storey double skin Façade

For the single storey double skin façade the velocity was also evaluated for two areas of the room, once between the two layers of the façade system 2 and on the entrance to the open cooling ceiling ceiling. The areas are marked in figure 7.13 for the single storey double skin façade (fs2).

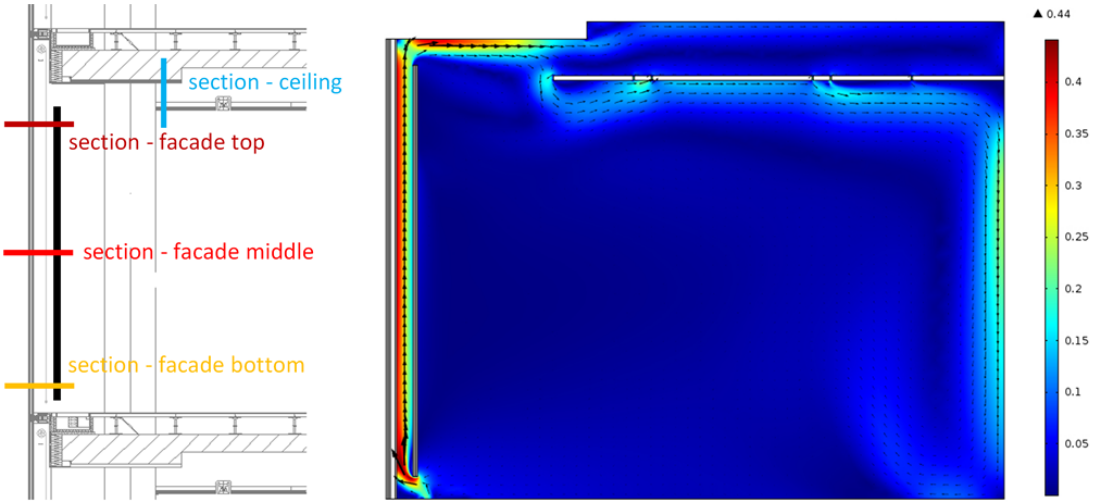

Figure 7.13: Visualization of the regarded areas for the velocity study; the colours of the cutting lines are referring to the diagrams

For façade system 2 - single storey double skin façade - the results for an incident radiation of 800 W/m^2 and an external temperature of 32 °C are shown in figure 7.14, were the left side represents the results for the façade area and the right side represent the result for the ceiling gap. The mean velocity within the façade gap is 0.20 m/s, for the ceiling gap there is a mean velocity of 0.05 m/s.

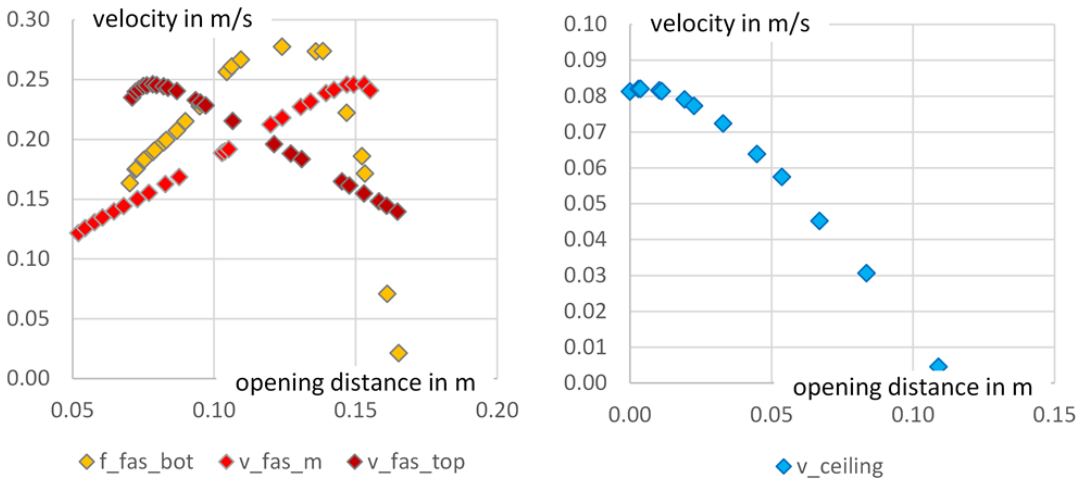

Figure 7.14: velocity field within the façade area (left diagram) and the ceiling gap (right diagram) for façade system 2 - single storey double skin façade, simulation result for an incident solar radiation of 800 W/m^2 and an external temperature of 32 °C

The comparison of the distribution of the air flow is shown in figure 7.15 for the single skin façade left side and the single storey double skin façade (right side). The results are regarding an incident radiation of 800 W/m^2. The total amount of air (about 50 m^3/h) was divided according to the results of the air flow calculation for the two façade systems.

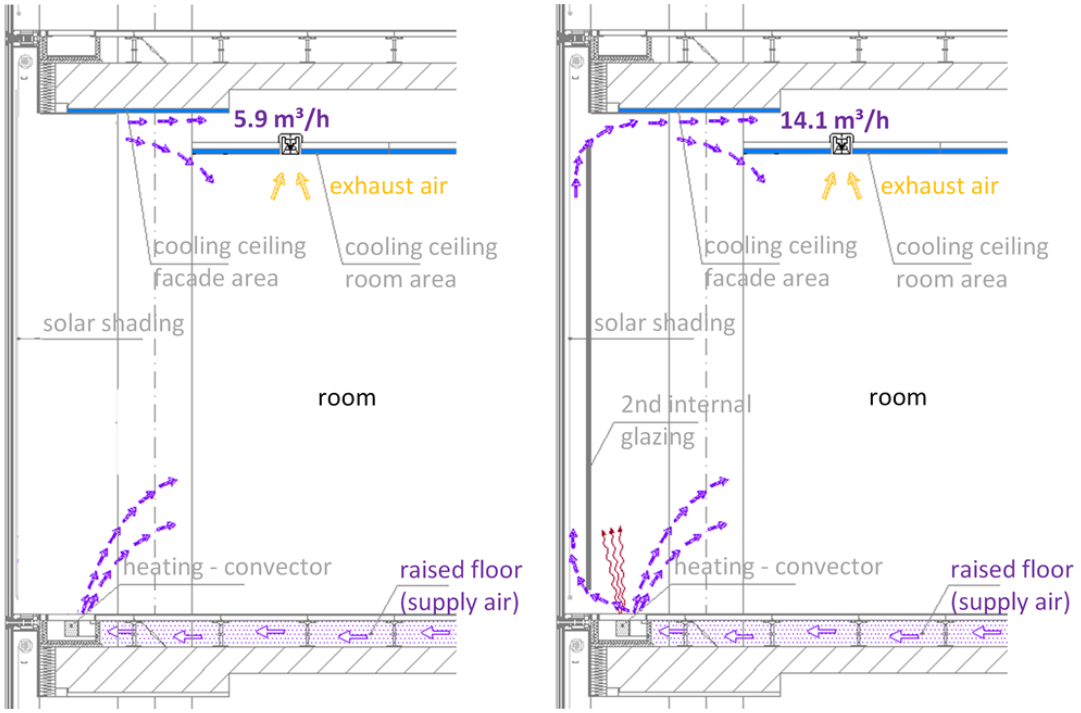

Figure 7.15: Air distribution for the two façade systems for an incident radiation of 800 W/m^2; left side: single skin façade; right side: single storey double skin façade

Design Day Simulation - Air Velocity

For the calculation of the air velocity a ”design day” simulation was done with the CFD model. The external temperature and solar radiation of this day are shown in figure 7.16. The boundary conditions regarding the surface temperatures were adapted according to the results of the thermal simulation, the range of the temperatures for the different surfaces are summarized in table 7.7.

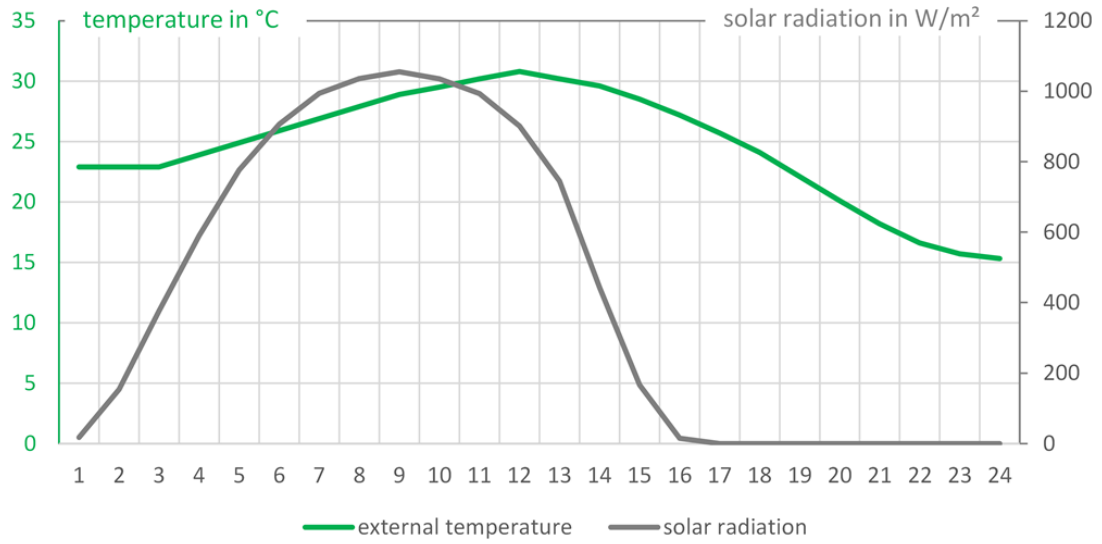

Figure 7.16: Design Day - external temperature and solar radiation

Table 7.7: Summary of the temperature range for the surrounding surfaces for the design day simulation

Description	Minimum temperature in °C	Maximum temperature in °C
Floor	21.0	23.0
Partition wall	20.0	25.0
Ceiling – room	21.0	23.0
Ceiling façade	21.0	32.0
Cooled ceiling (bottom)	18.0	19.0
Cooled ceiling (top)	18.0	19.0

The results of the mean velocity in dependence of the temperature difference of the air temperature in the room and the inside surface temperature of the façade (façade area) or the suspended cooling ceiling (ceiling area), are shown in figures 7.17 and 7.18.

The results regarding the single skin façade are shown in figure 7.17, the mean air velocity is very similar in both areas (façade area - orange marked dots; ceiling area - blue marked dots). The mean velocity for the façade area is 0.03 m/s and for the area regarding the cooling ceiling there is a mean air velocity of 0.02 m/s.

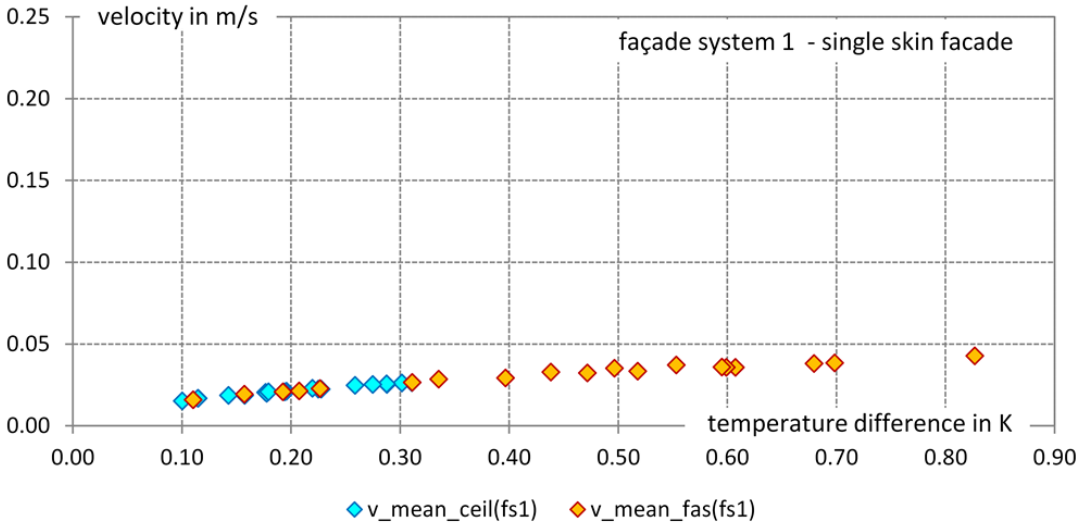

Figure 7.17: Simulation results regarding the mean velocity in the considered areas for the design day for façade system 1 - single skin façade; results regarding the façade: v_mean_fas(fs1); results regarding the ceiling: v_mean_ceil(fs1)

In figure 7.18 the result on the mean air velocity in the façade area and regarding the cooling ceiling are visualized, where the red dots belong to the results concerning the façade are and the blue ones to the cooling ceiling. The mean velocity for the façade area is 0.16 m/s and for the area regarding the cooling ceiling there is a mean air velocity of 0.03 m/s.

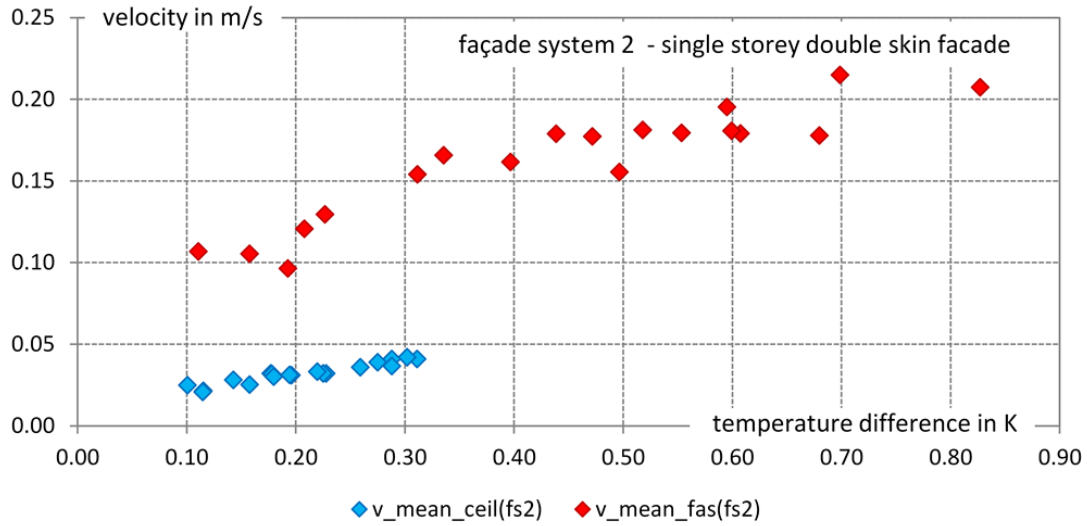

Figure 7.18: Simulation results regarding the mean velocity in the considered areas for the design day for façade system 2 - single storey double skin façade; results regarding the façade: v_mean_fas(fs2); results regarding the ceiling: v_mean_ceil(fs2)

The results of the mean velocity in dependence of the temperature difference (air temperature / surface temperature) were compared for both façade systems The results are visualized in figure 7.19, were fs 1 means façade system 1 - single skin façade and fs2 façade system 2 - single storey double skin façade. The results out of the CFD simulation regarding the convective heat flow show a higher velocity and therefore a higher convective heat flow regarding the change from single skin façade to single storey double skin façade is assumed. For the façade area the total convective heat flow for the single storey double skin façade is 5 times the value for the single skin façade, for the ceiling the factor between the two façade systems is 1.5.

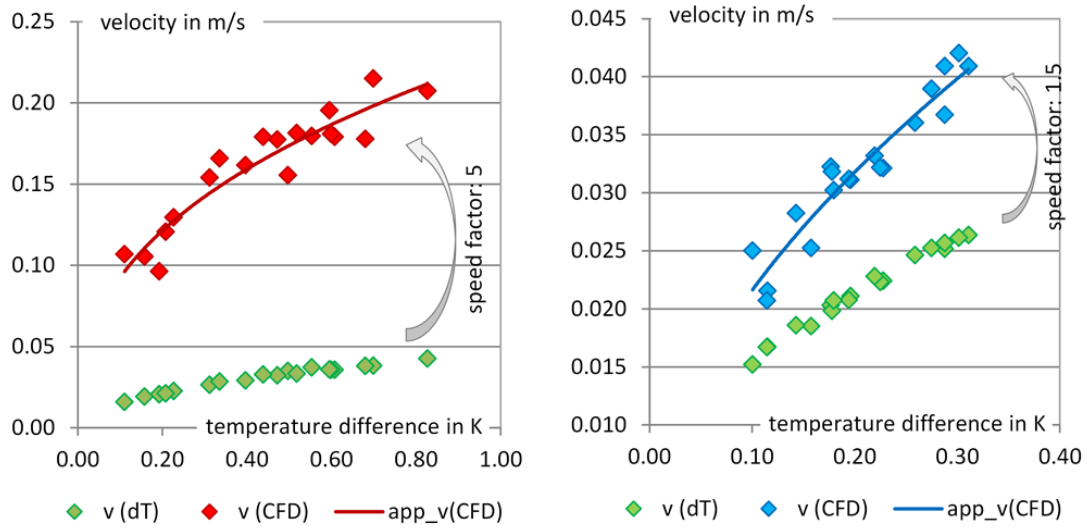

Figure 7.19: Comparison of the velocity - thermal calculation (velocity is calculated from the convective heat flow due the temperature difference air temperature and surface temperature; left side - façade area; right side - ceiling area)

7.5 Conclusions of the CFD calculation

The comparison of in situ measurements of operative temperature and the cooling capacity of a cooling ceiling and the calculation results of the CFD calculation show good agreement. The CFD model can therefore be used to characterize different façade systems regarding their impact on operative temperature and the capacity of the cooling ceiling.

The comparison of the two façade systems – the single skin façade (type 1) and the single storey double skin façade (type 2) – show that there is a decrease in operative temperature and an increase of the cooling capacity.

The CFD calculation results show the cooling capacity in dependence of the solar radiation the temperature difference between the mean medium temperature and the operative temperature in the middle of the room and the depth of the room. The results show, that there is an impact due to the solar radiation and the characteristics of the cooling capacity within the room geometry. The increase of the cooling capacity due to a higher air flow rate is limited on the first 3 m from the façade, then there is no longer an impact due to solar radiation.

The evaluation of the air velocities show, that there is an higher convective air flow rate due to the single storey double skin façade, than it is calculated regarding the temperature differences of surface temperature and air temperature. The simulation results show, that for the façade area the velocity is 5 times higher and for the cooling ceiling the velocity is 1.5 times higher with the single storey double skin façade than with the single skin façade.

The results of the CFD calculation can be used for an enhanced building model for future building design. There are two possibilities to integrate the results. First the results regarding the cooling capacity can be integrated directly and second there is the possibility of using the so called speed factors and increase the convective heat flow within the thermal model.

8 Air Flow Integrated Room Model

8.1 Introduction

The measurement and the calculation results show an impact on the cooling capacity by changing air flow conditions within the room. The design of the façade system can increase the capacity of a cooling ceiling and therefore decrease the operative temperature in the room. Neglecting the flow characteristics in the room can lead to incorrect results, especially for complex façade systems in combination with component activation (e.g. cooling ceiling).

Therefore an enhanced building model for the design of future buildings, taking into account the interaction of building envelope and building service systems should be developed using the results of the air flow calculation.

There are three ways of integrating the results from the air flow calculation to the room model.

- direct integration of the calculated cooling capacity to the room model
- use of the splitting factors for the air flow
- integration of temperature depending ”speed factors” of the convective heat flow

For the room model the decision was to integrate the speed factors, because it allows the most flexibility in terms of system changes and the results for the air velocity can be generated by the air flow model using the wall function. The comparison of the simulation results done with the model using the wall function and with the model using the Low Reynolds number $k-\epsilon$ turbulence model show the same results for the air velocity in the regarded areas. For a direct cooling capacity integration the detailed model has do be used because with the model using the wall functions there are no reasonable results.

8.2 Model description

The room model is built in Matlab/Simulink as an ”extension/enhanced” thermal model. The results of the air flow calculation which was done by CFD simulations with the program COMSOL Multiphysics version 4.3a and validated with a series of measurements are included in the room model. The model is divided in the following main parts (see figure 8.1 - blue frames):

- input
- geometry

- room
- enclosing surfaces
- façade
- ventilation
- internal heat gains
- output

The schematic overview is shown in figure 8.1, where the blue frames highlight the different parts of the room model, the green frame visualize the summary of the integration of the temperature depending air flow. The main parts of the model are described in the following sections.

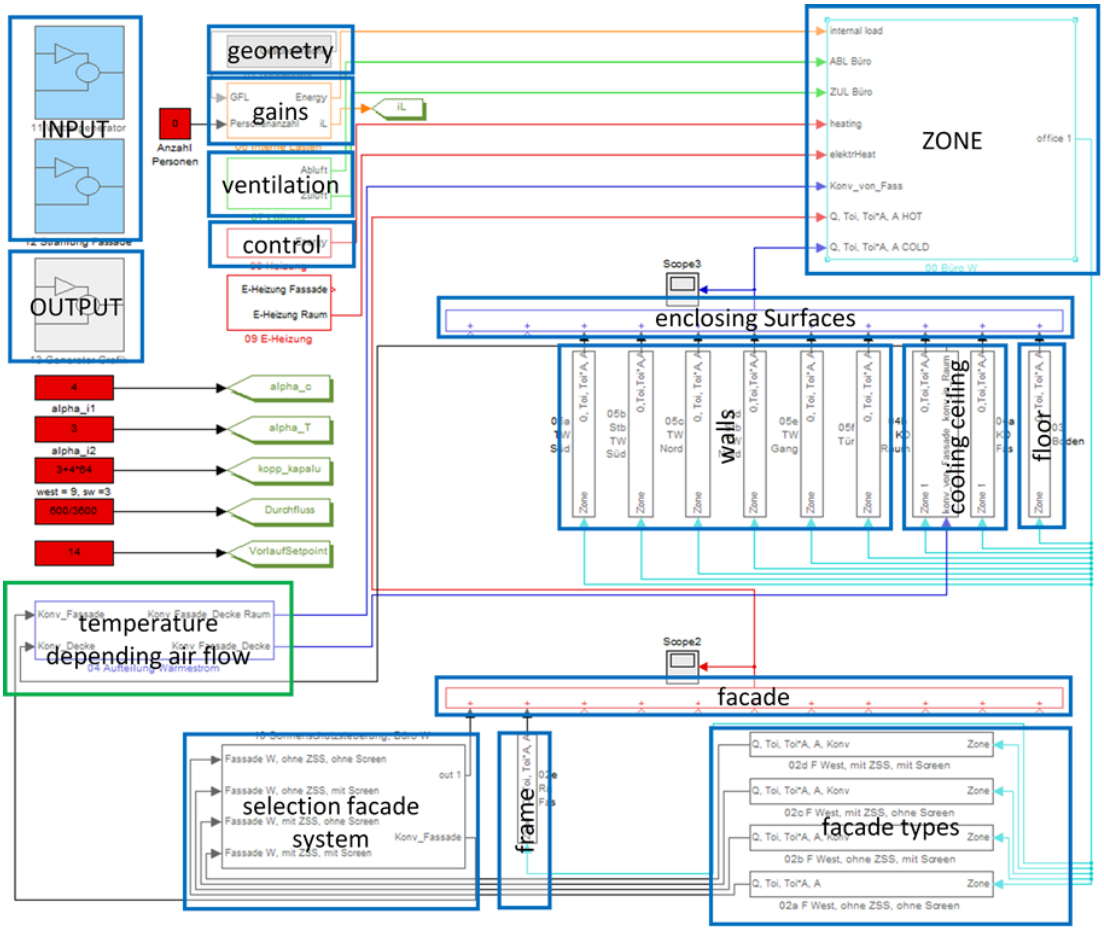

Figure 8.1: schematic overview of the **room model**; the main parts of the model are highlighted - room, enclosing surfaces, façade/façade types/shading control; cooling ceiling; ventilation; internal heat gains; geometry; input and output

8.2.1 Zone

The mapping of the zone comprises the summary of the calculation of the various input parameters and is shown in figure 8.2. The input variables include the geometry (grey frame), the calculation of the components (turquoise frame), the internal loads (red frame), the ventilation (violet frame), the calculation of the cooling ceiling (light blue frame) and the radiation (yellow frame). The resulting temperatures (air temperature, perceived temperature, mean radiant temperature) are calculated and given as output (blue frame) from the zone.

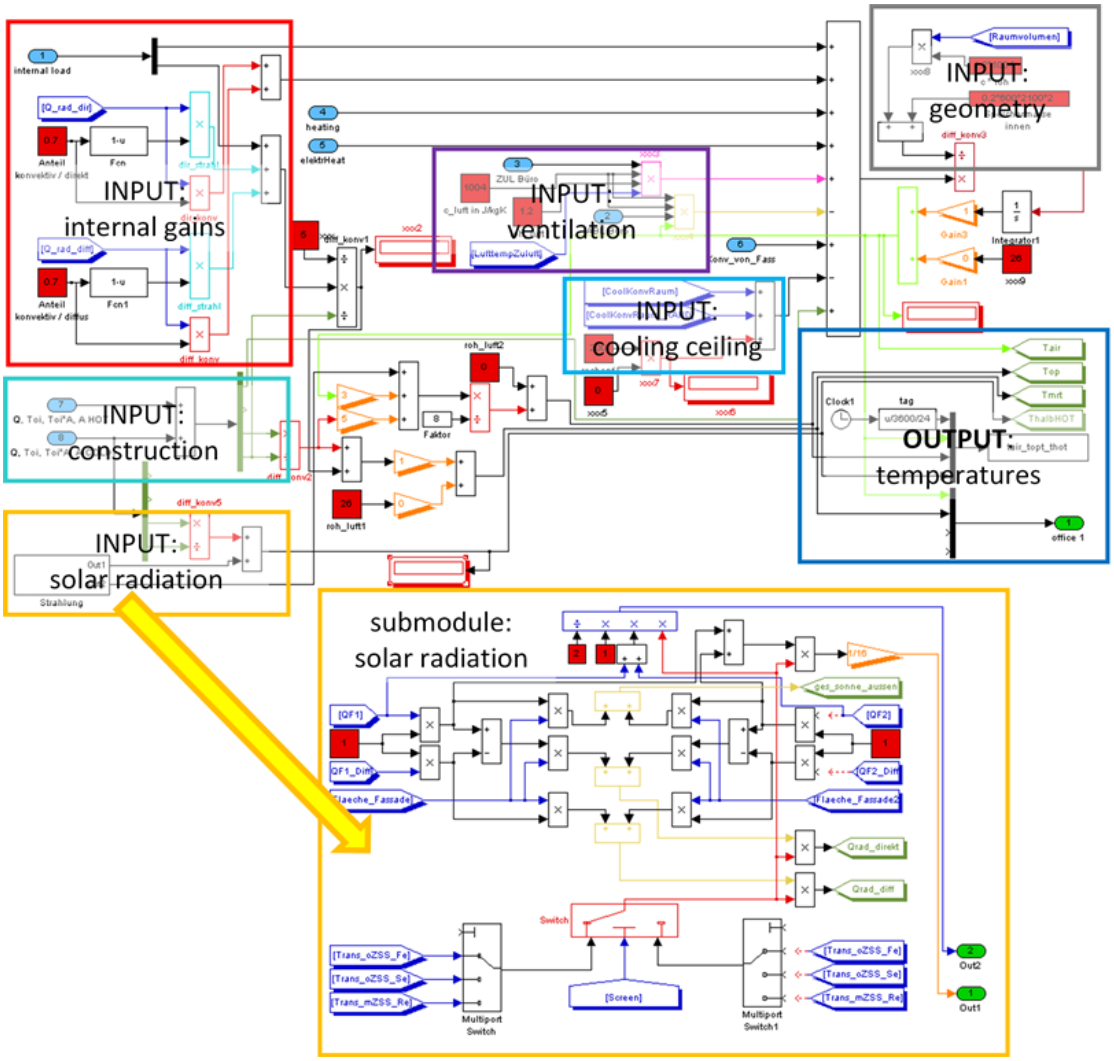

Figure 8.2: schematic overview of the model part - **zone**; summary of the various input parameters like geometry (grey frame), the calculation of the components (turquoise frame), the internal loads (red frame), the ventilation (violet frame), the calculation of the cooling ceiling (light blue frame) and the radiation (yellow frame); Output: resulting temperatures (blue frame)

8.2.2 Geometry

The module geometry describes the necessary input for determining the required geometry data for further simulations, an overview is shown in table 8.1.

Table 8.1: Summary of the geometric input parameters

nb	symbol	description	INPUT	unit
1	L_F	lenght of the facade	2.7	m
2	t_R	depth of the room	4.6	m
3	H_R	height between floors	3.5	m
4	h_r	ceiling height	3.0	m
5	$S_{TW,N}$	number of columns in north facing partition wall	1	unit
6	$S_{TW,S}$	number of columns in south facing partition wall	0	unit
7	O_F	orientation of the facade (π = Süd, $\pi/2$ =Ost, $3\pi/2$ = West)	$3\pi/2$	rad

In figure 8.3 schematic overview of the module geometry is shown, the left blue frame marks the input data shown in 8.1.

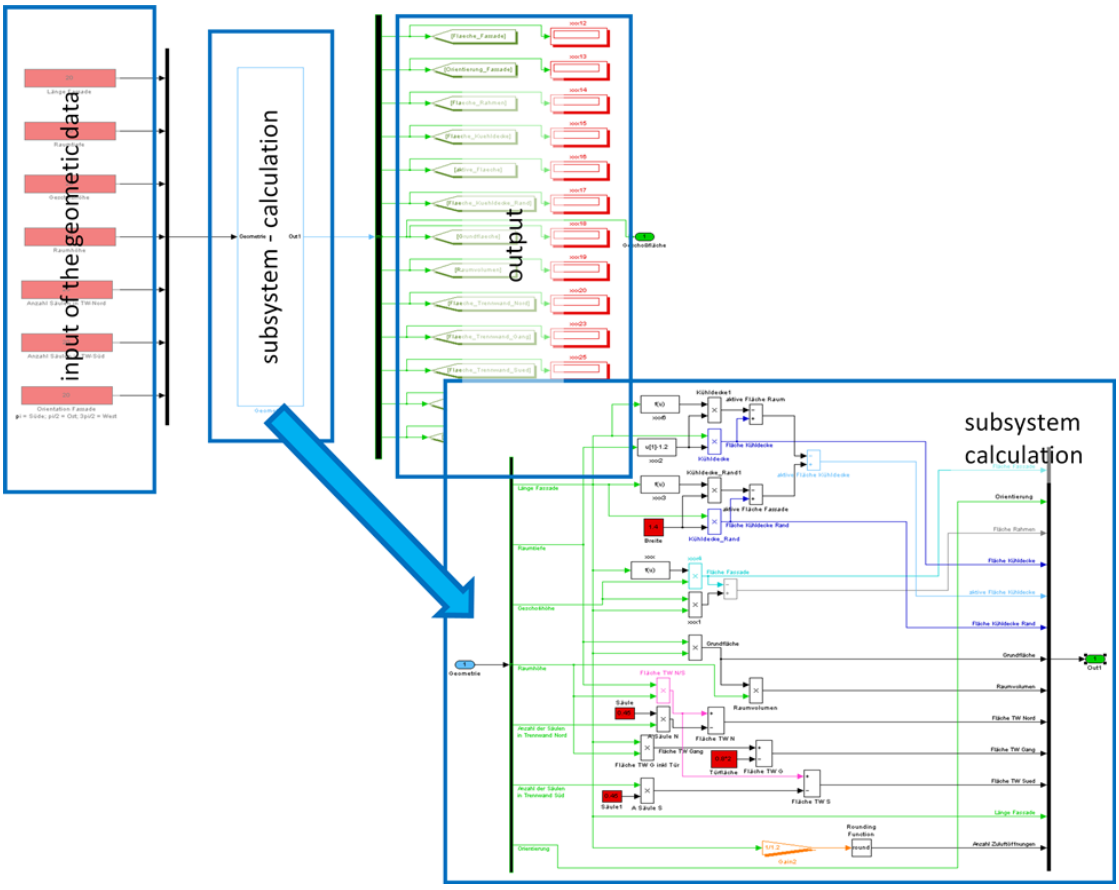

Figure 8.3: schematic overview of the model part - **geometry**; overview of the geometric input and calculated output parameters

The subsystem calculation processed on the data for the output (in figure 8.3) the output is marked by the third frame. In table 8.2 the parameter for further calculations are summarized.

Table 8.2: Summary of the geometric output data

nb	symbol	description	CALCULATED VALUE	unit
1	A_F	facade area		m^2
2	O_F	orientation of the facade		rad
3	A_R	frame area		m^2
4	$A_{KD,Raum}$	cooling ceiling area		m^2
5	$A_{KD,R,aktiv}$	active cooling ceiling area		m^2
6	$A_{KD,Rand}$	cooling ceiling edge surface		m^2
7	A_{GF}	floor area		m^2
8	V_R	room volume		m^3
9	$A_{TW,N}$	partition wall area - north		m^2
10	$A_{TW,G}$	partition wall area - corridor		m^2
11	$A_{TW,S}$	partition wall ares - south		m^2
12	L_F	lenght facade		m
13	ZUL	number of supply air outlets		-

8.2.3 Façade

The modeling of the façade system is one of the main points of the room model. The focus is set on the interaction between the façade system and the building service system (in this case the cooling ceiling). This section describes the calculation model of the considered façade systems within the in-situ measurements.

Façade Types

Four rooms were realized for in-situ measurements, the detailed description of the room set up and the measurements can be found in 2. Different façade systems were tested, the schematic overview of the single skin façade and the single storey double skin façade is shown in figure 2.3. The following bullet list summarize the 5 different façades systems (combination of glazing and shading)

- Façade system 1: single skin façade with internal shading element type 1
- Façade system 2: single skin façade with internal shading element type 2
- Façade system 3: single storey double skin façade with internal shading element type 2
- Façade system 4: single skin façade with internal shading element type 3 (blinds)
- Façade system 5: single storey double skin façade with internal shading element type 3 (blinds)

Within the room model the façade system was integrated by the following 4 façade types:

- Single skin façade, without shading
- Single skin façade, with shading
- Single storey double skin façade without shading
- Single storey double skin façade with shading

The differences are due to the shading element (with/without) and the layers of the façade (single skin façade versus single storey double skin façade). The shading system was modeled by its optical properties, the summary of the relevant values for the 3 tested shading types is shown in table 8.3.

Table 8.3: Summary of the differences regarding optical properties of the tested shading systems

optical properties	shading system 1	shading system 2	shading system 3
Solar transmittance τ	0.19	0.11	0.08
Reflectance ρ	0.37	0.39	0.39
Absorptance α	0.44	0.50	0.54
Light transmittance τ_L	0.19	0.10	0.07

For the modeling the main difference except the amount of layers is due to the air flow. A schematic overview for the different façade systems is shown in figure 8.4. The coloured frames refer to the systems of the modeling (see figure 8.5), the schematic picture of the air flow is shown by the violet arrows.

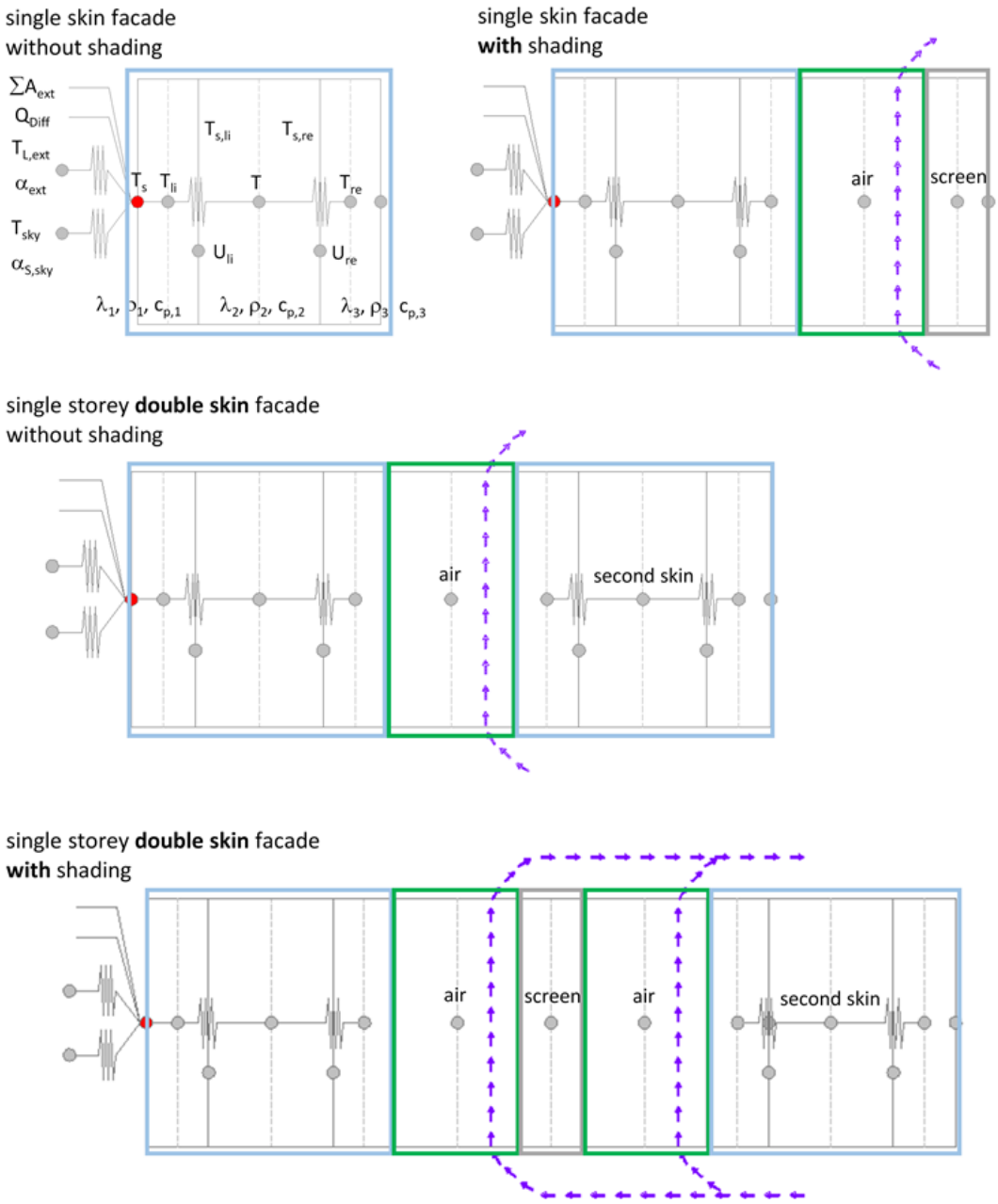

Figure 8.4: schematic overview of the façade types, the colours refer to the model components in figure 8.5; the air flow for the different façade types is highlighted with the violet arrows

In figure 8.5 the modeling of the façade type single storey double skin façade plus shading is visualized. The red frames mark the calculation of the layers according to the description of the thermal modeling done in chapter 6. The green frames mark the integration of the convective air flow according to the results of the air flow calculation (see chapter 7, section 7.4.3).

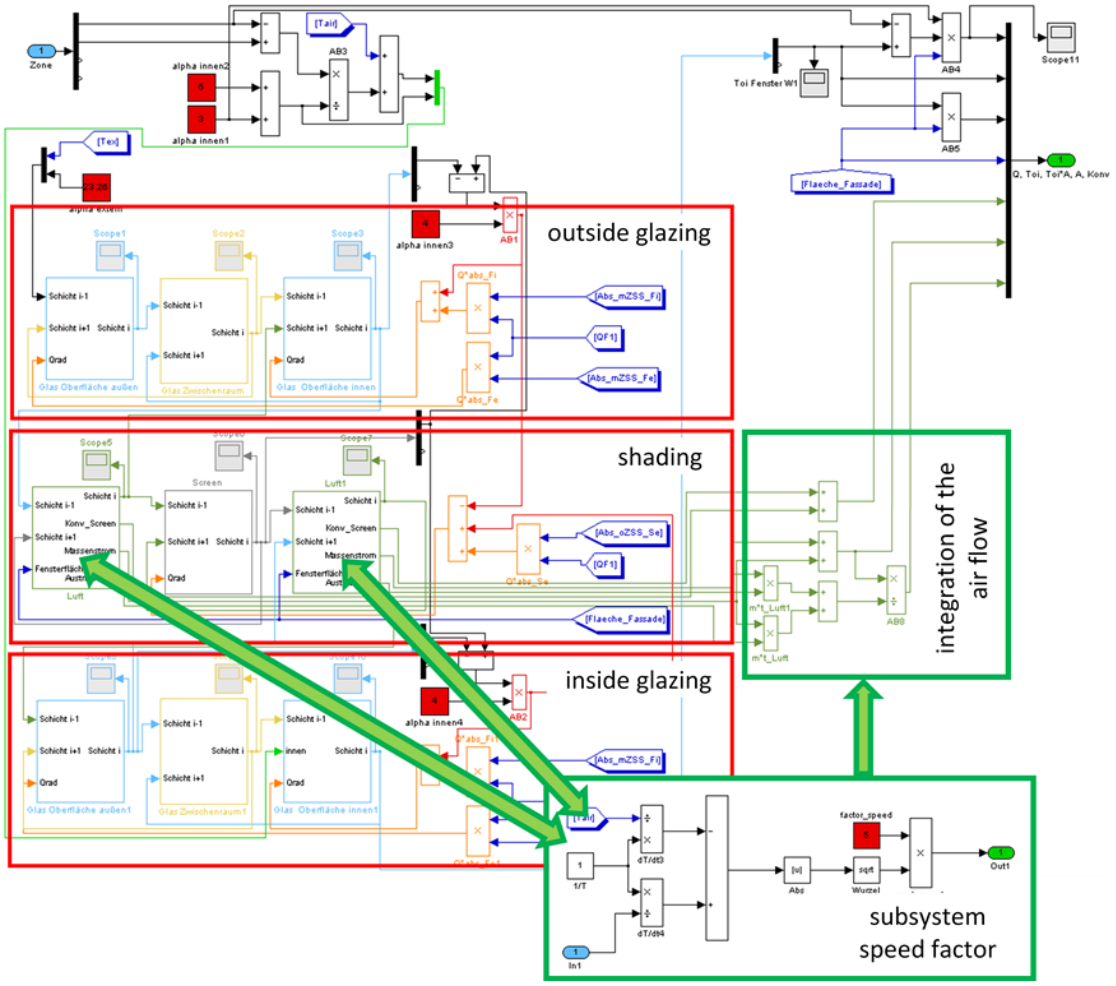

Figure 8.5: schematic overview of the model part - **façade type**; the picture show the façade type: single storey double skin façade plus shading; the red lines mark the calculation of the layers - the layers were adjusted to the façade type; the green field mark the integration of the air flow

Control of Façade and Shading System

This part describes the selection of the calculated façade type and if the shading is used or not. The modeling of the façade and shading type selection is visualized in a schematic overview in figure 8.6. The red frame mark the selection of the façade type, where 0 is for single sin façade and 1 is for single storey double skin façade.

The modeling for the two façade systems is marked by the blue frames on the left side, where the upper switch is for façade type 01 (single skin façade) and the switch below is for façade type 2 (single storey double skin façade). The control signal if the shading is on or off is given by a link named ”screen”. For the validation of the model the shading was fully closed. The input for the façade systems is given by the calculation of the layers according to the thermal modeling and the schematic overview of figure 8.4.

The output of the control strategy is marked by the blue filed on the right side. The outputs are the heat flow and the temperature for the used façade system in combination with the shading system (according to the thermal modeling) and the calculated air flow for the façade (according to the air flow modeling).

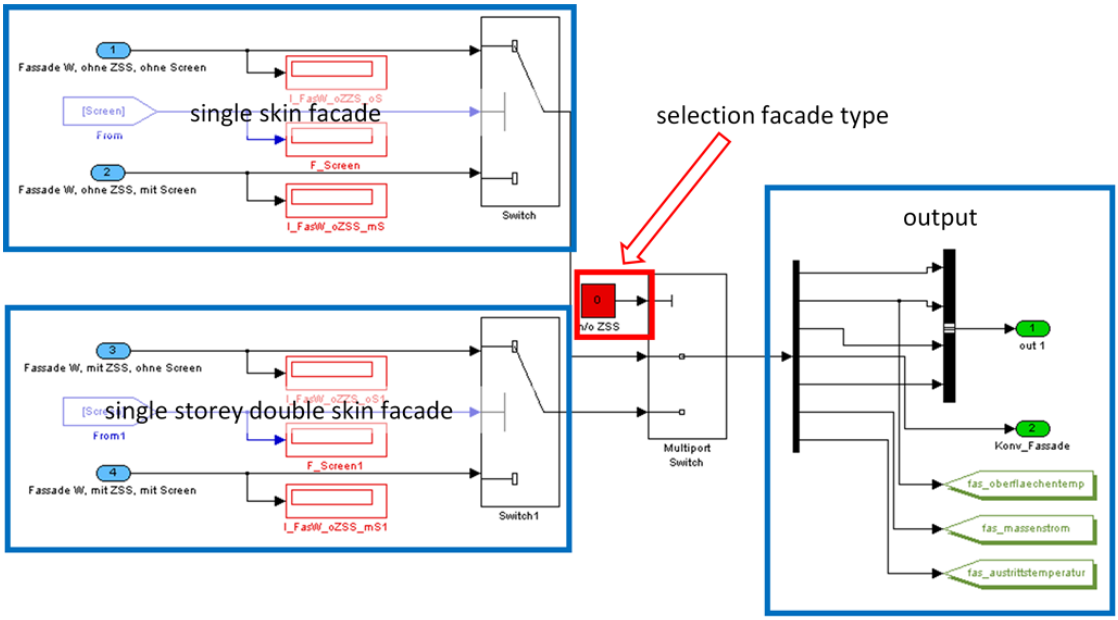

Figure 8.6: schematic overview of the model part - **control façade and shading system**; the red field mark the selection of the façade type; the upper switch is for façade type 01 (single skin façade) and the lower switch is for façade type 2 (single storey double skin façade); the marked field on the right side summarize the output

8.2.4 Enclosing Surfaces

This section describes the modeling of the enclosing surfaces like the floor / the ceiling and the partition walls. The modeling is done according to the description of the thermal modeling (see chapter 6.

Partition Walls

In figure 8.7 the modeling of the partition walls is shown. The upper red frame marks the inputs coming from the zone modeling like the zone temperatures (mean radiant temperature, operative temperature, air temperature) and additional input values for the component like the heat transfer coefficients or the boundary conditions. The red frame below show the modules for the layer calculation and the third red frame show the link to the input of the area of the partition wall.

The output of the calculation, which are the heat flow and the temperatures is marked by the blue frame at the right side of the picture.

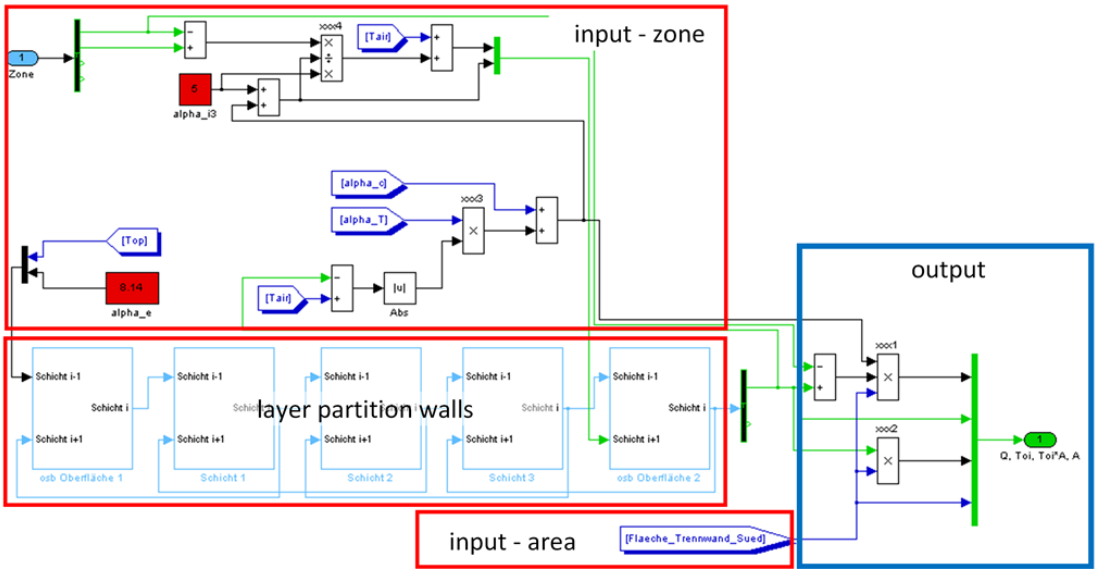

Figure 8.7: schematic overview of the model part - **partition walls**; 1st red frame (top): inputs coming from zone modeling; 2nd red frame (middle): modules for the layer calculation; 3rd red frame (bottom): link to the input data for the calculation; blue frame: outputs and results of the partition wall calculation

Raised Floor

The modeling of the raised floor is done according to the schematic overview in figure 8.8, where the red frame marks the thermal calculation of the component layers according to the description of chapter 6. The floor is divided into layers. The raised floor is air leading and therefore coupled with the module ”ventilation”. The subsystem marked by the blue frame is the visualization of the connection to the ventilation modeling.

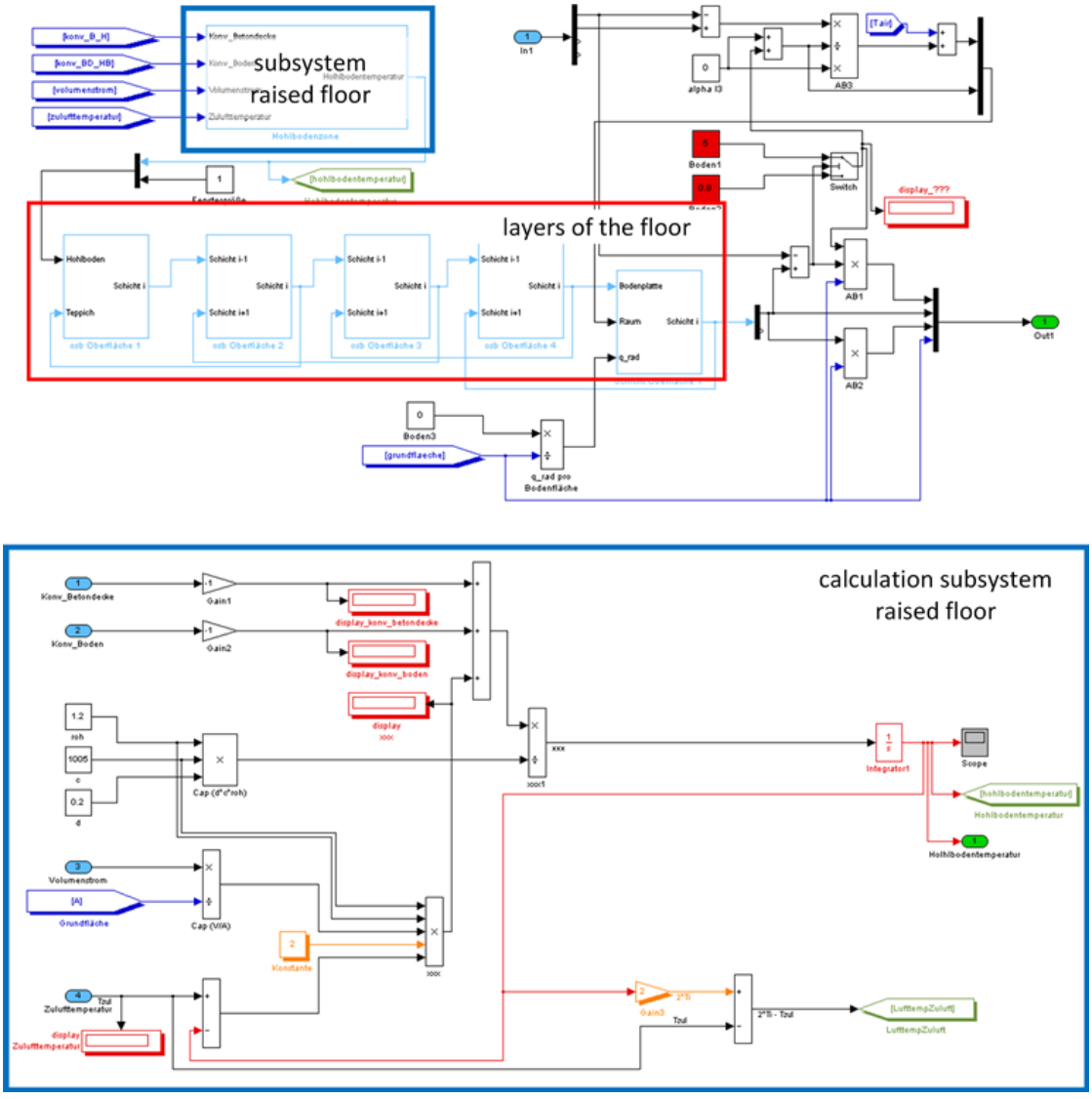

Figure 8.8: schematic overview of the model part - **raised floor**; red frame: thermal calculation of the floor; blue frame: integration / coupling to the ventilation of the room

Cooling Ceiling

The modeling of the cooling ceiling is divided into two parts - the cooling ceiling in the façade area and the cooling ceiling in the room area - regarding the system design of the building (detailed description see chapter 2, section 2.2.3). Figure 8.9 shows the modeling of the cooling ceiling regarding the room area, the model of the cooling ceiling belonging to the façade area is designed similar. The red frame marks the thermal modeling of the layer of the construction. The blue frame highlight the layer ”air” and the subsystem of the layer calculation is shown. The integration of the air flow with the modeling of the temperature depending ”speed factor” is done within this layer of the cooling ceiling and is highlighted by the green frame. The ”speed” factor for the cooling ceiling is defined due to the result of the air flow modeling and the definition is done in chapter 7, section 7.4.3.

The results of module ”cooling ceiling” are temperatures and the heat flow whcih are inputs for the module ”zone”. The simplified air flow calculation with the ”speed factor” is effecting on the module ”temperature depending air flow”.

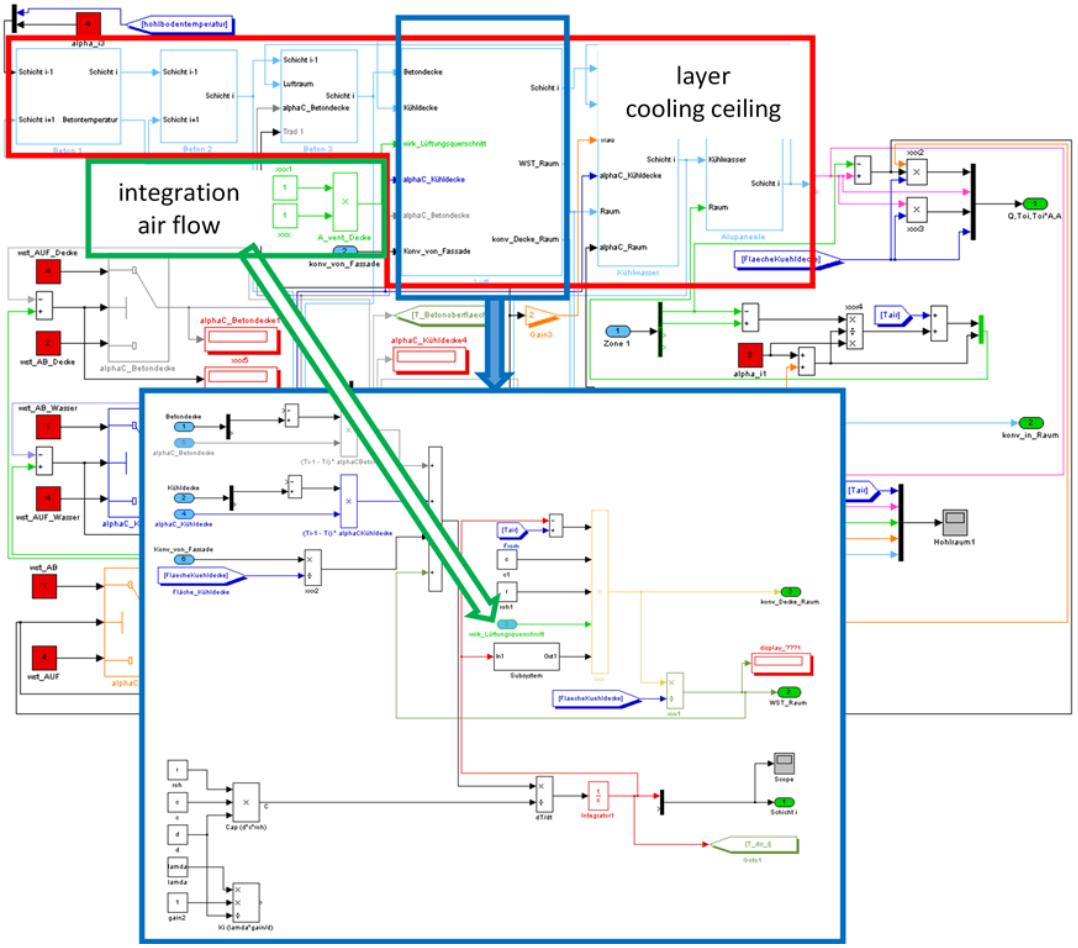

Figure 8.9: schematic overview of the model part - **cooling ceiling**; red frame: thermal calculation of the construction layers; blue frames: calculation of the layer ”air”; green frames: integration of the simplified air flow modeling

8.2.5 Internal Gains

The internal gains are considered according to the schematic scheme shown in figure 8.10. The heat gains are divided in a convective and a radiative part, furthermore there is a division due to different initiators like lights, technical equipment and people. The required input values like amount of people, degree of illumination / heat impact due to lights and technical equipment is marked by the red frame. The control of the internal gains is done by timer. For the calculation internal ains are assumed from 8.00am to 12.00am and from 1.00pm to 5.00pm. The output of the internal gains is reflecting on the zone calculation (see chapter 9, section 8.2.1)

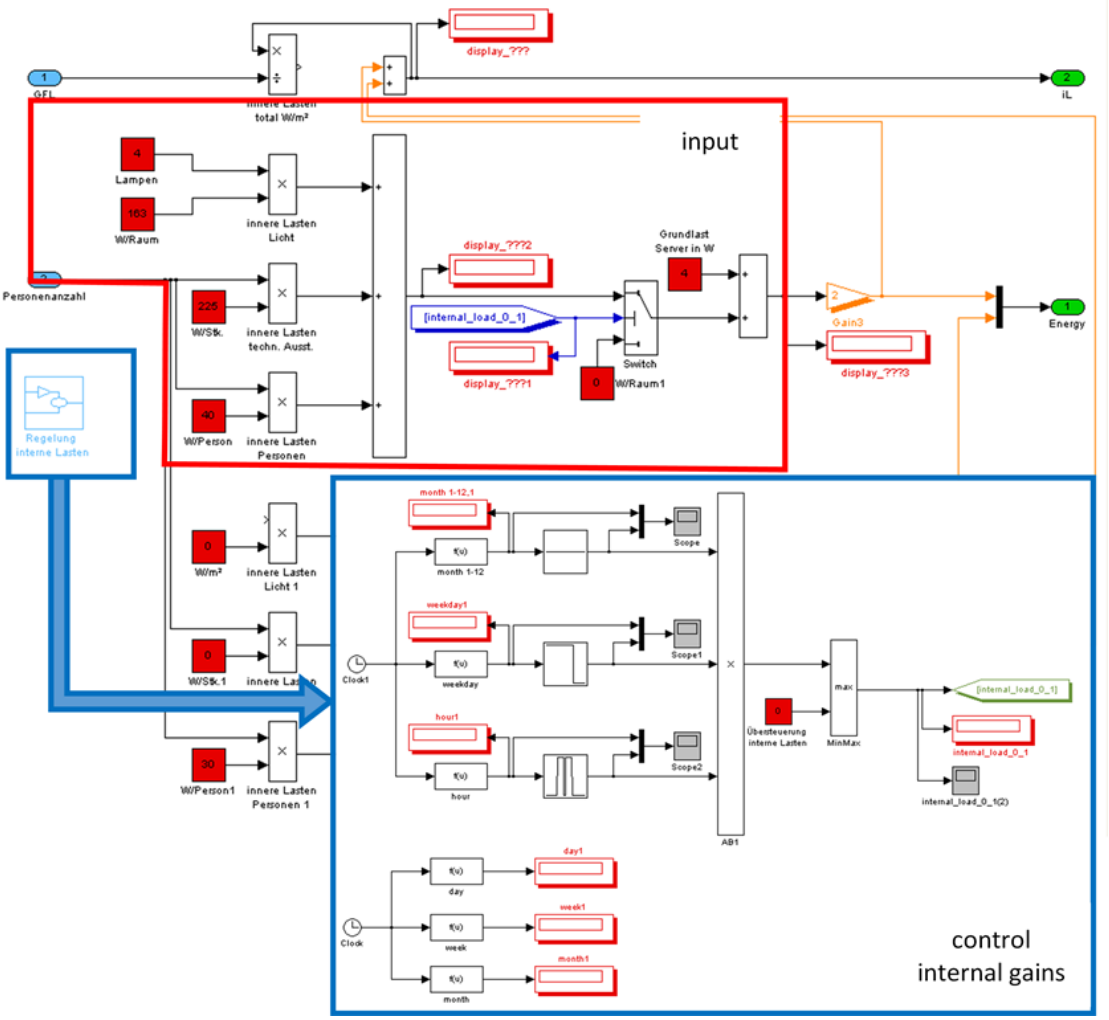

Figure 8.10: schematic overview of the model part - **internal gains**; red frame: input values - heat gains due to lights, technical equipment and people; blue frame: control of the internal gains

8.2.6 Ventilation

The supply air of the room is realized via the air leading floor (description see chapter 2, section 2.2.4. The modeling of the air flow is done by integration of the volume flow per each axes according to the measurement results presented in chapter 2, section 2.3.6. The supply air temperature was measured too (for results see chapter 2, section 2.3.7) and is integrated within the model by an external time series. Figure 8.11 show the schematic overview of the ventilation module, where the red frame marks the input due to volume flow rate and the blue one the control strategy by an hourly basis linked to the supply air temperature.

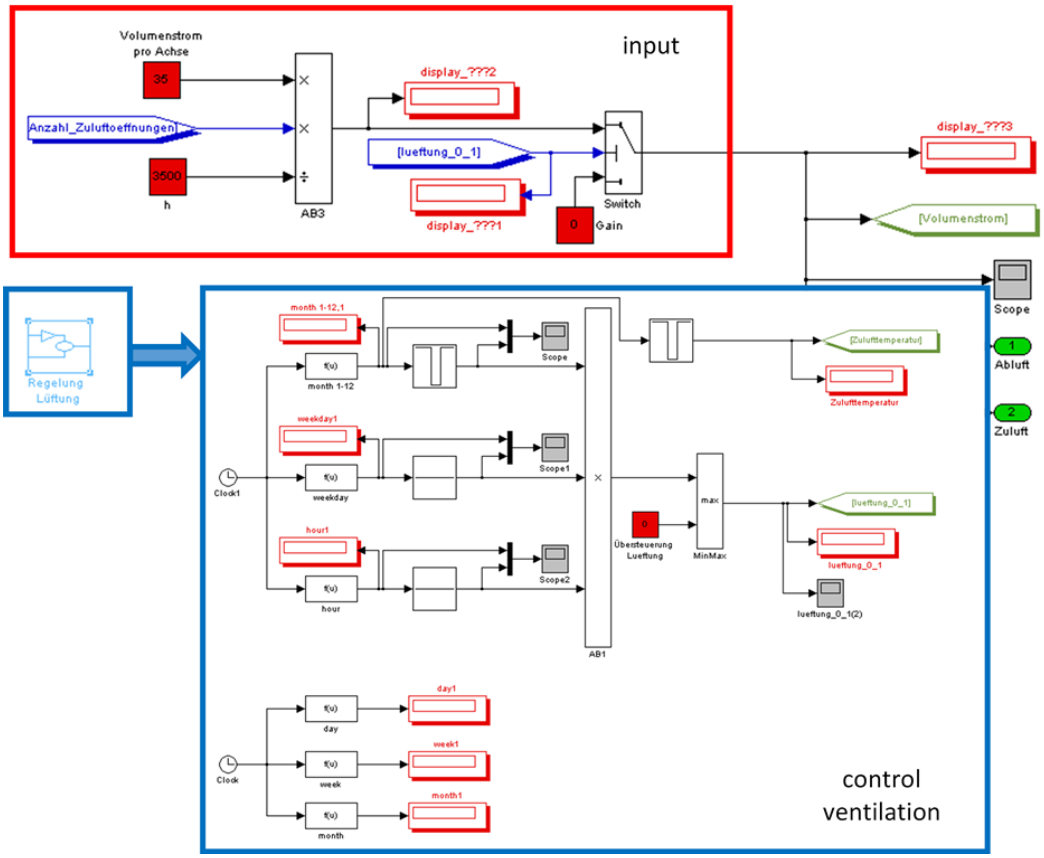

Figure 8.11: schematic overview of the model part - **ventilation**; red frame: input of volume flow rate; blue frame: control strategy of ventilation system and supply air temperature

8.2.7 Weather

The external boundary conditions like temperature , humidity and radiation are provided by an external data file. Figure 8.12 shows the schematic overview of the weather data, where the input is marked by the red frame, the blue one marks the output values for further calculations and the yellow one marks the calculation of the radiation on the surface.

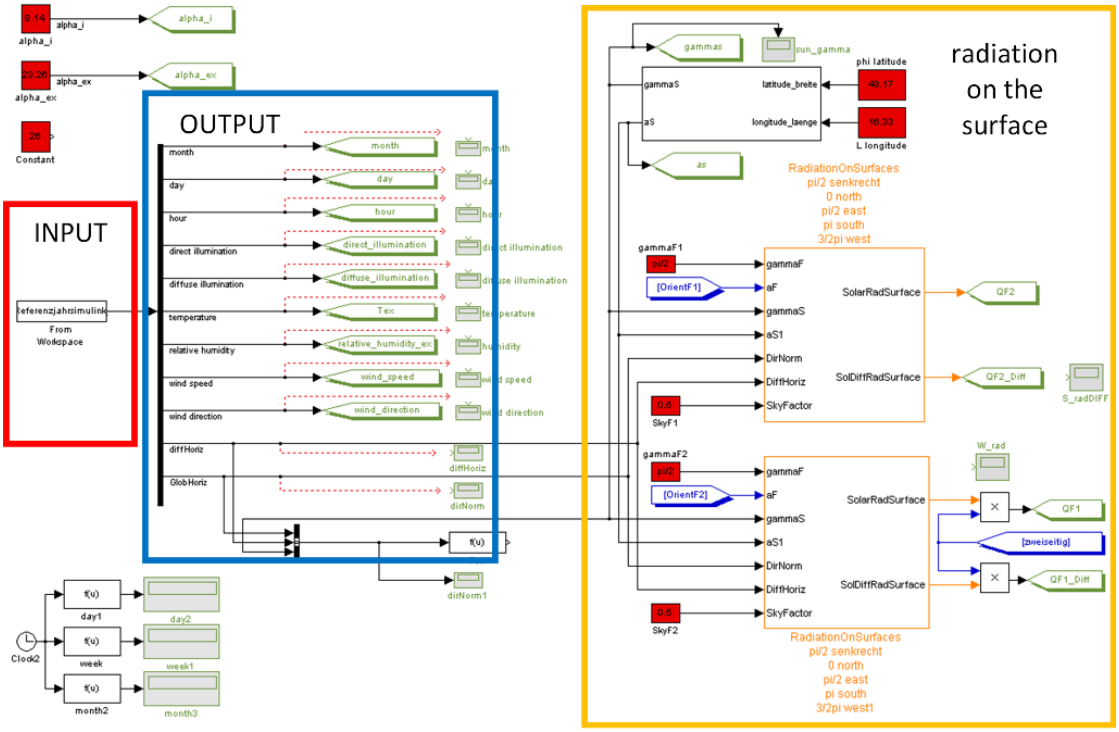

Figure 8.12: Schematic overview of the model part - **weather**; red frame: input data file; blue frame: output for further calculation; yellow frame: calculation of the radiation on the surface

8.3 Summary Air Flow Integrated Room Modeling

A room model was developed that integrates the thermal calculation and a simplified illustration of the three-dimensional flow phenomena. The integration is required for a correct calculation of transfer systems to the room (eg chilled ceilings).

The thermal calculation is based on the descriptions in chapter 6, which represent a summary of the description done in Clarke (2001) [18]. The consideration of the indoor air flow was determined by an air flow calculation. The results are presented in chapter 7. For the integration of the air flow speed factors were evaluated with the CFD calculation.

9 Validation of the Integrated Room Model

9.1 Introduction: Validation Enhanced Room Model

To validate the room model, it was compared with the available measurement data for operative temperature in the centre of the room and the cooling capacity (detailed description see chapter 2, 3, 4 and 5). The detailed comparison is done on room type 2 (single storey double skin façade), the calculation results for all room types is shown in subsection 9.5.

9.2 Air Flow Integration - Comparison of the Speed Factors

The calculated speed factors (result of the air flow calculation) were compared to the results of the air flow integrated room model. The results are shown in figure 9.1, where the air velocity in dependence of the temperature difference between the air temperature in the centre of the room and the surface temperature of the cooling ceiling or the façade is shown for the façade area (red) and the ceiling area (blue). The lines represent the results of the air flow calculation, the dots the results regarding the air flow integrated room model.

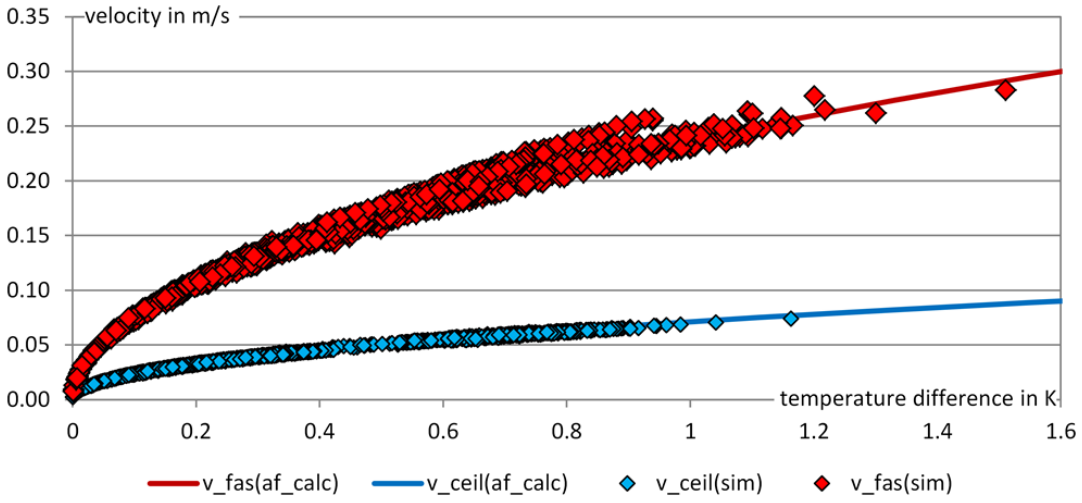

Figure 9.1: Comparison of the speed factors - result of the air flow calculation (lines) and output of the air flow integrated room model simulation (dots) for the façade area (red) and the cooling ceiling area (blue)

9.3 Comparison Measurement Results and Calculated Results on the Cooling Capacity

The comparison of the measurement results and the calculation results of the capacity of the cooling ceiling for room type 2 was done and the results are shown in figure 9.2. The cooling capacity of the cooling ceiling is shown in dependence of the temperature difference between the mean medium temperature and the operative temperature in the centre of the room, where the blue dots represent the measurement results and the red ones the calculated cooling capacities. The results of cooling capacity are related to the active cooling area in the room and not to the floor area. The comparison show a good accordance between these two values, the range of the calculated results is smaller than the measurement results.

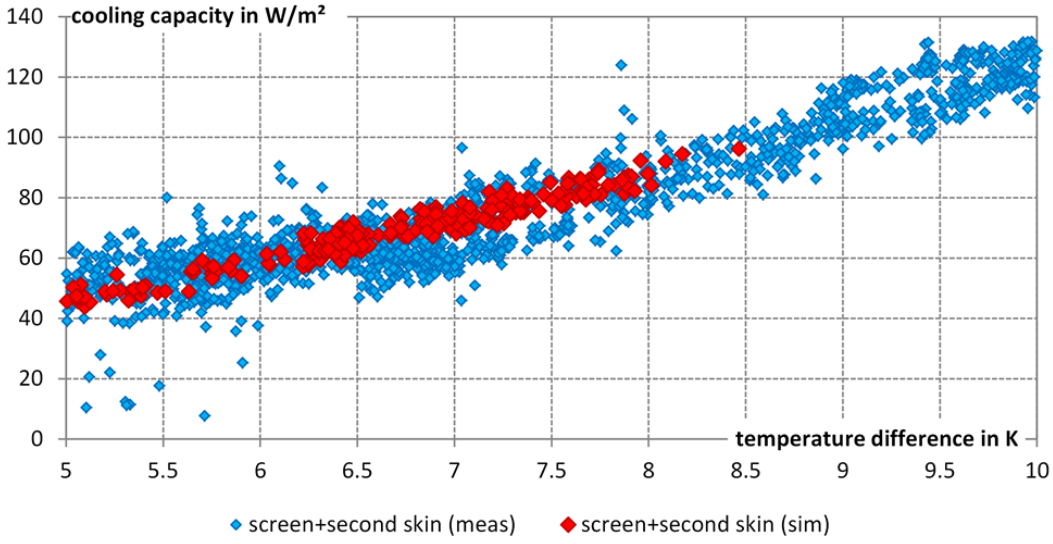

Figure 9.2: Comparison of the capacity of the cooling ceiling in dependence of the temperature difference between the mean medium temperature and the operative temperature in the centre of the room; red: calculation results, blue measurement results

9.4 Comparison Measurement Results and Calculated Results on Operative Temperatures

The room model was validated by comparing the calculation results with the available measurement data. For comparison the period from June 20th till the august 20th of the second summer period was used, where the data of July 27th was compared in detail. The results for the operative temperature in the centre of the room for this day are shown in 9.3, where the blue line represents the measurement data and the red line the calculated results of the developed room model. Both curves are for room type 2 (single storey double skin façade and screens as shading system).

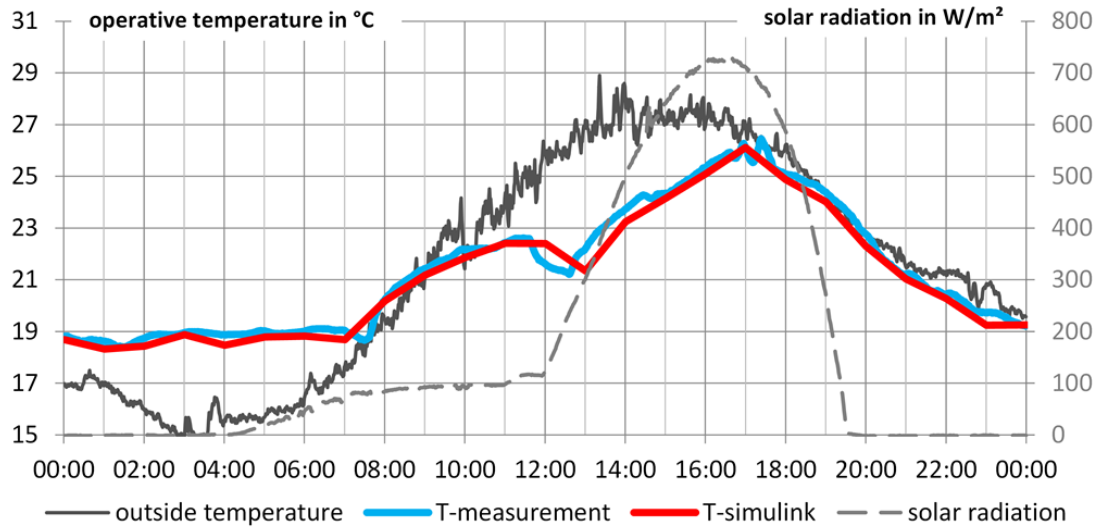

Figure 9.3: Comparison of the measurement results (blue line) and the results of the developed room model (red line) for room type 2; the difference between the measurement results and the simulation results around 5pm is due to the gap between the façade and the screen - direct sun is shining on the black ball meter (see figure 9.4)

The results show a good accordance, the difference during the lunch time is due to hourly time step of the simulation and a logging period of 1 min for the measurement data. The difference between the measurement results and the simulation results around 5.00 pm is due to the gap between the façade and the screen, which allows that direct sun is shining on the black ball meter (see figure 9.4).

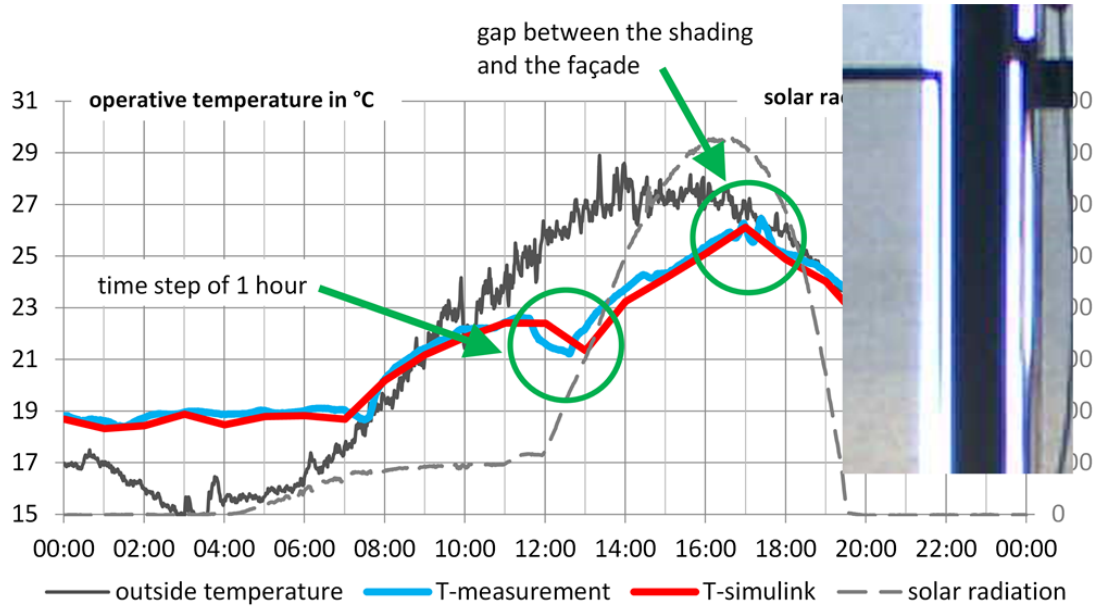

Figure 9.4: Comparison of the measurement results (blue line) and the results of the developed room model (red line) for room type 2 - **explanation of the differences**

9.5 Calculation Results for the different Room Types - Design Day

In figure 9.5 the results for room types 1, 2, 3 and 6 are visualized. The summary of the boundary conditions for the different room types is shown in table 9.1. The diagram shows the results for July 27th and the results are for the centre of the room. This diagram can be compared with the measurement results shown in figure 3.10 for the room types 0, 2, 3 and 6.

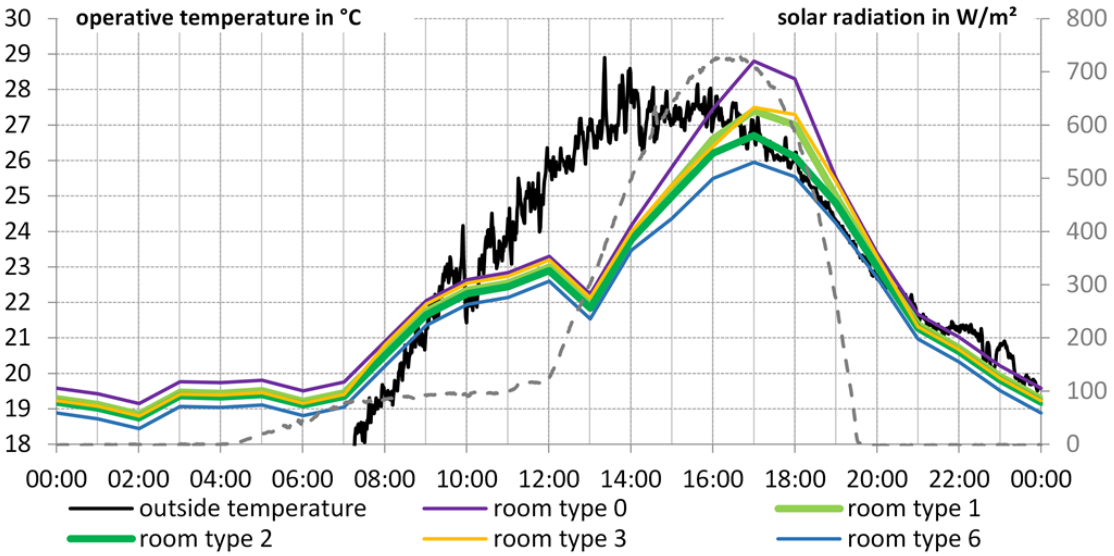

Figure 9.5: simulation results - room type 0 / 1 / 2 / 3 / 5; the simulation results are in a good accordance to the measurement results (see figure 3.20)

Table 9.1: Summary of boundary conditions referring to figure 9.5

name	room	façade	shading	additional cooling element
Room type 0	4	single skin	screen $\tau_L = 0.19$	---
Room type 1	1	single skin	screen $\tau_L = 0{,}10$	---
Room type 2	1	single storey double skin	screen $\tau_L = 0{,}10$	---
Room type 3	2	single skin	blinds	---
Room type 6	3	single storey double skin	screen $\tau_L = 0{,}10$	yes

9.6 Summary Validation Air Flow Integrated Room Model

The air flow integrated room model was validated by comparing the measurement results on cooling capacity of the cooling ceiling and the results on operative room temperature in the centre of the room for room type 2 (single storey double skin façade and screen as shading system). Furthermore the output values for the air velocity was compared to the air flow modeling results on air velocity.

The comparison of the simulation results with the air flow simulation results respectively the measurement results regarding the ”speed factors”, the cooling capacity of the cooling ceiling and the operative temperature in the centre of the room show a good accordance.

The calculated results for the operative temperature of the room model were validated with measured data of the test rooms and the comparison show a good correspondence. The differences between the measurement data and the calculated results with respect to the operating temperature are due to the time step or to structural conditions which have not been modeled.

With the developed room model the effect of different façade systems in combination with cooled ceilings can be evaluated. The enhanced room model combines the building physical planning and the building service planning and statements in terms of thermal comfort, with complex flow phenomena in closed or open façades and the dynamics of cooling delivery systems, can be done.

10 Summary and Outlook

10.1 Introduction

The goal of the work is to develop a mathematical model as a first step for an easy to handle design tool that can predict comfort in room for different building concepts. The key issue is the integration of a simplified model of complex flow phenomena within the room. The work is divided in two main parts. On the one hand there are in-situ measurements in an existing office building for (1) temperatures (air, surface and operative), (2) humidity, (3) capacity of the cooling ceiling and air flow measurements done by tracer gas measurements. Measurements on comfort with comfort level probes are carried out too. On the other hand there is the part of the mathematical modeling, which is divided into the following 3 subtasks (1) the thermal modeling, (2) the air flow modeling and the combination of these two model parts (3) the development of the air flow integrated room model

In figure 10.1 the schematic overview of the development of the room model is summarized. The development of the air flow integrated room model is an interactive work between different mathematical model parts (thermal modeling, air flow modeling) and measurement results to validate the model parts and the final room model.

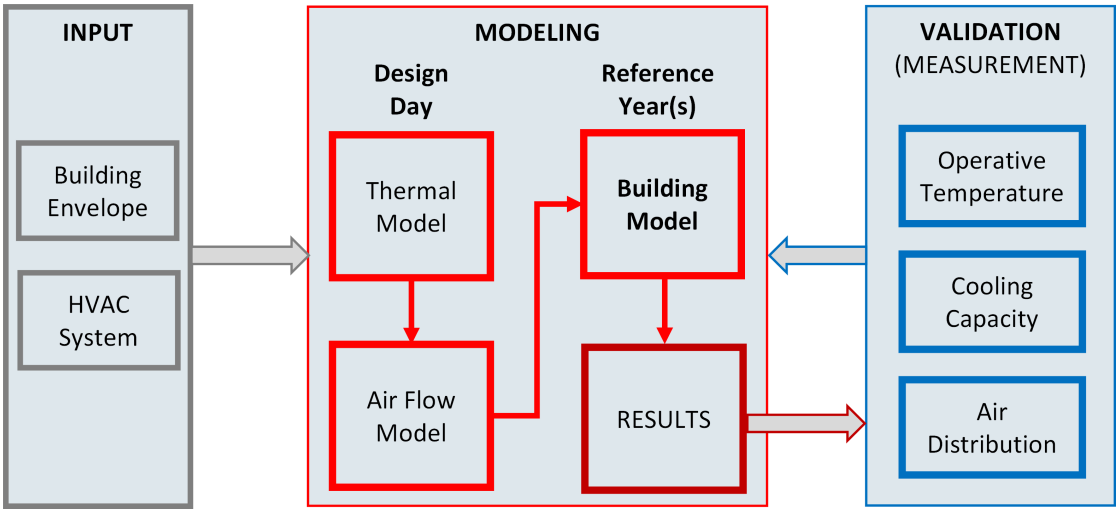

Figure 10.1: Schematic overview of the development of an enhanced room model

10.2 Summary of the work

The literature review shows, that non of the discussed (mostly used) building energy programs (TRNSYS, Energy Plus, IdaIce and ESP-r) can simulate the interaction of complex façade systems and cooling ceilings with the required level of detail. Although there are ”work-arounds” if specific parameters are known. For example in ESP-r it is possible to integrate a simplified air flow modeling by mass balances, which allows to describe the effect of buoyancy in dependence of façade systems and the cooling ceiling within the model if they are defined by a second party tool.

There is the possibility of doing coupled air flow and thermal simulations to get reliable results on room conditions and thermal comfort. These simulations are very time consuming at the moment and therefore not appropriate for the use of early planing phase support.

10.2.1 Measurement Results

A series of measurements have been done with different room types. The detailed description of the in-situ measurements is found in chapter 2, section 2.2.

The measurements took place in the 34th floor of an exiting office building in Austria. Four identical room each of around 11 m^2 were built. They were orientated to the west-side and have a fully glazed façade. In total 7 room types were tested, a summary regarding the measurement variations due to façade system, shading system and cooling system is shown in figure 10.2 and is summarized in table 10.1.

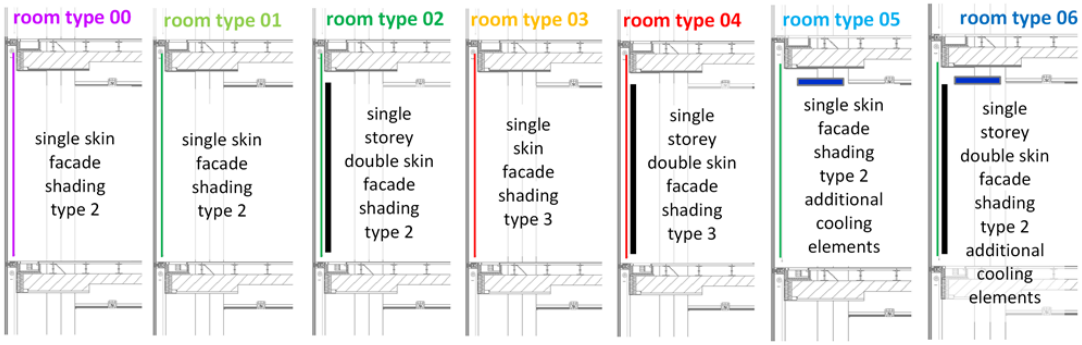

Figure 10.2: Visualization of the room types by section views - summary (detailed description see chapter 2.3.3)

Table 10.1: measurement variation, room types - summary (detailed description see chapter 2.3.3)

name	room	façade	shading	additional cooling element
Room type 0	4	single skin	screen $\tau_L = 0.19$	---
Room type 1	1	single skin	screen $\tau_L = 0{,}10$	---
Room type 2	1	single storey double skin	screen $\tau_L = 0{,}10$	---
Room type 3	2	single skin	blinds	---
Room type 4	2	single storey double skin	blinds	---
Room type 5	3	single skin	screen $\tau_L = 0{,}10$	yes
Room type 6	3	single storey double skin	screen $\tau_L = 0{,}10$	yes

Chapter 2.3 shows the detailed description of the measurement set-up. The schematic overview of the measurement equipment for the rooms s shown in figure 10.3, where the green marked positions are regarding temperature measurements, the blue ones are regarding humidity measurements and the red ones are referencing to the heat flow measurements. Additionally the mass flow of the cooling medium and the air flow were measured periodically. The main measurement points for the cooling capacity are also described separately in the section 2.3.5.

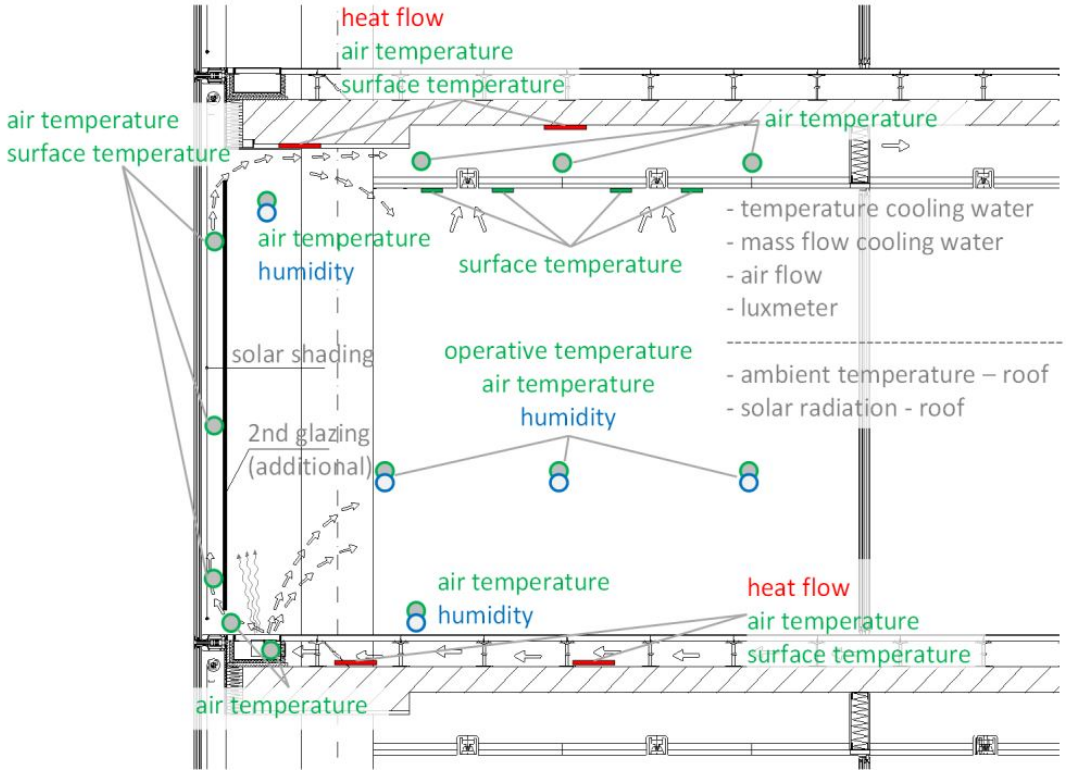

Figure 10.3: Measurement equipment of the test rooms

The relevant results regarding the measurement of the operative temperature is summarized in chapter 10, section 10.2.1. The main outcome of the measurements of the cooling capacity of the cooling ceiling is shown in chapter 10.2.1. The results of the

airflow measurements done by tracer gas are summarized in section 10.2.1. To make is easier to read the colour of the font in table 10.1 were used for creating the diagrams referring to the 7 different room set ups.

Operative temperature

The aim of the measurements is to identify the impact on operative temperature in the centre of the room and close to the façade regarding different façade systems. The impact of the different façade systems on the resulting cooling capacity was evaluated too. The room conditions were changed in the following three categories: (1) change of façade system, (2) change of shading system and (3) change of active cooling area

In figure 10.4 the result on the maximum operative temperature in the centre of the room for the different room types is shown. The change of the shading type from shading type 1 to shading type 2 reduces the maximum operative temperature of 1.4 K. The maximum operative temperature with room type 1 (shading type 2) is 27.4 °C. Due to the second glazing the operative temperature can be reduced of 0.7 K. With the additional cooling element there is a reduction of the maximum operative temperature by 2.5 K. The measured maximum operative temperatures and temperature difference to the reference room is shown in table 10.2.

Table 10.2: Summary of measurement results of the maximum operative temperature in the centre of the room

	Room type 0	Room type 1	Room type 2	Room type 3	Room type 4	Room type 5	Room type 6
temperature – totally closed	28.8 °C	27.4 °C	26.7 °C	27.3 °C	27.0 °C	26.2 °C	25.0 °C
temperature difference	-	- 1.4 K	- 2.1 K	- 1.5 K	- 1.7 K	- 2.5 K	- 3.8 K
temperature – half closed	-	29.3 °C	28.1 °C	29.0 °C	27.8 °C	27.9 °C	26.3 °C
temperature difference	-	+ 2.0 K	+ 1.4 K	+ 1.7 K	+ 0.8 K	+ 1.6 K	+ 1.3 K

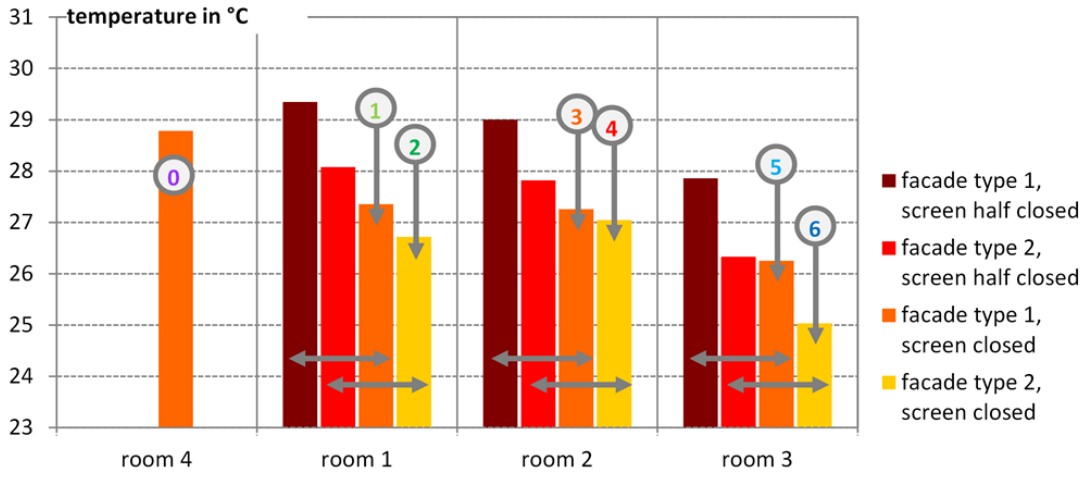

Figure 10.4: Measurement results on operative temperature - centre of the room

The measurement results next to the façade (distance of 1 m to the façade at the beginning of the working area) show a higher reduction of the maximum operative temperature. The results of the measurement are shown in figure10.5, the summary of the measured temperatures and the temperature difference to the reference room is shown in table 10.3. The change of the shading type from shading type 1 to shading type 2 reduces the maximum operative temperature of 1.4 K. The maximum operative temperature can be reduced of 1.2 K due to the second glazing from 28.3 °C (façade type 1) to 27.1 °C (façade type 2). With the additional cooling element there is a reduction of the maximum operative temperature of 2.9 K.

Table 10.3: Summary of measurement results of the maximum operative temperature next to the façade

	Room type 0	Room type 1	Room type 2	Room type 3	Room type 4	Room type 5	Room type 6
temperature – totally closed	29.7 °C	28.3 °C	27.1 °C	27.4 °C	26.8 °C	26.8 °C	25.4 °C
temperature difference	-	- 1.4 K	- 2.6 K	- 2.3 K	- 3.0 K	- 2.9 K	- 4.3 K
temperature – half closed	-	30.1 °C	28.5 °C	29.6 °C	28.2 °C	28.3 °C	26.9 °C
temperature difference	-	+ 1.8 K	+ 1.4 K	+ 2.4 K	+ 1.7 K	+ 1.5 K	+ 1.5 K

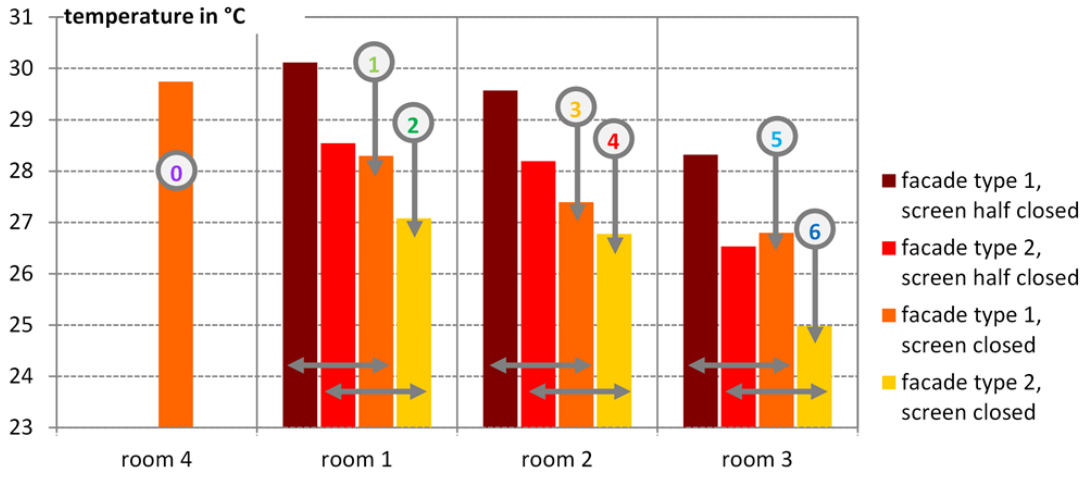

Figure 10.5: Measurement results on operative temperature - 1 m distance to the façade

Cooling Capacity

The summary of the measurement results visualize, that there is an impact on the cooling capacity by different room set-ups. The resulting cooling capacities of the different room types are shown in figure 10.6. The colour of the lines is referring to the description of the room types, which is summarized in table 10.1, the detailed description of the room types can be found in chapter 3 in section 3.2.2

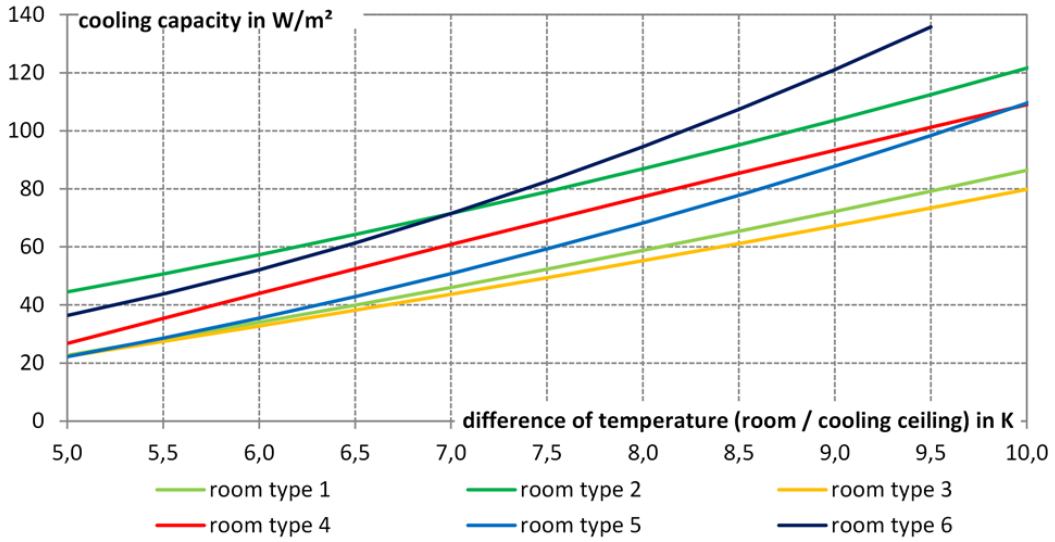

Figure 10.6: Comparison of the cooling capacity of different room types

The measurement results show that there is an increase of the cooling capacity due to different façade systems. There is an increase of the cooling capacity of about 20 $W/m^2_{coolingarea}$ in dependency of the temperature difference between the operative temperature in the centre of the room and the mean medium temperature due to the change of the façade system from single skin façade to single storey double skin façade. The verification of the assumption, that the capacity increase is because of a higher air flow rate over the ceiling and therefore a higher convection load, can be done by the mathematical model which is summarized in chapter 10.2.2.

Tracer Gas Measurement

The aim of the tracer gas measurements is to clarify how the façade system and the cooling ceiling impacts the air movement within a room. Therefore the measurements with different inject locations and different room set ups were done. As tracer gas CO_2 was used, as sensors Johnson Controls CD-W00-00-0 CO_2 transmitter were applied.

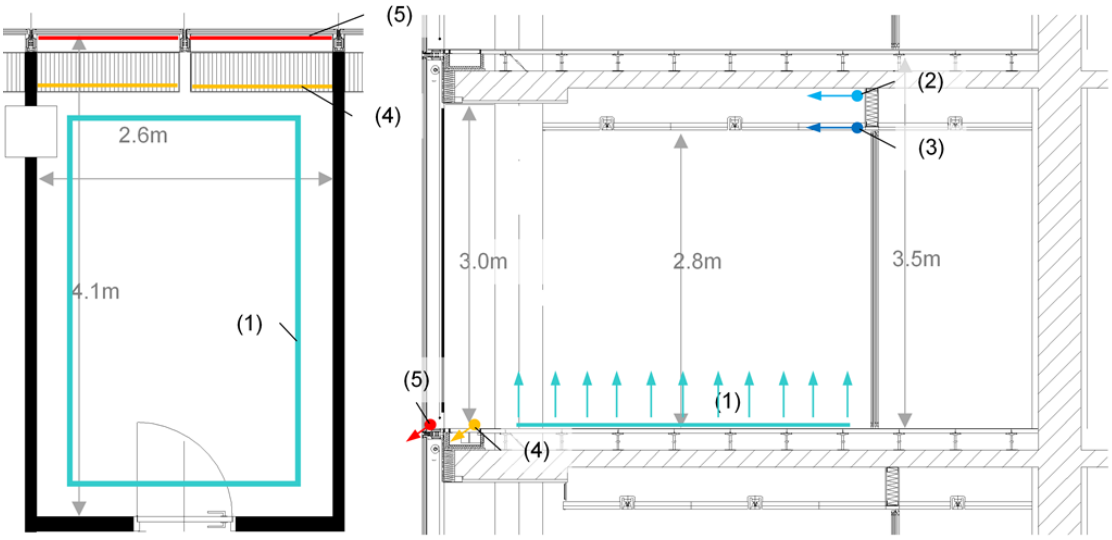

Figure 10.7: location of tracer gas injection - summary (detailed description see 2.2)

The detailed description of the test rooms and the general measurement set-up is done in chapter 2.2. Figure 10.7 shows the floor plan (left side) and the section view (right side) of the measurement room where the location of the tracer gas in injections are highlighted. (direct injection to the room (1); concrete ceiling (2) cooling ceiling (3); supply air area (4); façade area (5))The tracer gas measurement results show the impact by different concentration rates. The location of injections has no impact on the decay curves after the first 10 minutes.
Representative for the tracer gas measurement the measurement results of CO_2 concentration for the different room types with solar radiation, the tracer gas injection directly into the room (floor area) are shown in figure 10.8. The diagram shows an increase of concentration in the ceiling area due to the single stores double skin façade and a decrease due to the lack of natural ventilation for the cases with the closed suspended ceiling.

The single storey double skin façade leads to a significant increase of tracer gas concentration within the ceiling zone. The maximum concentration within the suspended ceiling variate between 720 ppm (room type 1) and 1491 ppm (room type 4). Due to the second glazing there is an increase of 350 ppm. The difference between the open and the closed ceiling is about 420 ppm.

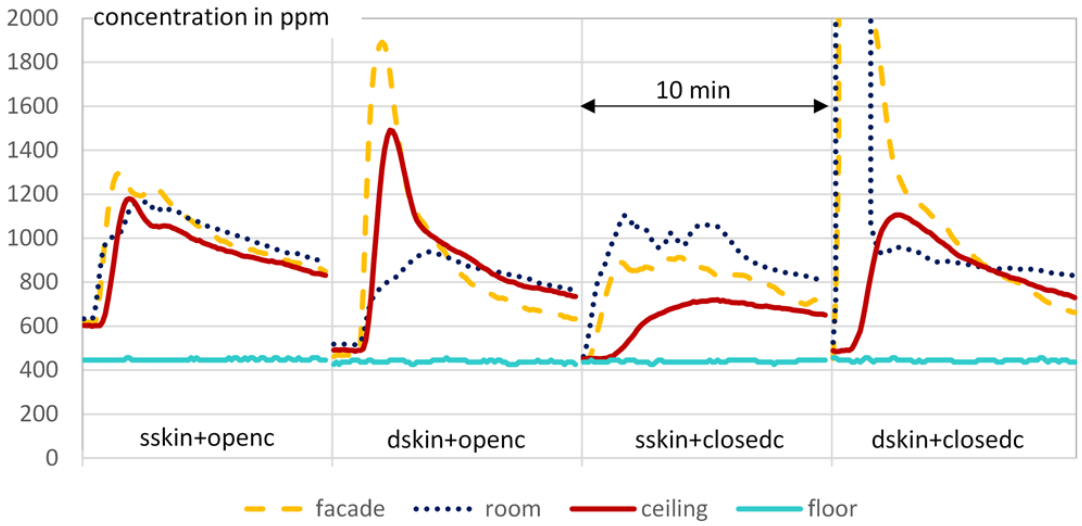

Figure 10.8: Measurement results of CO_2 concentration for the different room types with solar radiation, the tracer gas injection directly into the room (floor area). The diagram shows an increase of concentration in the ceiling area due to the single stores double skin façade and a decrease due to the lack of natural ventilation for the cases with the closed suspended ceiling.

The measurement results show an impact on the air flow due to different boundary conditions. These results were used for the detailed mathematical modeling of the air flow. To reach the aim of the research, which is the development of a simplified room model including the dynamic of three dimensional flow phenomena and possible to determine the impact on comfort with reasonable accuracy, the set of tracer gas measurement turned out to be the key part of the model validation.

10.2.2 Mathematical Modeling

The mathematical modeling was divided into three main parts - (1) the thermal modeling, (2) the air flow modeling and combining the first two (3) the air flow integated model. The thermal model was set up in Matlab/Simulink and the air flow modeling was done with the program Comsol Multiphysics. These two models form the basis for the air flow integrated room model, which was realised in Matlab/Simulink.

Thermal Modeling

For the development of a simplified room model a thermal model was set up in Matlab/Simulink. The mathematical model is based on separate modules, the model of the ”international Building Physics Toolbox” by Angela Sasic Kalagasidis (2007) [41] was used as template. The thermal model consists of four main groups - (1) construction, (2) zone, (3) systems and (4) sources and weather. The calculation of the room temperature and the capacity of the cooling ceiling was done with linked energy balances, wherein the calculation of components was done one-dimensional. The thermal cal-

culation is based on the descriptions in chapter 6, which represent a summary of the description done in Clarke (2001) [18].

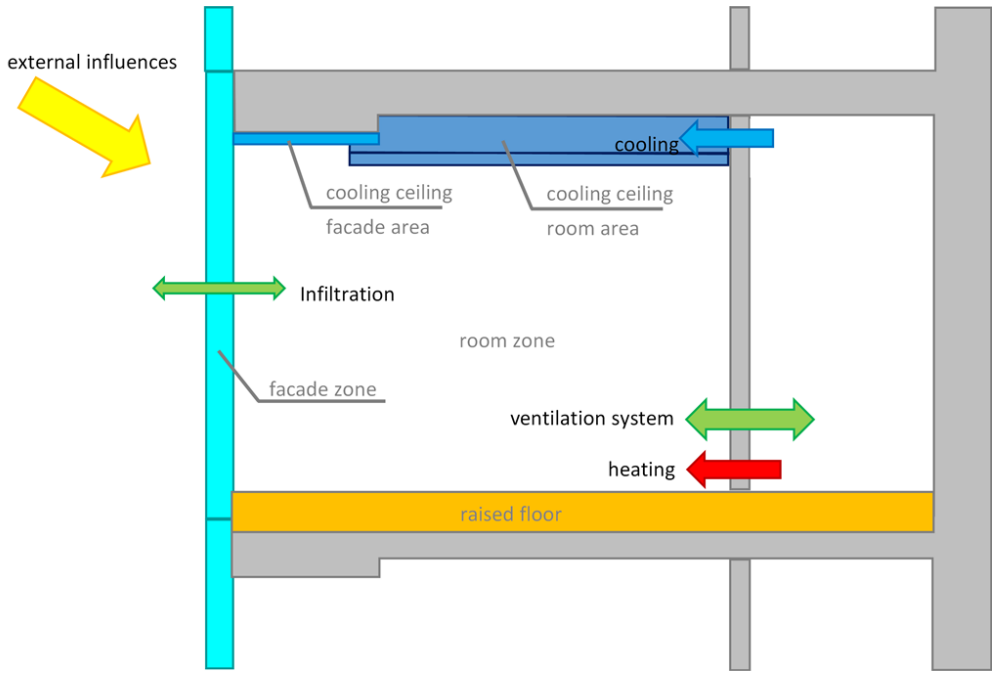

Figure 10.9: Schematic overview - room model

The thermal model is the first part of the air flow integrated room model. For the calculation, the rooms were divided into 5 zones like it's shown in figure 10.9. The calculation zones are (1) zone 01: room, (2) zone 02: façade, (3) cooling ceiling - façade area, (4) zone 04: cooling ceiling - room area and (5) zone 05: raised floor. In figure 10.9 the main impaction parameters are visualized, like the external influences due to temperature and radiation, the infiltration, the mechanical ventilation system and the heating and cooling system.

Air Flow Modeling

The air flow model is the second main part of the development of a air flow integrated room model which should calculate reliable results on comfort including the interaction of the envelope and the HVAC system. The software program COMSOL Multiphysics version 4.3a was used, with the aim to calculate the impact of air movement with different façade systems on the cooling capacity of the cooling ceiling. The influence on the cooling capacity due to the façade systems was measured by an intensive set of measurement and the results presented in chapter 2, 3, 4 and 5 are used for the validation of the mathematical model. The geometry of the simulation model is according to the architectural plans a section through the room. A simplification of the model, from three dimensions to two was done. The symmetry is along the depth of the room

The validation of the calculated results was done by the collected measurement data and is shown in figure 10.10. There is a good agreement between both for the operative temperature and the cooling capacity.

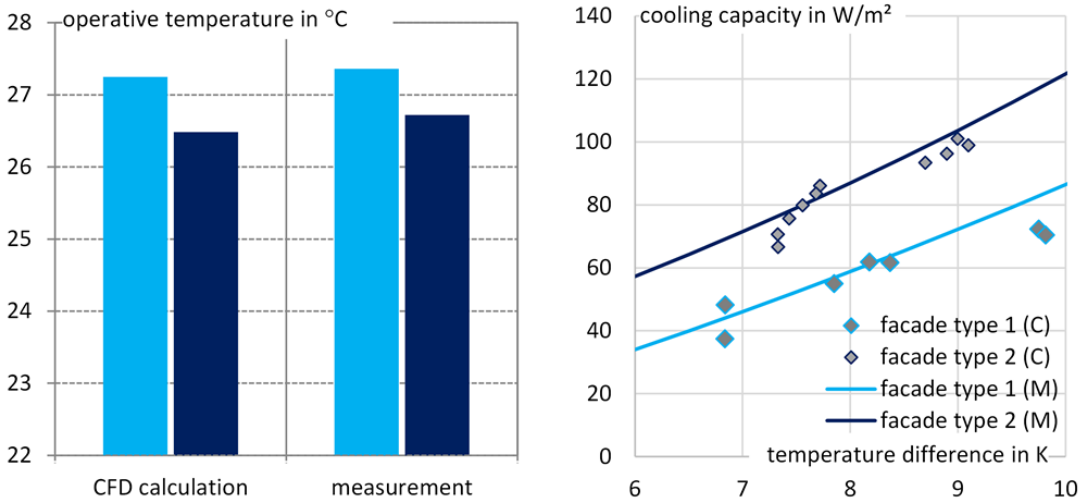

Figure 10.10: Measurement results on operative temperature (left side) and cooling capacity (right side; (M)..measurement; (C)..CFD calculation) – summary

In figure 10.10 on the left side the operative temperatures for two façade systems single skin façade and singe storey double skin façade with screen type 2 as shading system are shown. The left part in this diagram represents the result of the CFD calculation and the right part the measurement results, where the light blue colour refers to façade system 1 and the dark blue is regarding façade system 2. The compared value are for the position in the centre of the room, and the difference of the operative temperature in the middle of the room is about 0.2 K.
The right side diagram in figure 10.10 show the results regarding the cooling capacity of the cooling ceiling. The lines represent the measurement approximation done by the measurement results (detailed description see chapter 4). The points view the results out of the CFD calculation for the different tested boundary conditions. The diagram show a good agreement between the measurement results and the results of the CFD calculation for the cooling capacity of the cooling ceiling for both façade systems.

The comparison of the two façade systems – the single skin façade (type 1) and the single storey double skin façade (type 2) – show that there is a decrease in operative temperature and an increase of the cooling capacity.

In figure 10.11 the distribution of the air flow for the single skin façade left side and the single storey double skin façade (right side) according to the results of the air flow calculation is shown. The results are regarding an incident radiation of 800 W/m^2 and the total amount of air (about 50 m^3/h).

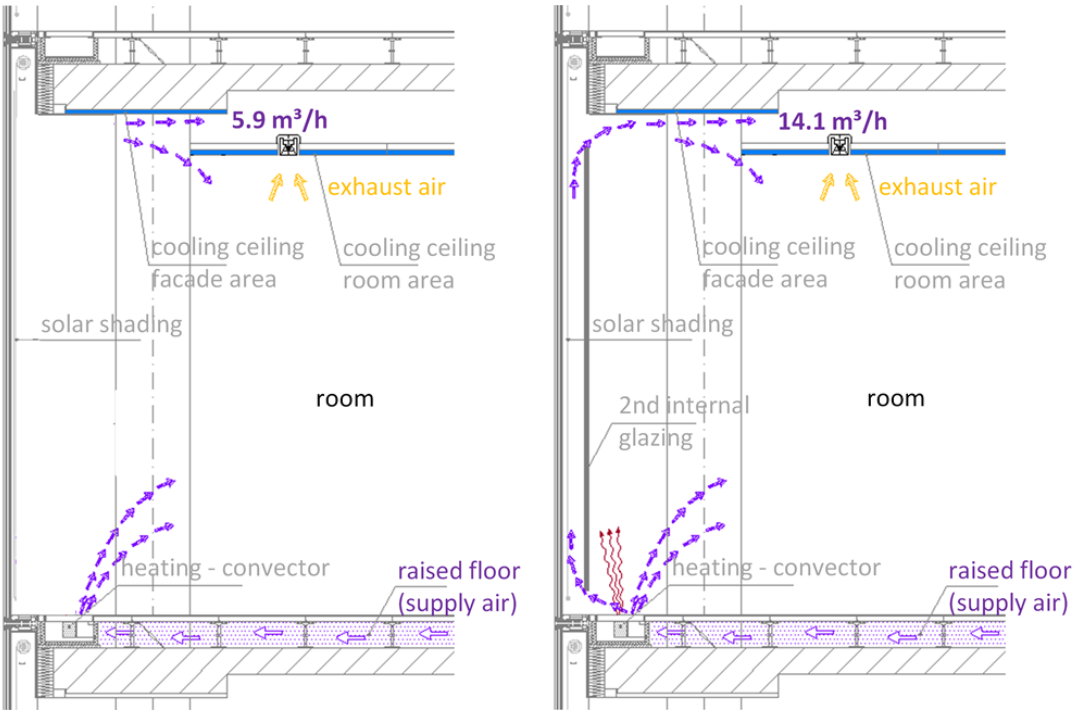

Figure 10.11: Air distribution for the two façade systems for an incident radiation of 800 W/m^2; left side: single skin façade; right side: single storey double skin façade

The results of the mean velocity in dependence of the temperature difference (air temperature / surface temperature) were compared for both façade systems The results are visualized in figure 10.12, were fs 1 means façade system 1 - single skin façade and fs2 façade system 2 - single storey double skin façade. The evaluation of the air velocities shows, that there is an higher convective air flow rate due to the single storey double skin façade. The velocities were calculated with respect to the temperature differences of surface temperature and air temperature. The simulation results show, that for the façade area the velocity is 5 times higher and for the cooling ceiling the velocity is 1.5 times higher with the single storey double skin façade than with the single skin façade.

The comparison of in situ measurements of operative temperature and the cooling capacity of a cooling ceiling and the calculation results of the CFD calculation show good agreement. The CFD model can therefore be used to characterize different façade systems regarding their impact on operative temperature and the capacity of the cooling ceiling as an input for the air flow integrated room model. There are two possibilities to integrate the results. First the results regarding the cooling capacity can be integrated directly and second there is the possibility of using the so-called speed factors and increase the convective heat flow within the thermal model.

10.2.3 Air Flow Integrated Room Model

The aim of the work is to develop an enhanced building model for the design of future buildings, taking into account the interaction of building envelope and building service systems. The realisation is done by a mathematical model that combines the thermal

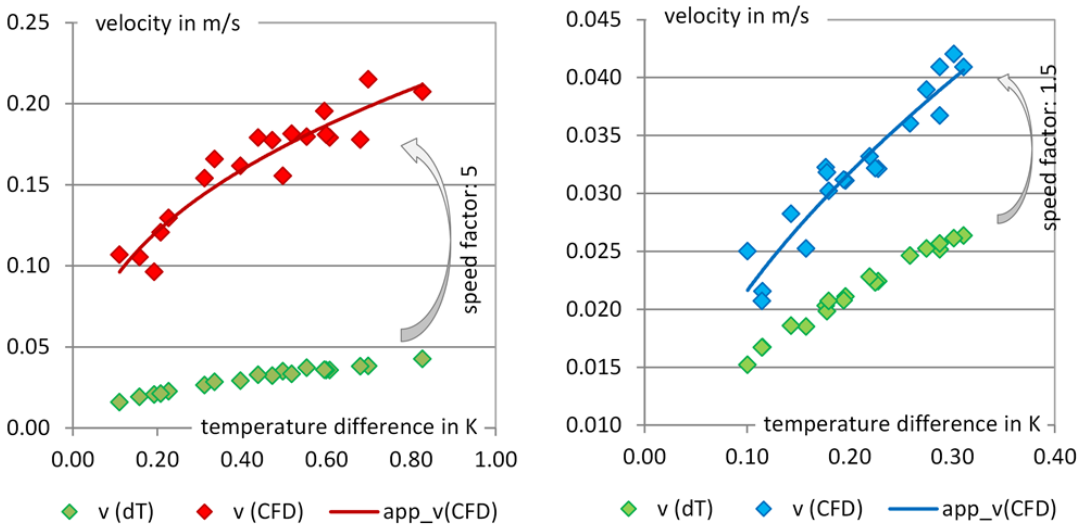

Figure 10.12: Comparison of the air velocity –> resulting speed factors - summary (detailed description see chapter 7.4.3)

modeling part with an simplified air flow calculation. A room model was developed that integrates the thermal calculation and a simplified illustration of the three-dimensional flow phenomena. The integration is required for a correct calculation of transfer systems to the room (eg chilled ceilings).

The room model is built in Matlab/Simulink as an ”extension/enhanced” thermal model. The results of the air flow calculation which was done by CFD simulations with the program COMSOL Multiphysics version 4.3a and validated with a series of measurements are included in the room model. There are three ways of integrating the results from the air flow calculation to the room model: (1) direct integration of the calculated cooling capacity to the room model, (2) use of the splitting factors for the air flow and (3) integration of temperature depending ”speed factors” of the convective heat flow. For the room model the decision was to integrate the speed factors, because it allows the most flexibility in terms of system changes and the results for the air velocity can be generated by the air flow model using the wall function. The comparison of the simulation results done with the model using the wall function and with the model using the Low Reynolds number $k - \epsilon$ turbulence model show the same results for the air velocity in the regarded areas. For a direct cooling capacity integration the detailed model has do be used because with the model using the wall functions there are no reasonable results.

The model is divided in the main parts: (1) input, (2) geometry, (3) room, (4) enclosing surfaces, (5) façade, (6) ventilation, (7) internal heat gains and (8) output. The schematic overview is shown in figure 10.13, where the blue frames highlight the different parts of the room model, the green frame visualize the summary of the integration of the temperature depending air flow.

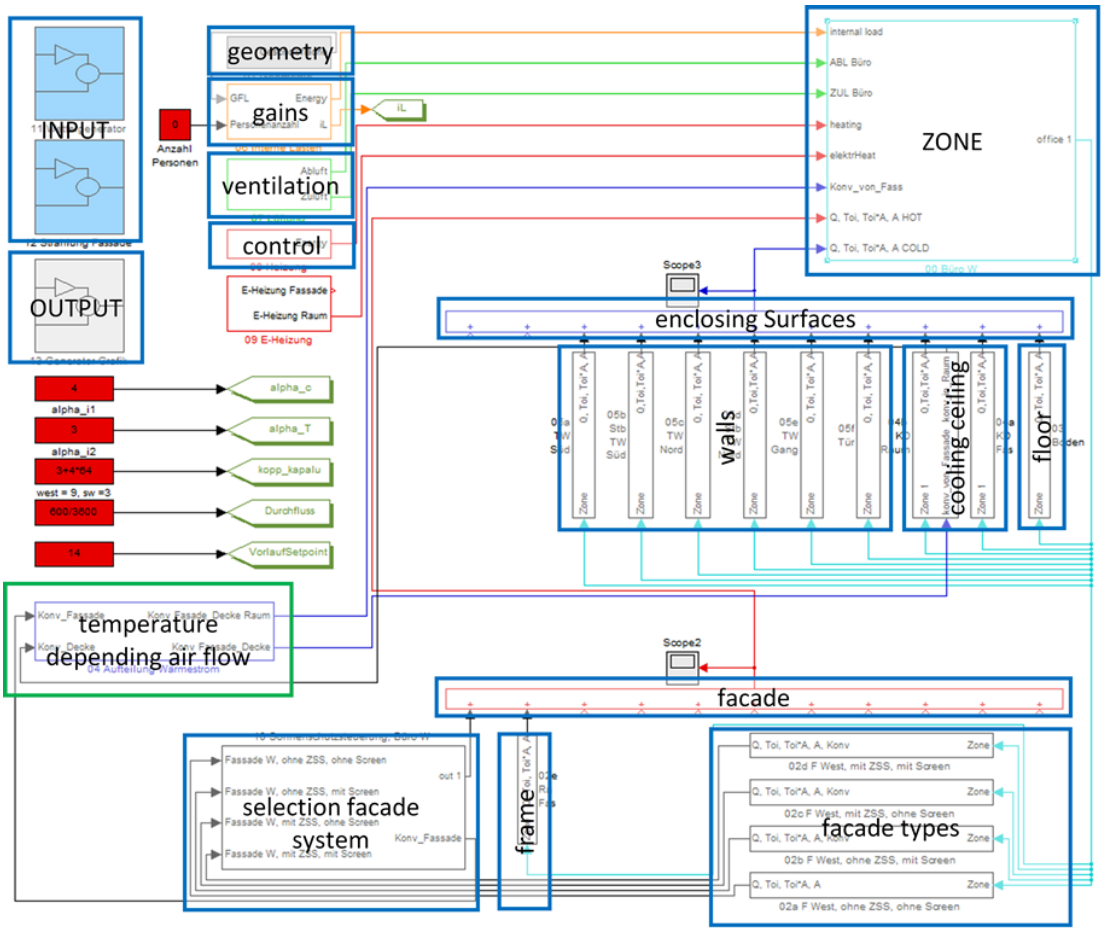

Figure 10.13: schematic overview of the **room model**; the main parts of the model are highlighted - room, enclosing surfaces, façade/façade types/shading control; cooling ceiling; ventilation; internal heat gains; geometry; input and output

To validate the room model, it was compared with the available measurement data for operative temperature in the centre of the room and the cooling capacity (detailed description see chapter 2, 3, 4 and 5). The detailed comparison is done on room type 2 (single storey double skin façade), the calculation results for all room types is shown in subsection 9.5.

For comparison the period from June 20th till the august 20th of the second summer period was used, where the data of July 27th was compared in detail. The results for the operative temperature in the centre of the room for this day are shown in 10.14, where the blue line represents the measurement data and the red line the calculated results of the developed room model. Both curves are for room type 2 (single storey double skin façade and screens as shading system). The results show a good accordance, the difference during the lunch time is due to hourly time step of the simulation and a logging period of 1 min for the measurement data.

After the successful validation of the air flow integrated room model the calculation was done for each room type to show the difference on operative temperature. In figure

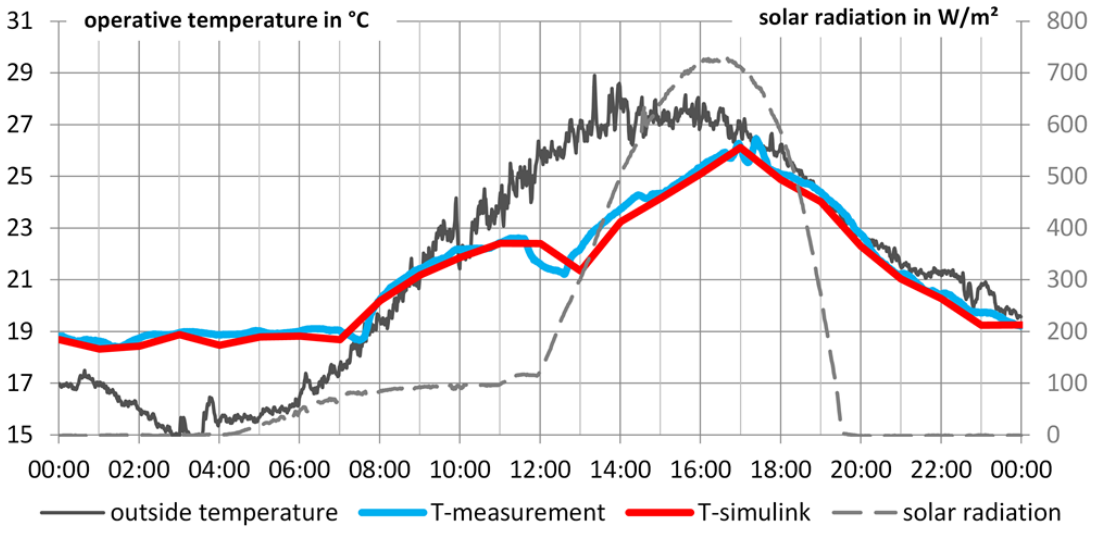

Figure 10.14: Comparison of the measurement results (blue line) and the results of the developed room model (red line) for room type 2 - summary

10.15 the results for room types 1, 2, 3 and 6 are visualized for the design day July 27th. The summary of the boundary conditions for the different room types is shown in table 10.1. The diagram shows the results for the operative temperature in the centre of the room. This diagram can be compared with the measurement results shown in figure 3.10 for the room types 0, 2, 3 and 6. The simulation results are in a good accordance to the measurement results (see figure 3.20)

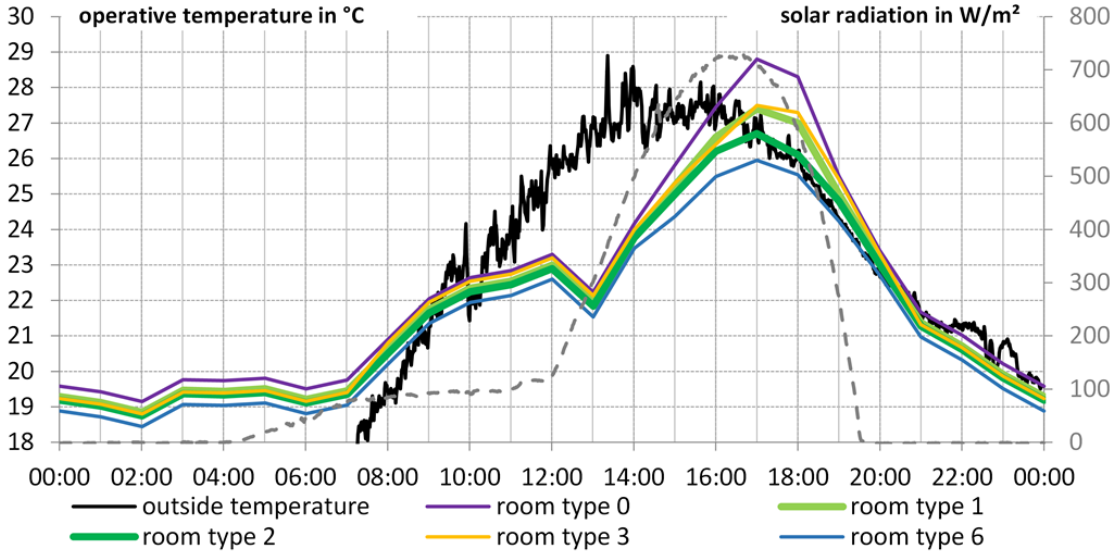

Figure 10.15: simulation results - room type 0 / 1 / 2 / 3 / 5;

The calculated results for the operative temperature of the room model were validated with measured data of the test rooms and the comparison show a good correspondence. The differences between the measurement data and the calculated results with

respect to the operating temperature are due to the time step or to structural conditions which have not been modeled.

For the air flow integrated room model the studies show, that the integration of temperature depending ”speed factors” of the convective heat flow is the simplest but still accurate enough way of realization. The need of detail is defined by the desired output, which in this case is the cooling capacity of cooling ceilings and the impact on the room temperature and therefore on the comfort in the room. The integration of ”speed factors” allows the most flexibility in terms of system changes and the results for the air velocity can be generated by the air flow model using the wall function.

10.3 Outlook

The simplification of the complex flow phenomena within the room by integrating speed factors calculated by an air flow model lead to similar results as the in-situ measurements for the cooling capacity of a cooling ceiling and the operative temperature. Within the work a validated air flow integrated room model was developed.

The air flow calculation done with the program COMSOL Multiphysics 4.3a needs inputs from a thermal calculation for the boundary conditions on surface temperatures and the solar radiation through the façade system is integrated by heat impacts directly to the different layers of the façade and the floor area. This is due to the radiation calculation of the program and is one point of improvement.

To get an easy to handle design tool for a planing support in an early stage planing phase of an building an interface and defined output values need to be realized. With the developed room model the effect of different façade systems in combination with cooled ceilings can be evaluated. The enhanced room model combines the building physical planning and the building service planning and statements in terms of thermal comfort, with complex flow phenomena in closed or open façades and the dynamics of cooling delivery systems, can be done.

Bibliography

[1] VDI 2078 Blatt 1. Cooling load calculation of air-conditioned buildings with room-conditioning from cooled walls and ceilings. Technical report, February 2003.

[2] DIN EN 1264. Water based surface embedded heating and cooling systems - Part 1: Definitions and symbols. Technical report, September 2011.

[3] EN 13363-2. Solar protection devices combined with glazing - Calculation of total solar energy transmittance and light transmittance - Part 2: Detailed calculation method. Technical report, June 2005.

[4] DIN EN 14240. Ventilation for buildings - Chilled ceilings - Testing and rating; German version EN 14240:2004. Technical report, April 2004.

[5] EN 15377-1. Heating systems in buildings - Design of embedded water based surface heating and cooling systems - Part 1: Determination of the design heating and cooling capacity. Technical report, February 2009.

[6] VDI 2078. Calculation of cooling load and room temperatures of rooms and buildings (VDI Cooling Load Code of Practice). Technical report, July 1996.

[7] DIN 4715-1. Cooling surfaces for rooms; part 1: measuring of the performance with free flow. Technical report, July 1994.

[8] EN 60584-1. Thermocouples - Part 1: EMF specifications and tolerances (IEC 60584-1:2013). Technical report, July 2014.

[9] DIN EN 60751. Industrial platinum resistance thermometers and platinum temperature sensors (IEC 60751:2008). Technical report, May 2009.

[10] ISO 7726. Ergonomics of the thermal environment - Instruments for measuring physical quantities. Technical report, 1998.

[11] ISO 7730. Ergonomics of the thermal environment - Analytical determination and interpretation of thermal comfort using calculation of the PMV and PPD indices and local thermal comfort criteria. Technical report, 2005.

[12] ISO 9060. Solar energy – Specification and classification of instruments for measuring hemispherical solar and direct solar radiation. Technical report, October 1990.

[13] EQUA Simulation AB. Ida indoor climate and energy, version 4.5. Manual, EQUA Simulation AB, 2013.

[14] Refrigerating American Society of Heating and Air-Conditioning Engineers. *2009 ASHRAE Handbook: Fundamentals*. 2009 Ashrae Handbook - Fundamentals. American Society of Heating, Refrigeration and Air-Conditioning Engineers, 2009.

[15] Manuel Andrés-Chicote, Ana Tejero-González, Eloy Velasco-Gómez, and Francisco Javier Rey-Martínez. Experimental study on the cooling capacity of a radiant cooled ceiling system. *Energy and Buildings*, 54:207–214, November 2012.

[16] Francesco Causone, Stefano P. Corgnati, Marco Filippi, and Bjarne W. Olesen. Experimental evaluation of heat transfer coefficients between radiant ceiling and room. *Energy and Buildings*, 41(6):622–628, June 2009.

[17] Battelle Memorial Institute. Defense Metals Information Center and W. Wood. *DMIC Report 177: Thermal Radiative Properties of Selected Materials*. Plenum Press handbooks of high-temperature materials. 1962.

[18] J. A. Clarke. *Energy simulation in building design*. Butterworth-Heinemann, Oxford, 2nd ed edition, 2001.

[19] Drury B. Crawley, Jon W. Hand, Michael Kummert, and Brent T. Griffith Griffith. Contrasting the capabilities of building energy performance simulation programs. technical report, United States Department of Energy, University of Strathclyde and Univerity of Wisconsin, 2005.

[20] Wolfgang Feist. Thermische Gebäudesimulation: kritische Prüfung unterschiedlicher Modellansätze. Müller, Jur. Verl., Heidelberg, 1994.

[21] Néstor Fonseca Diaz. Modeling of a hydronic ceiling system and its environment as energetic auditing tool. *Applied Energy*, 88(3):636–649, March 2011.

[22] Hossein Ghadamian, Mohammad Ghadimi, Mahdi Shakouri, Meisam Moghadasi, and Mohammad Moghadasi. Analytical solution for energy modeling of double skin façades building. *Energy and Buildings*, 50:158–165, July 2012.

[23] Bernd Glück. em Umweltschonende Raumheizung und -kühlung mit Kunststoff-Kapillarrohrmatten. Fachinstitut Gebäude-Klima, 2003.

[24] Bernd Glück. Wärmetechnisches Raummodell - Gekoppelte Berechnungen und wärmephysiologische Untersuchungen. C. F. Müller Verlag, 1997.

[25] Bernd Glück. Thermische Bauteilaktivierung: Nutzen von Umweltenergie und Kapillarrohren. C.F. Müller, Heidelberg, 1999.

[26] G.G. Gubareff, J.E. Janssen, and R.H. Torborg. em Thermal Radiation Properties Survey: A Review of the Literature. Honeywell Research Center ; Minneapolis-Honeywell Regulator Company, 1960.

[27] Neveen Hamza. Double versus single skin façades in hot arid areas. *Energy and Buildings*, 40(3):240–248, January 2008.

[28] W. M. Haynes. CRC handbook of chemistry and physics: a ready-reference book of chemical and physical data. Boca Raton: CRC Press., 2009.

[29] Wong Nyuk Hien, Wang Liping, Aida Noplie Chandra, Anupama Rana Pandey, and Wei Xiaolin. Effects of double glazed façade on energy consumption, thermal comfort and condensation for a typical office building in Singapore. *Energy and Buildings*, 37(6):563–572, June 2005.

[30] Teshome Edae Jiru and Fariborz Haghighat. Modeling ventilated double skin façades – a zonal approach. *Energy and Buildings*, 40:1567–1576, 2008.

[31] Refet Karadağ. The investigation of relation between radiative and convective heat transfer coefficients at the ceiling in a cooled ceiling room. *Energy Conversion and Management*, 50(1):1 – 5, 2009.

[32] Testo SE & Co. KGaA. Fibel-infrarot-messtechnik.pdf, 2016.

[33] R Külpmann. Untersuchungen zum Raumklimatisierungskonzept Deckenkühlung in Verbindung mit aufwärtsgerichteter Luftführung. PhD, TU Berlin, 1991.

[34] Detlef Laussmann and Dieter Helm. Air Change Measurements Using Tracer Gases: Methods and Results. Significance of air change for indoor air quality. 2011.

[35] H. Manz and Th. Frank. Thermal simulation of buildings with double-skin façades. *Energy and Buildings*, 37(11):1114–1121, November 2005.

[36] The Board of Trustees of the University of Illinois and the Regents of the University of California through the Ernest Orlando Lawrence Berkeley National Laboratory. Energyplus engineeringreference. Manual, The Board of Trustees of the University of Illinois and the Regents of the University of California through the Ernest Orlando Lawrence Berkeley National Laboratory., 2013.

[37] Charlesworth P.S. Air exchange rate and airtightness measurement techniques - an applications guide. technical report, Coventry, UK: Air Infiltration and Ventilation Centre, 1988.

[38] Guillermo Quesada, Daniel Rousse, Yvan Dutil, Messaoud Badache, and Stéphane Hallé. A comprehensive review of solar façades. Transparent and translucent solar façades. *Renewable and Sustainable Energy Reviews*, 16(5):2643–2651, June 2012.

[39] Hassan Radhi, Stephen Sharples, and Fayze Fikiry. Will multi-façade systems reduce cooling energy in fully glazed buildings? A scoping study of UAE buildings. *Energy and Buildings*, 56:179–188, January 2013.

[40] C. Riccabona, T. Bednar, and K. Mezera. Baukonstruktionslehre. 4. Bauphysik Manz, 2013.

[41] Angela Sasic Kalagasidis, P. Weitzmann, T. R. Nielsen, R. Peuhkuri, Carl-Eric Hagentoft, and C. Rode. The international building physics toolbox in Simulink. *Energy and Buildings*, 39:665–674, 2007.

[42] M.A. Shameri, M.A. Alghoul, K. Sopian, M. Fauzi M. Zain, and Omkalthum Elayeb. Perspectives of double skin façade systems in buildings and energy saving. *Renewable and Sustainable Energy Reviews*, 15(3):1468–1475, April 2011.

[43] University of Wisconsin-Madison Solar Energy Laboratory. Trnsys17 - volume 5 multizone building modeling with type56 and trnbuild. Manual, Solar Energy Laboratory, University of Wisconsin-Madison, TRANSSOLAR Energietechnik GmbH, CSTB – Centre Scientifique et Technique du Bâtiment, TESS – Thermal Energy Systems Specialists, 2005.

[44] University of Wisconsin-Madison Solar Energy Laboratory. Trnsys17 - volume 3 standard component library overview. Manual, Solar Energy Laboratory, University of Wisconsin-Madison, TRANSSOLAR Energietechnik GmbH, CSTB – Centre Scientifique et Technique du Bâtiment, TESS – Thermal Energy Systems Specialists, 2011.

[45] University of Wisconsin-Madison Solar Energy Laboratory. Trnsys17 - volume 4 mathematical reference. Manual, Solar Energy Laboratory, University of Wisconsin-Madison, TRANSSOLAR Energietechnik GmbH, CSTB – Centre Scientifique et Technique du Bâtiment, TESS – Thermal Energy Systems Specialists, 2012.

[46] Joana Sousa. Energy Simulation Software for Buildings: Review and Comparison. 2014.

[47] W. J. Stec and A.H.C.v. Paassen. Symbiosis of the double skin façade with the HVAC system. *Energy and Buildings*, 37(5):461–469, 2005.

[48] Kimura K Tanimoto J. Simulation study on an airflow window system with an integrated roll screen. page 317–325, 1997.

[49] Jürg Tödtli, Siemens-Aktiengesellschaft. *TABS Control Steuerung und Regelung von thermoaktiven Bauteilsystemen ; Handbuch für Planung, Auslegung und Betrieb*. Faktor-Verl., Zürich, 2009.

[50] Jeroen Van der Veken, Dirk Saelens, Griet Verbeeck, and Hugo Hens. Comparison of steady-state and dynamic building energy simulation programs. In *Proceedings of the Conference Performance of Exterior Envelopes of Whole Buildings IX, Ashrae, Atlanta USA*, 2004.

[51] viZaar AG. Homepage, 2014.

[52] Andreas Wagner. Energieeffiziente Fenster und Verglasung: Informationspaket. Solarpraxis, Berlin, 2007.

Curriculum Vitae

Katharina Eder
Sechshauser Strasse 36-38/7
1150 Vienna, Austria
+43(0)664 144.69.91

Education

2009–ongoing	PhD, Vienna University of Technology, Faculty of Mechanical and Industrial Engineering, Institute for Energy Systems and Thermodynamics, Vienna
2000–2004	Master Building Technology and Management, University of Applied Science Pinkafeld, Burgenland

Theses

2004	MasterTheses *Preparation of utilization data for dynamic thermal simulation of residential and non-residential buildings* Supervisors: Prof. Dr. Axel Seerig & Univ.-Doz. Dipl.-Ing. Dr.techn. Wolfgang Streicher

Experience

2013-ongoing	Research Engineer AIT Austrian Institute of Technology, Vienna, Austria dynamic thermal building and system simulation, energy concepts, scientific planning support
2010-2013	Research Assistant Vienna University of Technology, Institute of Building Construction and Technology, Vienna, Austria Development of dynamic building models, calculation of energy demand, energy strategies for low energy buildings
2006–2013	Technical Employee Vasko+Parnter Ingenieure, Vienna, Austria Dynamic thermal building simulation, energy strategies for low energy buildings
2003–2004	Research Assistant Graz University of Technology, Institute of Thermal Engineering,

	Graz, Austria CO2 reduction strategies
2005	Research Assistant University of Applied Science – Pinkafeld, Pinkafeld, Austria Dynamic thermal building simulation
2003–2004	Research Assistant Graz University of Technology, Institute of Thermal Engineering, Graz, Austria Dynamic thermal building simulation, energy monitoring

Additional Experience

2015-2016	Lecturer UAS Technikum Wien, Renewable Urban Energy Systems, Vienna, Austria Innovative cooling concepts
2013-2016	Lecturer University of Applied Science Salzburg, Smart Building, Salzburg, Austria Basics Smart Buildings, HVAC Technologies, Advanced HVAC Technologies
2008-ongoing	Fitness Trainer Holmes Place Vienna, Vienna, Austria LesMills BodyCombat

Computer Skills

Advanced	TRNSYS, ESP-r, BLAST
Intermediate	Matlab/Simulink, LaTeX, OpenOffice, AutoCad, COMSOL
Basic	Python, HTML, EnergyPlus, EQUA/IdaIce

Languages

German	Mothertongue
English	Intermediate Conversationally fluent
Italian	Basic Basic words and phrases only